DISSERTATION

EARLY OSTEOARTHRITIC CHANGES IN A CANINE CRANIAL CRUCIATE DEFICIENT MODEL

Submitted by

Troy Neal Trumble

Department of Clinical Sciences

In partial fulfillment of the requirements

For the Degree of Doctor of Philosophy

Colorado State University

Fort Collins, Colorado

Spring 2004

COLORADO STATE UNIVERSITY

June 23, 2003

WE HEREBY RECOMMEND THAT THE DISSERTATION PREPARED UNDER OUR SUPERVISION BY TROY TRUMBLE ENTITLED EARLY OSTEOARTHRITIC CHANGES IN A CANINE CRANIAL CRUCIATE DEFICIENT MODEL BE ACCEPTED AS FULLFILING IN PART REQUIREMENTS FOR THE DEGREE OF DOCTOR OF PHILOSOPHY.

Committee on Graduate Work

(Please print name under signature)

Adviser

Co-Adviser

Department Head/Director

ABSTRACT OF DISSERTATION

EARLY OSTEOARTHRITIC CHANGES IN A CANINE CRANIAL CRUCIATE DEFICIENT MODEL

Objective. To examine the early pathological, clinical, and biomarker responses that occur secondary to arthroscopic cranial cruciate ligament (CrCL) transection in the dog, for the purpose of determining the efficacy of a synthetic matrix metalloproteinase (MMP) inhibitor (BAY 12-9566) in slowing down the progression of osteoarthritis (OA).

Methods. An arthroscopic technique was developed and used to successfully transect the right CrCL in 39 dogs. Twenty and 19 dogs were orally administered BAY 12-9566 or a placebo, respectively, starting at 2 weeks post-transection and continued daily throughout week 18. Serum and synovial fluid collection, subjective pain scores (lameness, degree of weight bearing, response to joint extension, overall pain score, and effusion score), radiographs, and force plate analyses were all performed prior to CrCL transection, and then at various time points throughout the study until sacrifice at 18 weeks post-transection. At 18 weeks, gross and histologic grading was performed. Immunoassays were performed using the serum and/or synovial fluid in an attempt to determine the level of inflammation (prostaglandin-E_2), proteoglycan turnover (sulfated glycosaminoglycans-sGAG), bone formation (bone alkaline phosphatase-BAP, and osteocalcin-OC), collagen synthesis (carboxy-propeptide of type II collagen-CPII), type II collagen degradation (234CEQ neoepitope), type I and II collagen degradation (COL2-3/4C_{short} neoepitope), and type I collagen degradation (calculated as COL2-3/4C_{short} – 234CEQ). An additional 3 dogs underwent serial arthroscopic examinations of the stifle post-transection.

Results. Post-transection arthroscopic examinations demonstrated that articular cartilage and medial meniscal damage started as early as 2 weeks after transection and generally progressed. At 18 weeks, the gross and histologic lesions were highly variable between dogs with respect to incidence, location, severity, and type. Clinical parameters (lameness, degree of weight bearing, joint extension, overall pain score, and effusion score) became significantly worse after transection. PGE_2 concentration peaked at 2 weeks and correlated with the peak vertical force and impulse, and subjective lameness and effusion scores. Biomarker analyses demonstrated that type II collagen synthesis and degradation increased after transection, with synthesis predominating early and degradation at the end of the study. Synovial fluid type I collagen degradation was greater than type II collagen, predominating early while type II collagen degradation predominated later. Synovial fluid BAP levels from the operated stifle was significantly correlated to the total radiographic osteophyte score. All analyses did not reveal any significant differences between dogs treated with BAY 12-9566 compared to placebo treated controls.

Conclusion. Intra-articular damage starts to occur shortly after arthroscopic CrCL transection and progresses at a highly variable rate such that the MMP inhibitor BAY 12-9566 could not slow down the progression of OA when administered daily from 2 to 18 weeks post-transection. Biomarkers of inflammation, collagen synthesis and degradation, and bone formation can be successfully used in this cruciate-deficient model to characterize sequential patterns of intra-articular damage that occurs.

Troy Neal Trumble
Department of Clinical Sciences
Colorado State University
Fort Collins, Colorado
Spring 2004

ACKNOWLEDGEMENTS

To Bayer Corporation Inc., Animal Health Division, for providing the financial support for this study.

To Drs. Wayne McIlwraith and Clark Billinghurst for serving as my advisers and providing guidance and perspective throughout the good and bad personal and professional times I experienced throughout the last few years.

To Dr. Clark Billinghurst for passing on your knowledge about biomarkers and being the backbone upon which I could rely throughout the study.

To Drs. Richard Park, Chris Kawcak, and David Frisbie for serving on my committee and providing me with added knowledge and insight.

To Dr. Alison Bendele for sharing her knowledge about the pathological changes that occurred within this model of osteoarthritis.

To Elisa French, Steve Carey, Geri Baker, and Stephen Davis, and all of the members of the Colorado State University Lab Animal Resources and Orthopaedic Research Center, for your technical assistance that enabled this very large project to come to fruition.

To Megan Knowlton and Andi Hume for your patience in teaching and guiding me through the laboratory procedures used in this study.

To Dr. Elaine Carpenter for her artistic contribution.

To my beautiful bride, Cindy Trumble. My feelings for you go beyond words. Your inner strength is unparalleled and has allowed me to become a better and stronger person during the ups and downs of our life together. Thank you for putting up with the physical, emotional, financial, and time restrictions that have been placed upon our relationship since we have exchanged vows.

To my son, Eric Ronald Trumble. You provide me with the perspective of what is really important in life. Your smile and joy fill my heart.

DEDICATION

To my parents, Ronald Paul and Olive Elaine Trumble for providing me with a zest for life as well as the support and confidence to become the best person and professional that I can be. Based upon your example, I strive to become a better man, father and husband. Also, to my daughter, Taylor Nicole Trumble, it was a pleasure to meet you, even if it was short-lived. You changed my life forever and I'll never forget you. I am comforted knowing that you and grandpa are enjoying each others' company.

TABLE OF CONTENTS

Signature page.....ii

Abstract of dissertation.....iii-iv

Acknowledgements.....v

Dedication.....vi

1 Introduction.....1-50

1.1 Purpose of study.....1-2

1.2 Specific objectives.....2-3

1.3 Hypotheses.....3

1.4 Literature Review.....4-50

1.4.1 Normal canine stifle.....4-5

1.4.1.1 Anatomical overview.....4-5

1.4.2 Normal structure and function.....5-17

1.4.2.1 Cruciate ligaments.....5-7

1.4.2.2 Menisci.....7-8

1.4.2.3 Articular cartilage.....8-14

1.4.2.4 Synovium.....14-15

1.4.2.5 Synovial fluid.....15-16

1.4.2.6 Subchondral bone.....16-17

1.4.3 Normal homeostasis of articular cartilage.....18-26

1.4.4 CrCL transection as a model for osteoarthritis.....26-29

1.4.4.1 CrCL associated meniscal injuries.....29-30

1.4.4.2 Etiopathogenesis of OA after CrCL rupture.....30-33

1.4.5 Diagnosis of OA after CrCL rupture.....33-45

1.4.5.1 Clinical analysis.....33-34

1.4.5.2 Arthroscopy.....34-35

1.4.5.3 Imaging.....35-37

1.4.5.4 Force plate analysis.....37-40

1.4.5.5 Biomarker analysis.....40-45

1.4.6 Synthetic MMP inhibitors.....45-50

2 Technique for arthroscopic transection of the canine cranial cruciate ligament to induce osteoarthritis.....51-68

2.1 Summary.....52-53

2.2 Introduction.....53-54

2.3 Materials and methods.....54-56

2.4 Results.....56-63

2.5 Discussion.....63-68

3 Serial arthroscopic examination of the cranial cruciate deficient stifle in the dog.....69-91

3.1 Summary.....70

3.2 Introduction.....70-72

3.3 Materials and methods.....72-75

3.3.1 Experimental design.....72-74

3.3.2 Arthroscopic analysis.....74-75

3.4 Results.....75-83

3.4.1 Day 0.....77

3.4.2 Day 14.....77-78

3.4.3 Day 28.....78-79

3.4.4 Day 70.....79-80

3.4.5 Day 126.....80-83

3.5 Discussion.....83-91

4 Identification of changes in vertical ground reaction forces compared to meniscal pathology after cranial cruciate ligament transection in the dog.....92-115

4.1 Summary.....93-94

4.2 Introduction.....94-96

4.3 Materials and methods.....96-102

4.3.1 Animals and experimental protocol.....96-97

4.3.2 Gross pathology scores.....97-99

4.3.3 Force plate evaluation.....99-100

4.3.4 Calculations and groupings.....100-101

4.3.5 Statistical analysis.....102

4.4 Results.....102-110

4.4.1 Peak vertical force.....102-107

4.4.2 Vertical impulse.....107

4.4.3 Peak propulsion force.....108

4.4.4 Propulsion impulse.....108-109

4.4.5 Braking force and impulse.....109-110

4.5 Discussion.....110-115

5 Variability of macroscopic and microscopic pathology in osteoarthritis secondary to cranial cruciate ligament transection in dogs.....116-141

5.1 Summary.....117

5.2 Introduction.....118-119

5.3 Materials and methods.....119-125

5.3.1 Experimental design.....119-120

5.3.2 Macroscopic grading of lesions.....121-122

5.3.3 Microscopic grading of lesions.....122-124

5.3.4 Statistical analysis.....124-125

5.4 Results.....125-137

5.4.1 Macroscopic findings.....125-131

5.4.1.1 Synovial membrane.....125

5.4.1.2 Menisci.....125

5.4.1.3 Osteophytes.....125-126

5.4.1.4 Articular cartilage.....126-131

5.4.2 Microscopic findings.....131-137

5.4.2.1 Synovial membrane.....131

5.4.2.2 Osteophytes.....131

5.4.2.3 Articular cartilage.....131-137

5.5 Discussion.....137-141

6 Synovial fluid levels of bone-specific alkaline phosphatase correlate with osteophyte formation in a canine cranial cruciate ligament transection model of osteoarthritis.....142-164

6.1 Summary.....143-144

6.2 Introduction.....144-146

6.3 Materials and methods.....146-152

6.3.1 Experimental design.....146-147

6.3.2 Sample collection.....147-148

6.3.3 Radiographic analysis.....148-149

6.3.4 Molecular biomarker for bone alkaline phosphatase analysis.....149-150

6.3.5 Molecular biomarker for osteocalcin analysis.....150-151

6.3.6 Statistical analysis.....151-152

6.4 Results.....152-156

6.4.1 Serum bone alkaline phosphatase and osteocalcin.....152-153

6.4.2 Synovial fluid bone alkaline phosphatase.....153-154

6.4.3 Radiographic analysis.....155-156

6.4.4 Correlations.....156

6.5 Discussion.....157-164

7 Evaluation of collagen synthesis (type II) and degradation (type I and II) by collagenase cleavage and proteoglycan turnover in the synovial fluid and serum from a canine cranial cruciate transection model of osteoarthritis.....165-191

7.1 Summary.....166-167

7.2 Introduction.....167-170

7.3 Materials and methods.....171-177

7.3.1 Experimental design.....171-172

7.3.2 Sample collection.....172

7.3.3 Molecular biomarker of type II collagen synthesis.....172-173

7.3.4 Molecular biomarker of type I and II collagen degradation.....174

7.3.5 Molecular biomarker of type II collagen degradation.....174

7.3.6 Immunoblotting for 234CEQ specificity.....174-175

7.3.7 Estimation of type I collagen degradation.....175

7.3.8 Determination of proteoglycan turnover.....175-176

7.3.9 Statistical analysis.....176-177

7.4 Results.....177-184

7.4.1 Characterization of 234CEQ antibody as an antineoepitope antibody for collagenase-generated fragments of canine type II collagen.....177

7.4.2 Type II collagen synthesis, type I and II collagen cleavage by collagenases, and proteoglycan turnover in serum.....177-180

7.4.3 Type II collagen synthesis, type I and II collagen cleavage by collagenases, and proteoglycan turnover in synovial fluid.....180-182

7.4.4 Correlations.....182-184

7.5 Discussion.....185-191

8 Correlation of synovial fluid prostaglandin E_2 (PGE_2) concentrations to ground reaction forces and clinical parameters of pain and inflammation in a canine cranial cruciate transection model of osteoarthritis.....192-211

8.1 Summary.....193-194

8.2 Introduction.....194-196

8.3 Materials and methods.....196-202

8.3.1 Experimental design.....196-197

8.3.2 Synovial fluid collection.....197-198

8.3.3 Prostaglandin E_2 (PGE_2) analysis.....198-199

8.3.4 Force plate evaluation.....199-200

8.3.5 Subjective clinical pain scoring.....200-201

8.3.6 Statistical analysis.....201-202

8.4 Results.....202-206

8.4.1 PGE_2 analysis.....202

8.4.2 Force plate analysis.....202-204

8.4.3 Clinical parameters.....204-205

8.4.4 Correlations.....205-206

8.5 Discussion.....207-211

9 The ineffectiveness of a synthetic matrix metalloproteinase inhibitor determined in a canine cranial cruciate ligament transection model of osteoarthritis using pathology, clinical parameters, and biomarker analyses.....212-242

9.1 Summary.....213-214

9.2 Introduction.....214-217

9.3 Materials and methods.....217-226

9.3.1 Animals and experimental protocol.....217-218

9.3.2 Sample collection for biomarker analyses.....219

9.3.3 Analysis of pathology.....219-221

9.3.3.1 Macroscopic grading of lesions.....219-220

9.3.3.2 Microscopic grading of lesions.....220-221

9.3.4 Clinical parameters.....221-223

9.3.4.1 Subjective pain scoring.....221-222

9.3.4.2 Radiographic analysis.....222

9.3.4.3 Force plate evaluation.....222-223

9.3.5 Biomarker analyses.....223-225

9.3.5.1 Prostaglandin-E_2 (PGE_2) analysis.....223

9.3.5.2 Biomarker of type II collagen synthesis.....223

9.3.5.3 Biomarker of collagenase-induced type I and II collagen degradation.....223

9.3.5.4 Biomarker of collagenase-induced type II collagen degradation.....224

9.3.5.5 Estimation of collagenase-induced type I collagen degradation.....224

9.3.5.6 Determination of proteoglycan turnover.....224

9.3.5.7 Biomarker for early osteoblastic activity.....224-225

9.3.5.8 Biomarker for late osteoblastic activity.....225

9.3.6 Statistical analysis.....225-226

9.4 Results.....226-237

9.4.1 Pathology.....226-230

9.4.1.1 Macroscopic pathology findings.....226-228

9.4.1.2 Microscopic pathology findings.....228-230

9.4.2 Clinical parameters.....230-231

9.4.2.1 Subjective scoring.....230-231

9.4.2.2 Radiographic analysis.....231

9.4.2.3 Force plate analysis.....231

9.4.3 Biomarker analyses.....231-237

9.4.3.1 Articular cartilage markers in the serum.....231-233

9.4.3.2 Inflammatory and articular cartilage markers in synovial fluid.....233-236

9.4.3.3 Bone formation markers.....236-237

9.5 Discussion.....237-242

10 Summary.....243-251

10.1 Objective 1.....243-244

10.2 Objective 2.....244-245

10.3 Objective 3.....245-249

10.4 Objective 4.....250-251

Bibliography.....252-288

1 Introduction

1.1 Purpose of study

Osteoarthritis (OA) is a common musculoskeletal problem of dogs and humans, such that one or more joints become unable to move freely and without pain. It is represented by changes in the articular cartilage, synovial membrane, subchondral bone and synovial fluid, so that they are no longer able to absorb and dissipate the loads applied across the joint[1]. All of these components of joints are interrelated, so that any alteration to one will potentially change the properties of the others, resulting in possibly irreversible damage, leading to long-term morbidity. One of the most commonly injured joints in both dogs and humans is the stifle (knee), in which rupture of the cranial (anterior) cruciate ligament (CrCL) is the most commonly damaged structure[2]. The resulting abnormal forces placed across the stifle lead to functional and structural changes of the joint that are typical of OA. However, the exact etiopathogenesis of these catabolic changes are not completely understood.

For over 30 years, researchers have intentionally transected the CrCL in dogs and other animals in an attempt to create a model of osteoarthritis and increase our knowledge about this specific musculoskeletal problem in hopes that both dogs and humans would benefit from the results of their studies. One of the most beneficial aspects of this model is that it has helped to define the earliest changes that occur after injury as well as the cascade of events that follow. This has helped identify many of the mechanical and biochemical factors responsible for maintaining and potentiating the degradative processes. As a result, surgical intervention and/or medical treatments have been

developed in an attempt to block the degradative cascade before the catabolic state has reached a critical stage beyond which repair is not possible. However, even though we understand much more about the etiopathogenesis of OA now compared to 30 years ago, our main therapeutic interventions have not changed much. In other words, we still primarily attempt palliative means to control the clinical signs of inflammation and pain, but do little to reduce or reverse the actual destruction of the joint. This has prompted the development of disease modifying osteoarthritis drugs (DMOADs) that specifically attempt to block one or more aspects of the catabolic process so as to prevent further structural and functional damage to the joint. However, since these drugs do little to minimize clinical signs, efficacy must be proven by demonstrating that less destruction has occurred to the joint at both a macroscopic and biochemical level. Therefore, this study will examine the efficacy of a DMOAD using pathologic, clinical and biochemical examinations.

1.2 Specific objectives

The objectives of the research reported in this study were to:

1. develop and describe an arthroscopic approach to transect the CrCL in dogs for the creation of an experimental model of OA.
2. determine, using clinical, macroscopic, microscopic, and biomarker analyses, the efficacy of a disease modifying drug that inhibits the action of degradative enzymes responsible for catabolic changes in a joint after CrCL transection.
3. characterize the temporal pattern of clinical, macroscopic and biomolecular changes that occur in a joint after CrCL transection using non-invasive methods including: arthroscopy, force plate and radiographic analyses, as well

as biomarker analyses of inflammation, collagen synthesis and degradation, proteoglycan turnover, and bone formation.

4. analyze the macroscopic variability of this osteoarthritis model.

1.3 Hypotheses

The following hypotheses were proposed for this study.

1. The development and use of arthroscopic transection of the CrCL as a model of osteoarthritis will create consistent pathological changes in the stifle.
2. Articular cartilage degradation and meniscal damage will be established within the first few weeks after CrCL transection and severe meniscal damage can be identified using force plate analysis.
3. Treatment with the matrix metalloproteinase (MMP) inhibitor, BAY 12-9566, will result in significantly less pathologic changes, collagen degradation and proteoglycan turnover in stifle joints after CrCL transection compared to placebo-treated dogs.
4. Both type II collagen synthesis and degradation will increase after CrCL transection, with synthesis diminishing and degradation predominating over time.
5. PGE_2 concentrations in the synovial fluid will peak early and correlate to objective analysis of lameness via force plate analysis.
6. Serum levels of bone alkaline phosphatase (BAP) and osteocalcin (OC) will not differ from baseline after CrCL transection, but BAP levels in synovial fluid will increase and correlate with osteophyte progression identified radiographically.

1.4 Literature review

1.4.1 Normal canine stifle.

1.4.1.1 Anatomical overview. The structure of the canine stifle is the quadrupedal equivalent to the bipedal knee and is slightly different than most joints. In general, a joint is made up of two congruent bony surfaces that are held together by ligaments, and are covered by hyaline cartilage bathed in synovial fluid and surrounded by a joint capsule. The stifle, however, is a compound condylar synovial joint that does not have congruent bony surfaces (Figure 1.1)[3]. Semilunar fibrocartilages, called menisci, are interposed between the abaxial portion of the articular cartilages of the femur and tibia. They are almost triangular in cross-section, with the apex directed axially in an attempt to make the femoral and tibial surfaces congruent, leaving only the central portion of the tibial plateaus to articulate directly with the femoral condyles. The main

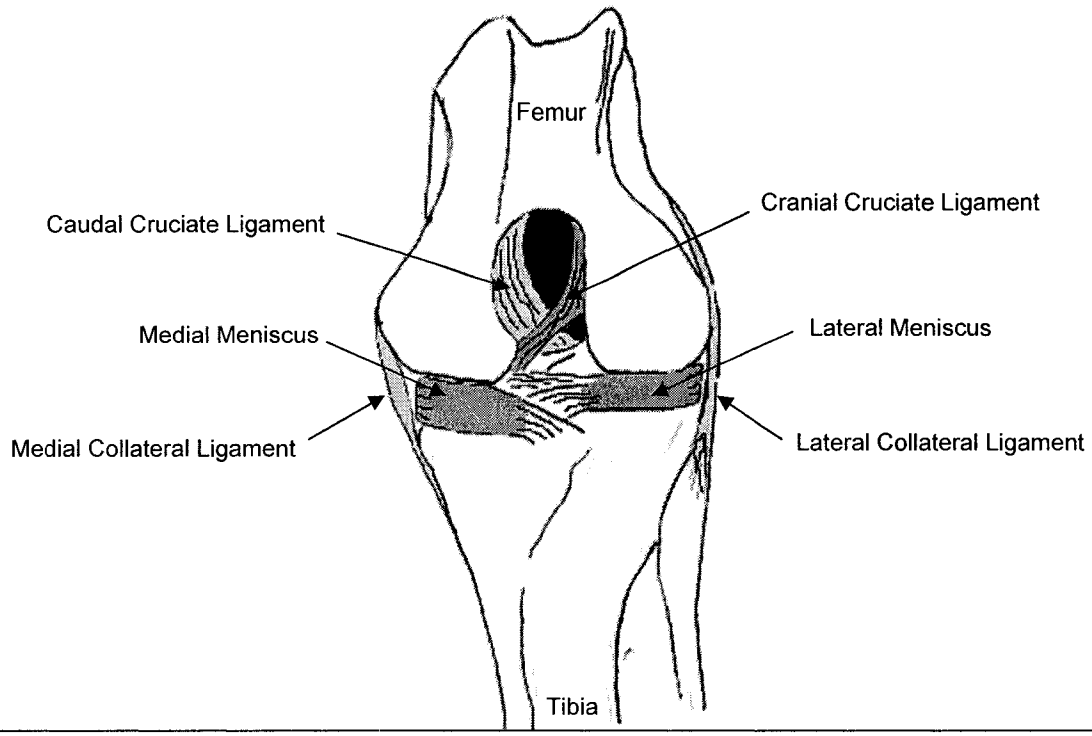

Figure 1.1. Schematic of the normal canine stifle with the femur maximally flexed to clearly demonstrate the cruciate ligaments. Structures are labeled accordingly. Adapted from Arnoczky, SP, et al., 1977.

stabilizers of the stifle include the collateral and cruciate ligaments (Figure 1.1). The collateral ligaments are attached to the medial and lateral aspects of the femoral epicondyles and proximal tibia, whereas the cruciate ligaments cross each other in the middle of the joint connecting the axial aspect of the femur and tibia. The stifle consists of one large synovial structure that is divided into four regions that are based on the anatomical structures that articulate, including: the femorotibial, femoropatellar, femorofabellar, and the proximal tibiofibular regions[3]. Most of the clinically important articulations occur in the femorotibial and femoropatellar areas, and will therefore be the focus of this report. The femorotibial joint articulation is the area between the femoral condyles and the tibial plateaus where the menisci are located, and the femoropatellar joint articulation is formed between the trochlea of the femur and patella.

1.4.2 Normal structure and function.

1.4.2.1 Cruciate ligaments. Within each stifle there are two intra-capsular, extra-synovial cruciate ligaments that are named according to where they insert on the tibia. The cranial cruciate ligament (CrCL) inserts on the cranial aspect of the proximal tibia, whereas the caudal cruciate ligament (CaCL) inserts on the caudal aspect of the proximal tibia (Figure 1.1). These are equivalent structures to the anterior cruciate ligament (ACL) and posterior cruciate ligament (PCL) in humans, representing relative differences in nomenclature between bipeds and quadrupeds. The cruciate ligaments are relatively acellular, with an abundant extracellular matrix that is composed primarily of type I and III collagens, elastin, proteoglycans, glycosaminoglycans (GAGs) and water[4]. The collagen fibers are arranged in slightly random parallel bundles to maximize tensile forces in all directions, and the proteoglycans and GAGs attract and hold water, adding

structure to the matrix as well as support of the collagen arrangement[5]. The elastin provides a small amount of elongation during tension of the ligament to protect the bony insertions[5].

The CrCL originates on the caudal axial surface of the lateral femoral condyle and courses cranially, medially, and distally, creating a slight outward (lateral) twist to insert slightly cranial and lateral to the intercondylar eminence of the tibia (Figure 1.1)[6]. The CrCL is further subdivided into two major bands, the craniomedial and caudolateral bands that are named for their relative attachment locations on the femur (cranial or caudal) and on the tibia (medial or lateral)[6]. When extended, the caudolateral band is taut while the craniomedial band is relatively lax, whereas during flexion, the craniomedial band tightens and the caudolateral band loosens[6]. The clinical importance of this is that the CrCL remains under tension throughout the range of motion of the stifle allowing the CrCL to have considerable reserve strength above the requirements for normal ambulation. As a result of this anatomy and orientation, the CrCL functions as the primary stabilizer of the knee in extension and internal rotation[6,7]. In other words, it has a primary role in the control of cranial tibial translation (cranial draw) and hyperextension, with a secondary role in the control of varus-valgus and rotational stability[8].

The CaCL originates on the axial surface of the medial femoral condyle and courses caudally and distally to attach into a depression on the caudal tibia between and 1 cm distal to the tibial plateaus (Figure 1.1)[6]. The CaCL is also comprised of two major bands named for their attachment sites on the femur and tibia. In extension, the craniomedial band is lax and the smaller caudolateral band is taut[6]. When flexed, the

caudal band becomes lax and the cranial band tightens[6]. As a result of this anatomy and orientation, the primary function of the CaCL is as a restraint to caudal displacement of the tibia, in addition to stabilizing the medial aspect of the joint by assisting the medial collateral ligament and resisting axial rotation (outward) of the tibial plateau during loading[6]. It is the secondary stabilizer against hyperextension, after the CrCL[6,9].

1.4.2.2 Menisci. The medial and lateral menisci are semilunar fibrocartilages interposed between the articular cartilages of the femur and tibia. The menisci consist primarily of type I collagen, water, and small amounts of proteoglycans and GAGs[4]. Similar to the cruciate ligaments, the proteoglycans and GAGs attract and hold water in the extracellular matrix providing extra support to the collagen network[5]. Each meniscus has a cranial and caudal ligamentous attachment to the tibia. The lateral meniscus also has a caudal femoral attachment. The size, orientation, and strength of the meniscal attachments determine the magnitude and direction of the load transmitted to the meniscal substance, and guides meniscal displacement during joint motions[10]. The lateral meniscus is slightly thicker than the medial meniscus due to the difference in shape of each condyle so as to provide for joint congruency. The medial meniscus is more firmly attached to the abaxial joint capsule and medial collateral ligament than the lateral, which only attaches to the joint capsule. Therefore, the lateral meniscus is more movable during flexion by sliding caudally on the tibia allowing it to be able to fully accept load transmission (Figure 1.2)[10].

The menisci function to protect the opposing articular surface by acting as a shock absorber, increasing the stability of the joint by deepening the articular surface on the

tibia, and relieving the incongruity between the femur and tibia[8]. The curvature of the condyles distributes the load optimally when the menisci are present, but not when

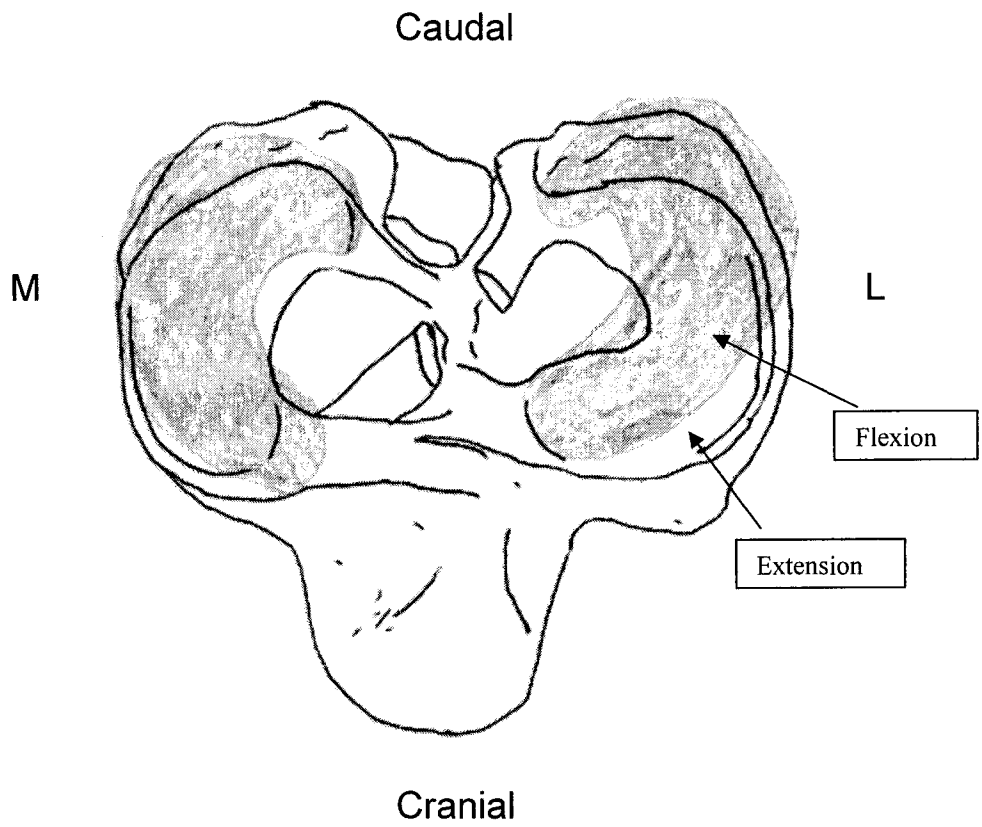

Figure 1.2. Schematic of the proximal aspect of the tibia with the menisci present, to demonstrate the amount of excursion of the menisci in normal extension and flexion (shaded). Note the limited amount of movement of the medial meniscus. Reprinted from Arnoczky, SP, et al. 1977.

absent[11]. The collagen fibrils are radially arranged on the surface and circumferentially arranged on the interior, allowing the menisci to transfer compressive forces into circumferential tensile forces minimizing the load placed upon the articular surface of the tibia[12]. Therefore, the menisci are capable of transmitting 40-60% of the applied load across the joint[11]. In addition, the menisci have also been shown to aid in lubrication, provide the articular cartilage with nourishment, and provide proprioception[8,13,14].

1.4.2.3 Articular cartilage. Hyaline cartilage is a smooth, glistening tissue on the ends of articulating surfaces of bones within diarthrodial joints. It

communicates with the synovial cavity superficially and attaches to the subchondral bone on its deepest surface. Hyaline cartilage is relatively acellular, and has no blood vessels, lymphatics, or nerve tissue. It is made up primarily of water (70-75%) and electrolytes that are maintained within the extracellular matrix created by chondrocytes surrounded primarily by collagen, proteoglycans, and glycosaminoglycans[15].

Microscopically, articular cartilage is divided into 4 major zones, including the superficial zone at the surface, followed by the middle or intermediate zone, the deep zone, and finally the calcified zone (tidemark) (Figure 1.3). In adult articular cartilage,

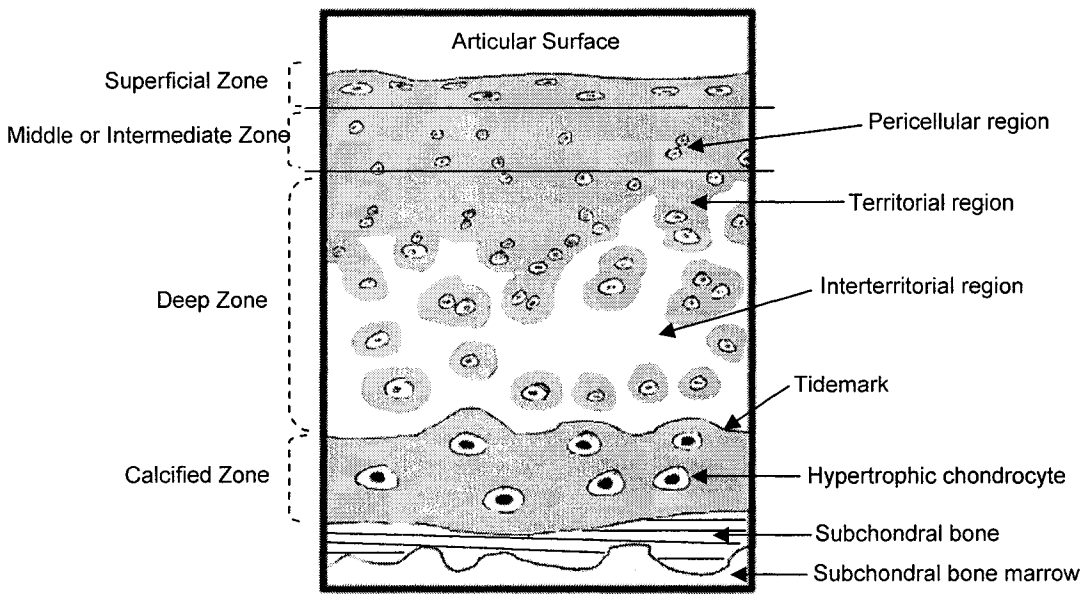

Figure 1.3. Schematic of the microscopic appearance of adult articular cartilage, with the respective zones and regions identified. Adapted from Eikenberry, EF, et al., 1999.

these zones consist of two major compartments, including the metabolically active cell-associated matrix, next to the chondrocytes, and the further removed interterritorial matrix[15]. Chondrocytes account for 2-5% of the articular cartilage volume and take on slightly different shape and function, depending upon their location within articular cartilage. Chondrocytes have the greatest cell density near the surface and are flattened

and oriented parallel to the surface, whereas in deeper zones, they are more spherical and extend slightly perpendicular (Figure 1.3). The deeper the chondrocytes, the more heterogeneity with respect to shape, surface receptors and metabolic activities[15]. Chondrocyte nutrition relies on the diffusion of nutrients from the synovial fluid since cartilage is avascular with the layers being subjected to different concentrations of nutrients and metabolites[15].

Collagen represents ~60% of the dry mass of articular cartilage[16]. The four types of collagen found in normal articular cartilage are types II, VI, IX, and XI[16]. Type II collagen accounts for 90% of the total collagen in hyaline cartilage, but is also located in the nucleus pulposus of the intervertebral discs, vitreous humor, and trachea[16]. It provides the primary torsional stability and tensile strength of cartilage by linking together with glycoproteins and proteoglycans. Type VI collagen forms a highly cross-linked, branched network in and around the type II collagen fibril that is highly adhesive for many cell types such as proteoglycans and may play a role in linking the larger collagens to the cell surface[15]. Type II collagen contains 3 identical α1 (II) polypeptide chains arranged in a right-handed triple helical pattern via a repeat of glycine residues to produce a tropocollagen subunit that forms collagen fibrils with a quarter stagger array extracellularly (Figure 1.4)[15]. Covalent crosslinks then form between the respective α chains and between other collagen molecules, conferring stiffness and strength to the fibril and the tissue. In addition, type IX collagen links to a type II collagen fibril in an antiparallel fashion to stabilize the 3-D organization of the collagen network by filling in the gaps, and interacting with other matrix components, as well as preventing fibril-fibril interactions[15]. Type XI collagen plays a pivotal role in the control of cartilage collagen

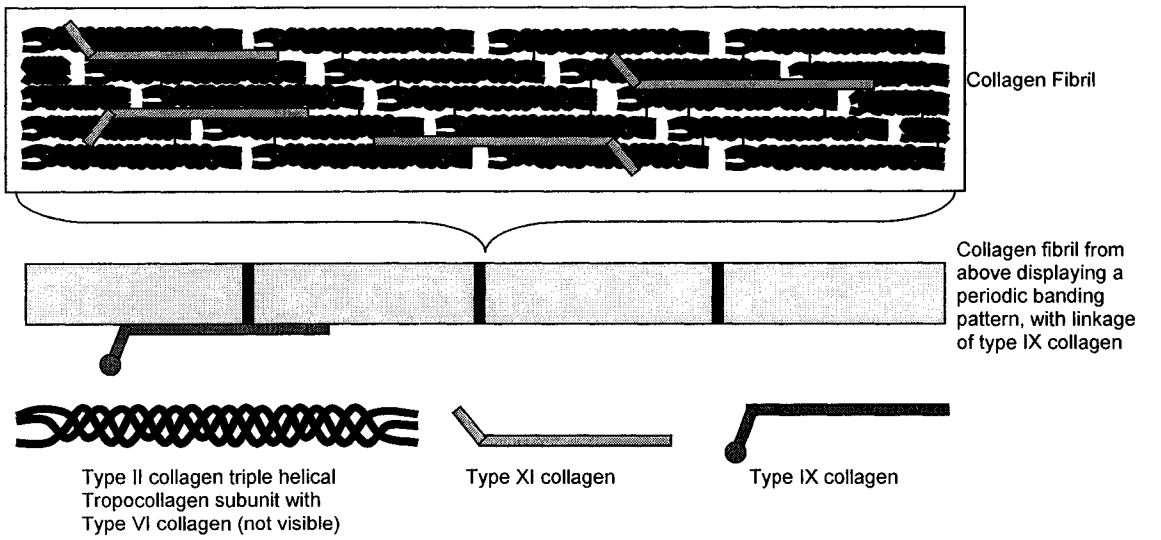

Figure 1.4. Schematic of collagen fibril assembly (top), including triple helical type II tropocollagen subunits packed into a quarter-staggered array that leads to a periodic banding pattern that is visible with electron microscopy (middle). The relative locations of types XI with respect to the type II collagen triple helix, and type IX collagens with respect to the entire collagen fibril are shown. A key of symbols is listed at the bottom. Adapted from von der Mark, K, 1999.

fibril assembly in articular cartilage by controlling the thickness of type II collagen and may be the core upon which type II collagen is deposited[15]. The arrangement of the collagen fibrils in articular cartilage varies depending upon the zone. At the surface, the fibrils align with the joint surface, whereas in the intermediate zone, the fibrils are randomly distributed in 3-dimensions. Finally, in the deep zone, the fibrils are nearly parallel to the long bone axis[15].

Proteoglycans account for 5-7% of the wet weight of articular cartilage[17]. The main proteoglycans present in articular cartilage include aggrecan, decorin, fibromodulin, and biglycan. Aggrecan is a large aggregating proteoglycan that represents 50-85% of the proteoglycans present in hyaline cartilage[17]. The basic structure for all proteoglycans consist of a protein core to which glycosaminoglycan (GAG) side chains of keratan sulfate (KS) and chondroitin sulfate (CS) are covalently bound. The aggrecan protein core is made up of three globular domains (Figure 1.5). Two globular domains (G1 and

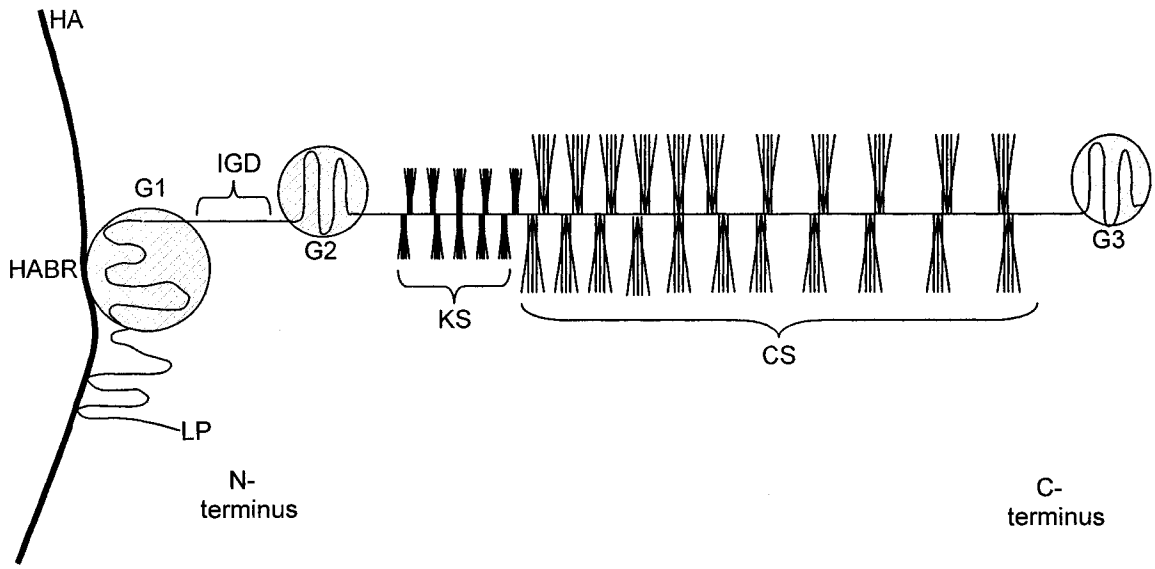

Figure 1.5. Schematic of the basic structure of the proteoglycan of aggrecan. The protein core is made up of three globular domains (G1, G2, G3), with multiple glycosaminoglycan side chains of keratan sulfate (KS) and chondroitin sulfate (CS) bound between G2 and G3. The G1 globular domain binds the aggrecan core to a long strand of hyaluronic acid (HA) at the hyluronan binding region (HABR), and is stabilized by link protein (LP). The interglobular domain (IGD) between G1 and G2 is a common site for proteolytic cleavage of aggrecan. Adapted from Hardingham, T, 1999.

G2) are present at the N-terminal region with the third (G3) located at the C-terminal region. G1 binds the aggrecan core protein to a long hyaluronic acid (HA) strand at a hyaluronan binding region (HABR) and is stabilized by link protein (LP)[18]. Because of this HA binding of aggrecan, many proteoglycans monomers can aggregate together along the HA chain (Figure 1.6), providing further structure to the cartilage matrix[17]. Biglycan, decorin, and fibromodulin are small proteoglycans that can bind to other constituents in the matrix, like collagen, and contribute to the structural network.

The structure of proteoglycans in cartilage is not uniform, in that there is often heterogeneity in the size of the aggregate, length of protein core, numbers present, and the positioning of KS and CS side chains[17]. The GAG side chains (KS and CS) of proteoglycans are composed of repeating disaccharide units and play a role in the resistance to interstitial fluid flow[19]. Within the tissue, CS and KS are negatively charged

and exert repulsive forces on each other. This fixed-charge density is variable, due to the variation in proteoglycan content and is responsible for the osmotic pressure of cartilage[20], which may ultimately contribute up to 50% of the overall compressive stiffness of articular cartialge[21].

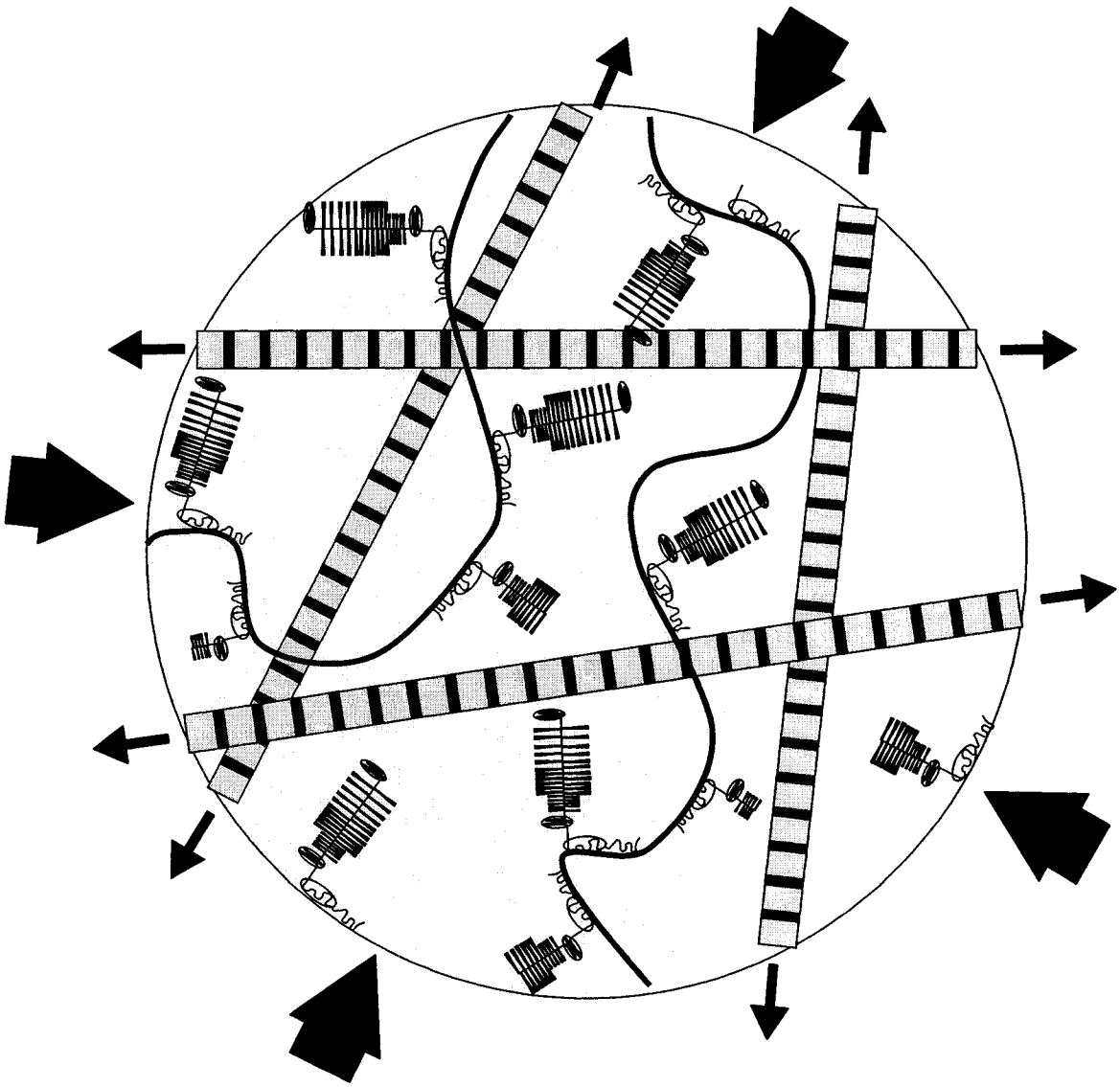

Figure 1.6. Schematic of the inter-relationship between type II collagen fibrils (tubular structure with periodic banding pattern described in Figure 4) and aggregates of the proteoglycan, aggrecan (Figure 5) bound to long strands of hyluronic acid (black lines). This demonstrates the osmotic environment created such that water and electrolytes (large arrows) enter cartilage, placing the collagen fibrils under tension (small arrows). Adapted from Hardingham T, 1999.

Even though the proteoglycans and collagens appear to have their own particular functions, they really function together. The viscoelastic property of cartilage is mainly attributable to the proteoglycans trapped in an aggregated meshwork between the collagen fibers, offering great resistance to fluid flow and redistribution of water[17]. The fixed negative charge creates an osmotic environment that allows water and electrolytes to fill the space between the collagen and proteoglycans, placing collagen fibrils under tension (Figure 1.6)[22]. When a load is placed across a joint, fluid is expelled at the leading edge of cartilage contact, but flows into cartilage at the trailing edge, in response to an increase in the swelling pressure until it is resisted by the tension developed in the collagen network[23]. Further joint loading will increase the congruity of the opposing surfaces of cartilage, increasing the volume utilized and ultimately increasing joint stability. As pressure is released, the GAGs move apart by charge repulsion and fluid flows back into the cartilage.

1.4.2.4 Synovium. In the canine stifle, the synovium covers all intra-articular surfaces of the joint except for the articular cartilage and articulating surfaces of the menisci. The superficial layer of the synovium, or the intimal layer, is only 1-3 cells thick, and lacks a basement membrane or tight junctions[24]. The cells that compose this layer are called synoviocytes, and they have phagocytic and immunologic functions (via macrophages)[25]. In addition, these cells synthesize the glycosaminoglycan, hyaluronan (HA), at the plasma membrane[25]. Deep to this intimal layer is the subintima which is the supporting layer of the synovium. This layer contains the primary connective tissue including collagen types I and III, proteoglycans, GAGs, fibroblasts, and mast cells, as

well as the lymphatics and neurovascular supply. The intimal layer is just a fine barrier between the intravascular and interstitial fluid of the subintima and synovial fluid[25].

The primary function of the synovium is to help determine the composition of the synovial fluid, by providing a selective barrier for ultrafiltration of the plasma. The proximity of the capillary plexus of the subintimal layer to the intimal surface facilitates exchange of water and solutes that is regulated by Starling forces in which there are pressure differences between the plasma and synovial fluid[26]. In general, for small molecules (<10kDa), simple diffusion allows the plasma and synovial fluid to equilibrate[26]. The production of HA by the synoviocytes also affects diffusion into the synovial fluid since HA on the synovial membrane surface will obstruct solute passage through steric hindrance[27]. The synovial membrane does not serve any known biomechanical function, but is capable of responding to mechanical stress by becoming fibrotic through the increased production of collagen in the subintimal layer, which can then alter the normal diffusion patterns and/or synoviocyte metabolism[28,29].

1.4.2.5 Synovial fluid. The synovial fluid is a viscous, transparent fluid that is an ultrafiltrate of plasma, containing most of the molecules present in plasma[13]. However, the relative concentrations of these molecules in the synovial fluid are usually quite different from that in the blood. The cellularity of the synovial fluid is relatively low and consists mostly of mononuclear cells as well as some polymorphonuclear leukocytes[30]. The synovial fluid contains a greater amount of HA compared to the plasma because of its production by the synoviocytes. HA is primarily responsible for giving the synovial fluid its viscosity[31]. Clearance of macromolecules and synovial fluid from the synovial cavity occurs through the lymphatics and veins in the subintimal layer

of the synovial membrane allowing for maintenance of the volume and composition of the synovial fluid. It is a complex process that appears to be affected by joint size[32], position of the joint with regard to flexion or extension[33], tension in the periarticular tissue[32], compliance of the joint capsule[33], the macromolecular content of the fluid[34], movement[35], and inflammation[36]. The normal synovial fluid volume in a canine stifle joint is relatively low at 0.2 to 0.7 ml[30]. Since articular cartilage is avascular and the intra-articular ligaments and menisci have limited blood supply, the primary functions of synovial fluid are to provide nutrition and lubrication to the articular cartilage and intra-articular ligaments[37-39]. In addition, synovial fluid helps transport and clear the by-products of metabolism from the intra-articular tissues.

1.4.2.6 Subchondral bone. Underneath the articular cartilage are the subarticular tissues. This includes the calcified cartilage and the subchondral bone. The calcified cartilage is the transition zone between the articular cartilage and subchondral bone (Figure 1.3). The junction of cartilage to bone is undulating and can therefore convert potential sheer stresses of weight-bearing into compressive and tensile forces[40]. The subchondral bone can be further divided into the subchondral plate closest to the calcified cartilage and the trabecular bone which is furthest from the calcified cartilage. Similar to cartilage, bone is composed of an extracellular matrix that is organized around a highly structured collagen lattice[41]. Osteoblasts are the primary bone-forming cells of the extracellular matrix, and are located directly on the surface. These osteoblasts secrete osteoid which eventually become mineralized by hydroxyapatite. Hydroxyapatite makes up 65% of the entire extracellular matrix of bone and helps provide its stiffness[42]. The remainder of the bone is composed primarily of collagen (95%), with proteoglycans and

some other noncollagenous proteins forming the remainder. Type I collagen accounts for 90% of the collagen within the bone and provides the primary load bearing properties, tensile strength, and torsional resistance of bone[41]. Once the osteoblast is surrounded by the mineralized matrix, it is called an osteocyte, and sits in a lacuna. Projections extend from the lacuna, called canaliculi, allowing cell-to cell contact between osteoblasts and osteocytes. In addition, osteoclasts are also present on the surface of bone and are responsible for invoking bone resorption. There is a close relationship b etween these cells with regards to formation and resorption of bone[41].

Normally, subchondral bone is responsible for maintaining the joint surface and absorbing stress placed on the joint[43]. In a normal joint, subchondral bone will actually maintain an uneven joint surface. In other words, the outer surfaces remain in contact while the center portion of the bone is not in contact. The purpose of this is to allow for the center of the joint to move axially during loading, thereby transmitting the load to the cortices, taking stress off of the articular cartilage. Therefore, subchondral bone provides the majority of the cushioning for the joint[43]. However, one must not think of subchondral bone as a static structure. It is rather dynamic in nature so that it can adjust to different amounts and types of stresses placed on a joint. In other words, the subchondral bone must allow for strength as well as cushioning. If the balance between cartilage and bone is not correct for the stresses placed on the joint, the bone can model or remodel to adjust for the difference. Modeling tends to refer to the formation of new functional bone, whereas remodeling is the replacement of old bone for more functional bone[41].

1.4.3 Normal homeostasis of articular cartilage.

In order to be able to understand what happens to the joint cartilage after CrCL transection/rupture, we must first consider how the articular cartilage replenishes itself under normal circumstances. In general, the structure of articular components is maintained in a functional homeostasis, or steady state, so that it can continue to transmit loads across the joint without any major damage occurring to any of its components. This balance is achieved by carefully regulated synthesis and degradation of the extracellular matrix. Bone is always in a constant flux in order to respond to changing loads, as well as to provide the body with necessary electrolytes (calcium). Cartilage turnover is slower, with aggrecan turning over more rapidly than type II collagen[44]. This normal turnover is initiated by a complex array of degradative enzymes and inflammatory mediators (Figure 1.7).

Collagen synthesis (type I and II) begins with transcription and translation of mRNA to form a procollagen α chain. Starting at the C-terminus, three procollagen α chains wind into a triple helix by forming disulphide bonds. Non-helical propeptides remain at each end of the helix as the procollagen molecules are secreted into the extracellular space. Here, the non-helical domains are enzymatically removed to form tropocollagen molecules. The tropocollagen molecules then orientate into the quarter-staggered array to form fibrils (Figure 1.4). Covalent cross-links form between the tropocollagen molecules to give the fibrils strength. Finally, the fibrils aggregate with other collagen molecules and proteoglycans in the process of fibrillogenesis[16].

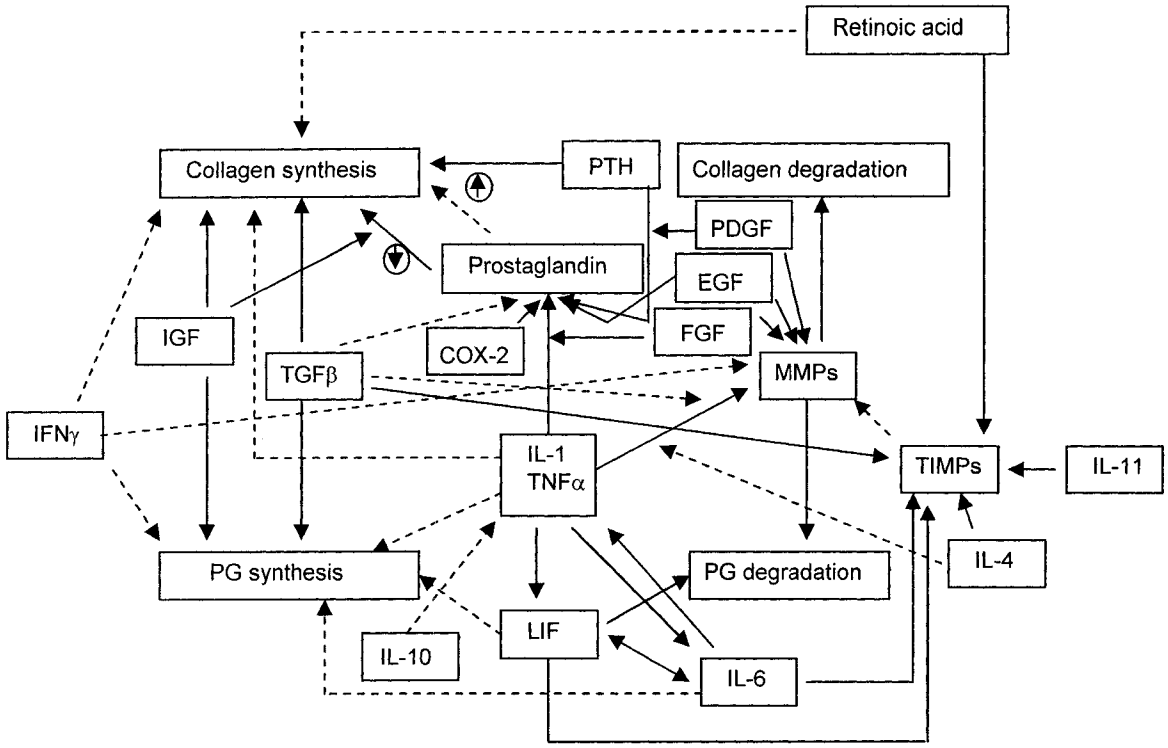

Figure 1.7. Schematic of the complex balance between degradative enzymes and inflammatory mediators that participate in homeostasis of collagen and proteoglycan synthesis and degradation, and can become unbalanced during OA. Complete lines and arrows represent stimulation, whereas the dashed lines and arrows represent inhibition. Arrows that point to another line demonstrate that the activity occurs within that pathway. ⊕ represents an action that occurs when the prostaglandin levels are low. ⊕ represents an action that occurs when the prostaglandin levels are high. IFN γ = interferon gamma, IGF = insulin-like growth factor, TGF β = transforming growth factor beta, IL = interleukin, TNF α = tumor necrosis factor alpha, COX-2 = cyclo-oxygenase-2, PTH = parathyroid hormone, LIF = leukemia inhibitory factor, FGF = fibroblastic growth factor, PDGF = platelet derived growth factor, EGF = epidermal growth factor, MMP = matrix metalloproteinase, TIMP = tissue inhibitor of metalloproteinase, PG = proteoglycan.

Similarly, to form proteoglycan aggregates, synthesis of aggrecan, link protein, and HA are all required. Aggrecan is synthesized as a protein core after which the KS and CS side chains are added. The sulphated core is then secreted into the pericellular matrix. Link protein is synthesized independently but usually at the same rate as aggrecan[45,46], while HA synthesis occurs separately at the plasma membrane. The G1 domain of aggrecan is not functional immediately after secretion and cannot bind HA[47]. This allows aggrecan to move from the cell and pericellular space into the interterritorial

zone (Figure 1.3)[22]. It then binds to HA via link protein at the HABR. Deep zone chondrocytes exhibit a faster rate of PG synthesis and a slower rate of PG turnover than superficial zone chondrocytes. Therefore, the net matrix accumulation is more pronounced around the deep zone than around the superficial zone chondrocytes[15].

Turnover of articular cartilage is primarily regulated by the combination of inflammatory mediators and degradative enzymes and their inhibitors. Most of the proteases are produced due to extrinsic stimuli that influence the synoviocytes and chondrocytes. Such external influences include cytokines[48], matrix components[49,50], mechanical forces[50], and hydrostatic pressure changes[51]. The primary family of enzymes responsible for turnover of articular cartilage is the matrix metalloproteinases (MMPs). MMPs are a family of greater than 20 zinc-containing, calcium-dependent endopeptidases that are produced by many different cells (Table 1.1)[52]. They are synthesized with a propeptide attached that blocks the active zinc-containing center[53]. Most MMPs are activated extracellularly by proteolytic cleavage of the propeptide, allowing the zinc atom to hydrolyze susceptible bonds in the protein substrate[54]. Once activated, these enzymes have the potential to destroy all of the matrix components of articular cartilage. There are many different types of MMPs that play a role in cartilage degradation, and their expression are both tissue specific and highly regulated[55]. MMPs are classified according to the substrate digested with tissue distribution and substrate specificity often differing between members of the same group (Table 1.1)[52].

Primary MMPs in OA include collagenase -1, -2, and -3 (MMP -1, -8, and -13), stromelysin -1 and -2 (MMP -3 and -10), gelatinases A and B (MMP -2 and -9) and membrane-type metalloproteinase 1 (MT-MMP-1 or MMP-14)[56]. The collagenases

Table 1.1. Table of known matrix metalloproteinases (MMPs) classified as collagenases, stromelysins, gelatinases, membrane-type metalloproteinases, and others. The alternative names, substrate digested, and the tissue inhibitor of metalloproteinase (TIMPs) that can inhibit each MMP are listed. Adapted from Elliott, 2001, Cawston, 1996, and Mengshol, et al., 2002.

MMP	Alternative Names	Substrates	TIMPs
Collagenases			
MMP-1	Interstitial collagenase, Collagenase-1	Collagens I, II, III, VII, VIII, X; aggrecan; gelatin; casein; link protein; α1-proteinase inhibitor; α2- macroglobulin; proTNF; proMMP-2; proMMP-9	1,-2,-3,-4
MMP-8	Neutrophil collagenase, Collagenase-2	Collagens I, II, III, V, VII, VIII, X; aggrecan; gelatin; fibronectin; α1-proteinase inhibitor; α2-antiplasmin	1,-2,-3
MMP-13	Collagenase-3	Collagens I, II, III, IV, X, XIV; aggrecan; gelatin; tenascin; plasminogen activator inhibitor -2; fibronectin; proMMP-2; proMMP-9	1,-2,-3
MMP-18	*Xenopus* collagenase	Unknown	1,-2,-3
Stromelysins			
MMP-3	Stromelysin-1	Aggrecan; collagens III, IV, IX, X, XI; gelatin; casein; fibronectin; laminin; elastin; link protein; versican; type I collagen telopeptides; α1-proteinase inhibitor; proTNF; proMMP-1; proMMP-7; proMMP-8; proMMP-9; proMMP-13	1,-2,-3,-4
MMP-10	Stromelysin-2	Collagens III, IV, V; gelatin; casein; aggrecan; link protein; fibronectin; elastin; laminin; proMMP-1; proMMP-8; proMMP-9	1,-2,-3
MMP-11	Stromelysin-3	Fibronectin; casein; laminin; proteoglycan; gelatin; α1-proteinase inhibitor	1,-2,-3
MMP-7	Matrilysin (PUMP-1)	Gelatin; casein; collagens IV, X; elastin; aggrecan; link protein; fibronectin; vitronectin; laminin; α1-proteinase inhibitor; proTNF; proMMP-1; proMMP-2; proMMP-3; proMMP-9	1,-2,-3,-4

Table 1.1. Continued.

MMP	Alternative Names	Substrates	TIMPs
Gelatinases			
MMP-2	Gelatinase A	Gelatin; collagens I, IV, V, VII, X, XI, XIV; aggrecan; link protein; fibronectin; elastin; versican; laminin; proTNF; α1-proteinase inhibitor; proMMP-9; proMMP-13	1,-2,-3,-4
MMP-9	Gelatinase B	Gelatin; collagens III, IV, V, VII, X, XIV; aggrecan; link protein; versican; elastin; fibronectin; α1-proteinase inhibitor; proTNF	1,-2,-3,-4
Membrane-type metalloproteinases			
MMP-14	MT1-MMP	Collagens I, II, III, gelatin; casein; aggrecan; fibronectin; vitronectin; laminin; elastin; proTNF; proMMP-2; proMMP-13	1,-2,-3
MMP-15	MT2-MMP	Gelatin; fibronectin; proMMP-2; tenascin; laminin	1,-2,-3
MMP-16	MT3-MMP	proMMP-2; collagens I, II, III	1,-2,-3
MMP-17	MT4-MMP	TNFα (convertase)	1,-2,-3
MMP-24	MT5-MMP	proMMP-2	1,-2,-3
MMP-25	MT6-MMP	Gelatin	1,-2,-3
Others			
MMP-12	Macrophage elastase, Metalloelastase	Elastin; collagen IV; gelatin; fibronectin; laminin; vitronectin	1,-2,-3
MMP-19		Aggrecan	1,-2,-3
MMP-20	Enamelysin	Amelogenin	1,-2,-3
MMP-21	XMMP	Unknown	1,-2,-3
MMP-22	CMMP	Gelatin; casein	1,-2,-3
MMP-23		Unknown	1,-2,-3
MMP-26	Endonetase	Gelatin	1,-2,-3

(MMP -1, -8, and -13)[57-60] as well as the membrane bound MMP-14[61] have been shown to cleave the fibrillar collagen triple helix at a specific site (Gly_{775}-Leu/Ile_{776})

approximately three fourths of the distance from the amino- terminal end of each α chain, resulting in the generation of a new three-quarter length fragment (TC^A) and one-quarter length fragment (TC^B)[57-59,61,62]. The most potent of these collagenases for type II collagen is MMP -13[59]. In addition, these collagenases can cleave aggrecan in multiple locations so that aggrecan is freed from its attachment with HA allowing it to diffuse out of the matrix. The major cleavage site is in the interglobular domain at Asn341 and Phe374 (Figure 1.5)[63]. Another important group of MMPs are the stromelysins (MMP-3, and -10) because they can degrade aggrecan, participate in collagen denaturation, and activate other MMPs[64-67]. The gelatinases (MMP -2 and -9) are primarily responsible for the denaturation (unwinding) of the triple helix of fibrillar collagens following collagenase cleavage, as well as some cleavage of aggrecan[68]. During homeostasis, these MMPs are carefully controlled by endogenous inhibitors, such as α2-macroglobulin, or a family of four tissue inhibitors of metalloproteinases (TIMPs) (Table 1.1)[52]. They are released from the synoviocytes and chondrocytes and form an irreversible, non-covalent 1:1 complex to prevent activation of proenzymes as well as blocking the action of previously activated MMPs[69,70].

Another important group of enzymes in matrix degradation are the aggrecanases. They are a sub-family of the ADAM (a disintegrin and metalloproteinase) family in that they lack a transmembrane domain and possess thrombospondin-like sequences. These aggrecanase enzymes are therefore classified as ADAM-TS 4 and 5[52]. Aggrecanases cleave aggrecan in multiple locations but the major cleavage site is at Glu373 and Ala374 in the interglobular domain (Figure 1.5)[71]. The actions of MMPs and aggrecanases appear to be by completely different processes with similar net effects. In addition, other

proteinases involved in matrix degradation include aspartic and cysteine proteinases. These are intracellular proteinases that are also released from synoviocytes and chondrocytes and degrade collagen and proteoglycans[56]. Serine proteinases, such as plasmin and plasminogen activators (tissue and urokinase) also play a major role in activation of the MMPs[53]. A general inhibitor of all of these proteinases (serine and MMPs) is α2-macroglobulin[72].

Cytokines are peptide regulatory factors that bind to cell surface receptors and stimulate the cell to undergo a cascade of intracellular events, often influencing cellular replication[73]. Cytokines include interleukins, interferons, growth factors, and other mediators[48]. Probably the most important pro-inflammatory cytokines with respect to articular cartilage turnover are interleukins 1 α and β (IL-1 α and β) and tumor necrosis factor α (TNF α). The major cellular source of interleukin-1 is the macrophage/monocyte system[74], as well as fibroblasts, chondrocytes[75], and osteocytes. The action of IL-1 on cells is mediated by two types of receptors (IL-1R)[76], that bind the α and β forms with different affinities[74]. Once IL-1 binds to these receptors, it stimulates the chondrocytes to produce more IL-1[77]. A natural inhibitor, called the interleukin receptor antagonist protein (IRAP), prevents IL-1 from binding to the receptor[78]. IL-1 causes degradation of the cartilage matrix by stimulating collagenase, stromelysin, and prostaglandins (Figure 1.7)[74,77]. It also increases the release of aggrecan via aggrecanase stimulation[79], as well as directly decreasing aggrecan and type II collagen synthesis[80,81]. Tumor necrosis factor is produced by the same cellular sources as IL-1. There are also two cell-surface receptors (TNF-R) for TNF α[82]. The number of these receptors on the cells is variable and depends on stimuli received by the cell. The presence of TNF α

bound to the receptor will actually induce receptor degradation and the cell will become refractory to further stimulation[74]. This proteolytic cleavage of the receptors produces TNF-R-derived proteins, which act as natural TNF inhibitors[83]. Just like IL-1, TNF α stimulates cartilage degradation via increasing collagenase, stromelysin, and prostaglandin synthesis (Figure 1.7).

As opposed to IL-1 and TNF α, there are also naturally occurring anti-inflammatory cytokines that actually have a protective role in cartilage (Figure 1.7). IL-10 inhibits synthesis of IL-1 and TNFα[84]. IL-6 is released by many cells, including chondrocytes[85], mostly in response to IL-1, and TNF α, and it can actually up-regulate IL-1 and TNFα production[73,86]. IL-6 does not induce MMP production, and in fact, increases expression of TIMPs[87,88]. Similarly, IL-4 and IL-11 enhance TIMP-1 production[84]. The production of another member of the IL-6 family, leukemia inhibitory factor (LIF) is stimulated by IL-1, TNFα, and IL-6[84]. It also enhances TIMP-1 production, but decreases proteoglycan synthesis while increasing proteoglycan degradation[84].

Various growth factors play a role in homeostasis, including insulin-like growth factor (IGF), transforming growth factor (TGF), fibroblast growth factor (FGF), platelet derived growth factor (PDGF), and epidermal growth factor (EGF) (Figure 1.7). IGF has two functionally distinct types (I and II)[89], that stimulate chondrocytes to produce type II collagen and proteoglycans[90]. TGF has three isoforms (β1, β2, β3). They inhibit the IL-1 effects on chondrocytes due to prostaglandins. They stimulate ECM production by chondrocytes by increasing proteoglycan synthesis and decreasing proteoglycan degradation, as well as increasing synthesis and secretion of TIMP[91]. FGF enhances IL-1

mediated prostaglandin and proteinase release[92]. PDGF is capable of stimulating MMP-13 as well as PTH[93], and EGF similarly stimulates collagenase synthesis and induces cyclo-oxygenase-2 (COX-2) expression[94].

During the process of homeostasis of articular cartilage, as well as bone, all of the above pathways are used to varying degrees to maintain a functional tissue that can withstand the normal loads applied. Each act as a check and balance on the other. For example, IL-1 and TNF α will stimulate MMP production and therefore, cartilage breakdown. However, the amount of degradation is held in check by IL-6, IL-4, and the TIMPs. Based on this oversimplified example, it is easy to see that if one or more of the cytokines or proteases starts to become over produced, or if there is a lack of TIMP synthesis, then the scales will no longer be balanced, allowing degradation to predominate over synthesis. This is what occurs during the process of osteoarthritis.

1.4.4 CrCL transection as a model for osteoarthritis.

Canine CrCL transection models of OA have been developed because of the difficulties in obtaining human cartilage and the need to study the early and sequential events of OA[95]. Use of the CrCL transection model in the dog has demonstrated that the OA changes that develop are mostly due to altered joint mechanics and not due to the inflammation associated with the surgery itself. This has been demonstrated by immobilizing the operated limbs of dogs immediately after transection and identifying cartilage atrophy without any evidence of OA changes[96]. In addition, control of hemostasis during CrCL transection did not lessen the OA changes compared to those without any hemostasis, indicating that the mechanical changes are of greater importance that the synovial inflammation[97]. Overall, it has been a viable model of human OA, by

showing typical progressive OA changes[98], including full thickness cartilage ulceration[1], and subchondral plate sclerosis[99].

One of the earliest reports was by Marshall[100], and then Pond and Nuki popularized the stab technique[101]. The three main approaches used for surgical transection of the cruciate ligament have included the percutaneous stab[101-117], arthrotomy (medial or lateral)[1,96-100,104,118-128], and arthroscopic techniques[129-132]. No differences have been noted between these procedures with regards to the pathological, ultrastructural and biochemical OA changes produced[104,130,131,133]. The arthroscopic technique has been the least used of the procedures, and in those studies where it has been applied, it is poorly described. Therefore, a consistent arthroscopic technique for CrCL transection was developed in this study and will be described.

Most of the studies utilizing this model of OA have used a heterogeneous population of dogs, (mixed breed[96,104,107,108,110-114,118,121], mongrels[1,98,99,105,123-127,129,130], or a mixture of different breeds[100,102,107,117,119,120,134]) whereas fewer studies have used one specific breed (Beagles[103,106,116,132], American Foxhounds[122,128], and Greyhounds[115]). The dogs have generally been adults, ranging in age from the time of epiphyseal closure (~1.5 years) up to 8 years of age, and their weight has ranged from 6.8 to 40 kg, with most being between 12 and 30 kg. Most dogs have been kept in cages/pens[96,99,100,104,105,108,110,113,116-121,123,132], or runs[1,98,102,122,124-127,129,130] whereas only a few studies have utilized more controlled exercise regimens[106,107,111,112,114,115].

Historically, the canine CrCL transection model has been used to determine the earliest osteoarthritic changes that occur to the intra-articular components, especially articular cartilage, after CrCL transection[95,102,106,107,120], as well as characterizing the

sequence of events that occur up to 54 months after transection[1,98,99,103,105,120,128]. Most of these studies have looked at many different time points to identify the early changes that occur after CrCL transection, averaging less than 5 dogs (often 1-2 dogs) per interval[1,98,99,102,103,105-107,118-120,125-130,134]. Many have described histological changes in articular cartilage that occur prior to macroscopic evidence of cartilage fibrillation, including increased surface proteoglycan loss[96,100,101,107], hypercellularity of chondrocytes in the middle and deep zones[107,118,121], and hypertrophy of the articular cartilage[102,118,121,135,136] that varies in degree depending upon the area of the joint examined[128]. This hypertrophy of articular cartilage has been shown to persist for 3 years after CrCL transection[98,99,137,138], and may be due to hyperhydration and an increase in the concentration of proteoglycans due to increased synthesis that occurs within days after CrCL transection[102,137]. These processes likely results in increased interfibrillar spacing of collagen fibrils[106]. These results suggest that repair of articular cartilage attempts to keep pace with articular cartilage breakdown, but that this repair tissue can't hold up to mechanical stresses as well as the original cartilage and eventually degradation of the matrix occurs to a level that is equivalent to end-stage OA in humans[139].

The rate of progression, location, and severity of lesions, however, has varied tremendously when using this model of OA. It has been hypothesized that the differences in the lesions generated were most likely due to the differences in the breed, age, weight, surgical technique used to sever the CrCL, and the amount of exercise the dog required post-transection[140]. For example, Marshall described non-progressive lesions when dogs were followed out to 2 years[119], whereas, Vignon, et al. noted progressive cartilage fibrillation out to 8 months[120]. In addition, there has been no consensus as to where

articular cartilage is most damaged, with some reporting that it is more severe on the tibia[102] and others on the femur[98,104], with large differences in the amount, timing, and degree of meniscal damage[102,118,119]. Therefore, although the use of this model has been advantageous in identifying the early and sequential changes after CrCL transection, it appears to have a large degree of variability. To make matters worse, as previously noted, many of these studies used a small number of dogs per interval studied (usually 1-2 dogs)[110-115,123,124,141], making extrapolations to humans with OA more difficult. By using a larger group of dogs, this study will attempt to analyze this variability.

1.4.4.1 CrCL associated meniscal injuries. Once the CrCL is naturally and completely ruptured or experimentally transected, unrestrained cranial tibial thrust occurs that creates craniotibial translation with respect to the femur (cranial draw)[142]. In addition, an increased amount of internal rotation of the tibia with respect to the femur results when the limb is in flexion, but not in extension[6]. The combination of increased internal rotation and cranial tibial translation make it likely that meniscal damage will result[143]. Isolated meniscal lesions without concurrent cruciate ligament injury do occur in dogs, but are rare, and can be from sudden compressive forces acting directly on the meniscus such as would occur from a jump with the stifle extended[8].

Since the lateral meniscus is more mobile, making it less likely to get caught between the femur and tibia, it rarely gets injured unless multiple ligaments are damaged[144]. The incidence of medial meniscal injury, post-CrCL rupture in the naturally occurring disease process, is reported to be from 48 to 80%[14,143,145-155]. The types of meniscal injury have been well described in dogs[14,149], and usually involve the caudal horn of the medial meniscus, which is similar to the human condition, where the posterior

region of the meniscus is subjected to the highest compressive load[156]. The location of the tear, combined with the cranial tibial thrust allows the torn portion of the meniscus to slide between the femur and the tibia. This abnormal impingement of the meniscal tissue will presumably cause the dog to have an acute exacerbation of its lameness[10,143,151]. Meniscal injury has been reported to be present as early as 2 weeks after CrCL transection[157], suggesting that the longer the stifle is unstable, the greater the incidence of meniscal injuries. However, no correlation between the incidence of meniscal injury and the duration of CrCL deficiency has been identified[146]. In addition, no real explanation exists as to why all dogs don't sustain meniscal damage following CrCL rupture or transection. Therefore, the temporal pattern and variability of the meniscal damage that occurs after CrCL rupture is poorly defined. We will attempt to describe the temporal pattern and variability of meniscal damage in our study using serial arthroscopic examinations after CrCL transection.

1.4.4.2 Etiopathogenesis of OA after CrCL rupture. The etiopathogenesis of osteoarthritis in the dog is a complex, dynamic process that involves the interaction of the subchondral bone, synovium, synovial fluid, and articular cartilage, and is therefore referred to as an organ system failure[139]. This means that there is no one decisive initiating pathway, and regardless of the cause, the end-product that is recognized as OA is indistinguishable[158]. Historically, this end-product has been characterized by focal erosion and ulceration of articular cartilage, sclerosis of subchondral bone, marginal osteophytes, enthesiophytes, as well as variable inflammation and hyperplasia of the synovial membrane[1].

Regardless of the cause, often the main early response of the joint is due to an inflammatory reaction to the joint insult. This results in extensive synovial infiltration with mononuclear cells and lymphoid aggregates resulting in hyperplasia of the synovial lining and eventual capsular fibrosis[1,159]. During this inflammatory process, vascular leakage causes a greater amount of diffusion of water and solutes into the synovial fluid than the clearance of synovial fluid through the lymphatic system. The net result of this is synovial membrane edema, effusion and leakage of protein into the synovial fluid[31]. Effusion of the joint has many important effects such as creating a local ischemia in the synovial membrane as well as ischemic-like conditions in the articular cartilage since the synovial fluid is the primary supplier of nutrients and oxygen to the articular cartilage, as well as the key depository of its waste products for subsequent removal from the joint[160].

During this inflammatory process, IL-1 and TNF α have been presumed to be the prime candidates for mediating the catabolic processes occurring in the articular cartilage. Even though the absolute concentrations of the cytokines may be high in the synovial fluid, this does not necessarily represent the activity level of these molecules, due to the consistent presence of their natural inhibitors, including soluble cell surface receptors. The cytokines ultimately cause increased production and release of MMPs from invading inflammatory cells[161], synovial fibroblasts[162], and chondrocytes[163]. These proteinases are initially released as latent proenzymes, but are often rapidly activated by other MMPs or proteinases. The levels of the endogenous inhibitors of MMPs, TIMPs, are often increased as well, most likely due to anti-inflammatory cytokines such as IL-6 and -4 (Figure 1.7). However, there usually exists a molar excess of MMPs compared to TIMPs in inflammation[164]. Presumably, during this period, growth factors, such as TGF-β and

IGF attempt to stimulate the chondrocytes for increased synthesis of the matrix components as well[165]. This anabolic response attempts to keep pace with the degradative processes, but often the net stimulatory effect is not enough to be able to counteract the degradation that ensues.

The earliest identified changes that occur in articular cartilage are due to this biochemical cascade of events. There is an initial increase in hydration[107], along with an increase in total proteoglycan content[136]. The net result of this is an increase in cartilage thickness (hypertrophy)[136]. Chondrocyte activity is also markedly upregulated for type II collagen synthesis in the early phases of OA[117,166]. However, this upregulation of proteoglycan and type II collagen synthesis is not uniform throughout the entire matrix. The superficial layer of cartilage is the first area depleted of proteoglycans and collagen, suggesting that the increase in synthesis may be insufficient for protection of the superficial layer[117,167,168]. In addition, the newly synthesized proteoglycans may actually be altered, in that the size of the aggrecan molecules is smaller than normal and the ratio of CS to KS increases[107]. As the disease progresses, there is a large amount of heterogeneity in the degree and extent of damage despite no apparent differences in the ultimate histologic, biochemical and metabolic changes to articular cartilage[1]. Often, the disease process progresses to full-thickness cartilage erosions.

The response of bone is usually what is used to ultimately identify the presence of OA, by radiographically identifying the presence of osteophytes or narrowed joint space. Osteophytes usually form at the marginal surface of the joints when gross instability is present. However, the factors that determine the extent to which the osteophytes develop is not clear, and may include cytokines and growth factors, such as TGF-β[169], and IGF[170].

These systemic factors may play a role in osteophyte formation for joints in which there has been no evidence of instability. Enthesiophytes will also form at the sites of attachment of tendons and ligaments in response to gross instability due to increased stresses placed on the intact tendons and ligaments to maintain stability[95,171]. Over time, subchondral bone sclerosis will become radiographically evident in osteoarthritis as well[171]. Whether this is the cause of cartilage degradation or is a reaction to cartilage degradation is debatable. It has been suggested that the switch from compensated repair of articular cartilage to progressive loss may be associated with the stiffening and thickening of the subchondral bone plate[1,99]. However, quite often, changes in the bone are not radiographically evident at the time of the first visible cartilage lesions. Regardless, when there is a difference in stiffness of the subchondral bone plate, shear stress is placed on the overlying articular cartilage, potentiating degradation[172].

1.4.5 Diagnosis of OA after CrCL rupture.

1.4.5.1 Clinical analysis. Physical examination for CrCL injury includes the combination of careful palpation along with identification of lameness at a walk and/or trot. Palpation is generally performed on both hind limbs simultaneously to identify muscle atrophy, pain, joint swelling, or other asymmetries. In general the CrCL deficient dog will have atrophy of the quadriceps muscles and a medial buttress in the region of the medial collateral ligament[7,173]. This medial buttress is a firm swelling in this region that can develop within hours of CrCL rupture, and some feel that the presence of this medial buttress is almost pathognomonic for CrCL rupture[173]. Manipulation of the limb to identify an increase in the range of motion can also help diagnose CrCL rupture, since the limb becomes more unstable. However, over time, the

range of motion may actually decrease as a result of the secondary OA changes that have developed[7].

Specific diagnostic tests can also be performed that generally require further manipulation of the limb to test for joint laxity. The cranial drawer test has been the hallmark diagnostic exam used for determining cruciate ligament instability. The goal of the examination is to see if the tibia can be moved cranially or caudally with respect to the femur. Any degree of positive drawer movement (cranial or caudal) indicates likely injury to the cruciate ligament. A positive cranial drawer sign is diagnostic for CrCL rupture, but the absence of cranial drawer does not rule out CrCL rupture because the dog may stabilize the joint by contracting the surrounding musculature[7]. In addition, a tibial compression test can be used to diagnose CrCL rupture by identifying the presence of tibial thrust. In this test, one finger is placed over the patellar tendon to the tibia crest. The hock is then flexed until tension of the common calcanean tendon is achieved. If the CrCL is ruptured, the tensed gastrocnemius muscle pushes the tibia forward in relation to the femur[7,173]. The tibial compression test is easier to perform in large dogs, but can also result in false negatives when there is a great amount of periarticular fibrosis present[7]. In addition, arthrocentesis can be used as a diagnostic technique. It can be used to collect synovial fluid for further analysis, or as a means for injection of a local anesthetic for elimination of lameness. Synovial fluid analysis can help distinguish between acute and chronic inflammation, as well as ruling out septic or immune-mediated processes[7].

1.4.5.2 Arthroscopy. Arthroscopy has been shown to be a valuable and reliable tool for identifying CrCL rupture as well as grading osteoarthritic changes in the dog[174-179]. It is considered a minimally invasive technique that causes much less trauma

and inflammation of the joint when compared to an arthrotomy and allows early detection of intra-articular pathology[177,179]. In addition, arthroscopy has been shown to be an accurate method of diagnosing stifle injury with a reported 83-99% correlation with arthrotomy[174-176]. As compared to gross necropsy and arthrotomy findings, arthroscopy provides more detailed information about the morphological changes that occur within the joint[174,177,180]. For example, arthroscopy is more sensitive than arthrotomy when examining cartilage fibrillation, because of the magnification and fluid flow through the joint[174]. Therefore, arthroscopy has the potential to be able to diagnose early irreversible articular cartilage damage that cannot be identified during arthrotomy, providing more accurate assessment of the stage of OA present within a CrCL deficient joint.

Arthroscopy has usually been used to examine the CrCL deficient stifle at one given time point after transection to compare the arthroscopic findings to the arthrotomy and gross findings[174]. Only one study in dogs has used serial arthroscopic examinations of CrCL deficient joints to determine the long term intra-articular changes[157], and the identification of the temporal patterns of intra-articular changes that occurred after CrCL transection were poorly defined. Therefore, we will attempt to determine the temporal pattern and severity of changes that occur in the acute period after CrCL transection by serially examining 3 dogs after CrCL transection. Description of these changes should be beneficial to the clinician with regards to understanding the progression of events that occur in the unstabilized joint. In addition, it has the potential to help explain changes that could be identified by biomarker and force plate analyses.

1.4.5.3 Imaging. Ancillary diagnostic techniques that can be used to identify the cause of hind limb lameness include survey radiographs, stress radiography

of an affected joint, nuclear scintigraphy, magnetic resonance imaging and computerized tomography[173]. In general, lateral and cranial-caudal radiographs of the stifle aid in the diagnosis of CrCL rupture by ruling out many bone and soft tissue abnormalities[7]. Radiography is not essential in diagnosis of CrCL rupture, and in fact, Roush reports that radiographs are neither necessary nor useful in diagnosing CrCL rupture[173]. However, radiographs are most useful in documenting the degree of secondary OA that has developed, providing a baseline for the amount of OA changes present. This allows for comparative follow-up radiographs to determine the progression of the OA process. Radiographic assessment of OA in humans is usually performed by determining the degree of articular cartilage damage (joint space narrowing) and osteophyte formation. However, for joint space measurements to be accurate, the patient should be weight bearing, which is impractical in the dog[171]. In addition, it should be noted, that even though articular cartilage damage and the presence of osteophytes are induced by the same factor (instability in the CrCL transection model), they develop independently[100,181-183]. In general, the radiographic findings after CrCL rupture in the dog vary based on the chronicity. In the acute stage, the radiographic signs are indicative of synovial effusion and a decrease in the dimension of the fat pad that will further diminish over time, while the number and size of osteophytes increase over time[171]. Periarticular osteophytes are generally first identified on the medial and lateral femoral trochlear ridges and the distal edge of the patella, and then later occur around the femoral and tibial condyles[119].

Stifle ultrasound as well as magnetic resonance (MR) imaging of the stifle could be useful in diagnosing CrCL rupture, but are limited due to availability and expertise[173]. MR has become the diagnostic imaging technique of choice for human knee disorders[184].

It is a noninvasive technique that allows for imaging of the cruciate ligaments, menisci, and articular cartilage in any plane. In humans, it has a 95% correlation with arthroscopic findings with respect to evaluation of the cruciate ligaments[185]. MR has proven useful in a research setting when examining the cartilaginous defects, as well as the generalized soft tissue changes that occur in the long standing CrCL deficient stifle[138,171,186]. In addition, nuclear scintigraphy and computed tomography have both been used in the experimental CrCL model to determine the degree of changes that occur in the underlying bone[99,187-189]. Use of MR imaging, nuclear scintigraphy, and computed tomography has been mostly limited due to its low availability and high cost compared to other diagnostic modalities for CrCL rupture. They are not needed to diagnose the majority of CrCL injuries of dogs, but in complicated cases they all have the potential to determine the degree of damage present in all tissues of the joint.

1.4.5.4 Force plate analysis. Kinesiology is the study of motion, and it is divided into two major categories, kinematics and kinetics. Kinematics is the description of movement with regard to its temporal and geometric characteristics, irrespective of the forces applied, whereas kinetics is the study of the relationship of movement to the forces that produce, modify, or stop motion[190,191]. Force plate analysis is the main example of kinetic analysis of movement performed by recording the ground reaction forces of a limb or pair of limbs as the subject steps on and across a specialized plate. It has become one of the most productive objective measurements of limb movement and pain response in human and veterinary medicine, and is often combined with 2- or 3-dimensional kinematic analysis. This kinematic analysis is commonly performed by placing targets on a subject such that when the subject moves in a calibrated space, their movement can

be tracked and analyzed by a computer. Traditionally, motion has been analyzed subjectively by trained observers, to identify differences from normal in movement as a result of injury. When compared to subjective analysis of a dysfunctional gait, kinesiology removes bias based on human observation, as well as providing improved accuracy and data collection capability[191]. However, no single method of gait analysis can evaluate every parameter of locomotion[190].

In general, force plates record the magnitude, direction, duration, and position of the applied forces based on acceleration or resistance of the object being placed on the force plate[190]. The force plate measures 3 orthogonal ground reaction forces, vertical, craniocaudal, and mediolateral, that result from limb placement during the gait cycle (Figure 1.8). These forces only represent the summation of limb function via forces transmitted through that limb to the ground, and are therefore, not joint-specific[191]. Peak vertical force and vertical impulse are the best measures of normal and pathologic gait because they have the greatest magnitude and most directly measure weight-bearing[192,193]. Impulses are the measure of force over time (force applied throughout the stance phase). Craniocaudal forces represent limb forces that affect forward progression

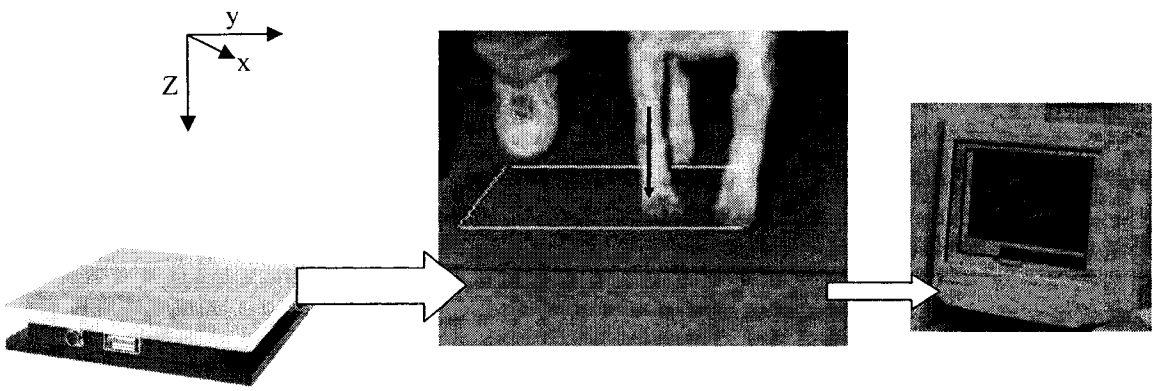

Figure 1.8. Photograph of the force plate (left) with the representative forces that can be measured. The force in the Z direction (peak vertical force) represents the amount of force applied to the plate when the dog bears weight on the limb, as it crosses the plate (outlined in the center). This force and respective contact area can be examined and analyzed via software on the computer (right).

with the stance phase being divided into braking (deceleration) and propulsion (acceleration). Braking is the impulse needed to decrease the dogs' momentum in the early stance phase, and propulsion is the increase in momentum in the late stance phase, allowing the dog to be able to push off with its foot. The forelimbs have been shown to be mostly responsible for braking and the hindlimbs for propulsion of the entire dog[192]. Mediolateral forces represent a very small portion of the dog's body weight (< 6%) and therefore have the largest variation[192].

Budsberg, et al. demonstrated that for a controlled study, dogs should have a homogeneous morphology, since the peak vertical force and impulse are inversely correlated with physical size, and the duration of stance phase (braking and propulsion forces) increases with increased physical size[192]. Limb speed also affects the ground reaction forces in a predictable manner[194-196], such that the peak vertical hind limb force increases and the respective impulse decreases with increasing dog velocity[196]. In fact, a variation of as little as 0.3 m/s in velocity can significantly affect the ground reaction forces[196]. Force plate analyses cannot test for specific pathologies or measure successive events during locomotion unless more than one plate is utilized. This means that multiple passes over the force plate are required to collect a representative data sample. This trial repetition as well as individual dog variation account for a relatively large percentage of the total variance in force plate measurements. Jevens, et al. demonstrated that the percentage of the total variance accounted for by trial repetition was 29-85% whereas individual dog variation accounted for 14-69%[197]. Part of these difference could be accounted for by the fact that most force plates have decreased sensitivity at the edges,

making it necessary to strike the center of the plate for the most accurate results[190]. Jevens, et al. also noted that the number of experienced handlers used to collect the force plate data on dogs resulted in only 0-7% of the percentage of total variance[197]. Therefore, the number of dogs used in a study, as well as the trial repetitions, are more important then minimizing the number of handlers.

When examining CrCL deficient dogs, the peak vertical force and impulse, as well as the braking and propulsion impulses are significantly reduced[198-201]. Force plate analyses demonstrate that without surgical treatment, these CrCL deficient dogs show a severe drop in the ground reaction forces followed by a gradual increase that plateaus by about 10 months after CrCL rupture[198-201]. Budsberg showed that when these dogs are followed out 3 years after CrCL transection, the ground reaction force remained at this level, and did not return to normal pre-transection levels[202]. In addition, force plate analysis has been shown to be sensitive enough to detect the improvement in ground reaction forces, back to normal pre-injury levels, within 5-6 months of surgical repair for CrCL rupture[198,199]. However, force plate analysis does not have the capability to demonstrate differences in OA development since it has been shown that OA progresses after CrCL rupture in spite of the surgical technique used[155]. In this study, we will use the force plate analysis as an objective measure of the lameness that occurs after CrCL transection and that could be related to inflammation or potential meniscal damage.

1.4.5.5 Biomarker analysis. Biomarkers of joint tissue metabolism are molecules that are derived directly or indirectly from turnover of articular cartilage, bone, or synovium. Biomarkers can be used to provide information about the synthesis and degradation of specific molecules in the early phase of clinical

trials, allowing for the early diagnosis of disease with the potential to determine the eventual prognosis, and for monitoring or predicting the response of a specific therapeutic agent[203]. In this study we will use biomarkers to monitor the tissue response to our therapeutic agent as well as attempt to diagnose early pathology. The ideal biomarker of OA would be one that identifies either synthesis or degradation of a specific tissue, by easily obtaining fluid in which the biomarker is measurable with its levels correlating to the pathological changes of OA. However, to date, there is no such biomarker available, but many candidates exist (Table 1.2).

Table 1.2. Table of biomarkers that can be identified by either enzyme immunoassay (EIA) or colorimetric assay in the dog, based upon the tissue of interest, as well as the metabolic stage of interest (Syn = synthesis, Deg = degradation). Companies are listed if commercial kits exist.

Tissue	*Biomarker*	*Syn or Deg*	*Type of Assay*	*Name of Assay*	*Company*
Cartilage	C-propeptide of type II procollagen	Syn	EIA	CPII	IBEX Tech.
	Chondroitin sulfate (CS) epitope 846	Syn	EIA	CS-846	IBEX Tech.
	Cleaved type II collagen (234CEQ)	Deg	EIA	234CEQ	None
	Sulfated glycosaminoglycans (sGAG)	Deg	Colorimetric	DMMB	None
	Keratan sulfate (KS) epitopes	Deg	EIA	5D4	None
		Deg	EIA	7D4	None
	Cartilage oligomeric matrix protein (COMP)	Deg	EIA	None	None

Table 1.2. Continued Tissue	Biomarker	Syn or Deg	Type of Assay	Name of Assay	Company
Bone	Bone-specific alkaline phosphatase (BAP)	Syn	EIA	Metra™ BAP	Quidel Corp.
	Osteocalcin (OC)	Syn	EIA	BTI Intact Human Osteocalcin	Biomedical Technologies Inc. (BTI)
	Cleaved type I and II collagen ($COL2\text{-}3/4C_{short}$)	Deg	EIA	None	None
	C-telopeptide of type I collagen (CTx)	Deg	EIA	Serum CrossLaps	Nordic Bioscience A/S
	Deoxypyridinoline crosslinks (DPD)	Deg	EIA	Metra™ DPD (urine)	Quidel Corp.
		Deg	EIA	Metra™ Total DPD (serum/urine)	Quidel Corp.
	Pyridinium crosslinks (PYD and DPD)	Deg	EIA	Metra™ PYD (urine)	Quidel Corp.
	Pyridinoline (PYD)	Deg	EIA	Metra™ Serum PYD (serum)	Quidel Corp.
Synovium	Hyaluronic acid (HA)	Syn	Colorimetric	Alcian Blue analysis	None
	COMP	Syn	EIA	None	None
	Eicosanoids	Deg	EIA	Correlate-EIA	Assay Designs, Inc.
	Cytokines IL-1β, TNFα, IL-6	Deg	EIA	Correlate-EIA	Assay Designs, Inc.

Most of the biomarkers of OA can be identified in the synovial fluid, serum, or urine depending upon the stability of the analyte. In general, when examining a single joint, the synovial fluid is the most valuable fluid to obtain due to its proximity to the articular cartilage and synovium combined with the long half life of most markers in this fluid. This makes it more likely to identify the majority of fragments that diffuse out of cartilage prior to the further processing that occurs in the lymphatic system or in the liver and kidney after they reach the blood[204]. Therefore, joint disease related changes to the biomarkers and their levels should be easier to assess. However, in the dog, synovial fluid is harder to collect than blood due to its low volume, requirement for sedation, and the concentration of the marker is dependent on the clearance rate of the joint that changes with inflammation[205]. Collection of blood is best for systemic musculoskeletal disease, not for disease of a single joint, since the cartilage marker of interest gets diluted and is combined with similar biomarkers from all of the cartilaginous tissues of the body (Figure 1.9). Therefore, blood levels of a specific marker from an OA joint won't change unless the damage is pronounced and rapid[203]. In addition, biomarker levels in the blood and urine are affected by further processing in the liver and kidney. In fact, some markers are present in normal serum at concentrations below the limit of detection of available assays, such as deoxypyridinoline collagen cross-links which are excreted in urine in a concentrated form. Collection of urine in the dog, however, is not easy, and offers no real advantage for those markers that can be examined in the synovial fluid and blood. The general approach of most OA studies is to ideally collect synovial fluid, if possible, but to also collect serum, especially if a lavage technique was used to collect the synovial fluid[206].

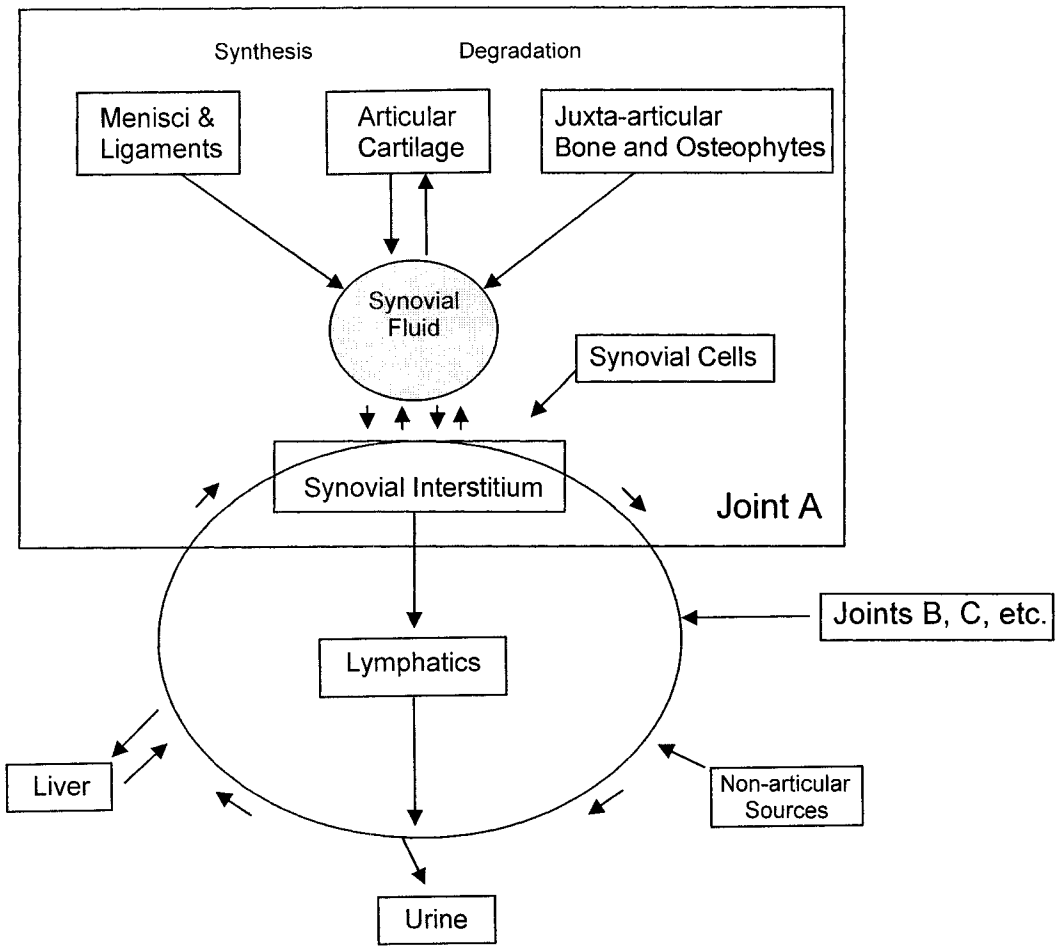

Figure 1.9. Schematic representation of the relationship between the biomarker concentrations in the synovial fluid from Joint A, the blood, and the urine. The concentrations of a biomarker in the single joint depend upon the rates of synthesis and degradation, as well as the clearance from the joint. Biomarkers in the serum are influenced by contributions from other joints (Joints B, C, etc.), as well as by metabolism in the liver and clearance by the kidney. Adapted from Lohmander, et al. 1997, Simkin, 95, and Myers, 1999.

Most of the biomarkers examined in the dog with either naturally-occurring or experimental transection of the CrCL have focused on proteoglycan metabolism in the synovial fluid and/or serum[207-219]. These include analyses of sulfated glycosaminoglycans (sGAG)[208,212-216], keratan sulphate epitopes (5-D-4, 7-D-4)[207-209,211-216] and chondroitin sulphate epitopes (3-B-3, 846)[208,211,214-216,219]. In addition, HA has been examined in this model in the serum and synovial fluid[220,221]. Very few studies have examined markers of type II collagen cleavage[219] or bone formation (osteocalcin)[217]. Therefore, considering

the acceptance and long term use of this model of OA, there is plenty of potential to examine many more biomarkers in the serum and synovial fluid of dogs after CrCL transection. This study will examine biomarkers of inflammation (prostaglandin E_2– PGE_2), type II collagen synthesis (carboxy-propeptide of type II collagen – CPII)[222], type II or type I and II collagen degradation by collagenase cleavage (234CEQ neoepitopes and COL2-3/4C_{short}, respectively)[62,223], proteoglycan turnover (sulfated glycosaminoglycans – sGAG)[224], and bone formation markers (bone alkaline phosphatase – BAP, and osteocalcin – OC) before and after CrCL transection.

1.4.6 Synthetic MMP inhibitors.

The action of most currently available treatment for OA is directed toward control of pain and/or inflammation associated with synovitis, but does little to reduce joint destruction. Since MMPs have been determined to be a primary factor in cartilage degeneration, they have been identified as a potential component of the OA process that could be inhibited to prevent or limit actual structural breakdown of articular cartilage. MMPs can be controlled at a number of points, including during the stimulation of expression and production of proMMPs (i.e. cytokine inhibitors), during the activation of proMMPs (i.e. proteinases and TIMPs), and by inhibiting activated MMPs (i.e. α2-macroglobulin or TIMPs)[56]. Corticosteroids are a commonly used therapeutic in OA that can block MMP gene expression by binding directly to DNA or transcription factors[225], but are not specific for MMPs. Synthetic inhibitors of MMPs, on the other hand, have been designed to block the MMP activity at the protein level with a variable degree of specificity towards MMP type.

Many different types of inhibitors have been designed to counteract the action of MMPs in cancer and OA (Table 1.3)[226]. The initial inhibitors had a zinc chelating ligand attached to a peptide that mimicked the cleavage site of the MMPs in the target substrate, blocking the action of the MMP on the substrate[56]. Many of these first inhibitors had low oral bioavailability and were broad-spectrum. They were replaced by second generation inhibitors that were based on the 3-dimensional structure of specific MMPs identified by X-ray crystallography[227]. Since it has been suggested, through the use of genetically engineered mice,[228] that loss of a single MMP family member is not sufficient to prevent OA, these inhibitors are generally broad spectrum. The second-generation inhibitors have better specificity to certain groups of MMPs (stromelysins or collagenases). In addition, these inhibitors have the potential to be more potent, with good bioavailability such that they can reach the articular cartilage at therapeutic concentrations with minimal side effects[56]. However, one of the greatest hurdles for any drug is its capability to penetrate the dense, highly charged matrix of the articular cartilage[229]. In fact, the therapeutic benefits of MMP inhibitors in both OA and RA have yet to be seen[227,230] with MMP inhibitors being used mostly to evaluate the importance of various MMPs via *in vitro* cartilage explant systems[60,223,231-236].

Tanomastat (BAY 12-9566) is a non-peptidic biphenyl second generation MMP inhibitor with a zinc-binding carboxyl group (Figure 1.10)[237]. It is a broad-spectrum inhibitor that selectively targets MMP-3, -2, -9, and -14, and is less inhibitory to the collagenases (MMP -1, -8, and -13). It inhibits metastasis and angiogenesis in cancer patients[238] and halts or slows the progression of OA[239,240]. It has good oral bioavailability at multiple doses, with good penetration into the synovial fluid and

Table 1.3. Table of MMP inhibitors described in the literature for use on cancer or OA. Known inhibitory constants (IC_{50}) are listed for MMP -1, -2, -3, -7, -8, -9, -12, -13, - and -14. If the drug reached a clinical trial, the highest testing phase is listed. RA = rheumatoid arthritis, IBD = inflammatory bowel disease.

			MMP IC_{50} (nM)									
Compound	***Company***	***Use***	***MMP-1***	***MMP-2***	***MMP-3***	***MMP-7***	***MMP-8***	***MMP-9***	***MMP-12***	***MMP-13***	***MMP-14***	***Clinical Trial***
Marimastat	British Biotech	Cancer	5	6	200	20	2	3		2		III Cancer
Prinomastat (AG3340)	Agouran	Cancer, macular degeneration	8.3	0.08	0.27	54		0.26		0.04		III Cancer II Macular degeneration
BMS-275291 (D 2163)	Bristol-Myers Squibb & Celltech Chiroscience	Cancer	25	41	157		10	25		4		III Cancer
Metastat	CollaGenex	Cancer										
Neovastat	Aeterna	Cancer										III Cancer
Solmastat	British Biotech	Cancer, multiple sclerosis	10	80	30	5		70				I Cancer
CGS 27023A	Novartis	Cancer, OA, *in vitro* cartilage	33	20	43			8	7.7	1.9		Cancer (suspended)
Tanomastat (BAY 12-9566)	Bayer	Cancer, OA, *in vitro* cartilage	>5000	11	134		2200	301		66000	414	III Cancer (withdrawn) II OA (withdrawn)

Table 1.3 (Continued)

Compound	*Company*	*Use*	MMP IC_{50} (nM)									*Clinical Trial*
			MMP-1	*MMP-2*	*MMP-3*	*MMP-7*	*MMP-8*	*MMP-9*	*MMP-12*	*MMP-13*	*MMP-14*	
Batimastat (BB-94)	British Biotech	Cancer, *in vitro* cartilage	10	4	20		10	1		3		II Cancer (withdrawn)
Cipemastat (Ro-323555)	Roche Biosciences	OA, RA, *in vitro* cartilage	3	154	527		4	59		3		III RA (suspended)
Rs-130,830	Roche Biosciences	OA	590	0.22	9.3	1200		0.58		0.52		II OA (suspended)
Ro-113,830	Roche Biosciences	OA										II OA
BB-87	British Biotech	*In vitro* cartilage explants										
Rs-102,481	Roche Biosciences	*In vitro* cartilage	1100		19		18	32		0.08	1.8	
Ro-31-9790	Roche Biosciences	*In vitro* cartilage										
GI-168	Glaxo Inc.	RA	3	3	225							
Periostat (Doxycycline)	CollaGenex	Periodontitis, RA										Licensed: Periodontitis
D 1927	Celltech Chiroscience	RA, IBD										II RA
Ilomastat (GM 6001)	Glycomed	Corneal ulcers										III corneal ulcer (withdrawn)

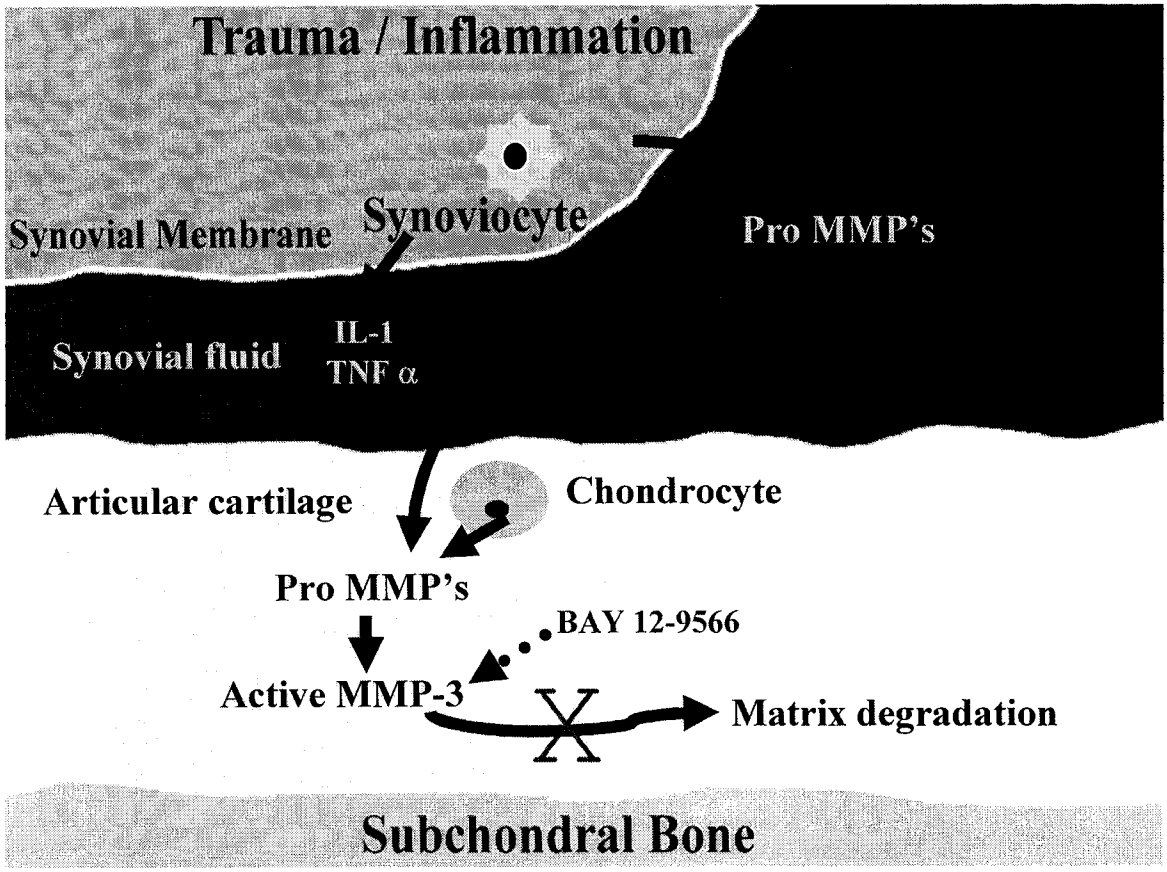

Figure 1.10. Schematic of events (oversimplified) that occur within the joint after trauma or inflammation. The synovial membrane, synovial fluid, articular cartilage, and subchondral bone are each represented. The relative location and action of the MMP inhibitor, BAY 12-9566, in blocking matrix degradation within articular cartilage is demonstrated.

articular cartilage, even though it is highly protein bound (99.9%)[239-241]. In IL-1 stimulated cartilage explant studies, BAY 12-9566 has been shown to reduce the amount of proteoglycan release and collagen degradation in a dose-dependent manner[223,242]. Histologic evidence of significant decreases in cartilage lesions after administration of oral BAY 12-9566 has been demonstrated in a rat adjuvant arthritis model[243]. as well as in canine and guinea pig meniscectomy models of OA[241], with cartilage loss being reduced by 50-60% compared to controls in the canine model. These reports suggest that BAY 12-9566 has the potential to be a useful anti-arthritic therapy. Therefore, we will

evaluate the efficacy of orally administered BAY 12-9566 in slowing down or halting the progression of degradative changes in the joint that occur secondary to CrCL transection in the dog. This will be evaluated based on differences detected in the degree of pathology (gross and histologic), the clinical parameters of pain and inflammation, radiographs, force plate analysis, and biomarker analyses.

2 TECHNIQUE FOR ARTHROSCOPIC TRANSECTION OF THE CANINE CRANIAL CRUCIATE LIGAMENT TO INDUCE OSTEOARTHRITIS

Troy N. Trumble, DVM, MS, C. Wayne McIlwraith, BVSc, PhD, R. Clark Billinghurst, DVM, PhD

To be submitted to *American Journal of Veterinary Research* Spring 2003

Presented at the 11th Annual ACVS Veterinary Symposium, Chicago, IL, October 11-14, 2001.

2.1 Summary

Objective. To develop a technique for arthroscopic transection of the cranial cruciate ligament (CrCL) in dogs for the creation of a model of osteoarthritis (OA).

Methods. Initial cadaveric study (using 35 canine stifles), after which the technique was applied to a large group of dogs (60 mature male Walker Hounds) used in an osteoarthritis study. Cadavers or anesthetized dogs were positioned in dorsal recumbency and the right hind limb was secured in maximal flexion. The arthroscope was inserted lateral to the patellar ligament, midway between the distal patella and the proximal tibia. The craniomedial band of the CrCL was identified, and the instrument portal was made medially, cranial to the medial femoral condyle and proximal to the medial meniscus. A meniscectomy blade was used to transect the cruciate ligament, and the arthroscope was directed between the transected ends to verify complete transection. If incomplete, the meniscectomy blade was repositioned to complete transection. Transection was confirmed by the presence of a cranial drawer response.

Results. Complete CrCL transection required an average of 14 minutes (range, 4-40 minutes) and was verified in 59 of 60 dogs at post-mortem. Two passes of the meniscectomy blade were required for complete transection in the majority of dogs (57%). The fat pad was resected in 13% of the dogs. Intra-operative complications included iatrogenic fibrillation of cartilage on the axial aspect of the medial femoral condyle (12%), intra-articular hemorrhage (12%), and periarticular accumulation of saline (18%). Of the instances requiring fat pad resection, 5/8 (63%) also had hemarthrosis and/or periarticular saline accumulation.

Conclusion. The described arthroscopic technique causes little iatrogenic damage or morbidity while providing reliable transection of the CrCL of the dog that mimics the clinical condition of CrCL rupture and subsequent development of OA.

2.2 Introduction

Transection of the cranial cruciate ligament (CrCL) in dogs is a commonly used model of experimental osteoarthritis (OA). This model is characterized by mechanical instability that leads to progressive clinical, biochemical, morphologic, and radiographic changes in the articular cartilage that closely mimic the early events of canine and human OA[104,129-131,244]. The severity of the induced arthritis can vary greatly within the model itself, as well as amongst the different induction techniques available[104,129-131]. Three previously described techniques used for CrCL transection are a percutaneous stab incision[101], an open arthrotomy[100], and arthroscopy[130].

Historically, the most common, least invasive technique for CrCL transection is the percutaneous stab incision (Pond-Nuki model)[101]. However, even though this technique is relatively non-invasive since it is performed through a small stab incision, it has the potential to cause a great deal of iatrogenic damage to intra-articular structures such as articular cartilage[104,129-131]. Moreover, this technique does not allow direct visualization of the CrCL, therefore potentiating incomplete or overzealous transection of the CrCL, with partial transection of the caudal cruciate ligament[104].

An open arthrotomy avoids many of the problems inherent with the percutaneous stab incision technique, because it allows direct visualization of the CrCL[104,131]. However, it has its own inherent problems since it requires extensive soft tissue dissection, creating a variable degree of injury to periarticular neurovascular structures[245].

This can then result in altered mechanical activity of the joint and thus prolonged morbidity. In addition, an extensive arthrotomy alone can cause pathological changes in all of the ligaments associated with the stifle[245].

Because of the problems inherit in these two methods, other investigators have performed arthroscopically guided CrCL transection[129-132,244,246-248]. The main advantage of arthroscopy is that it allows direct visualization for transection of the CrCL with minimal damage to the articular cartilage or caudal cruciate ligament[129]. It maximizes the advantages of the other techniques by performing the surgery through a small stab incision, while at the same time allowing a thorough examination of intrasynovial structures. This results in less incisional morbidity as well as less damage to intra-articular structures, thereby allowing for quicker rehabilitation[129,130]. Moreover, arthroscopic transection of the CrCL in the dog (unilateral and bilateral) has been shown to be similar to the Pond-Nuki and the open arthrotomy models, in terms of the amount and degree of degenerative intra-articular changes produced[129-131]. However, to the authors' knowledge, a detailed description of the arthroscopically guided CrCL transection technique is lacking. Therefore, the purpose of this paper was to describe, in detail, the technique for arthroscopic CrCL transection in the dog as it was applied to an investigative study of a novel anti-arthritic agent. It was not the purpose of this paper to describe the articular lesions produced from this model, since they have already been previously reported[129-131,244].

2.3 Materials and methods

A 30-degree, 2.7-mm arthroscope was used for this procedure, and was connected to a light source and a videoendoscope (Dyonics, Smith and Nephew, Inc., Andover,

MA), allowing collection of video and digital still images. An adjustable constant rate infusion pump was used to allow continuous infusion of the joint with saline. The only arthroscopic instruments required for completion of the CrCL transection included a meniscectomy blade (CSU Meniscus Knife, Sonatec Instruments, Englewood, CO), (Figure 2.1) and a vacuum-assisted motorized synovial tissue resector. In order to

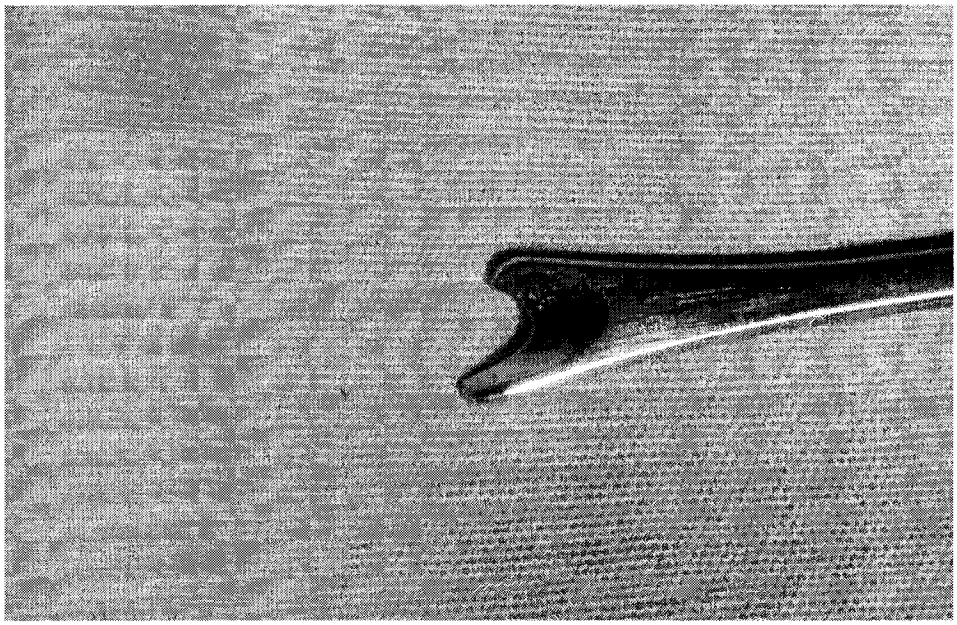

Figure 2.1. Photograph of the meniscectomy blade used to transect the cranial cruciate ligament. Note the difference in lengths between the two blunt ends. The long blunt end was placed underneath the craniomedial band of the CrCL so that the cutting surface (concave portion) surrounds the CrCL.

ensure a reproducible approach for arthroscopic CrCL transection, the techniques were developed and standardized on 35 stifles of canine cadaver specimens prior to use in a live animal study. All stifle joints of the cadavers were dissected to document complete CrCL transection, and to determine the extent of damage to other intra-articular structures. After standardization of the technique on cadavers, 60 adult, purpose bred, male Walker hounds, with an average weight of 24.1 kg (range, 16.8 - 33.3 kg) were used in this study. All dogs had normal physical, orthopaedic, radiographic, and force plate examinations.

All dogs were premedicated with a mixture of acepromazine (0.05-0.1 mg/kg intramuscularly), morphine (1 mg/kg intramuscularly), and atropine (0.04 mg/kg intramuscularly). Sodium thiopentathol (12-24 mg/kg intravenously) was used for induction, followed by maintenance with 1-2% isoflurane during the surgical procedure. The heart rate and blood pressure were continuously monitored. Analgesia was administered via a 5 mg fentanyl patch (2.0 μg/kg/hr) that was applied the day before surgery and was maintained for 72 hours post-operatively. Morphine (1 mg/kg subcutaneously) was also administered for pain post-operatively as needed. Cephalexin (Keflex) was given intravenously during surgery, and was continued orally (10 mg/kg) every 12 hours for 3 days to prevent infection.

Dogs were obtained through approved sources by the Colorado State University Laboratory Animal Resources, and the study was conducted under a protocol approved by the Colorado State University Animal Care and Use Committee.

2.4 Results

Each dog was placed in a supine position, and the right hind limb was firmly secured in maximal flexion. The right hind limb was then routinely prepared for surgery and draped. A 20-guage needle was placed in the medial aspect of the joint and directed into the intercondylar region in an attempt to avoid distention of the fat pad with injected saline. Synovial fluid was aspirated from the joint to confirm intra-articular needle placement and the joint was then distended with 10 ml of saline. This provided maximal distention of the joint, making the optimal site for the arthroscopic portal easily identifiable on the lateral aspect of the joint. A 3-mm lateral parapatellar skin incision was made at the point of maximal distention, lateral to the patellar tendon, midway

between the femur and tibia (Figure 2.2). A stab incision was then made through the

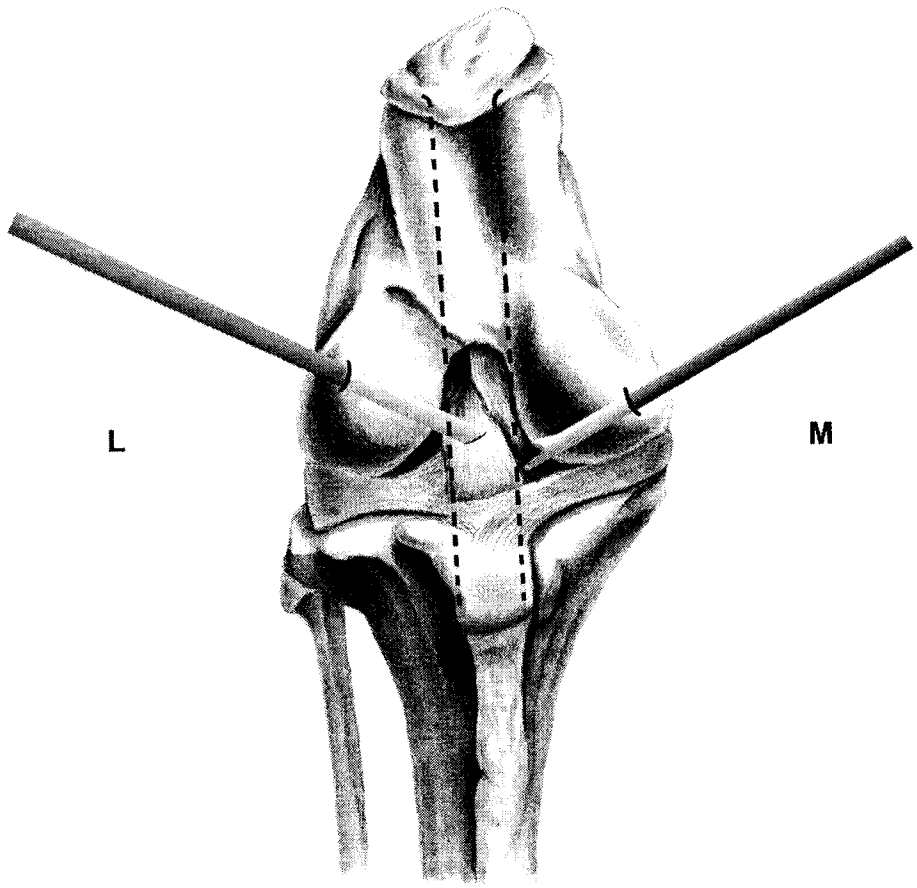

Figure 2.2. Schematic representation of the described arthroscopic technique in a canine stifle placed in maximal flexion. The dashed lines represent the patellar ligament. Medial (M) and lateral (L) are labeled accordingly. A 30-degree, 2.7-mm arthroscope was inserted laterally, midway between the distal aspect of the patella and the proximal aspect of the tibia. The instrument portal was made cranial to the medial femoral condyle, and proximal to the medial meniscus, and the meniscectomy blade was inserted. Placement of this portal allowed access to the midbody of the cranial cruciate ligament so that there is minimal iatrogenic damage during transection.

subcutaneous tissues and into the joint using a # 11 blade. If the portal was made too distal, then either menisci could be damaged. A 2.7-mm arthroscopic sleeve and blunt trochar were introduced into the joint via this lateral incision, and then directed caudally into the intercondylar region. The trochar was removed from the sleeve allowing fluid to escape from the joint, confirming intra-articular placement. The arthroscope was inserted into the sleeve and continuous low-pressure lavage of the joint with saline was started

and maintained at 40 cm of H_2O pressure. The cranial femorotibial compartments of the joint were then examined for the presence of any intra-articular abnormalities.

The arthroscope was initially directed into the medial compartment of the stifle allowing visualization of the medial femoral condyle, medial meniscus, and craniomedial band of the CrCL (Figure 2.3). Determination of the site for the instrument portal was

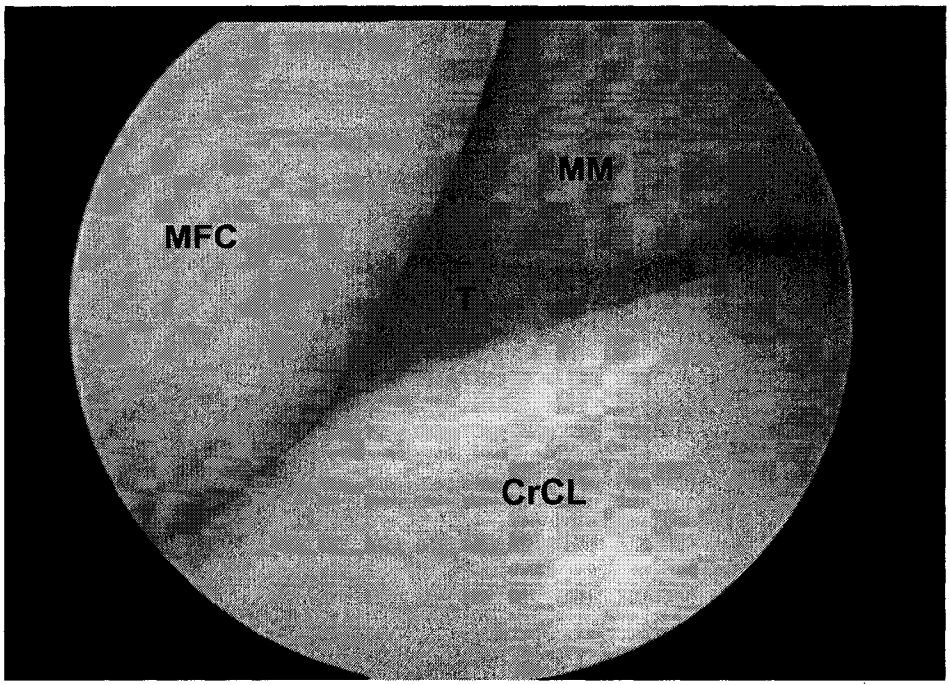

Figure 2.3. Arthroscopic photograph of the medial femorotibial compartment of the canine stifle via a lateral parapatellar approach, with the limb positioned in maximal flexion. Notice the clear visualization of the medial femoral condyle (MFC), medial meniscus (MM), proximal medial tibia (T), and the medial aspect of the craniomedial band of the cranial cruciate ligament (CrCL). This was the typical view of the CrCL that should be obtained prior to insertion of the meniscectomy blade.

best obtained by inserting a 20-gauge needle directly into the medial pouch, mimicking the direction of the meniscectomy blade (Figure 2.2). The needle was then removed and the incision made in the same direction as the needle, with the blade being observed arthroscopically, thereby minimizing iatrogenic damage. The instrument portal needed to be large enough so that when the meniscectomy blade was inserted, it did not enlarge the joint capsule more than the skin. If the skin portal was too small, extravasation of fluid

would increase rapidly, which tended to collapse the joint. Placement of a needle for identification of the instrument portal allowed placement of the meniscectomy blade cranial, parallel, and slightly proximal to the level of the medial meniscus (Figure 2.2), so as to minimize damage to other intrasynovial structures. The most common area that could be traumatized was the intercondylar fossa of the lateral condyle. Moreover, if the portal was placed slightly more distal, then it was possible to damage the lateral meniscus or the cranial intermeniscal ligament during transection.

Once inside the joint, the meniscectomy blade was then manipulated until the longer blunt end of the blade could be positioned underneath the CrCL with the short end of the C-shaped blade partially encircling the ligament (). If the blade could

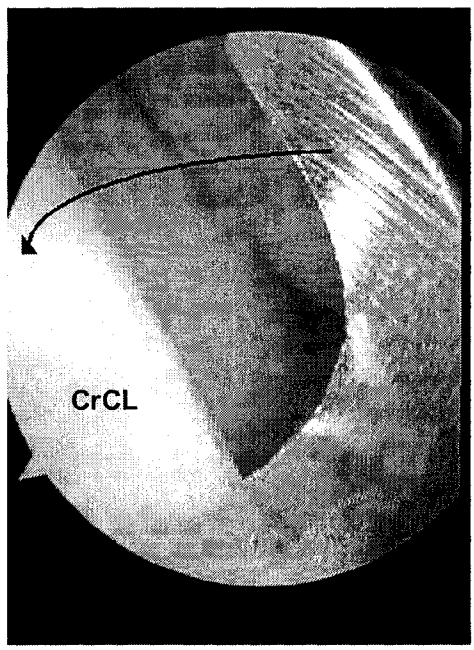

Figure 2.4. Arthroscopic photograph of the medial femorotibial compartment of the canine stifle via a lateral parapatellar approach with the limb positioned in maximal flexion. The long blunt end of the meniscectomy blade was placed underneath the medial aspect of the cranial cruciate ligament (CrCL). The blade was then directed caudally (arrow) so that the concave cutting surface could completely surround the CrCL, maximizing the potential for complete transection.

not be adequately positioned due to poor visualization of the CrCL due to the fat pad, then a vacuum-assisted mechanical synovial tissue resector was used to debride the fat pad until the craniomedial band of the CrCL could be seen. Once encompassing the CrCL, the blade was then directed slightly caudally (downward) in an attempt to completely encircle the medial aspect of the craniomedial band of the CrCL (). The limb was held rigid and the midbody of the cranial cruciate ligament was transected by directing the blade in a medial to lateral direction, with constant caudally directed pressure. No attempt was made to prevent hemorrhage during transection. The arthroscope was directed between the transected ends to evaluate the thoroughness of the CrCL transection. If complete transection had occurred, the arthroscope could be successfully directed through the lateral portion of the CrCL, and the caudal aspect of the joint could be completely visualized (Figure 2.5). However, if there was incomplete

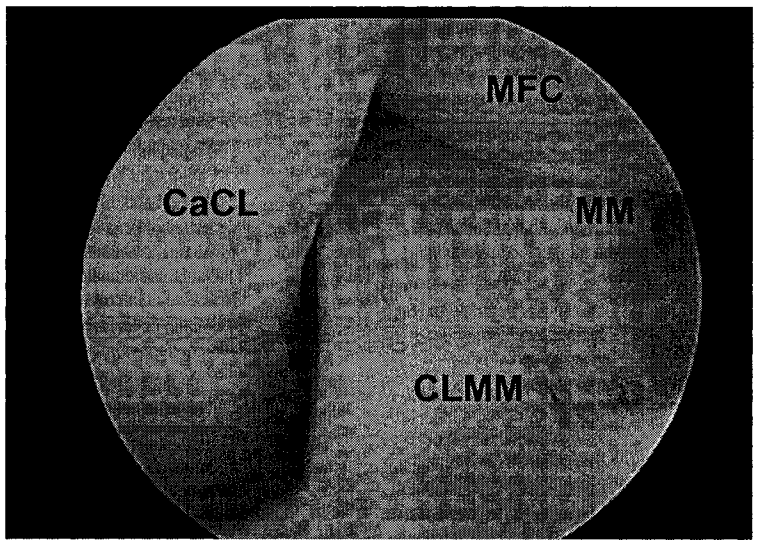

Figure 2.5. Arthroscopic photograph of the caudal medial aspect of the canine stifle via a lateral parapatellar approach with the limb in maximal flexion after complete arthroscopic transection of the CrCL with a meniscectomy blade. The arthroscope was placed between the transected ends of the CrCL, allowing examination of the entire caudal aspect of the joint. Note how the caudal cruciate ligament (CaCL), axial surface of the medial femoral condyle (MFC), caudal horn of the medial meniscus (MM) and the caudal meniscotibial ligament of the medial meniscus (CLMM) was clearly visible after transection. This view was not possible if transection was incomplete (see Figure 2.6).

transection, the arthroscope could not be directed completely through the lateral portion of the CrCL (Figure 2.6). In this situation, additional medial to lateral passes of the meniscectomy blade were performed until complete transection of the CrCL was obtained. After the initial pass of the meniscectomy blade through the midbody of the CrCL, the fat pad would occasionally prevent visualization of the transected ends of the ligament. A vacuum-assisted synovial tissue resector was used to debride the fat pad until the transected ends could be adequately visualized.

Any remaining fluid in the joint was removed via the arthroscopic sleeve. The skin portals were closed using 3-0 Nylon, and the incision was lightly bandaged with

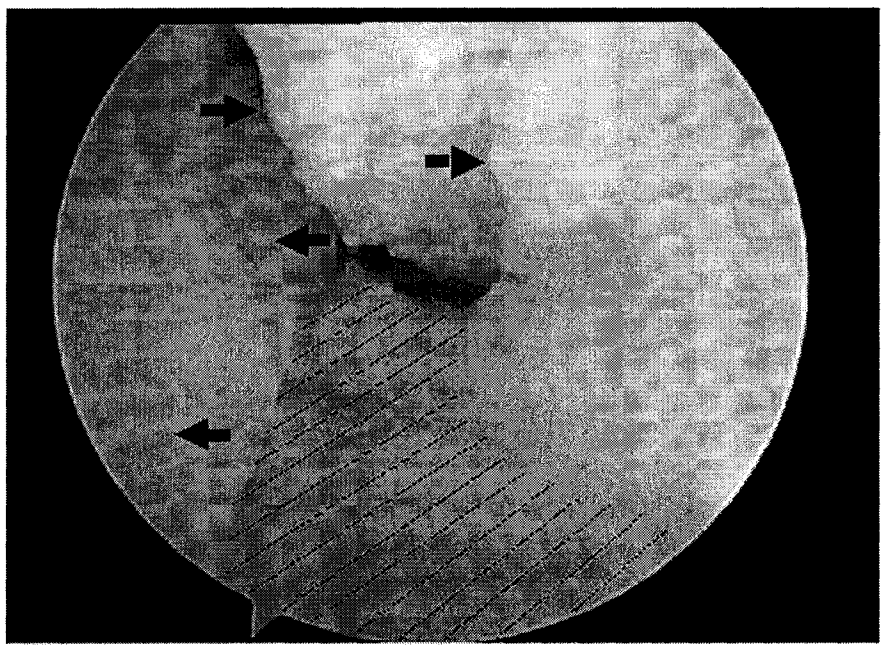

Figure 2.6. Arthroscopic photograph of the canine stifle via a lateral parapatellar approach with the limb in maximal flexion after partial transection of the CrCL with one pass of the meniscectomy blade. The arthroscope was directed between the medially transected ends of the CrCL (arrows), and identifies incomplete transection of the lateral aspect of the CrCL (outlined by parallel lines).

gauze and adhesive tape. The limb was then manipulated after suture placement for final conformation of CrCL transection by a positive cranial drawer response. The animals

were closely monitored during the first 48 hours post-operatively for any signs of pain, infection, anorexia, or intestinal complications. The skin sutures were removed after 2 weeks. To encourage the development of OA, the dogs were placed in an exercise protocol that required leash walking for 30 minutes every day for 5 days/week from the second day post-operatively until sacrifice at 4 months. All dogs were euthanized with sodium pentobarbital euthanasia solution (88 mg/kg) via intravenous injection. At the time of sacrifice, both stifles were disarticulated and examined grossly for verification of CrCL transection. Grading of osteoarthritic changes as well as further sample collection was performed for a concomitant study of a novel anti-arthritic agent.

For the 60 dogs, a mean of 14 minutes (range, 4-40 minutes) was needed to complete the CrCL transection from the first skin incision to the closure of the last portal. Surgery time decreased as experience with the technique improved. To achieve complete transection of the CrCL, 34 (57%) of the dogs required two passes with the meniscectomy blade, while 15 (25%) required one, and 11 (18%) required 3 or more passes with the blade. Gross examination of the operated stifles upon necropsy confirmed transection of the CrCL and the induction of OA in all but one dog. This dog had its CrCL only partially transected with minimal induction of OA. All dogs could walk on the limb within 36 hours of surgery and there were no post-operative complications.

Intra-operative complications included iatrogenic fibrillation of the cartilage on the axial aspect of the medial femoral condyle in 7 (12%) dogs. This was a direct result of trauma from the trochar during creation of the arthroscope portal. In addition, 7 (12%) of the dogs had hemorrhage into the joint at some point during the procedure, and 11

(18%) had periarticular accumulation of saline. None of these complications were considered severe enough to prevent completion of the CrCL transection. The fat pad had to be resected in 8 (13%) of the dogs, with half of these occurring in the initial 10 surgeries. Of the 8 dogs that had the fat pad resected, 5 (63%) also had hemarthrosis and/or periarticular fluid accumulation.

2.5 Discussion

Traditionally, the percutaneous stab incision and the open arthrotomy techniques have been the most commonly used procedures for transecting the cranial cruciate ligament in dogs to create an experimental model of OA[104]. The authors of this report decided to use the arthroscopic technique for CrCL transection in an attempt to maximize the advantages of small portals and good visualization. Even though there are other studies reporting the use of arthroscopy for CrCL transection[129-132,244,246-248], a complete description of the technique was lacking. In order to have a reproducible model of OA via arthroscopic transection, we felt that development of a consistent technique was critical for success. There is little margin for error throughout the entire procedure. Therefore, the purpose of this paper was to describe our arthroscopic technique for CrCL transection that produced a consistent model of OA with little post-operative morbidity.

During standardization of this procedure with cadavers, different degrees of flexion were examined, and full flexion allowed for the best visualization and access to the cranial cruciate ligament. When the limb was placed in maximal flexion, the cranial cruciate ligament became easily identifiable at the medial aspect of the craniomedial band and it was clearly separated from the caudal cruciate ligament[6]. In contrast, when the limb was placed in partial flexion, it was difficult to separate the CrCL and caudal

cruciate ligament. The craniomedial band of the CrCL remains taut in maximal flexion[6], allowing reliable placement of the meniscectomy blade around the CrCL for transection. An additional advantage of maximal flexion of the stifle, was that it allowed for less iatrogenic injury to other intrasynovial structures, because it placed the midbody of the CrCL in the middle of the joint, away from both menisci and the caudal cruciate ligament. It was also easier to insert the arthroscopic trochar and sleeve into the joint by allowing more entry space into the intercondylar region[179]. Overzealous entry of the arthroscopic trochar and sleeve into the intercondylar region can still damage the articular cartilage of the axial, non-weight-bearing surface of the medial femoral condyle as seen in our study. It should be noted that as we became more experienced with the technique, this iatrogenic damage was minimized.

It was also important to place the limb as perpendicular to the surgery table as possible, to minimize the amount of abduction/adduction that can occur. The procedure was much more difficult if the limb had even a small degree of abduction/adduction because of the potential for periarticular accumulation of saline. This would occur because of a change in the tissue planes of the initial incision, thereby trapping fluid in the subcutaneous tissues. This, in turn, made it increasingly difficult to insert the instrument into the joint and to maintain joint distention[174,177,178]. Periarticular fluid accumulation also decreased the visibility within the joint because of collapse of the joint capsule itself. In addition, because the tissue planes were under more pressure with fluid accumulation, it became more difficult to interpret the presence of a cranial drawer response after transection.

As with any arthroscopic procedure, distention of the stifle prior to insertion of the arthroscopic trochar/sleeve was very important to ensure that the arthroscopic sleeve and trochar were inserted into the joint and not subcutaneously. If the joint was adequately distended, but no fluid escaped from the arthroscopic sleeve after the blunt trochar was removed, then the blunt trochar and arthroscopic sleeve were redirected until fluid escaped from the sleeve after removal of the trochar. This ensured that the cannula was in the joint prior to saline infusion. If the cannula was placed subcutaneously and fluid was pumped extrasynovially, then it became very difficult to enter and remain in the joint due to collapse of the joint capsule.

Many studies describe making a skin and subcutaneous incision only for the arthroscopic portal[174,176-179]. The joint capsule is then entered using a sharp trochar in a slow twisting motion. This procedure can make it difficult to introduce the arthroscopic sleeve/trochar, and can also create a large hole through the joint capsule, potentiating periarticular extravasation of fluid. In addition, this increases the chances of iatrogenic damage of intrasynovial structures. The authors minimized the potential for the occurrence of this problem by making a small stab incision through the subcutaneous tissue and the joint capsule. This stab should still be made as small as possible to minimize collection of fluid periarticularly.

It was important to make sure that the meniscectomy blade remained sharp. Once the blade became blunt, it was difficult to completely transect the CrCL. In addition, it became very easy to damage the arthroscope, in addition to the lateral joint capsule. In our study, a dull blade was the main reason for requirement of multiple passes in order to completely transect the CrCL. The blade starts to dull after successive use in 4 dogs,

which was minimized by having a second sharp meniscectomy blade available during each surgery period of 5 or more dogs. With a sharp blade, the CrCL could be entirely transected with one pass of the meniscectomy blade. With this procedure, if part of the CrCL remained intact, it was on the caudal lateral aspect of the ligament (Figure 2.6). This portion of the ligament remains loose when the limb is in maximal flexion[6]. When transecting the cranial cruciate ligament, the blade should be directed caudally (down) after encompassing the medial aspect of the ligament (Figure 2.4). If not directed caudally, then the loose caudal lateral portion will not be transected on the first pass. Since the arthroscope is introduced laterally, it was difficult to adequately view the lateral aspect of the ligament. One can attempt to switch the instrument and arthroscopic portals to better visualize the lateral aspect of the ligament, but it has the potential to result in extrasynovial fluid accumulation. With experience, any intact portion of the CrCL can be identified via the lateral arthroscopic portal. The remaining intact portion of the cruciate ligament can be transected by inserting the meniscectomy blade through the previously transected medial section allowing access to the non-transected portion.

The fat pad did not have to be transected in most dogs with this technique. It was only transected in 13% of the dogs in this study. The fat pad tended to obstruct the view of the entire joint if saline was infused into it during the initial injection or if the joint was egressed immediately. The infusion rate of saline was only increased above 40 cm H_2O pressure if there was adequate visualization of the joint, and was not increased above 100 cm H_2O pressure, in order to minimize the risk of periarticular fluid extravasation[174]. In our experience, the fat pad interfered at two stages of the surgery. It either initially obstructed visualization of the medial aspect of the CrCL, or when the arthroscope was

directed between the transected ends of the CrCL. Once the fat pad obstructed visualization, then it had to be resected in order to view the CrCL. This could be done with any arthroscopic ronguer[177,178], but because of the size of the joint it was most easily accomplished using a motorized soft tissue resector. Only enough of the fat pad had to be resected to allow visualization of the CrCL. As more of the fat pad was resected, the potential for hemorrhage increased, which obstructed the surgical field even further. In addition, the more fat pad resection required, resulted in greater periarticular fluid extravasation. This proved to be the case in this study since 63% of those dogs that had the fat pad resected had hemarthrosis and/or periarticular saline accumulation as well.

Only one dog out of 60 dogs in this study had partial transection of the CrCL using the described technique. This dog was in the first group of 10 dogs that had CrCL transection. In this dog, there was difficulty in visualization of the CrCL due to the fat pad, and periarticular fluid accumulation. In this case, the fat pad was liberally resected, leading to hemarthrosis and additional periarticular fluid accumulation. This made it difficult to identify the lateral portion of the CrCL, and interpret a cranial drawer response. The lack of visibility of the lateral portion of the CrCL is the major drawback to using this procedure, since the key to its success and one of its major advantages over the percutaneous stab incision method is the visual verification of transection. This became less of a problem with experience, as surgical time decreased and more success was obtained with trying to avoid the fat pad and preventing periarticular fluid accumulation.

The arthroscopic procedure for CrCL transection described in this study provides a reproducible model of OA with little morbidity and iatrogenic damage to other

intrasynovial structures. It is probably equivalent to the best-case scenario with the Pond-Nuki model (i.e. no iatrogenic damage with complete CrCL transection) because it minimizes the post-operative morbidity through small stab incisions. The arthrotomy method not only has the potential to injure periarticular neurovascular structures[129,130,245], but it also could make the stifle inherently more stable compared to other techniques due to fibrosis of the incision. This fibrosis may negatively impact on the degree of OA changes that occur over time as CrCL transection creates OA through instability of the joint.

Arthroscopy of the canine stifle requires patience and practice[177-179]. However, once the surgeon has experience with the arthroscopic procedure for CrCL transection described in this report, it is a very reliable and reproducible technique for the induction of OA in the dog. This experimental OA model can then be used to evaluate novel anti-arthritic agents for both animals and humans.

3 SERIAL ARTHROSCOPIC EXAMINATION OF THE CRANIAL CRUCIATE DEFICIENT STIFLE IN THE DOG

Troy N. Trumble, DVM, MS, C. Wayne McIlwraith, BVSc, PhD, R. Clark Billinghurst, DVM, PhD

To be submitted to *Veterinary Surgery* in spring 2003.

Presented in part at the 12th Annual ACVS Veterinary Symposium, San Diego, CA, October 17-20, 2002.

3.1 Summary

Objective. To determine the temporal pattern and severity of intra-articular changes in the early period after cranial cruciate ligament (CrCL) transection in the dog.

Methods. Three adult purpose bred male Walker Hounds had the right CrCL transected arthroscopically at day 0. Serial arthroscopic examinations were then performed at 14, 28, 70, and 126 days post-CrCL transection. The temporal pattern and severity of changes to the synovium, joint capsule, menisci, and articular cartilage were described and graded for each day. Arthroscopic findings were verified grossly at 126 days post-CrCL transection.

Results. Articular cartilage and medial meniscal damage started as early as 2 weeks after CrCL transection and generally progressed from there. Stretching or rupture, to a variable degree, of the cranial meniscotibial ligament of the medial meniscus was identified in all 3 dogs. The degree of synovitis peaked at one month after CrCL transection, and then decreased over time.

Conclusion. Clinically relevant osteoarthritic changes start to occur shortly after CrCL transection and will generally progress when the joint is not stabilized.

3.2 Introduction

Cranial cruciate ligament (CrCL) rupture in dogs has been reported to be a common cause of hind limb lameness[2], and may actually be under-diagnosed[173]. CrCL rupture causes gross instability and inflammation that creates a cascade of events in the joint that can lead to osteoarthritis (OA). OA is a rapidly progressive process that is ultimately represented by degradation of articular cartilage and damage to menisci and subchondral bone[1,249]. This degradation is believed to be irreversible, and is usually

clinically evident within the first few months after CrCL rupture. The goal of treatment of CrCL rupture is to attempt to minimize the instability created by stabilizing the joint surgically, thereby preventing further deterioration of the joint and facilitating early return to full function[148,155]. Surgical stabilization for CrCL rupture has undergone a pronounced evolution and includes many different procedures[250].

In a study of CrCL deficient dogs that were not stabilized, Vasseur stated that joint stabilization should be performed immediately after rupture because, regardless of size, all dogs developed OA[251]. However, in most referral hospitals, dogs will generally present with a chronic history of rupture in which OA is already established prior to surgery[7]. The range from the time of injury to surgical repair is reported to be 3 to 18 weeks, with most being performed closer to the later time point[145,152-154,252,253]. This suggests that duration from injury to surgery is likely a major contributing factor to the overall progression of OA. In fact, one large prospective study of post-operatively stabilized CrCL deficient stifles demonstrated a positive correlation between disease duration and the amount of osteophytes and cartilage fibrillation present[146].

To complicate matters even further, the medial meniscus also tends to become injured at some stage post-CrCL rupture. The types of meniscal injury have been well described in dogs[14,149], and usually involve the caudal horn of the medial meniscus. However, the duration of disease has not been shown to correlate with the incidence of meniscal injury[146]. Meniscal damage can occur either at the same time as the insult that resulted in the cruciate rupture, or more likely secondary to the abnormal forces placed across the joint as a result of CrCL rupture[143,154]. This tends to indicate that it would be important to attempt to stabilize the joint to minimize the potential for meniscal damage.

Little is reported in regard to the temporal pattern of clinically relevant osteoarthritic changes that occur within the articular cartilage and medial meniscus of the canine stifle after CrCL rupture. A better understanding of these changes would potentially help the clinician to make decisions that would improve the overall care and prognosis of CrCL deficient dogs. Experimental transection of the CrCL provides the capability to examine the intra-articular changes that occur within the joint immediately after transection. This provides many advantages, including the ability to know the temporal pattern of damage to intra-articular structures. Arthroscopy has been shown to be a valuable and reliable tool for identifying CrCL rupture as well as grading osteoarthritic changes in the dog[174-179]. Arthroscopy has usually been used to examine the CrCL deficient stifle at one given time point after transection to compare the arthroscopic findings to those after arthrotomy as well as with the gross findings[174]. However, to the authors' knowledge, only one study in dogs has reported serial arthroscopic examinations of CrCL deficient joints to determine the long term intra-articular changes[157]. Therefore, the purpose of this study was to arthroscopically examine the stifles of three dogs, post-CrCL transection, to determine the temporal pattern and severity of changes that occur in the early period after CrCL transection. Our hypothesis was that articular cartilage degradation and meniscal damage would be established within the first two weeks after CrCL transection.

3.3 Materials and methods

3.3.1 Experimental design. Three purpose-bred adult male Walker hounds (20.5, 22.1, and 22.9 kg) were studied. Inclusion criteria required the dogs to be free of

pre-existing orthopaedic disease of the stifles based on routine physical, orthopaedic, lameness, radiographic, and force plate examinations.

All dogs were anesthetized and the right hind limb was prepared for aseptic surgery. A lateral parapatellar arthroscopic approach to the right stifle was used to examine the joint for the presence of any intra-articular pathology of the articular cartilage, cruciate ligaments and menisci. The CrCL was then transected arthroscopically using a meniscectomy blade (Chapter 2). Serial arthroscopic examinations were performed at 14, 28, 70, and 126 days post-CrCL transection. The stifles were evaluated systematically, starting in the medial femorotibial compartment followed by the intercondylar region and finishing in the lateral femorotibial compartment.

Analgesia was administered via a 5 mg fentanyl patch (2.0 μg/kg/hr) that was applied the day before each surgery and was maintained for 72 hours post-operatively. Morphine (1 mg/kg subcutaneously) was also administered post-operatively for pain, as needed. Cephalexin (Keflex) was administered intravenously during surgery and was continued orally (10 mg/kg) every 12 hours for 3 days to prevent infection. Throughout the study, all dogs were housed in individual runs. The animals were closely monitored during the first 48 hours post-operatively for any signs of pain, infection, anorexia or intestinal complications. To encourage the development of OA, dogs were placed in an exercise protocol that required leash walking for 30 minutes every day for 5 days/week from the second day post-operatively until 126 days post-operatively. All dogs were euthanized with sodium pentobarbital euthanasia solution (88 mg/kg) via intravenous injection at day 126 post-transection. At the time of sacrifice, the stifles were

disarticulated and examined grossly for the location and extent of osteoarthritic changes present. The gross pathology was descriptively recorded and digitally photographed.

Dogs were obtained through approved sources by the Colorado State University Laboratory Animal Resources, and the study was conducted under a protocol approved by the Colorado State University Animal Care and Use Committee.

3.3.2 Arthroscopic analysis. For the purposes of recording the changes identified during arthroscopic examination, the intra-articular changes were documented on videotape and via digital photography. For each observation period, descriptive analysis as well as grading of the severity of the gross changes of the synovium, fibrous tissue reaction, menisci, and articular cartilage were recorded by the surgeon (TNT). Descriptive analyses consisted of identifying the arthroscopic changes as none, mild, moderate, or severe based on the location and extent of injury during each arthroscopic examination.

Severity grading was performed after all of the serial arthroscopies were performed, and was based on a 0-3 scale. The degree of synovitis was graded as 0 = no synovitis present, 1 = mild synovitis represented by slightly hyperemic synovial membrane, 2 = moderate synovitis represented by a moderate amount of hypertrophy and hyperemia of the synovial membrane, or 3 = severe synovitis represented by villous hypertrophy and thickening and hyperemia of the synovial membrane, such that it bleeds on contact. The degree of fibrous reaction was graded as 0 = no fibrinous or fibrous reaction, 1 = consolidation of the fat pad and the presence of fibrin on and around the transected ends of the CrCL, 2 = increased size/consolidation of the fat pad with more organized fibrin on and around the CrCL ends, as well as moderate capsular fibrosis or

the presence of fibrinous tags, or 3 = organized fibrous response on or around the CrCL or joint capsule and/or the presence of mature fibrous adhesions.

Meniscal damage was graded for the medial meniscus only. Overall damage of the medial meniscus was graded as 0 = no change, 1 = mild fibrillation or tearing of the axial surface, 2 = moderate fibrillation and/or small transverse tearing of the axial surface, or 3 = severe fibrillation and or longitudinal tearing of the caudal horn. Specific changes that occurred around the cranial horn of the medial meniscus were graded as 0 = no change, 1 = slight proximal and/or abaxial displacement of the cranial horn, 2 = moderate proximal or abaxial and caudal displacement of the cranial horn and/or increased vascularity at the junction of the cranial meniscotibial ligament, or 3 = severe abaxial and caudal displacement of the cranial horn with fibrinous/fibrous reaction and/or increased vascularity around the junction of the cranial meniscotibial ligament. Articular cartilage lesions on the medial and lateral femoral condyles, as well as the medial and lateral tibial plateaus were graded as 0 = no change, 1 = mild fibrillation, 2 = moderate fibrillation and/or the presence of clefts or score lines, or 3 = severe fibrillation and/or full thickness cartilage erosion.

3.4 Results

A summary of the arthroscopic findings for dogs A, B, and C is presented by examination period. Specific severity gradings of arthroscopic lesions for each observation period of each dog are listed in Table 3.1.

Table 3.1: Severity grading for the intra-articular changes noted arthroscopically, based on a 0-3 scale for each dog (A,B,C) for each examination (day 14, 28, 70, 126) after CrCL transection. The severity grade for each change was averaged for the 3 dogs for each examination (Avg). Articular cartilage fibrillation (Fib) was calculated by combining the 4 areas assessed. The total severity score for each day was calculated by taking the average of all of the scores for all of the intra-articular changes examined on each day. Cr = cranial, Med = medial, and Men = meniscus.

	Day 14				***Day 28***				***Day 70***				***Day 126***			
	Dog				***Dog***				***Dog***				***Dog***			
Intra-articular changes	***A***	***B***	***C***	***Avg***	***A***	***B***	***C***	***Avg***	***A***	***B***	***C***	***Avg***	***A***	***B***	***C***	***Avg***
Synovitis	1	1	2	***1.3***	2	2	3	***2.3***	1	2	1	***1.3***	1	1	1	***1***
Fibrous Reaction	2	1	1	***1.3***	2	1	2	***1.7***	3	2	3	***2.7***	3	3	3	***3***
Meniscal Fibrillation	1	1	1	***1***	1	1	2	***1.3***	2	1	3	***2***	2	2	3	***2.3***
Displacement Cr Med Men	0	0	0	***0***	1	2	2	***1.7***	2	2	3	***2.3***	2	3	3	***2.7***
Articular Cartilage Fibrillation																
Lateral Femoral Condyle	0	0	0	***0***	1	0	0	***0.3***	1	1	0	***0.7***	1	1	1	***1***
Medial Femoral Condyle	0	0	1	***0.3***	1	0	1	***0.7***	1	1	1	***1***	2	2	2	***2***
Lateral Tibial Plateau	0	2	0	***0.7***	0	2	0	***0.7***	2	2	2	***2***	2	2	3	***2.3***
Medial Tibial Plateau	0	0	0	***0***	0	0	0	***0***	2	0	2	***1.3***	2	2	3	***2.3***
Articular Cartilage Fib Avg				***0.25***				***0.43***				***1.25***				***1.9***
	Day 14 Ave			***0.58***	***Day 28 Ave***			***1.09***	***Day 70 Ave***			***1.66***	***Day 126 Ave***			***2.08***

3.4.1 Day 0. Transection of the CrCL was successfully performed in all dogs, with no complications. All of the dogs were non weight-bearing lame on the limb immediately after surgery, and 2/3 (A and B) began toe-touching within the first few days after surgery. Lameness continued to improve throughout the first two weeks, and remained mild to moderate throughout the rest of the study for these two dogs. The other dog (C) remained non weight-bearing through day 70 and began toe-touching by day 126.

3.4.2 Day 14. There was mild synovitis present throughout the joint in 2/3 dogs (A and B) and moderate synovitis present in the third (C). The fat pad was slightly enlarged and consolidated, and there was a mild to moderate amount of fibrin present on the transected ends of the cruciate ligament in all dogs. The entire axial surface of the medial meniscus could be easily observed without manipulation of the limb with a mild amount of fibrillation present on the cranial axial surface of the medial meniscus in all dogs (Figure 3.1A). One dog (C) had mild cartilage fibrillation on the medial femoral condyle, whereas another dog (B) had a moderate degree of articular cartilage fibrillation

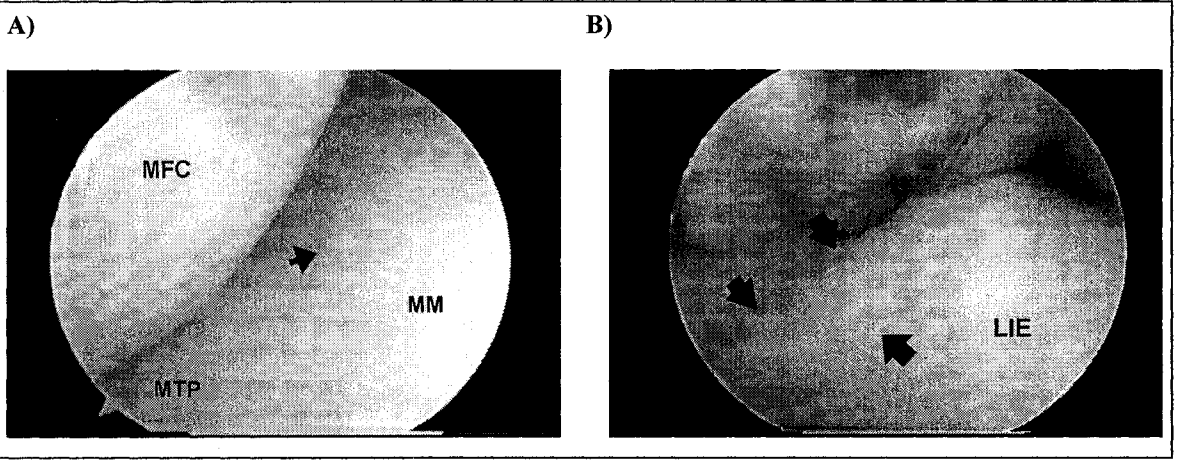

Figure 3.1. Day 14 post-CrCL transection arthroscopic view of the medial femorotibial compartment **(A)** and the intercondylar region **(B)** of dog A and B, respectively, demonstrating mild fibrillation (small arrow) on the axial surface of the medial meniscus **(A)** and moderate articular cartilage fibrillation (large arrows) on the lateral intercondylar eminence (LIE) of the tibia **(B)**. MFC = Medial Femoral Condyle, MTP = Medial Tibial Plateau, MM = Medial Meniscus.

on the proximal lateral intercondylar eminence of the tibia (Figure 3.1B).

3.4.3 Day 28. There was now moderate to severe synovitis present throughout the joint with a varying degree of hyperemia and villous hypertrophy in all dogs (Figure 3.2A). The fat pad consolidation and fibrin on the transected ends of the CrCL remained relatively unchanged from day 14 in all dogs. The entire axial surface of the medial meniscus remained visible without limb manipulation and the degree of fibrillation in that region remained unchanged from day 14 in two of the dogs (A and B). The third dog (C)

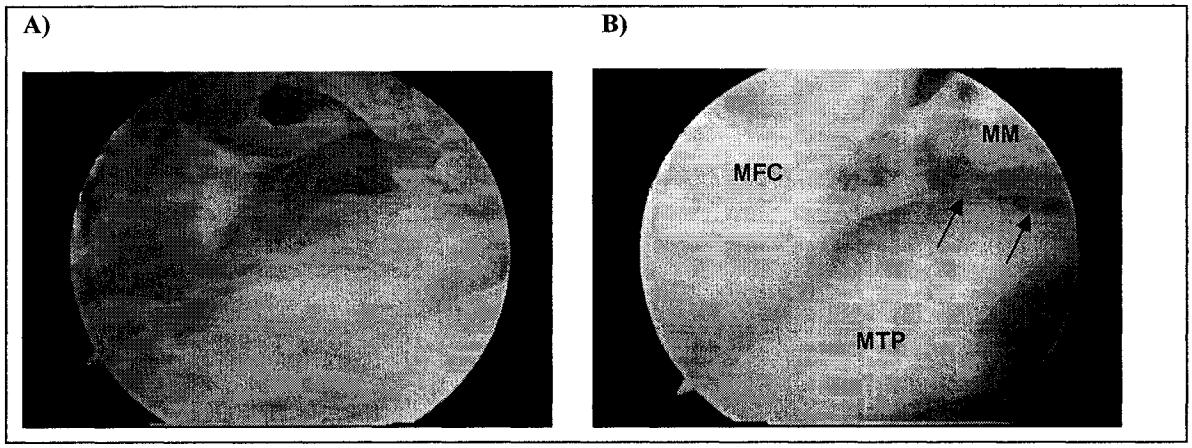

Figure 3.2. Day 28 post-CrCL transection arthroscopic view of the synovial membrane **(A)** and medial femorotibial compartment **(B)** of dog C and A, respectively, demonstrating severe synovitis with villous hypertrophy and hyperemia **(A)** and slight proximal and abaxial displacement of the cranial horn of the medial meniscus **(B)** along with increased vascularity (arrows). MFC = Medial Femoral Condyle, MTP = Medial Tibial Plateau, MM = Medial Meniscus.

had a slight tear on the axial surface of the medial meniscus that was on the caudal portion of the fibrillated area identified on day 14. Associated with this tear was a thin frond-like portion of the medial meniscus. The cranial horn of the medial meniscus appeared to be more mobile in all of the dogs, being slightly abaxially and proximally displaced with neovascularization present near the junction of the cranial meniscotibial ligament. (Figure 3.2B). A mild amount of articular cartilage fibrillation was present on the weight bearing portion of the medial femoral condyle of two dogs (A and C). One

dog (A) also had a mild amount of articular cartilage fibrillation on the axial, non weight bearing portion of the lateral femoral condyle. The degree of fibrillation of the proximal lateral intercondylar eminence of the tibia in dog B was unchanged.

3.4.4 Day 70. There was a moderate amount of wear debris in the synovial fluid in the presence of a mild to moderate degree of synovitis in all dogs. The size of the fat pad increased and appeared more consolidated with a hematoma in one dog (C), remained unchanged in another (A), and decreased in the third (B). In all of the dogs, the transected ends of the CrCL have atrophied and the amount of fibrin appeared to be less and more organized. In one dog (C), there were numerous fibrous tags in the intercondylar region, adhering to the caudal cruciate ligament. The entire axial surface of the medial meniscus was still observed in all dogs without limb manipulation. The fibrillation of the medial meniscus remained unchanged in one dog (B), but progressed to a small transverse tear in another (A). In the third dog (C), a longitudinal tear of the caudal horn was now present, with this portion of the caudal horn protruding cranially underneath the medial femoral condyle (Figure 3.3A). The cranial horn of the medial meniscus was still slightly displaced both proximally and abaxially in all dogs with increased vascularity at the junction of the cranial meniscotibial ligament. The mild degree of articular cartilage fibrillation on the weight-bearing surface of the medial femoral condyle and axial non weight-bearing surface of the lateral femoral condyle was unchanged in two dogs (A and C), and started to appear in the third (B). A moderate degree of articular cartilage fibrillation on the proximal cranial medial tibial plateau (Figure 3.3B) developed in two of the dogs (A and C) and all dogs had moderate fibrillation on the lateral intercondylar eminence of the tibia.

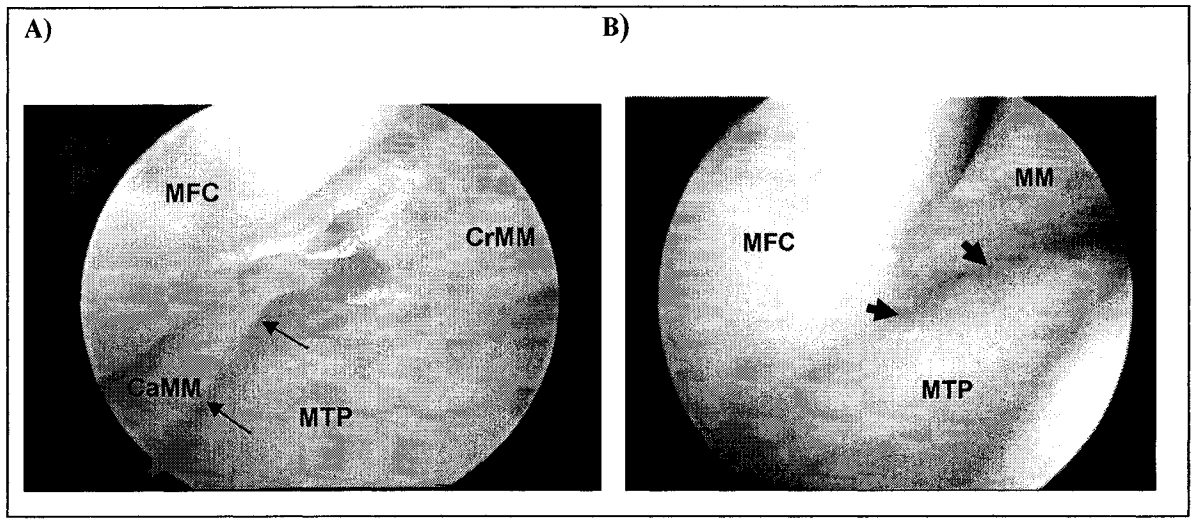

Figure 3.3. Day 70 post-CrCL transection arthroscopic view of the medial femorotibial compartment **(A and B)** of dog C and A, respectively, demonstrating a large bucket handle tear of the caudal horn of the medial meniscus (CaMM) protruding cranially (small arrows) between the medial femoral condyle (MFC) and the medial tibial plateau (MTP) **(A)**, and a moderate degree of articular cartilage fibrillation (large arrows) on the medial tibial plateau **(B)**. CrMM = Cranial horn of the medial meniscus, MM = Medial Meniscus.

3.4.5 Day 126. There was still a moderate amount of wear debris present in the synovial fluid in the presence of a mild synovitis in all dogs. A moderate amount of fibrous tissue was present throughout the entire joint in all of the dogs, with two of the dogs (A and C) forming mature fibrous adhesions in the intercondylar region (Figure 3.4A). The transected ends of the CrCL were further atrophied in all dogs and covered by mature fibrous tissue. In two of the dogs (A and B), the entire axial surface of the medial meniscus was observed without limb manipulation, with the small cranial axial tear remaining unchanged in one dog (A), while a small transverse tear in the previously fibrillated cranial axial portion appeared in the other dog (B). In the third dog (C), the medial meniscal tear progressed into a large bucket handle tear of the caudal horn that was traced back to the caudal meniscotibial ligamentous attachment. The torn caudal horn was displaced cranially, and the cranial horn was no longer visible, indicating rupture or stretching of the cranial meniscotibial ligament with major abaxial and caudal

displacement of the cranial horn of the medial meniscus (Figure 3.4B). In the other two

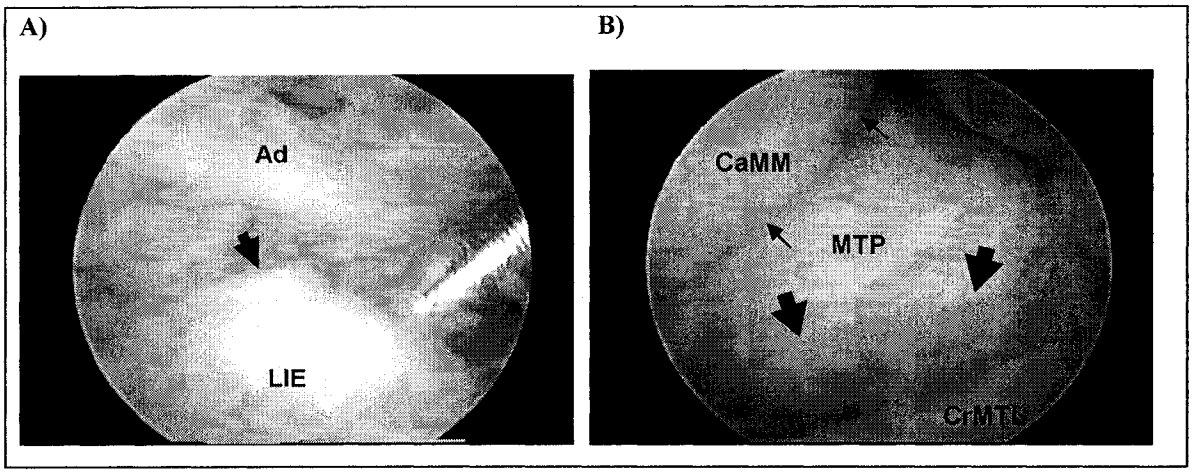

Figure 3.4. Day 126 post-CrCL transection arthroscopic view of the intercondylar region **(A)** and medial femorotibial compartment **(B)** of dog C demonstrating a large fibrous adhesion (Ad) and an osteophyte (arrow) on the lateral intercondylar eminence (LIE) **(A)**, and rupture/stretching of the cranial menisctibial ligament (CrMTL) of the medial meniscus so that the cranial horn of the medial meniscus is no longer visible on the cranial aspect of the medial tibial plateau (MTP) **(B)**. The bucket handle tear of the caudal horn of the medial meniscus (CaMM) is still protruding cranially (small arrows), and complete articular cartilage erosion is present (large arrows) on the cranial medial tibial plateau where the cranial horn usually sits **(B)**.

dogs (A and B), the cranial horn of the medial meniscus was moderately (B) to severely (A) displaced abaxially and caudally, with a moderate amount of fibrin in the location of the cranial meniscotibial ligament. There was a moderate degree of articular cartilage fibrillation present on the weight bearing surface of the medial femoral condyle, proximal cranial medial tibial plateau, and the lateral intercondylar eminence of 2 dogs (A and B). All dogs also had mild articular cartilage fibrillation on the non weight-bearing surface of the lateral femoral condyle. In the dog with the bucket handle tear (C), there was severe articular cartilage erosion on the proximal medial tibia where the cranial horn used to sit, as well as on the cranial proximal aspect of the lateral tibia.

Gross examination of all of the dogs' joints demonstrated a moderate to severe amount of fibrous tissue surrounding the joint capsule. Complete CrCL transection was verified in all dogs and the transected ends had atrophied toward each respective bony

attachment by about 1/3 of its transected length. There was a moderate to severe amount of fibrous tissue present in the intercondylar fossa, surrounding the two transected CrCL ends, with fibrous adhesions in two dogs (A and C). A minimal to moderate amount and size of osteophytes were present along the femoral trochlear ridges, the proximal borders of the tibial plateau, and/or the distal patella in 2/3 dogs (A and C). A moderate amount of osteophytosis was present in the femoral intercondylar region in 2/3 dogs (A and C), combined with a mild to moderate amount of bony resorption.

The lateral menisci appeared grossly normal in all dogs, but 2/3 dogs (A and B) had thinning and an irregular surface/small tear on the cranial axial surface of the medial meniscus. The third dog (C) had a large bucket handle tear of the caudal horn of the medial meniscus that extended from the caudal meniscotibial ligament to just beyond the middle of the axial meniscus (Figure 3.5A). The width of the tear was approximately

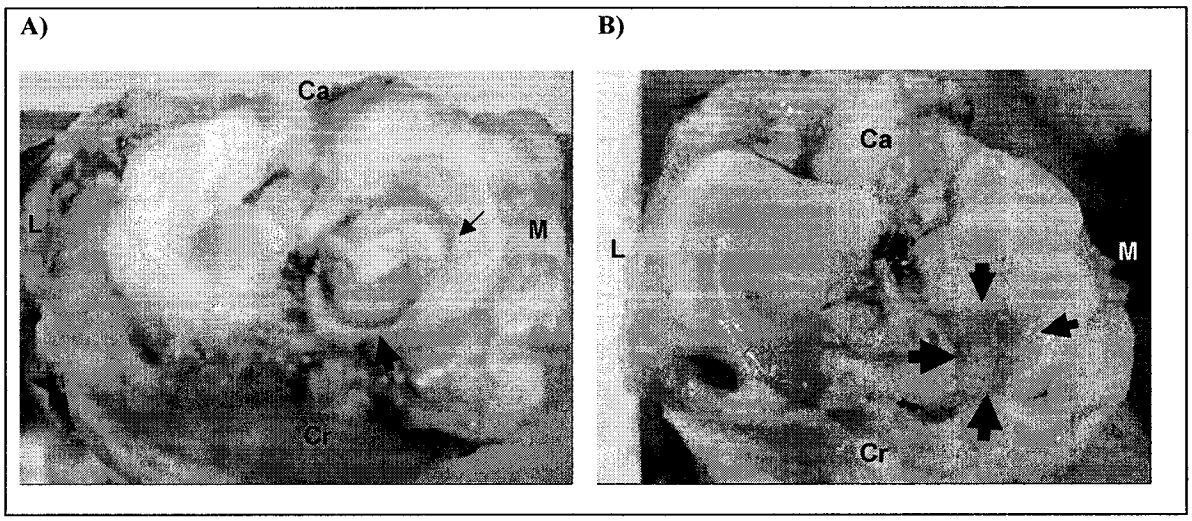

Figure 3.5. Gross appearance at day 126 post-CrCL transection of the medial meniscus of dog C after disarticulation of the stifle **(A)**, and of the articular cartilage of the tibia after further removal of the menisci **(B)**. A large bucket handle tear of the caudal horn of the medial meniscus (small arrow), as well as a mature fibrous adhesion (large arrow) was observed in the typical location of the cranial meniscotibial ligament of the medial meniscus **(A)**. Full-thickness erosion of the articular cartilage (arrows) was observed on the cranial aspect of the medial tibial plateau where the cranial horn of the medial meniscus was located **(B)**. M = Medial, L= Lateral, Cr = Cranial, Ca = Caudal

50% of the normal meniscal width in the caudal horn, with a moderate amount of fibrous tissue present along the entire periphery of the medial meniscus. The cranial aspect of the medial meniscus was intimately embedded within this fibrous tissue and was displaced proximally off of the tibial plateau. There was a mature fibrous adhesion in the typical location of the cranial meniscotibial ligament, but no ligamentous tissue could be identified (Figure 3.5A). In the other 2 dogs (A and B), only about ¼ of the cranial meniscotibial ligament of the medial meniscus was intact with a moderate amount of fibrous tissue at its junction with the medial meniscus. There was a mild degree of gross articular cartilage fibrillation present on the proximal medial and lateral surfaces of the tibial plateaus not protected by the menisci in one dog (B), that was moderate (A) to severe (C) in the other two dogs, with damage extending to the lateral intercondylar eminence. In dog C, severe erosion of the articular cartilage was present on the cranial proximal medial tibia where the cranial horn of the medial meniscus normally sits (Figure 3.5B). Mild articular cartilage fibrillation and linear score lines were present on the weight-bearing surface of the medial and lateral femoral condyles of all dogs.

3.5 Discussion

Arthroscopy has been identified as a valuable tool for identifying changes that occur within the joint during the development of OA, especially to the articular cartilage, ligaments or menisci[174-179]. Few studies have looked at the serial use of arthroscopy in an experimental setting. Siemering, over 1 year, serially examined the stifles of 4 dogs that underwent a variety of experimental transections, including CrCL transection, and reported no adverse effects from the arthroscopic procedure itself[157]. Arthroscopy is considered a minimally invasive technique that causes much less trauma and

inflammation of the joint than an arthrotomy[177,179]. The major negative aspect of the arthroscopic procedure identified in our study was iatrogenic damage to the articular cartilage. Most of the linear score lines and some of the fibrillation on the axial non weight bearing surface of the lateral femoral condyle or the weight bearing portion of the medial femoral condyle noted in this report were presumed to be iatrogenically created by insertion of the blunt trochar and arthroscopic sleeve through an increasingly thickened joint capsule.

In this study, arthroscopy was identified as a sensitive method to detect early, subtle changes occurring in the joint such as early identification of articular cartilage fibrillation that would be difficult to identify grossly or by routine imaging. Fibrillation occurs when there has been damage to the collagen network of the articular cartilage[254], that is thought to be irreversible, and will rapidly progress if the joint environment is not biomechanically stabilized. It has been reported that collagen in the superficial zone of cartilage becomes thinner and more widely spaced so that fibrillation can occur within the first week after CrCL rupture[106,255,256]. The earliest fibrillation noted in this study was present at 2 weeks in dog B on the lateral surface of the intercondylar eminence of the tibia. This was an unexpected location since it is not a true weight bearing area of the tibia. It is logical to assume that this damage is a direct result of the instability, but it could be due to the difference in stiffness of the subchondral bone[172]. For this to have occurred in our study, one would have to assume that underlying differences in the subchondral bone would be present by 2 weeks which were not evident radiographically. Once fibrillation was present, the damage in that location either maintained itself or progressed (Table 3.1). Innes and Barr demonstrated, through a series of naturally

occurring CrCL ruptures, that cartilage fibrillation scores positively correlated with disease duration[146], further suggesting that this damage is associated with the period of instability. The early evidence of articular cartilage fibrillation in the current study is important clinically, because it demonstrates that cartilage damage will likely be present in most dogs prior to joint stabilization as it is currently performed.

Meniscal injury is a common sequelae of the instability created after cruciate ligament rupture[14,145]. It has been reported that 48-80% of dogs that ruptured their CrCL will sustain meniscal damage, usually to the medial meniscus[14,143,145-155]. The high rate of meniscal injuries reported may be due to the chronicity of CrCL injuries seen at referral centers[143]. The types of meniscal injuries sustained have been previously defined for the dog[14,149], as well as possible reasons for the higher rate of medial compared to lateral meniscal injury[10]. Most of the injuries occur to the axial surface of the caudal horn[14,149] such that folding of the damaged caudal horn flips cranially and becomes impinged between the medial femoral condyle and the proximal medial tibia[10,149], as occurred in dog C in our study.

This meniscal damage can occur either at the same time as the insult that resulted in the cruciate rupture, or more likely occurs secondary to the instability of the joint[143,154]. Siemering reported arthroscopic evidence of damage as early as two weeks post-transection[157], demonstrating that serial arthroscopic exams have the ability to identify early meniscal changes as well as the overall temporal nature of this injury. In the current study, initial medial meniscal damage started as fibrillation on the axial surface two weeks after CrCL transection. By day 28, the medial meniscus in dog C sustained a small transverse tear at the caudal extent of the initial fibrillation. This then transitioned

into a longitudinal tear by day 70 and worsened by day 126. Interestingly, this same damage was present by day 14 in the other 2 dogs, but it progressed minimally after that. This suggests that damage to the meniscus is set up by day 14, and other factors such as muscular function, and joint instability play a role in the extent of further damage. One of these factors may be dependent on the amount of injury sustained to the cranial meniscotibial ligament of the medial meniscus.

The cranial meniscotibial ligament of the medial meniscus attaches the cranial horn to the proximal aspect of the cranial intercondylar area of the tibia just cranial to the lateral edges of the CrCL and the intermeniscal ligament[10,14]. The meniscotibial ligaments play a vital role by providing secure fixation of the cranial and caudal horns of the menisci allowing the body of the meniscus to withstand circumferential hoop stress applied during weight-bearing[257,258]. The circumferential hoop stress is produced in an attempt to counteract abaxial extrusion of the menisci as a result of an applied load so that forces are transmitted evenly throughout the meniscus and across the joint[257,258]. Presumably then, if damage occurs to one of the cranial meniscotibial ligaments, an increased amount of force would be placed on the body of the meniscus leading to failure of the fibers and eventual tearing[143].

All three dogs of this study had arthroscopic evidence of proximal, abaxial, and caudal displacement of the cranial horn of the medial meniscus, associated with increased vascularity at the junction of the craniomedial meniscotibial ligament as early as day 14. This increased vascularity was likely in response to injury being sustained by the meniscotibial ligament, and often became more pronounced over time, suggesting that stretching or tearing of the ligament had occurred. To the authors' knowledge, this has

not been previously reported. The authors theorize that damage to the cranial medial meniscotibial ligament may be sustained after CrCL transection/rupture due to the cranial tibial thrust which causes a small amount of repetitive hyperextension[142]. This repetitive hyperextension would likely cause the cranial medial meniscotibial ligament to be wedged between the cranial aspect of the proximal tibia and the transition area between the medial trochlear ridge and femoral condyle. This repetitive trauma combined with the relative immobility of the medial meniscus is likely to traumatize this ligament over time causing it to stretch initially, and then eventually rupture, if the joint remains unstable. This relationship to the degree of instability of the joint could be demonstrated in our study by the differences seen between dog C and dogs A and B. Dogs A and B experienced only mild to moderate stretching/tearing of this ligament, respectively, and they became inherently more sound on their CrCL deficient limb sooner than dog C who sustained complete rupture of the meniscotibial ligament. Each dog may respond differently, depending upon the insertional anatomic variation that may exist in the cranial meniscotibial ligament, especially if the attachment is to either the cruciate ligament or the intermeniscal ligament, as described in humans[259,260].

This also suggests that the degree of tearing or stretching of the cranial meniscotibial ligament may either contribute to, or be a result of the amount of damage sustained by the remainder of the meniscus. Evidence of this is supported by the fact that dog C had the most severe tearing/rupture of this ligament and also the most meniscal damage. When the cranial meniscotibial ligament ruptures, presumably the circumferential fibers would likely not be able to withstand the forces applied to the meniscus[257]. The mobility of the entire meniscus would likely increase, with the cranial

horn moving much more than the caudal horn, causing the axial portion to get stretched. This would conceivably make it easier for the caudal horn to exceed the mechanical capabilities of the radial and circumferential fibers of the caudal pole, resulting in its subsequent tearing and allowing it to become impinged between the medial femoral condyle and the medial tibial plateau. In addition, the increased mobility of the cranial horn of the medial meniscus can lead to the mechanical damage that is often identified on the articular cartilage of the cranial aspect of the tibial plateau where the cranial horn used to sit (Figure 3.5B)[149], as well as on the femur at the junction between the trochlear ridges and the medial femoral condyles[145,249].

Clinical evidence of this tearing of the cranial medial meniscotibial ligament may be difficult to identify at the time of stabilization of CrCL deficient stifles due to chronicity of the injury. Often the area of the cranial medial meniscotibial ligament is covered in thick fibrous tissue, which is likely the secondary response of the joint to repair this ligament as well as stabilize the joint. Nevertheless, it can be difficult to distinguish this fibrous reaction from the actual ligament itself. Therefore, it would be difficult to diagnose this injury later in the disease process when most clinically affected joints are operated. There is also the potential that this is an injury that only occurs in the experimental transection and not in the clinical situation, although injury sustained due to instability would presumably be the same. To definitely identify and characterize this injury, further serial arthroscopic studies would need to be performed on a larger group of experimentally transected CrCL joints, or in the acute stages of naturally-occurring CrCL rupture. The clinical significance of this injury requires further investigation.

Mechanical instability of a joint, causes the synovial membrane to become inflamed along with a fibrinous and subsequent fibrous reaction of the joint capsule. The inflammatory reaction is presumed to occur in the acute stages of the injury process and then decline over time as the joint becomes more stable due to the fibrous and bony response to the instability. The severity of inflammation identified in this study was based on the morphologic changes that occurred in the synovium which were mild at day 14, and then peaked in severity by day 28. It then decreased, despite the increase in joint debris, but was not completely eliminated by day 126 (Table 3.1). The temporal synovial membrane response identified in this study is most likely a multifactorial process, that results in blockage of the lymphatics and sluggish venous drainage, and upregulation and activation of enzymes that would degrade the articular cartilage[97]. This would suggest that early stabilization may be of benefit in decreasing the amount of damage that would ensue from the instability and inflammation. However, it is important to note that since we are examining these joints only at certain defined time points, there could very well be other peaks of inflammation that were missed. The continuation of a low grade inflammatory process, in the face of increased stability by day 70 and 126, is likely due to the increased amount of particulate wear debris present within the joint, as this has been shown to cause inflammation[261].

The fibrinous and subsequent fibrous reaction of the joint after CrCL transection noted in this study was quite pronounced. Much of the initial fibrinous reaction occurred in the intercondylar region of the femur where the atrophied ends of the cruciate ligaments were covered with fibrin. Over time, this became more organized as the transected ends atrophied toward their respective bony attachment. The formation of

multiple fibrous adhesions are likely the inherent response of the joint to stabilize itself, or could simply be due to the joint instability/pathology. The joint capsule became increasingly more fibrotic in all of these dogs throughout the study. This capsular reaction is likely a generalized reaction of the joint to the instability since it has been shown that in clinical cases of CrCL rupture, the degree of periarticular thickening was significantly associated with tearing of the CrCL[146], indicating that instability plays an important role.

The results of this study are a direct result of experimental transection of the CrCL, which is more representative of the acute traumatic rupture than the chronically injured CrCL that structurally and functionally deteriorates over time[7]. Therefore, presumably, many of the same temporal changes that were found in the current study can be extrapolated to the clinical situation of acute rupture. The CrCL transection model of OA produces changes that are quite variable between dogs. This makes it difficult to say that certain pathology will occur in every dog, but even as this small group of dogs demonstrated, there are general trends in certain locations and types of injury that occur following CrCL transection. To more definitively document the early intra-articular changes that occur after CrCL transection, a larger group of dogs should be studied. The femoropatellar region was not examined in this study because it was deemed that articular cartilage damage present on the weight-bearing surfaces of the femorotibial joints would be more clinically relevant than changes to the patella. In addition, histology would allow better identification of the severity of lesions with regard to depth and extent of lesion that was created in the articular cartilage, menisci and meniscal ligaments, but this was not performed for any of these dogs.

In conclusion, this study allowed temporal identification of the damage sustained to the synovium, articular cartilage, meniscal, and meniscotibial ligament after CrCL transection. Articular cartilage and medial meniscal damage started as early as 2 weeks after CrCL transection, and generally progressed from there. Stretching or rupture of the cranial meniscotibial ligament of the medial meniscus was identified to a variable degree in all three dogs, and the clinical importance of this injury still needs to be defined. The degree of synovitis peaked at one month after CrCL transection and then decreased over time but never completely subsided. Overall, this study demonstrated that clinically relevant osteoarthritic changes start to occur as early as 2 weeks after CrCL transection and will likely progress when the joint is not stabilized.

4 IDENTIFICATION OF CHANGES IN VERTICAL GROUND REACTION FORCES COMPARED TO MENISCAL PATHOLOGY AFTER CRANIAL CRUCIATE LIGAMENT TRANSECTION IN THE DOG

Troy N. Trumble, DVM, MS, R. Clark Billinghurst, DVM, PhD, Alison M. Bendele DVM, PhD, C. Wayne McIlwraith, BVSc, PhD

To be submitted to *American Journal of Veterinary Research* in spring 2003.

4.1 Summary

Objective. To determine whether decreases in the peak vertical force of a cranial cruciate ligament (CrCL) deficient limb in the dog would be suggestive of meniscal injury when compared to gross meniscal damage.

Methods. Thirty-nine purpose-bred adult male Walker Hounds had the right CrCL arthroscopically transected and force plate measurements of the right hind limb were performed prior to, and then 2, 4, 10, and 18 weeks after transection. Only those dogs with $\geq$ 10% decrease in peak vertical force were considered to have potential meniscal injury. Based on this dividing point, dogs that did not have $\geq$ 10% decrease in peak vertical force at any point between successive measurements after week 2 were placed into group 1, which represented the "typical" response of most dogs after CrCL transection. The remainder of the groups (2-4) were defined based on when the $\geq$ 10% decrease in peak vertical force was measured. Group 2 had $\geq$ 10% decrease in peak vertical force from week 2 to week 4, and groups 3 and 4 had $\geq$ 10% decrease in peak vertical force from week 4 to week 10 and week 10 to week 18, respectively. The menisci and articular cartilage of all of the CrCL transected limbs were graded for damage at week 18 and the grades for groups 2-4 were compared to group 1.

Results. Group 1 was comprised of 27/39 (69%) dogs, and groups 2-4 had 4 dogs in each group (12/39, 31%). The percent change in peak forces and impulses (vertical and propulsion) were significantly lower in groups 2-4 at each respective measurement period (weeks 2, 4, 10, and 18) compared to group 1. The meniscal grade for groups 2-4 was significantly higher ($p=0.0035$) than for group 1, indicating significantly more damage.

Conclusion. In the CrCL deficient dog, force plate analysis can identify an acute exacerbation in lameness which may be due to secondary meniscal injury, providing a non-invasive way to delineate the temporal pattern of meniscal injury.

4.2 Introduction

Force plate analysis has been used as a research tool in dogs to objectively measure normal and abnormal forces[192,193,196-202,262-267]. It allows for description of the peak forces and impulses (total force applied over time) applied in a vertical, craniocaudal (braking and propulsion), and mediolateral directions. Many canine orthopaedic studies have included analysis of these ground reaction forces to objectively determine the normal forces applied for different gait cycles at varying velocities[192,193,196,197,262-266]. In addition, force plate analysis has measured the abnormal forces that result from insult to the appendicular skeleton, as well as the response of the limb to various surgical techniques or medical therapies used to treat the joint impairment[198-202,267].

Cranial cruciate ligament (CrCL) transection in dogs has been an accepted experimental model of osteoarthritis (OA) resulting in changes typical of the early stages of OA in both humans and dogs[98]. Transection of the CrCL in the dog causes lameness due to the instability and inflammation that is created and ultimately results in damage to all of the intra-articular structures, including the synovium, menisci, articular cartilage and subchondral bone[98,101,249]. Force plate analysis has been used to document changes in the ground reaction forces that occur as a result of CrCL rupture/transection compared to preoperative values[198-202]. These studies have shown that after CrCL rupture/transection, the mean peak vertical, braking and propulsion forces and respective impulses decreased

dramatically within the first few weeks after insult, but then slowly improved over time. Certain surgical techniques have been shown to improve this kinetic data in the early period, suggesting that the force plate is a sensitive tool for identification of subtle differences that can occur over time[199].

Medial meniscal damage is a common sequela to CrCL rupture/transection in the dog[14,145]. It is believed to occur secondary to the unrestrained cranial tibial thrust that creates cranial tibial translation with respect to the femur[10]. The types and locations of meniscal injuries have been well described in the dog[14,149], but the exact timing of meniscal tearing after CrCL rupture/transection is unknown. It has been suggested that meniscal damage could occur simultaneously with CrCL rupture, but more than likely occurs secondary to abnormal biomechanical loading due to CrCL insufficiency[143]. It is a common clinical impression that CrCL deficient dogs that have sustained meniscal injury will be more lame than those dogs that have CrCL deficiency alone[10,143,145,151]. This could be in the early period after CrCL rupture, especially if meniscal damage occurred at the same time. However, it is usually suspected in the dog that was acutely lame in the first few weeks and then started to improve, only to suffer a worsening in the lameness in the first couple of months after rupture/transection. Presumably, this worsened lameness due to meniscal damage should be detectable using the ground reaction forces generated from force plate analysis. To the authors' knowledge, comparison of objective analysis of lameness with meniscal damage after CrCL rupture/transection has not been previously reported.

The purpose of this study was to evaluate the ground reaction forces of dogs following CrCL transection and compare the decrease in peak vertical force of a cranial

cruciate deficient limb to the actual degree of meniscal injury at the end of the study. Our hypothesis was that dogs that sustained substantial meniscal injury (grade 3/3) would have a $\geq$ 10% decrease in the peak vertical force between successive measurement periods from 2 to 18 weeks after CrCL transection.

4.3 Materials and methods

The study was conducted under a protocol approved by the Colorado State University Animal Care and Use Committee. Dogs were obtained through approved sources by the Colorado State University Laboratory Animal Resources. The opportunity to study the effect of meniscal injury on the ground reaction forces developed as an adjunct to a study examining a novel therapeutic agent.

4.3.1 Animals and experimental protocol. Thirty-nine purpose-bred adult male Walker Hounds with a mean ± SD weight of 22.40 ± 2.69 kg (range, 16.8 – 29.5 kg) were studied. Upon arrival, dogs were given routine physical and hematologic examinations. Orthopedic examination included a separate lameness and physical examination of both hind limbs as well as radiographs of both stifles. In anticipation of gait analyses, each dog was acclimated for several weeks to the force platform analysis laboratory and were led by a leash at a trot across the force plate prior to inclusion. Selection and subsequent inclusion required the dogs to be free of pre-existing orthopedic disease of the stifles based on orthopedic examination and radiographs. In addition, the dogs had to be able to adequately trot across the force plate with minimal effort or coaxing from the handler.

All dogs were anesthetized, and the right hind limb was prepared for aseptic surgery. A lateral parapatellar arthroscopic approach to the right stifle was used to

examine the joint for the presence of any intra-articular pathology of the articular cartilage, cruciate ligaments and menisci. The CrCL was then transected arthroscopically using a meniscectomy blade (Chapter 2). Analgesia was administered via a 5 mg fentanyl patch (2.0 μg/kg/hr) that was applied the day before surgery and was maintained for 72 hours post-operatively. Morphine (1 mg/kg subcutaneously) was also administered post-operatively for pain, as needed. Cephalexin (Keflex) was administered intravenously during surgery and was continued orally (10 mg/kg) every 12 hours for 3 days to prevent infection. Throughout the study, all dogs were housed in individual runs. The animals were closely monitored during the first 48 hours post-operatively for any signs of pain, infection, anorexia, or intestinal complications. To encourage the development of OA, dogs were placed in an exercise protocol that required leash walking for 30 minutes every day for 5 days/week from the second day post-operatively until sacrifice at 18 weeks. All dogs were euthanized with sodium pentobarbital euthanasia solution (88 mg/kg) via intravenous injection at 18 weeks post-operatively and both stifles were disarticulated and examined grossly.

4.3.2 Gross pathology scores. Pathological grading of the menisci and articular cartilage was performed blindly by a board-certified pathologist (AMB). Meniscal degeneration was graded on a scale from 0-3 with 0 = no lesion, 1 = mild fraying or incomplete tears with or without significant fibrous replacement/repair, 2 = moderate fraying or tearing (longitudinal surface or small transverse tears) with or without significant fibrous replacement/repair, 3 = severe fraying or tearing (such as penetrating longitudinal tears – bucket handle) without significant effective fibrous replacement/repair (Figure 4.1). Cartilage damage was graded on a scale from 0-4 with 0

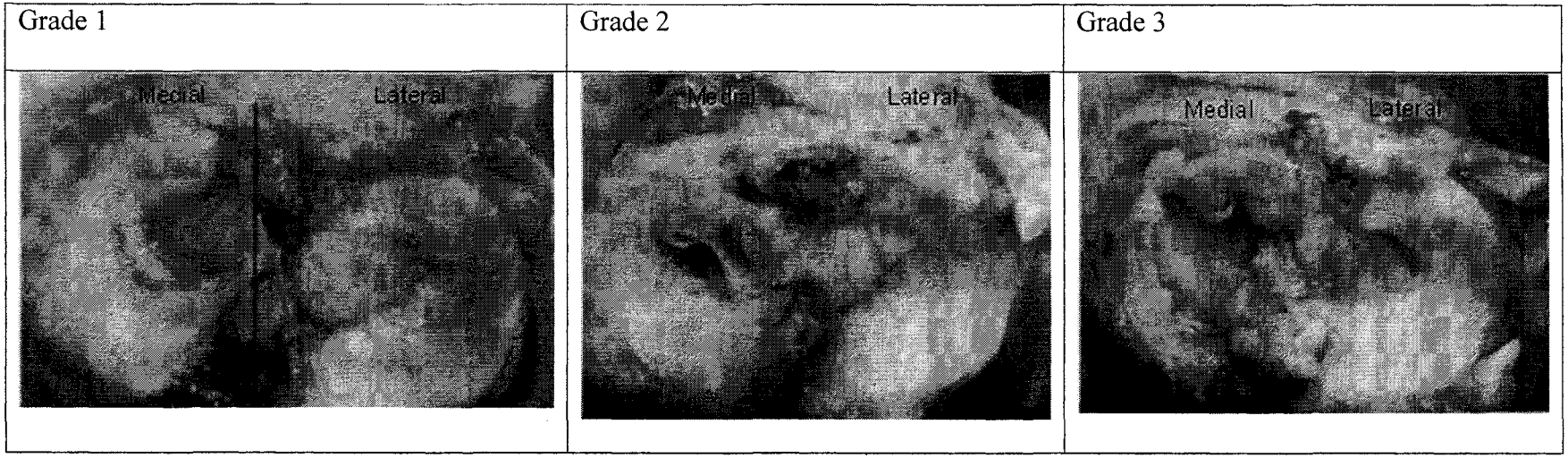

Figure 4.1. Gross appearance of the menisci after disarticulation of the stifle for each representative grade of medial meniscal damage (1-3). Medial and lateral are laballed accordingly. Grade 1 meniscal degeneration was defined as mild fraying or incomplete tears with or without significant fibrous replacement/repair. Grade 2 was defined as moderate fraying of tearing (longitudinal surface of small transverse tears) with or without significant fibrous replacement/repair. Grade 3 was defined as severe fraying of tearing (such as penetrating longitudinal tears – bucket handle) without significant effective fibrous replacement/repair.

= normal, 1 = minimal superficial fibrillation, 2 = mild to moderate fibrillation presumably into the upper middle zone, 3 = mild to moderate fibrillation and/or loss of cartilage extending to the middle zone, and 4 = severe cartilage loss extending to the deep zone or subchondral bone. A total subjective cartilage severity score was calculated by summing the cartilage damage scores on the medial and lateral tibia plateaus as well as on the medial and lateral femoral condyles (maximum score of 16).

4.3.3 Force plate evaluation. The force plate (Model ORS6-5, Advanced Mechanical Technologies Inc., Newton, MA) was mounted in the center of, and level with, the surface of a 15-m runway. The signal from the force plate was processed and stored by use of computer software programs (IBM 486Dx, IBM Co., Boca-Raton, FL and Acquire, Version 6.3W, Sharon Software Inc., Dewitt, MI). As each dog was trotted over the force plate, velocity was recorded by use of 2 photoelectric cells, placed 2 m apart, and a start-interrupt timer system. Care was taken to ensure that the dog triggered the photoelectric cells and that a constant speed was maintained across the force plate during each trial. Dogs were trotted across the force plate by one handler prior to having the CrCL transected (baseline), and then again at 2, 4, 10, and 18 weeks post transection. An evaluation was considered valid if the dog struck the plate with its right forelimb followed by its right hind limb at a velocity between 1.45 and 2.05 m/s with less than 10% acceleration/deceleration. If a dog was distracted during an evaluation, or any other paw or combination of limbs struck the force plate, then the data was considered invalid. Due to the severity of lameness present in some dogs, each dog was trotted across the force plate a maximum of 75 times per trial session, and the first five acceptable trials were collected per dog, per session. If the dog did not have five acceptable trials, then

that number of acceptable trials was used in the analysis. If the dog was completely non-weight bearing on the right hind limb, then the value entered for each trial was zero. All trials were recorded and archived on digital video. Peak vertical, braking and propulsion forces and each respective impulse were recorded for each limb at 1-millisecond intervals for 650 milliseconds after foot strike. All forces were normalized to the dog's body weight at each measurement period.

4.3.4 Calculations a nd g roupings. The acceptable trials for each dog were averaged for each ground reaction force for all force plate sessions (baseline, weeks 2, 4, 10, and 18). In order to evaluate periodic worsening in the lameness that might be associated with meniscal injury, these values were used to calculate the percent change in each ground reaction force and impulse (vertical, braking and propulsion) from one force plate session to another (baseline to week 2, week 2 to week 4, etc.). This percent change was calculated by subtracting the value for the initial measurement period from the subsequent measurement period, and this total was divided by the subsequent measurement period, and multiplied by 100. To be able to complete this calculation for those dogs that were non weight-bearing, all dogs had a value of 1 added to the peak vertical force and impulse, 0.1 to the braking and propulsion forces, and 0.001 to the braking and propulsion impulses to eliminate 0 from the calculations. A sample calculation for a positive percent change from week 2 to week 4 was determined using the described formula: [(week 4-week 2)/week 4]x100, such that [(30.78-23.17)/30.78]x100 = 25% increase from week 2 to week 4. An example of a negative percent change is [(26.26-31.78)/26.26]x100 = -21% decrease from week 2 to week 4. An increase in the percentage indicated that the dog was placing more weight on the limb

and becoming more sound, whereas a decrease indicated a worsening of the lameness. All dogs demonstrated a large decrease from preoperative values (baseline) to the two week mark after transection that has been reported to be due to the increased instability[198-202]. Meniscal injury most likely occurs when there is a period of increased lameness in the chronic CrCL deficient dog[10,143,145,151]. Therefore, only those dogs in this study that had $\geq$ 10% decrease in the peak vertical force from week 2 to week 18 were considered to have sustained recent meniscal injuries. The percent change throughout this manuscript will be described according to the subsequent measurement period since the meniscal damage could have occurred anytime between the two measurement periods. Therefore, using the example above, the percent change from week 2 to week 4 will be listed under week 4 since this is when the decrease was measured.

For further analysis, peak vertical force was used to group the dogs. Dogs were grouped according to if and when they had a $\geq$ 10 % decrease in peak vertical force between two consecutive force plate sessions after week 2. Group 1 was defined as those dogs that had an increase or < 10% decrease in peak vertical force from week 2 through to week 18. This group seems to represent the "typical" response of most dogs after CrCL transection/rupture[199-202]. Group 2 was defined as those dogs that had $\geq$ 10% decrease in peak vertical force from week 2 to week 4. Groups 3 and 4 were defined as those dogs that had $\geq$ 10% decrease in peak vertical force from week 4 to week 10 and week 10 to week 18, respectively. Table 4.1 demonstrates the percent change calculated for each grouping and ground reaction force.

4.3.5 Statistical analysis. The percent change in the mean values for the peak vertical, braking, and propulsion forces, as well as the corresponding impulses were used as the dependent variables in a mixed model ANOVA. The four groups were used as a fixed effect class variable over subsets of time, allowing examination of the differences in each respective ground reaction force between each group, at each measurement period (weeks 2, 4, 10, and 18). Tukey's pairwise comparison was also performed to distinguish differences between each group at the given force plate measurement period. All of the ground reaction forces were normally distributed based on the Kolmogorov-Smirnov test. Descriptive statistics were reported for the meniscal grades and subjective gross cartilage severity scores. The meniscal grades were not normally distributed. Two tail t-tests were used to examine differences between the groups for the meniscal and cartilage scores, respectively, and a Spearman rank correlation was performed to compare the meniscal grade to the cartilage severity scores. A value of $P<0.05$ was considered significant.

4.4 Results

4.4.1 Peak vertical force. Graphic and tabular representation of the changes in peak vertical force for each group are represented in Figure 4.2. There were 27/39 (69%) dogs that were placed into group 1, by having an increase or < 10% decrease in the peak vertical force between two successive measurements from week 2 through week 18 (Figure 4.2). All of the dogs in group 1 had a large decrease in peak vertical force at week 2 from preoperative values at baseline, which then increased at each subsequent measurement period throughout the remainder of the study (Table 4.1). The remaining 12 (31%) dogs had a $\geq$ 10% decrease in the peak vertical force between two successive measurements at some stage after week 2. Groups 2-4 were each comprised of 4 dogs

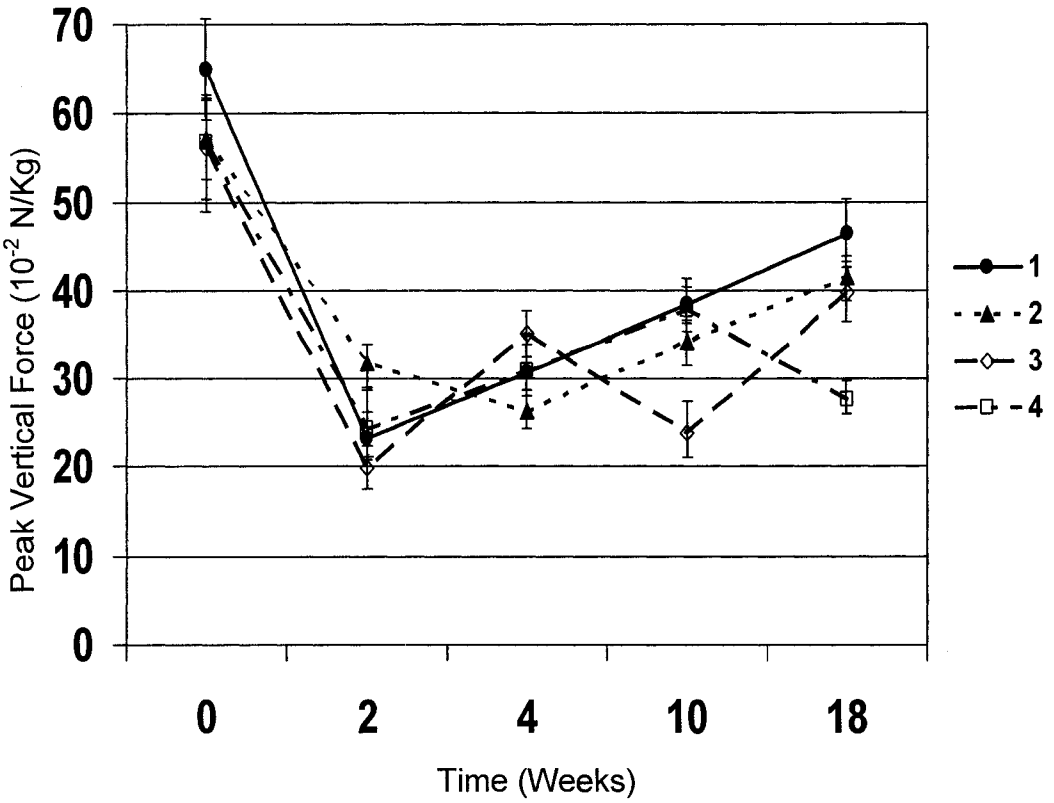

	Time (weeks)				
Group	0	2	4	10	18
1 (•) (n=27)	65.02 ± 5.81	**23.17** ± 2.67	30.78 ± 3.60	38.46 ± 2.89	46.37 ± 3.87
2 (▲) (n=4)	57.20 ± 4.77	**31.78** ± 2.90	**26.26** ± 1.89	34.20 ± 3.11	41.54 ± 2.12
3 (◊) (n=4)	56.12 ± 6.35	**19.80** ± 1.87	35.12 ± 1.81	**23.83** ± 2.49	39.75 ± 3.58
4 (□) (n=4)	56.78 ± 6.14	**24.22** ± 3.77	30.90 ± 3.48	37.78 ± 2.54	**27.68** ± 1.85

Figure 4.2: Graphical and tabular representation of the mean (± SD) peak vertical force of each group (1, 2, 3, and 4) for each measurement period (0, 2, 4, 10, and 18). Decreases in the peak vertical force from one measurement period to the next are highlighted in bold in the table. Each decrease in peak vertical force was ≥ 10% of the previous measurement period. Notice that all dogs had a large decrease at week 2. Group 1 (•) then increased throughout the remainder of the study. This is the typical response after CrCL rupture. Group 2 (▲) continued to decrease at week 4 and then increased. Group 3 (◊) increased at week 4, but then decreased at week 10 before increasing at week 18. Group 4 (□) increased from week 2 to week 10, and then decreased at week 18.

Table 4.1. The mean (± SD) calculated percent change for each ground reaction force for each group of dogs (groups 1, 2, 3, and 4) for each respective measurement period (2, 4, 10, and 18), such that week 2 represents the percent change from the measurement at week 2 compared to baseline. Negative values are highlighted in bold representing the percentage in which the ground reaction force decreased from the previous measured value.

		Time (weeks)			
Ground Reaction	**Group**	**2**	**4**	**10**	**18**
Peak Vertical	**1**	**-804** ± 1885	24 ± 26	19 ± 12	17 ± 20
	2	**-88** ± 51	**-21** ± 13	23 ± 9	16 ± 15
	3	**-1881** ± 3580	40 ± 39	**-772** ± 1510	43 ± 37
	4	**-138** ± 22	20 ± 13	19 ± 13	**-39** ± 21
Vertical Impulse	**1**	**-226** ± 258	21 ± 22	14 ± 13	13 ± 19
	2	**-104** ± 55	**-27** ± 20	31 ± 10	12 ± 17
	3	**-360** ± 509	29 ± 39	**-113** ± 196	41 ± 30
	4	**-132** ± 38	14 ± 18	16 ± 15	**-37** ± 18
Peak Propulsion	**1**	**-1170** ± 3130	19 ± 32	19 ± 17	16 ± 23
	2	**-76** ± 67	**-33** ± 22	16 ± 33	20 ± 29
	3	**-2857** ± 5674	15 ± 74	**-1514** ± 2977	30 ± 47
	4	**-109** ± 90	21 ± 19	18 ± 16	**-60** ± 34
Propulsion Impulse	**1**	**-10914** ± 32136	18 ± 37	21 ± 21	10 ± 28
	2	**-76** ± 75	**-38** ± 32	20 ± 43	11 ± 37
	3	**-27327** ± 54449	41 ± 45	**-14777** ± 29482	34 ± 50
	4	**-113** ± 190	2 ± 51	14 ± 23	**-62** ± 64
Peak Braking	**1**	**-739** ± 1328	**-1** ± 120	**-15** ± 85	17 ± 44
	2	**-985** ± 1793	25 ± 59	**-329** ± 485	1 ± 12
	3	**-2309** ± 4288	**-147** ± 262	**-63** ± 107	**-14** ± 88
	4	**-1000** ± 1162	41 ± 34	13 ± 84	**-72** ± 163
Braking Impulse	**1**	**-3007** ± 5834	**-12** ± 168	**-77** ± 260	20 ± 59
	2	**-4409** ± 8264	14 ± 124	**-1121** ± 1929	**-14** ± 75
	3	**-8600** ± 16002	**-1720** ± 2656	21 ± 49	17 ± 56
	4	**-3591** ± 4941	10 ± 65	**-44** ± 179	14 ± 71

(Figure 4.2). By definition, group 2 dogs had an additional $\geq$ 10% decrease in the peak vertical force from force plate measurements taken at week 4 compared to week 2 (Table 4.1). Group 3 dogs had an additional $\geq$ 10% decrease in the peak vertical force at the week 10 measurement period compared to week 4, and group 4 dogs had a decrease in peak vertical force at week 18 compared to week 10 (Table 4.1). Table 4.2 contains the pairwise comparisons (Tukey's) of the percent change in ground reaction forces for groups 2, 3, and 4 versus group 1 for each measurement period. There was no statistical difference between groups in the percent decrease at the week 2 measurement period for any of the ground reaction forces. However, the percent change in peak vertical forces in group 2 at week 4 was significantly lower ($p=0.0021$) than that for group 1. At week 10 and week 18, the percent change in peak vertical force was significantly lower for group 3 ($p=0.002$ and 0.0304, respectively) than group 1, and the percent change in the peak vertical force for group 4 was significantly lower than group 1 ($p=0.0001$) at week 18.

The mean $\pm$ SD meniscal grade for the 12 dogs in groups 2-4 was 2.58 $\pm$ 0.67, (Table 4.3) which was significantly higher ($p=0.0035$) than for the 27 dogs in group 1 (1.56 $\pm$ 0.89). When compared to all of the meniscal grades, these 12 dogs represented 8/14 (57%) grade 3, 3/7 (43%) grade 2, 1/17 (6%) grade 1, and 0/1 (0%) grade 0 lesions. The mean $\pm$ SD subjective gross cartilage severity score for the 4 dogs in group 2 (10.75 $\pm$ 3.30) was significantly higher ($p=0.0082$) than for the 27 dogs in group 1 (6.63 $\pm$ 2.63). However, when the cartilage severity score for the 12 dogs in groups 2-4 were combined, (Table 4.3) the mean $\pm$ SD score was only 8.67 $\pm$ 3.28, which was significantly higher ($p=0.046$) than group 1. There were no significant correlations between the

Table 4.2: Tukey's multiple pairwise comparisons of the percent change at each respective measurement period (2, 4, 10, and 18) focusing on the comparison between groups 2, 3, and 4 to group 1 for each ground reaction force. P values are shown for each comparison. The overall group significance for each ground reaction force is underlined and italicized for each measurement period. Level of significance was set at $P<0.05$ and significant differences are highlighted in bold only if there was an overall significant group effect.

Pairwise Comparisons	Time (weeks)			
	2	4	10	18
Peak Vertical	*0.0989*	*0.0001*	*0.0291*	*0.0001*
Group 1 vs. 2	0.4941	**0.0021**	0.9864	0.9521
1 vs. 3	0.3058	0.2598	**0.0020**	**0.0304**
1 vs. 4	0.5242	0.7903	0.9993	**0.0001**
Vertical Impulse	*0.0003*	*0.0001*	*0.0051*	*0.0001*
Group 1 vs. 2	0.4038	**0.0005**	0.5936	0.9593
1 vs. 3	0.3582	0.4834	**0.0003**	**0.0117**
1 vs. 4	0.5177	0.5794	0.9614	**0.0001**
Peak Propulsion	*0.1643*	*0.0247*	*0.0306*	*0.0001*
Group 1 vs. 2	0.5236	**0.0117**	0.9959	0.7813
1 vs. 3	0.3270	0.8450	**0.0023**	0.3425
1 vs. 4	0.5362	0.9082	0.9980	**0.0001**
Propulsion Impulse	*0.2181*	*0.0156*	*0.0343*	*0.0046*
Group 1 vs. 2	0.5309	**0.0110**	0.9998	0.9695
1 vs. 3	0.3443	0.2818	**0.0029**	0.2176
1 vs. 4	0.5323	0.4386	0.9987	**0.0006**
Peak Braking	*0.0201*	*0.2524*	*0.0071*	*0.1717*
Group 1 vs. 2	0.8012	0.7171	**0.0011**	0.6377
1 vs. 3	0.1145	0.0439	0.5935	0.3776
1 vs. 4	0.7896	0.5522	0.7533	0.0162
Braking Impulse	*0.0302*	*0.0038*	*0.0168*	*0.4954*
Group 1 vs. 2	0.7268	0.9514	**0.0030**	0.3158
1 vs. 3	0.1687	**0.0003**	0.7652	0.9258
1 vs. 4	0.8841	0.9597	0.9181	0.8616

Table 4.3: The mean (± SD) meniscal grade (0-3) and corresponding total subjective gross cartilage severity score for each group (1, 2, 3, and 4). The Spearman rank correlation between the meniscal grade and cartilage severity score is listed for each group.

Group	Meniscal Grade (Mean ± SD)	Cartilage Severity Score (Mean ± SD)	Spearman Rank Correlation
1	1.56 ± 0.89	6.63 ± 2.63	r=0.1628 (p=0.4172)
2	2.50 ± 0.58	10.75 ± 3.30	r=0.2357 (p=0.9167)
3	2.75 ± 0.50	7.00 ± 3.74	r=0.7746 (p=0.3333)
4	2.50 ± 1.00	8.25 ± 2.22	$r=7.38X10^{-20}$ (p=0.2530)

meniscal grades and gross cartilage severity scores for any of the groups, or combination of groups (Table 4.3).

4.4.2 Vertical impulse. Similar to the peak vertical force, the vertical impulse for all dogs in group 1 decreased at week 2, but then increased at week 4, week 10, and week 18 (Table 4.1). Group 2 dogs had a 27% average decrease in the vertical impulse from force plate measurements taken at week 4 compared to week 2, whereas group 3 dogs had a 113% decrease at week 10 compared to week 4, and group 4 dogs had a 37% decrease in vertical impulse at week 18 compared to week 10 (Table 4.1). There was no statistical difference between groups in the percent decrease in vertical impulse at the week 2 measurement period (Table 4.2). However, at week 4, group 2 had a significantly lower percent change (p=0.0005) compared to group 1. At week 10 and week 18, group 3 had a significantly lower percent change (p=0.0003 and 0.0117, respectively) than group 1, and the percent change in the vertical impulse for group 4 was significantly lower than group 1 (p=0.0001) at week 18 (Table 4.2).

4.4.3 Peak propulsion force. The changes in the peak propulsion force were similar to the findings of peak vertical force, in that the percent change in peak propulsion force for all dogs in group 1 decreased at week 2, but then increased at week 4, week 10, and week 18 (Table 4.1). Group 2 dogs had a 33% average decrease in the peak propulsion force from force plate measurements taken at week 4 compared to week 2, whereas group 3 dogs had a 15-fold decrease at week 10 compared to week 4, and group 4 dogs had a 60% decrease in peak propulsion force from week 18 compared to week 10 (Table 4.1). There was no statistical difference between groups in the percent decrease at the week 2 measurement period (Table 4.2). However, at week 4, group 2 had a significantly lower percent change ($p=0.0117$) compared to group 1. At week 10, group 3 had a significantly lower percent change ($p=0.0023$) than group 1, and the percent change in the vertical impulse for group 4 was significantly lower than group 1 ($p=0.0001$) at week 18 (Table 4.2).

4.4.4 Propulsion impulse. The changes in the propulsion impulse were similar to the findings of the peak propulsion force, in that the percent change in propulsion impulse for dogs in group 1 decreased at week 2, but then increased at week 4, week 10, and week 18 (Table 4.1). Group 2 dogs had a 38% average decrease in the propulsion impulse from force plate measurements taken at week 4 compared to week 2, whereas group 3 dogs had a 148-fold decrease at week 10 compared to week 4, and group 4 dogs had a 62% decrease in propulsion impulse at week 18 compared to week 10 (Table 4.1). There was no statistical difference between groups in the percent decrease at the week 2 measurement period (Table 4.2). However, at week 4, group 2 had a significantly lower percent change ($p=0.0110$) compared to group 1. At week 10, group 3 had a significantly

lower percent change (p=0.0029) than group 1, and the percent change in the vertical impulse for group 4 was significantly lower than group 1 (p=0.0006) at week 18 (Table 4.2).

4.4.5 Braking force and impulse. The peak braking force and impulse did not follow the same pattern of percent change as described for the other ground reaction forces. The mean percent change in the peak braking force and impulse for group 1 decreased in all of the dogs at week 2, and then continued to decrease at week 4 and week 10 before increasing at week 18 (Table 4.1). Instead of dogs in groups 2-4 all experiencing decreases in the peak breaking force and impulse, as was the case with the other ground reaction forces, 6/12 had an increase in the peak braking force and 9/12 had an increase or no change in the braking impulse. Of the 6 dogs that had an increase in the peak braking force, 3 were in group 1, 1 in group 3, and 2 in group 4. For these 6 dogs that had an increase in the peak braking force, there was also an increase in the braking impulse. An additional dog in group 3 had an increased braking impulse, and 2 dogs had no change in the braking impulse. Because of this relative difference, the mean ± SD changes in peak braking force and impulse did not follow a predictable pattern, and are summarized in Table 4.1. Significant differences in the percent changes for groups 2, 3, and 4 compared to group 1 at each measurement period are listed in Table 4.2. The mean ± SD meniscal grade for those 6 dogs that had an increase in the peak braking force was 2.83 ± 0.41 compared to 2.33 ± 0.82 for those that had decreased, but this difference was not statistically different (p=0.21). The mean ± SD meniscal grade for those 7 dogs that had an increase in the braking impulse was 2.80 ± 0.38 compared to 2.67 ± 0.58 for those

had decreased, with there being no statistical difference (p=0.54) between these two groupings.

4.5 Discussion

Many force plate studies have documented the changes that occur in the ground reaction forces of the hind limb after rupture or transection of the cranial cruciate ligament[198-202]. The most predictable changes have been reported to occur with the peak vertical force and its respective impulse (total force applied over time). For both of these ground reaction forces, there is a large decrease from preoperative values for the dogs in the first 2 to 4 weeks that is presumed to be a direct result of pain related to instability[198-202]. Over time, most dogs will then start to use the limb more as the inflammation subsides and the joint becomes more stable as the capsule becomes more fibrotic. This is demonstrated by continual improvement in the amount of force placed on the ground by the injured limb until a plateau is reached by about 10 months post-transection with the peak vertical force remaining below original baseline levels out to 3 years[202]. The results for the peak vertical force for the 27 dogs in group 1 of our study fit this pattern. They all had a large decrease in peak vertical force by 2 weeks, with a gradual increase in the amount of weight being placed on the limb from that time on (Figure 4.2, Table 4.1). Therefore, group 1 was used as the comparative group in this study. In other words, it was viewed as the typical response that most dogs would follow after CrCL transection, such that if any dog had a decrease in the peak vertical force that was different than this group, it would be suspicious of meniscal damage.

Often in the clinical situation when there is an acute exacerbation of lameness in the CrCL deficient dog, medial meniscal damage is suspected[10,143,145,151]. Damage to the

medial meniscus has been thought to occur as a result of the instability created by the CrCL deficiency, not as a result of the initial injury[143]. The most common meniscal damage identified during CrCL surgery is a longitudinal tear of the caudal horn of the medial meniscus which likely happens because the caudal horn acts as the main secondary stabilizer to the cranial tibial thrust[268,269]. The location of the tear, combined with the cranial tibial thrust, allows the torn portion of the meniscus to slide between the femur and the tibia. This abnormal impingement of the meniscal tissue will presumably cause the dog to become acutely more lame. Therefore, clinically, following CrCL rupture, any dog that either remains very lame in the initial period, or becomes acutely lame within the first few months after it has shown improvement, is assumed to have sustained secondary meniscal damage[10,143,145,151]. To the authors' knowledge, this has been a subjective assessment only and has not been monitored using force plate analysis.

Since this is the first description of trying to identify meniscal damage using the force plate, we had to define the magnitude of decrease that would be presumptive of meniscal damage. Since meniscal injury tends to cause a rather large increase in lameness, we presumed that only those dogs with $\geq$ 10% decrease in peak vertical force would be representative of possible meniscal injury. This percent decrease was chosen as a value that would be identifiable as an acute onset of lameness on subjective assessment. Most of the dogs that had a noticeable increase in lameness had a $\geq$ 10% decrease in the peak vertical force, whereas an increase in the degree of lameness was not as obvious for the 8 other dogs that had smaller decreases in peak vertical force (mean $\pm$ SD 3.32% $\pm$ 2.10%) at some point throughout the study. Therefore, it appeared that a cutoff at a 10% decrease appeared to best mimic the clinical picture of detectable meniscal injury.

Based on this dividing point, dogs that did not have a $\geq$ 10% decrease in peak vertical force at any point between successive measurements after the week 2 measurement period, were placed into group 1. The remainder of the groups (groups 2-4) were defined based on when the $\geq$ 10% decrease in peak vertical force was measured. Our results demonstrated that there was a significantly higher (p=0.0035) average meniscal grade for these 12 dogs in groups 2-4 compared to group 1 (Table 4.3). In fact, when examining all of those dogs with grade 3 meniscal injury in this study, the majority (57%) were in groups 2-4. In a concurrent study performed in this laboratory, 3 dogs underwent force plate examinations and serial arthroscopies at the same time points (Chapter 3). One of the dogs developed a bucket handle tear of the caudal pole of the medial meniscus between the week 4 and week 10 arthroscopies and also experienced a 27% decrease in peak vertical force at the week 10 force plate measurement period (unpublished data). Based on this arthroscopic data and the typical clinical situation after CrCL rupture[10,143,145,151], it is reasonable to extrapolate that the acute exacerbation in lameness observed in these dogs could be due to recent meniscal injury. In the CrCL deficient joint, the menisci are one of the few structures that can become acutely injured and cause an acute exacerbation in lameness since it causes mechanical interference that can lead to pain from inflammation, as well as a "locking" or "giving way" of the limb[10]. However, the fact remains that this is a presumption based on our arthroscopic findings and clinical impression, because the menisci of the dogs in this study were not examined or graded until the end of the study at 18 weeks.

Articular cartilage damage could potentially contribute to the increase in lameness, but rarely does cartilage damage occur rapidly enough to cause an acute

worsening in the lameness unless a cartilage flap is present. More than likely, cartilage damage is going to result in a slowly progressive lameness that probably contributes to CrCL deficient dogs never reaching preoperative peak vertical force levels[202]. However, dogs in groups 2-4 of this study did have slightly significantly higher cartilage severity scores ($p = 0.046$) when compared to group 1. The most likely explanation for this would be that cartilage damage likely increases as meniscal damage increases, but the results of a previous report[249], as well as the failure to detect significant correlations for our data do not support this. Therefore, we cannot rule out that cartilage damage might contribute to some of the changes in the ground reaction forces found in this study.

The division of the dogs into groups 2-4 was according to when the decrease in peak vertical force occurred. This allowed us to examine the relative time frame in which meniscal injury may occur. As demonstrated in Figure 4.1, presumed meniscal injury occurred as early as 2-4 weeks, and as late as 10 to 18 weeks after CrCL transection. Since there were 4 dogs in each of these groups, there did not appear to be a predominate time in which most dogs injured their meniscus. Those dogs that experienced a decrease in peak vertical force at week 4 compared to week 2 could have simply represented a continuation of the pain response due to the instability, and not represent meniscal injury. In fact, this group of dogs had the most prominent cartilage changes present of any of the groups, suggesting that there was longer lasting effects of the instability. However, since the cartilage and menisci were not examined until the end of the study, it is impossible to determine exactly what caused the continued decrease in peak vertical force in these 4 dogs. In the separate serial arthroscopic study of 3 CrCL deficient dogs performed in this laboratory (Chapter 3), both medial meniscal and cartilage fibrillation started as early as 2

weeks after CrCL transection. However, by 4 weeks, medial meniscal damage tended to progress more rapidly than the cartilage degeneration. Therefore, the potential for meniscal injury causing an increase in lameness cannot be ruled out 4 weeks after CrCL transection.

The changes in the vertical impulse, peak propulsion force, and propulsion impulse in this study were similar to previous reports of CrCL deficient dogs[198,199], and mirrored the changes in the peak vertical force in each respective group (Table 4.1 and 4.2). However, the changes in the peak braking force and braking impulse after CrCL deficiency were different from these previous reports. The changes in group 1 decreased relative to preoperative values, as expected, but the changes in groups 2-4 were unpredictable. After week 2, 50% of the dogs increased their peak braking force and 58% increased their braking impulse in groups 2-4. A plausible explanation for this may be that this increase in the braking forces may be related to greater meniscal pathology, where the dog is forced to stab its paw down when placing it on the ground. However, even though the meniscal grade was higher for those dogs that showed an increase in the peak braking force and the braking impulse, there was no statistical difference from those dogs that had a decrease. These changes in braking force and impulse may be somewhat inconsequential since the hind limbs are mostly responsible for propulsion of the dog at a trot, making minor differences in the braking forces irrelevant[192].

The collection of the force plate data in this study was performed so that the previously identified sources of variability would be minimized[196,197,264,265]. However, individual variation among and within each dog with regards to its response to CrCL transection was difficult if not impossible to control for, and could have affected some of

the results. Twenty of the dogs used in this study, were administered a novel therapeutic agent, but were included in this study because there were no differences identified in the ground reaction forces between the treatment and placebo groups. Therefore, the likely affect of the drug on the results of the force plate analyses are minimal.

In summary, this study demonstrates that a $\geq$ 10% decrease in the peak vertical force identified in successive measurements made at some point between 2 and 18 weeks could represent recent medial meniscal injury since there was a significantly higher meniscal grade for these dogs when compared to dogs that had improved lameness during the same period. This provides a potential non-invasive way to objectively delineate the temporal pattern of meniscal injury after CrCL rupture/transection.

5 VARIABILITY OF MACROSCOPIC AND MICROSCOPIC PATHOLOGY IN OSTEOARTHRITIS SECONDARY TO CRANIAL CRUCIATE LIGAMENT TRANSECTION IN DOGS

Troy N. Trumble DVM, MS, Alison M. Bendele DVM, PhD, R. Clark Billinghurst DVM, PhD, C. Wayne McIlwraith BVSc, PhD

To be submitted to *Osteoarthritis and Cartilage* in spring 2003.

5.1 Summary

Objective. Cranial cruciate ligament (CrCL) transection in the dog is a commonly used model of osteoarthritis (OA) even though there is little reported on the variability in the pathological changes produced between dogs. The present study evaluates the variability in the gross and histologic pathology between a large group of dogs after CrCL transection.

Methods. Nineteen mature purpose-bred male Walker Hounds had the right CrCL transected arthroscopically, and the dogs were subjected to a controlled exercise regimen for 18 weeks. Gross and histologic analyses of both stifles were subsequently performed to determine the relative incidence, type, location and severity of intra-articular degenerative changes present.

Results. The gross and histologic lesions induced by CrCL transection were highly variable between dogs with respect to incidence, location, severity, and type. The coefficient of variation (CV) for the macroscopic and microscopic scores ranged from 21-436% and 27-424%, respectively. The majority of degenerative changes were present on the medial tibial plateau, especially on the cranial aspect. The most common change on the femoral condyle was located at the junction between the medial femoral condyle and the trochlear ridge.

Conclusion. The presently described between-subject variation in degenerative changes produced secondary to CrCL transection should be an important consideration when planning to use this model for future projects, or when drawing conclusions from studies that use a small number of dogs.

5.2 Introduction

Many different animal models of osteoarthritis (OA) have been used to mimic the early stages of OA in humans and dogs. One of the most common models used is the cranial (anterior) cruciate ligament (CrCL) transection model in the dog[139]. Transection of the CrCL in the dog causes instability and inflammation within the joint that leads to changes in the synovium, menisci, articular cartilage, and subchondral bone[1,249]. Many studies have utilized this model to either describe the pathological changes that occur in the intra-articular structures over time following transection[1,98,100-102,105-107,118-120,128,134], or utilize it to determine whether different therapeutic agents are capable of modifying the intra-articular changes that occur with secondary OA[109-116,124,270].

It has been stated that one of the main advantages of the CrCL transection model is that the time of onset of the insult is known and that lesions are reproducible in certain locations[95]. However, the reality is that different laboratories have found differing locations and degrees of articular cartilage and meniscal injuries with the use of this model. It has been suggested that this variability may be due to many potential factors that can differ between each laboratory, including the breed, age and weight of the dogs used, the technique used to transect the cruciate ligament, and the amount of exercise the dog receives after transection[140]. Another important factor that has been rarely mentioned is the fact that there can be considerable between-subject variation in the types and locations of lesions present within the same laboratory setting. In other words, even when the same relative age, weight, breed of dog, surgical technique, and exercise protocol are used, there can be considerable variation in the pathology present between the dogs. For example, Brandt, et al. examined the long term OA changes that developed

in 3 dogs after cruciate ligament transection and found extensive cartilage ulceration on > 50% of the medial and lateral tibial plateaus of one dog, > 50% ulceration of only the medial tibial plateau on the second, and only mild fibrillation of both tibial plateaus on the third[1].

Most of the studies that have been performed utilizing this model have been to elucidate the temporal patterns of response of the articular cartilage, synovium, menisci, and/or subchondral bone to the instability created by CrCL transection. Many of these studies have utilized less than 4 dogs per time point in order to be able to examine different stages of the disease process, and conclusions have drawn based on the results from only a few dogs[1,98,99,102,103,105-107,118-120,128-130,134]. When this OA model has been used to determine the usefulness of different therapeutic agents, more dogs have generally been used, but rarely more than 7 per treatment group[109-116,123,124]. Since most of the therapeutic agents being tested are expected to have some effect on the degree of articular cartilage damage, there must not be a large amount variability present between the treated and control dogs, or else a treatment response may be masked.

This study will demonstrate that with a larger group of dogs (19), there is considerable variability present between dogs in the incidence, type, location and severity of lesions that are created after CrCL transection. Knowledge of this amount of variability is important when trying to compare the gross and histopathologic scores of various groups.

5.3 Materials and methods

5.3.1 Experimental design. Nineteen purpose-bred adult male Walker Hounds with a mean ± SD weight of 22.42 ± 2.39 kg (range, 19-28.5 kg) were studied. These

dogs were the placebo control group in a larger study of a novel therapeutic agent. Inclusion criteria required the dogs to be free of pre-existing orthopedic disease of the stifles (equivalent to the human knee) based on routine physical, orthopaedic, lameness, radiographic, and force plate examinations.

All dogs were anesthetized, and the right hind limb was prepared for aseptic surgery. A lateral parapatellar arthroscopic approach to the right stifle was used to examine the joint for the presence of any intra-articular pathology of the articular cartilage, cruciate ligaments and menisci. The CrCL was then transected arthroscopically using a meniscectomy blade (Chapter 2). Analgesia was administered via a 5 mg fentanyl patch (2.0 μg/kg/hr) that was applied the day before surgery and was maintained for 72 hours post-operatively. Morphine (1 mg/kg subcutaneously) was also administered post-operatively for pain, as needed. Cephalexin (Keflex) was administered intravenously during surgery and was continued orally (10 mg/kg) every 12 hours for 3 days to prevent infection. Throughout the study, all dogs were housed in individual runs. The animals were closely monitored during the first 48 hours post-operatively for any signs of pain, infection, anorexia, or intestinal complications. To encourage the development of OA, dogs were placed in an exercise protocol that required leash walking for 30 minutes every day for 5 days/week from the second day post-operatively until 18 weeks post-operatively. All dogs were humanely euthanized at 18 weeks with an overdose of pentobarbital (88 mg/kg).

All dogs were obtained through approved sources by the Colorado State University Laboratory Animal Resources, and the study was conducted under a protocol approved by the Colorado State University Animal Care and Use Committee.

5.3.2 Macroscopic grading of lesions. Immediately after sacrifice, the right and left stifles of all dogs were opened and the lesions were described, measured, and photographed by a board-certified pathologist (AMB). Gross pathology was subjectively graded for synovial thickening, the degree of medial and lateral meniscal damage, osteophyte formation, and articular cartilage degeneration. The synovial membrane was subjectively graded on a scale of 0-3, where: 0 = normal, 1 = mild thickening, 2 = moderate thickening, or 3 = severe thickening. Meniscal degeneration was graded on a scale from 0-3 with 0 = no lesion, 1 = mild fraying or incomplete tears with or without significant fibrous replacement/repair, 2 = moderate fraying or tearing (longitudinal surface or small transverse tears) with or without significant fibrous replacement/repair, 3 = severe fraying or tearing (such as penetrating longitudinal tears – bucket handle) without significant effective fibrous replacement/repair. The presence of osteophytes on the tibia and femur were subjectively graded on a scale of 0-3 as follows: 0 = none, 1 = small (1-2 mm), 2 = medium (2-3 mm, many or a few large $\geq$ 4 mm), or 3 = large (3-5 mm, many, often with recontouring of the shape of the surface).

The evaluations of articular cartilage degeneration and osteophyte formation were divided into two basic compartments: one being the tibial plateaus, and the other being the femoral condyles. Lesion locations for the tibial plateaus were identified as cranial, middle, the area not protected by the meniscus, and caudal. Lesion locations for the femoral condyles were proximal, central weight bearing, and central non-weight bearing. Actual measurements of articular cartilage lesions were made using a micrometer to derive a calculated set of data points based on length X width X depth score. The depth of articular cartilage damage was graded on a scale from 0-4 with 0 = normal, 1 =

minimal superficial fibrillation, 2 = mild to moderate fibrillation presumably into the upper middle zone, 3 = mild to moderate fibrillation and/or loss of articular cartilage extending to the middle zone, and 4 = severe cartilage loss extending to the deep zone or subchondral bone.

5.3.3 Microscopic grading of lesions. After gross examination, the proximal end of the tibia and distal end of the femur were removed using a band saw to preserve the articular surfaces in 10% neutral buffered formalin for 5 days. The sections of femurs and tibias from both stifles were then decalcified in formic acid and prepared for histopathologic evaluation. The surface area of the tibia and femur were divided into 4 compartments of the articular surface (medial tibia, lateral tibia, medial femur, and lateral femur). Each compartment was further subdivided into 3 basic regions (cranial, weight bearing, and caudal). For each region, 1-2 slabs of bone/cartilage, approximately 2-3 mm thick, were processed, embedded in paraffin, and sectioned for each dog (Figure 5.1). A similar approach was applied to the femoral condyles. Histologic sections were stained with toluidine blue. Synovial membrane was removed from the cranial portion of the joint and was placed in formalin for sectioning (5μm) and staining with hematoxylin and eosin.

Synovial pathology was scored on scale from 0-3 with 0 = none to minimal cellular infiltrate, 1 = mild subacute inflammation with evidence of synoviocyte hyperplasia, 2 = moderate subacute inflammation with mild to moderate synovial hyperplasia, and 3 = severe subacute inflammation with moderate to severe synovial hyperplasia. Osteophytes for each compartment (medial tibia, lateral tibia, medial femur and lateral femur) were measured using a previously described imaging system[97]. They

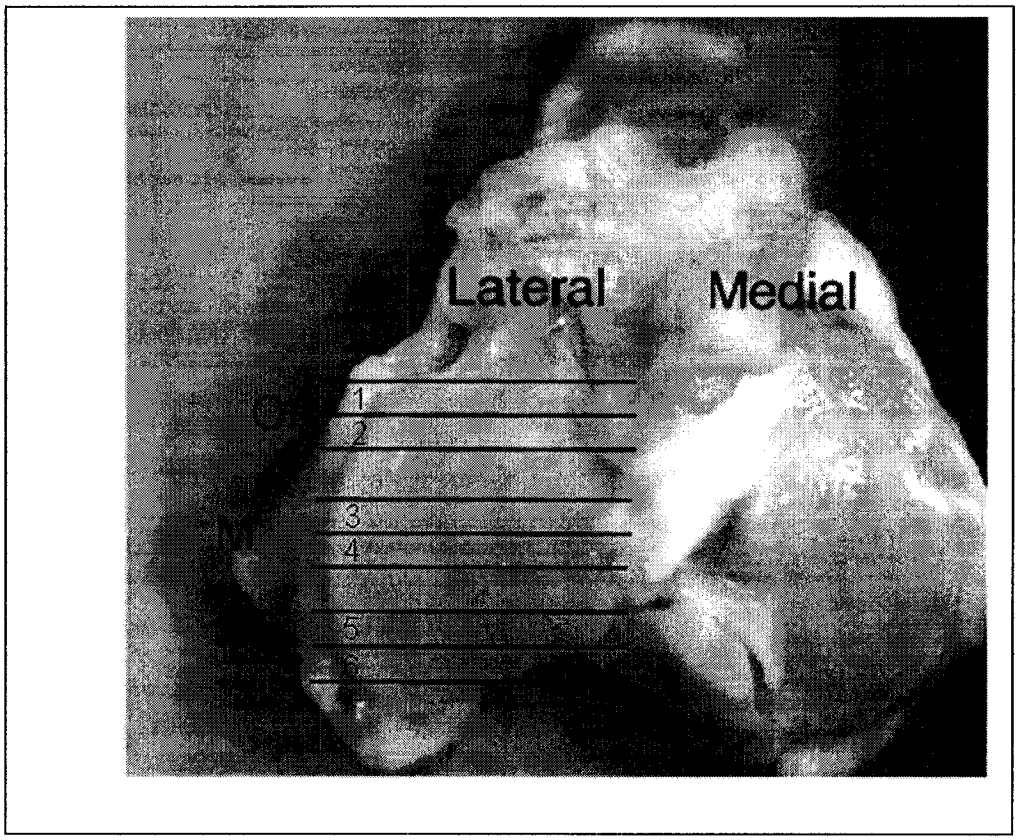

Figure 5.1. Normal left tibial plateau with lines superimposed on the lateral compartment of the tibial plateau to show the approximate regions of tissue trimming into slabs prior to processing and embedding for histologic analysis. The Cr lines represent the generation of 2 cranial sections (1 and 2), the M lines approximate areas of the middle weight bearing sections (3 and 4) and the Cd lines show the areas where caudal sections (5 and 6) were taken. Medial tibial plateaus were similarly sectioned. Medial and lateral tibial plateaus were separated prior to trimming. A similar approach was applied to the trimming of the femur.

were measured from the basal endochondral ossification to the surface of the cartilage cap and severity grades were assigned according to the size, as follows: 0 = none, 1 = up to 2000 μm, 2 = 2001 to 3000 μm, and 3 = 3001 or greater μm.

Compartmentalized articular cartilage lesions on medial tibia, medial femur, lateral tibia and lateral femur were scored for each of the regions. If 2 sections of tissue were present on the slide, the lesion score reflects the worst case scenario. For cartilage degeneration, lesions were graded according to the depth/severity and area involved. The depth/severity was graded on a scale of 0-5 (0 = none, 1=superficial, 2=upper 1/3,

3=middle zone, 4=deep zone but not to tidemark, 5=extending to tidemark) based on depth and character of the lesion. The area involved (fraction of the total surface, i.e. 1/3, 1/2, etc. up to 1=entire surface) was multiplied by the depth/severity score to arrive at a value for a single section. Values for each of the 3 regions were then summed to give a total for each compartment. Total values for cartilage degeneration parameters were separately determined for tibia and femur. Single objective depth measurements in areas of greatest lesion severity were taken using a previously described imaging system[97] for each section, and consisted of measurements taken from the surface (or estimated original surface when severe degenerative changes were present) to the point where cartilage appeared normal. A second measurement was taken in this same area to the depth of the tidemark so that the number expressed was a ratio of lesion depth vs. depth of tidemark. Measurements of the width of the total lesion of any type (chondrocyte death, cloning, fibrillation, proteoglycan loss) were taken across the tibial and femoral surfaces to give a total lesion width.

Subchondral bone was subjectively examined for each section, and changes were described, but no scoring pattern was assigned.

5.3.4 Statistical analysis. Descriptive statistics including the mean, standard deviation, variance, and coefficient of variation (CV) were generated for all of the gross and histologic data. Spearman rank correlation was used to correlate the medial meniscal grade to the gross articular cartilage score on the cranial aspect of the medial tibial plateau. Power analysis was performed using a one sample t-test on the overall mean and standard deviation for the gross scores listed in Table 5.1, using the average variance (0.6) as smallest difference that would be important to detect a significant difference. A

value of $P<0.05$ was considered significant for all analyses. All statistical analyses were performed using SAS software (SAS Institute, Cary, NC).

5.4 Results

5.4.1 Macroscopic findings. Gross pathologic changes to the synovium, menisci, articular cartilage and bone were minimal to non-existent in the left non-operated stifles. A few dogs had mild superficial fibrillation of the articular cartilage on the region of the medial tibial plateau not protected by the meniscus. Moreover, no osteophytes were present in these non-transected stifles.

5.4.1.1 Synovial membrane. There was moderate to severe thickening and fibrosis of the synovium and joint capsule in the operated right stifles, with villous hypertrophy often present as reflected in a mean ± SD grade of 2.42 ± 0.51 (Table 5.1).

5.4.1.2 Menisci. Meniscal damage was much greater on the medial versus lateral side (Table 5.1) with changes varying from mild fraying to near complete destruction with inadequate attempts at fibrous repair. Bucket handle tears of the caudal horn of the meniscus were a common finding. Fraying of the lateral meniscus was minimal to mild, if present, and many (12/19) joints had no lateral meniscal fraying.

5.4.1.3 Osteophytes. In the operated joints, osteophytes were generally largest and most numerous in the area of the femoral trochlear ridges (2.58 ± 0.61), but recontouring (shape change) of the tibial plateaus was a common finding (Table 5.1). Common locations for especially large osteophytes included the caudal and outside edges of the medial tibial plateau, the axial edge (adjacent to cruciate attachment area) of the lateral tibial plateau, and upper axial surface of the lateral femoral condyle. The presence of the large osteophytes on the axial surface of the lateral femoral condyle was often

associated with bone resorption of non-weight bearing areas of the lateral femoral condyle.

Table 5.1. Subjective gross pathology scores for each dog. The mean ± SD and coefficient of variation (CV) for each category are listed. Syn = Synovium, Med = Medial, Lat = Lateral, Men = Meniscus, Osteo = Osteophyte, Fem = Femur, Tib = Tibia

Dog	*Syn*	*Med Men*	*Lat Men*	*Med Fem Osteo*	*Lat Fem Osteo*	*Med Tib Osteo*	*Lat Tib Osteo*	*Trochlear Ridge Osteo*	*Med Fem Condyle Cartilage*	*Lat Fem Condyle Cartilage*	*Med Tib Plateau Cartilage*	*Lat Tib Plateau Cartilage*
1	2	2	1	0	1	2	1	3	0	0	1	1
2	2	1	0	0	3	2	1	3	0	0	3	0
3	3	3	1	1	1	3	2	3	2	1	4	0
4	2	1	0	1	0	2	1	2	2	0	4	1
5	2	2	0	1	0	3	2	2	1	0	1	1
6	3	3	1	1	3	3	1	3	3	1	4	1
7	2	1	0	1	1	1	1	2	3	0	4	2
8	2	1	1	1	1	2	2	3	4	0	2	2
9	3	3	1	1	3	1	2	3	1	1	3	2
10	3	2	0	1	0	2	1	3	4	1	4	4
11	2	3	0	0	2	1	1	2	1	0	2	2
12	2	1	0	1	1	1	1	1	2	0	2	1
13	3	3	1	0	1	1	1	3	2	1	3	0
14	2	1	0	1	1	1	1	2	2	1	2	2
15	3	3	0	0	2	1	2	3	3	1	4	2
16	2	1	0	1	2	2	1	2	1	2	1	1
17	3	3	0	1	1	1	1	3	2	1	4	2
18	3	1	0	1	1	1	1	3	2	1	4	2
19	2	1	1	1	2	1	1	3	2	1	3	0
Mean	**2.42**	**1.89**	**0.37**	**0.74**	**1.37**	**1.63**	**1.26**	**2.58**	**1.95**	**0.63**	**2.89**	**1.37**
SD	0.51	0.93	0.49	0.45	0.96	0.76	0.45	0.61	1.13	0.60	1.15	1.01
CV	**21**	**49**	**135**	**61**	**70**	**47**	**36**	**24**	**58**	**95**	**40**	**74**

5.4.1.4 Articular Cartilage. Articular cartilage lesions on the femoral condyles were generally located in the proximal, non-load bearing junction of the medial

femoral condyle and trochlear ridge and were focal, small but often deep (Figure 5.2, Table 5.2). These lesions were seldom present on the lateral femoral condyle (Table 5.1 and 5.2). Central weight bearing areas of the medial femoral condyle were at risk for development of larger lesions that ranged in severity from diffuse superficial roughening to severe extensive cartilage degeneration. Lateral femoral condyles were affected by degenerative changes in similar locations but damage was always much less severe than that seen on the medial femoral surface (Table 5.1 and 5.2).

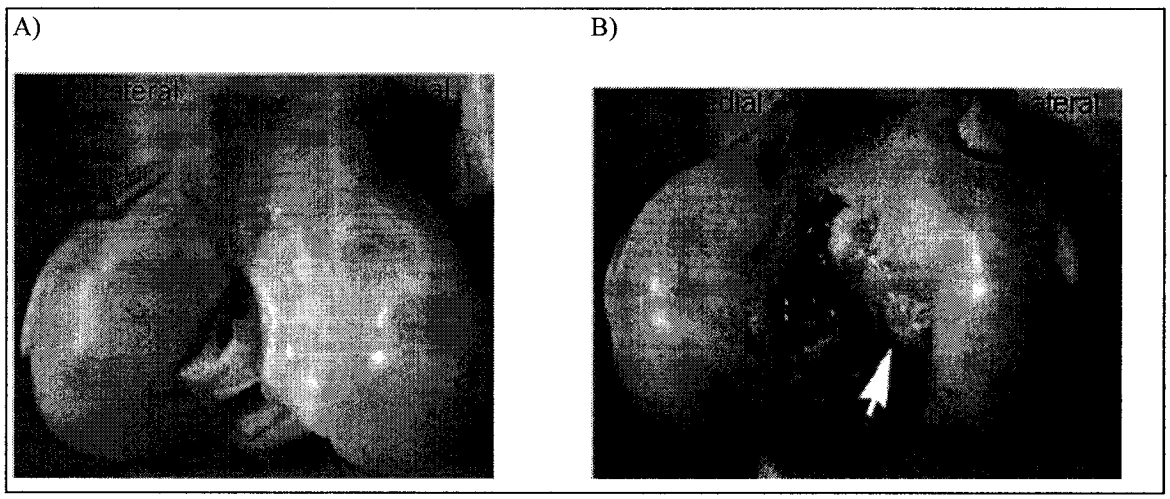

Figure 5.2. Disarticulated and sectioned femoral condyles from a normal left, non-operated stifle (A) compared to the degenerative changes present in an operated stifle (B). Note the focal articular cartilage degeneration on the proximal medial femoral condyle at the junction of the trochlear ridge (black arrow) as well as the osteophyte formation on the axial surface of the lateral femoral condyle (white arrow). Medial and lateral for each section is labeled accordingly.

Articular cartilage of the cranial, non-load bearing area of the medial tibial plateau, a region where there is normally a transition from hyaline to fibrocartilage or fibrous tissue in normal weight bearing animals, was at risk for development of severe degenerative changes (Figure 5.3, Table 5.2). Animals that had severe medial degeneration in this area often had similar but usually less severe changes on the lateral tibial plateau. The area not protected by the meniscus, a common location for superficial spontaneous degenerative changes, had superficial areas of degeneration in some animals.

Dog	*Medial Tibial Plateau*				*Lateral Tibial Plateau*				Total	*Medial Femoral Condyle*			*Lateral Femoral Condyle*			Total
	Cran	Mid	ANPM	Caud	Cran	Mid	ANPM	Caud	Tib	Prox	CWB	CNWB	Prox	CWB	CNWB	Fem
1	0	0	35	0	0	0	9	0	44	0	0	0	0	0	0	0
2	105	0	35	0	0	0	0	0	140	0	0	0	0	0	0	0
3	300	0	0	0	0	0	0	0	300	6	18	0	0	0	0	24
4	84	0	49	0	9	0	4	0	146	12	9	0	0	0	0	21
5	0	0	0	0	0	0	0	0	0	3	0	0	0	0	0	3
6	243	0	0	6	0	0	4	0	253	24	0	0	0	0	0	24
7	75	0	0	3	0	0	8	0	86	9	0	0	0	0	0	9
8	6	0	0	0	4	0	9	0	19	63	0	0	0	0	0	63
9	30	0	0	0	1	0	0	0	31	12	0	0	0	0	0	12
10	252	0	0	30	60	0	0	0	342	28	360	0	0	0	0	388
11	18	0	12	6	24	0	9	0	69	10	0	0	0	0	0	10
12	18	0	16	0	0	0	16	0	50	3	25	0	0	0	0	28
13	56	0	0	8	0	0	0	0	64	0	3	0	0	0	0	3
14	12	0	3	0	6	0	3	0	24	48	0	0	0	0	2	50
15	98	0	35	12	16	0	24	0	185	12	0	6	0	0	0	18
16	4	0	0	0	0	0	16	0	20	3	0	0	0	16	0	19
17	147	0	25	9	18	0	9	0	208	8	0	4	0	0	0	12
18	147	0	25	0	35	0	9	0	216	8	0	0	0	0	0	8
19	90	0	0	3	0	0	0	0	93	27	0	0	0	0	0	27
Mean	**88.68**	**0**	**12.37**	**4.05**	**9.11**	**0**	**6.32**	**0**	**120.53**	**14.53**	**21.84**	**0.53**	**0**	**0.84**	**0.11**	**37.84**
SD	92.08	0	16.38	7.33	15.88	0	6.83	0	103.19	16.93	82.18	1.61	0	3.67	0.46	86.33
CV	**104**	**-**	**132**	**181**	**174**	**-**	**108**	**-**	**86**	**117**	**376**	**306**	**-**	**436**	**436**	**228**

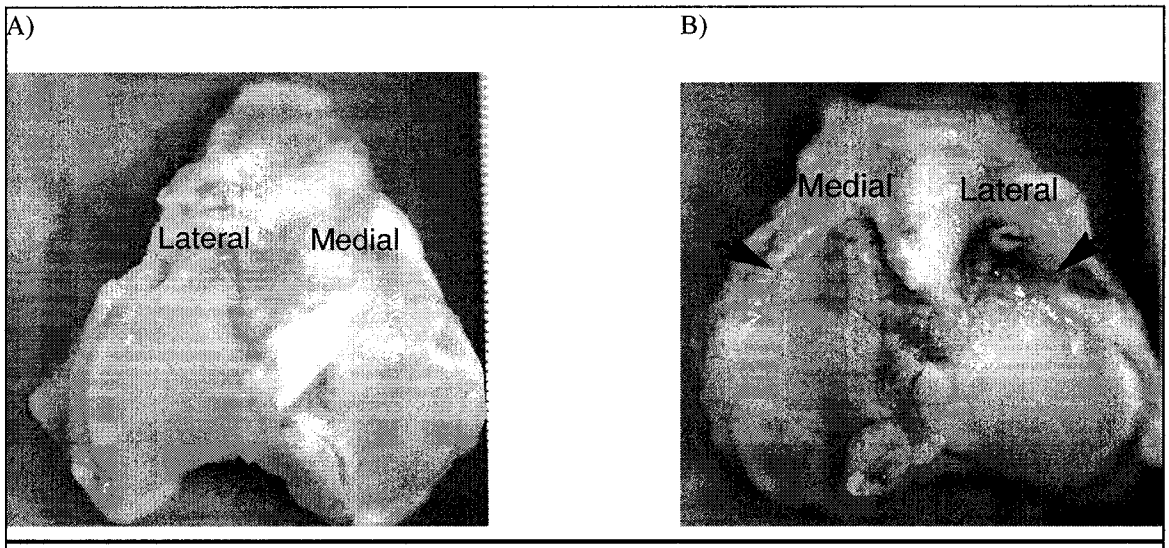

Figure 5.3. Disarticulated tibial plateau from a normal left non-operated stifle (A) and one from a CrCL transected stifle (B). Notice the severe articular cartilage degeneration on the cranial medial and lateral region (black arrows) in the operated stifle compared to the normal stifle. Medial and lateral for each section is labeled accordingly.

Caudal aspects of the medial tibial plateau often had superficial to medium-depth degenerative changes which interfaced with marked recontouring and osteophyte formation at the caudal aspect of the surface. Medial tibial cartilage subjective gross scores for cartilage degeneration were greater than lateral scores (Table 5.1). The cranial medial tibial plateau had the highest overall calculated values for articular cartilage damage (Table 5.2). Therefore when the data was expressed as a sum of calculated gross scores for tibia or femur, the greatest cartilage damage was identified on the tibia where values were almost 3 times greater than the values calculated for the femur (120.53 ± 103.19 vs. 37.84 ± 86.33; Table 5.2).

The coefficients of variation (CV) for each category of the macroscopic grading are listed in Tables 5.1 and 5.2. The range of CVs for all of the subjective macroscopic gradings listed in Table 5.1 was 21-135%. The range of CVs was much greater (86-436%) in the calculated articular cartilage scores that were based on specific locations of the lesions listed in Table 5.2. Representative examples of the variability in gross

pathology scores are shown in Figure 5.4. The correlation between the medial meniscal grade (Table 5.1) and the gross cartilage damage on the cranial aspect of the medial tibial plateau (Table 5.2) was not significant ($r = 0.2757$, $P = 0.2533$). Based on the mean, standard deviation, and variances of the gross scores in Table 5.1, the power for this study was 96%.

5.4.2 Microscopic findings. There were minimal to no histologic changes in the left non-operated stifles. Only minimal to occasionally mild spontaneous degenerative changes consisting of tangential layer loss, superficial zone chondrocyte and proteoglycan loss with minimal or mild fibrillation were seen on the medial and lateral tibial plateaus in the area not protected by the meniscus.

5.4.2.1 Synovial membrane. The synovial membrane had mild to severe subacute inflammation (2.11 ± 0.57) with mononuclear inflammatory cell infiltrate and distinct lymphoid aggregates and synovial hyperplasia in the operated stifles (Table 5.3).

5.4.2.2 Osteophytes. Osteophytes in the operated stifles were identified by the presence of basal endochondral ossification on the edge of the articular surface, often recontouring the shape of the joint surface. The medial tibial plateau had the highest incidence followed by the lateral tibial plateau, medial femoral condyle, and the lateral femoral condyle (Table 5.3).

5.4.2.3 Articular cartilage. Articular cartilage lesions in the operated stifles of these dogs ranged from focal superficial, to focal severe degeneration characterized by chondrocyte loss, proteoglycan loss, fibrillation and cleft formation with subjacent cloning of chondrocytes. In addition to these obvious focal degenerative changes, large areas of the cartilage (extending from the surface toward the tidemark) had

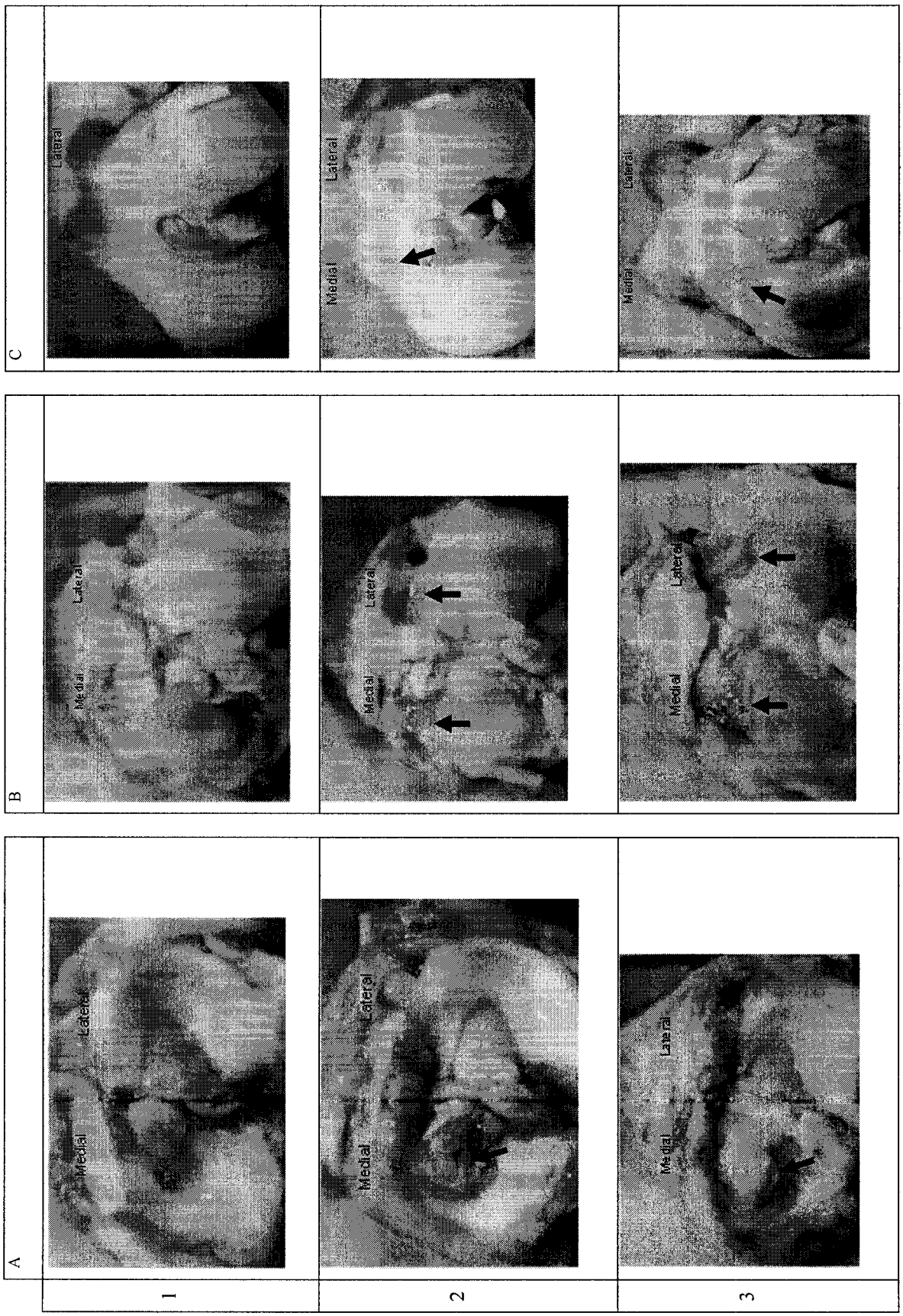

Table 5.3. Histologic pathology scores for each dog for the synovium, osteophytes, and lesion depth compared to the tidemark (TM). Osteophyte scores were calculated by averaging the osteophyte grade for the cranial or proximal, weight bearing, and caudal sections of the tibial plateaus or the femur. The lesion depth was calculated in the most severe location and is reported as a ratio of the tidemark depth. The mean ± SD and coefficient of variation (CV) for each location are listed. Syn = Synovium, Med = Medial, Lat = Lateral, Fem = Femur, Tib = Tibia, Osteo = Osteophyte.

Dog	*Syn*	*Med Fem Osteo*	*Lat Fem Osteo*	*Med Tib Osteo*	*Lat Tib Osteo*	*Med Fem Lesion Depth*	*Lat Fem Lesion Depth*	*Med Tib Lesion Depth*	*Lat Tib Lesion Depth*
1	2	0.67	0.67	2.67	1.67	0	0	0.26	0.11
2	2	1.00	0.33	1.67	1.33	0.11	0	0.04	0.05
3	2	0.67	0	2.33	1.00	0.14	0	0.22	0.07
4	3	0	0	0.67	0.67	0.03	0	0.05	0.08
5	3	1.33	0	1.67	1.50	0.33	0.29	0.11	0.11
6	2	0.67	1.00	1.67	1.67	0.3	0	0.40	0.06
7	1	0.67	0.67	0.33	0.67	0.33	0	0.08	0.22
8	2	0.33	0	1.33	2.00	0.36	0	0.62	0.24
9	2	1.67	1.00	0.67	2.33	0.25	0.37	0.35	0.11
10	3	1.00	1.00	2.67	1.00	1.00	0	0.85	0.45
11	2	2.00	1.67	2.00	1.33	0.10	0.19	0.12	0.08
12	1	1.67	1.67	2.00	2.00	0.39	0	0.07	0
13	2	1.00	1.00	1.00	1.00	0.06	0	0.46	0.08
14	2	1.33	2.00	0.67	1.00	0.25	0	0.13	0.08
15	2	1.33	1.67	1.00	1.67	0.38	0	0.12	0.07
16	2	1.00	1.00	2.67	1.67	0	0.16	0.33	0.05
17	3	2.67	3.00	1.67	1.33	0.17	0.07	0.15	0.13
18	2	2.00	1.67	1.33	2.00	0.46	0	0.19	0.13
19	2	1.00	0.67	1.00	1.33	0.19	0	0.14	0.07
Mean	**2.11**	**1.16**	**1.00**	**1.53**	**1.43**	**0.26**	**0.06**	**0.25**	**0.12**
SD	0.57	0.64	0.80	0.73	0.47	0.23	0.11	0.21	0.10
CV	**27**	**55**	**80**	**48**	**33**	**90**	**197**	**86**	**86**

marked diffuse chondrocyte cloning/hypercellularity associated with matrix changes which resulted in altered toluidine blue staining. This change in the staining was characterized by a shift from orthochromatic (blue) to metachromatic (purple). In some

dogs there was also the formation of a fibrous pannus-like tissue on the surface of the articular cartilage. This pannus-like change was most commonly seen in the cranial aspects of the tibial plateaus, an area which normally has morphology of fibrous to fibrocartilagenous tissue (Figure 5.5).

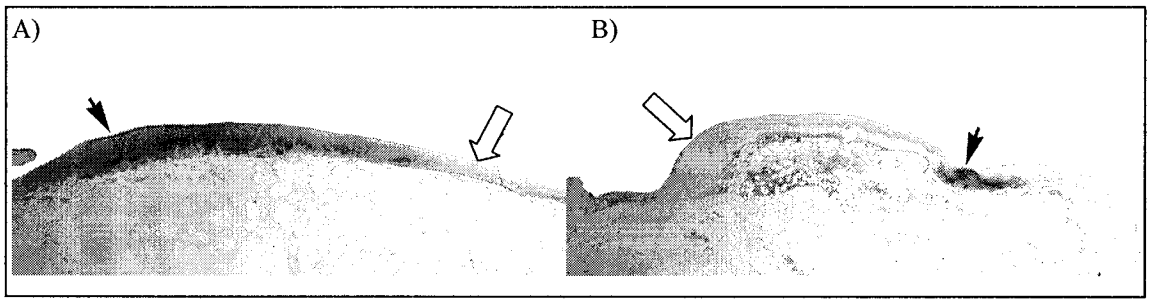

Figure 5.5. Microscopic section (16X) of the cranial section of the medial tibial plateau from the normal left unoperated stifle (A), and the CrCL transected stifle (B) depicted in Figure 3. Section A shows the normal appearance of this region, with thicker more cartilaginous areas (black arrow) and thinner more fibrous areas (open arrow). Section B depicts a highly irregular surface with fibrous areas (open arrow) as well as residual fibrocartilage areas (black arrow).

In the operated knees, the mean depth of articular cartilage degeneration when compared to the tidemark was generally greater on the medial side than lateral with no difference between the relative depths of femoral compared to tibial degeneration (Table 5.3). However, microscopic alterations based on calculated cartilage lesion scores (width X depth) were more severe on the tibial plateaus than femoral condyles (Table 5.4). Of the 4 compartments, evaluation of cartilage degeneration using calculated scores revealed that the cranial aspect of the medial tibial plateau was the most severely affected, (1.31 ± 1.33) followed by the proximal aspect of the medial femoral condyle (0.73 ± 0.63).

Bone changes in the subchondral area of operated joints included mild to marked trabecular thickening in various locations on both medial and lateral plateaus. A change from adipose to hematopoietic marrow often accompanied the increase in trabecular width.

Table 5.4. Histologic cartilage degeneration scores for each dog for the medial and lateral tibial plateaus and femoral condyles. Scores for each compartment (cranial or proximal, weight bearing, or caudal) were calculated by averaging the product of the width X depth of the lesions present in all 3 compartments. The sum of the tibial and femoral scores are the cumulative total of the respective medial and lateral scores. The mean ± SD and coefficient of variation (CV) for each location are listed. NS = no section available for analysis. Med = Medial, Lat = Lateral, Tib = Tibia, Fem = Femur, Plat = Plateau, Cond = Condyle, Cart = Cartilage, Cran = Cranial, Wt = Weight, Bear = Bearing, Caud = Caudal, Prox = Proximal

Dog	*Med Tib Plat Cart Degeneration*			*Lat Tib Plat Cart Degeneration*			Total Tib	*Med Fem Cond Cart Degeneration*			*Lat Fem Cond Cart Degeneration*			Total Fem
	Cran	Wt Bear	Caud	Cran	Wt Bear	Caud		Prox	Wt Bear	Caud	Prox	Wt Bear	Caud	
1	0.33	0.50	0	0	0.50	0.25	1.58	0	0	0	0	0	0	0
2	0	0.50	0	0	0.50	0.50	1.50	0	0	0.38	0	0	0	0.38
3	0	0.66	2.00	0	0.25	0.17	3.08	0	1.00	0.66	0	0	0	1.66
4	1.00	0.33	0.33	0.25	0.17	0.33	2.41	0	0.33	0	0	0	0	0.33
5	0	0.33	0.25	NS	0.75	0	1.33	1.65	0	0	NS	1.34	0.13	3.12
6	0.80	0.50	1.34	0	0.66	0	3.30	1.00	0.17	0	0	0	0	1.17
7	0.50	0.50	0	1.34	0.33	0.66	3.33	1.25	0	0	0	0.10	0	1.35
8	2.00	1.00	1.34	0.33	0.84	0.25	5.76	2.31	0.17	0	0	0	0	2.48
9	1.32	0.84	0	1.34	0.50	0.66	4.66	0.66	0.66	0.17	0	2.01	0.51	4.01
10	3.75	1.00	4.00	2.50	2.01	0.25	13.51	1.16	3.25	3.25	0	0	0	7.66
11	0.50	0.50	0.50	0.67	0.50	0.33	3.00	0.17	0.17	0	0	0	0.34	0.68
12	0.66	0	0	0	0	0	0.66	0.52	0.13	0	0	0	0	0.65
13	2.50	1.75	1.00	0.33	0.33	0	5.91	0.75	0	0	0	0	0	0.75
14	0.66	0.66	0	0.34	0	0.33	1.99	1.16	0	0	0	0	0	1.16
15	1.34	0.33	0.67	0.66	0.33	0	3.33	0.85	0.50	0	0	0	0	1.35
16	5.00	0	0	2.00	0.33	0	7.33	0	0	0	0	1.00	0.10	1.10
17	2.50	0.50	1.00	0.50	0	0	4.50	0.99	0	0	0.50	0	0	1.49
18	1.00	0.66	0	1.00	0.17	0.33	3.16	0.90	0.66	0.25	0	0	0	1.81
19	1.00	0.50	0	0.50	0	0	2.00	0.51	0.33	0	0	0	0	0.84
Mean	**1.31**	**0.58**	**0.65**	**0.65**	**0.43**	**0.21**	**3.81**	**0.73**	**0.39**	**0.25**	**0.03**	**0.23**	**0.06**	**1.68**
SD	1.33	0.39	1.01	0.73	0.46	0.22	2.92	0.63	0.75	0.75	0.12	0.57	0.14	1.75
CV	**101**	**67**	**154**	**111**	**107**	**105**	**77**	**87**	**194**	**302**	**424**	**242**	**242**	**104**

The CVs for the microscopic grading are listed in Tables 5.3 and 5.4. The range of CVs for all of the histologic grading was 27-424%, with the CVs being much greater the more specific the analysis.

5.5 Discussion

The lesions induced by CrCL transection in our study were highly variable amongst the dogs with respect to incidence, location, severity, and type. This between-subject variation has been rarely mentioned as an important consideration when using this model.

Historically, the canine CrCL transection model has been used to determine the earliest osteoarthritic changes that occur to the intra-articular components, especially articular cartilage, after CrCL transection[95,102,106,107,120], as well as the entire temporal sequence of events that occurs up to 54 months after transection[1,98,99,103,105,120,128]. When investigators have tried to compare their findings to those of other laboratories, the results have been highly variable with respect to the time of onset and the severity of OA lesions produced[140]. It has been hypothesized that these differences in the lesions generated were most likely due to the differences in the breed, age, weight, surgical technique used to sever the CrCL, and the amount of exercise the dog required post-transection[140].

Indeed, when comparing the cruciate ligament transection studies, most have used a heterogeneous population of dogs, (mixed breed[96,104,107,108,110-114,118,121], mongrels[1,98,99,105,123-127,129,130], or a mixture of different breeds[100,102,107,117,119,120,134]) whereas fewer studies have used specific purebreds (beagles[103,106,116,132], American Foxhounds[122,128], and Greyhounds[115]). Most dogs have been adults, ranging in age from the time of epiphyseal closure (~1.5 years) up to 8 years of age, and their weight has

ranged from 6.8 to 40 kg, with most being between 12 to 30 kg. The three main approaches used for surgical transection of the cruciate ligament have included the percutaneous stab[101-117], arthrotomy (medial or lateral)[1,96-100,104,118-128], and arthroscopic techniques[129-132]. Most dogs have been allowed to regulate their own exercise by being kept in cages/pens[96,99,100,104,105,108,110,113,116-121,123,132], or runs[1,98,102,122,124-127,129,130], whereas only a few studies have utilized more controlled exercise regimens[106,107,111,112,114,115].

All of these differences undoubtedly make it difficult to compare findings between different laboratory settings. However, because most of these studies have looked at many different time points to identify the early changes that occur after CrCL transection, $\leq$ 4 dogs (often 1-2 dogs) per interval have been used to draw conclusions[1,98,99,102,103,105-107,118-120,125-130,134]. However, when CrCL transection has been used to monitor the effectiveness of specific therapeutic agents, more dogs per treatment group (usually 5 to 7) have been used[110-115,123,124,141]. Based on the variability of the lesions reported in our study, the authors argue that the relatively low numbers of dogs used in those studies also contributes to the differences in the lesions identified and the conclusions that have been drawn. In fact, based on calculations using our gross data, 12 dogs would be required per group to obtain a power of 80%.

In general, the histologic evaluation was similar in outcome to the gross evaluation in our study. Measurements and lesion scoring were sometimes complicated by the diverse morphologic changes that were present. This included matrix degenerative changes that resulted in outright and reasonably easily quantifiable matrix loss as well as proliferative changes that altered the appearance of the cartilage and resulted in excessive fibrocartilage, fibrous tissue or combinations with pannus. These diverse morphologies

were most common in the cranial areas of the tibial plateaus. Normally this is not a load-bearing area and so the cartilage morphology is not hyaline, but fibrous or fibrocartilage. Transection of the CrCL resulted in this area, as well as the proximal medial femoral condyle, becoming load-bearing and subjected to mechanical forces. In the proximal femoral area, if lesions were present, they were generally degradative resulting in focal defects, often with substantial peripheral thickening of cartilage matrix and osteophyte formation at margins. When this occurred in the cranial areas of the tibial plateaus, lesions were often irregular areas of degeneration coupled with areas of intense fibrocartilage formation and overall recontouring of the area. These irregularities made these lesions much more difficult to score and quantify.

The focal articular cartilage defect on the cranial aspect of the medial tibial plateau, to our knowledge, has rarely been reported, whereas the focal lesion at the junction between the medial trochlear ridge and femoral condyle has been reported in a few studies[104,124,130,249]. These are both most likely defects that occur in the articular cartilage in response to the instability that is created in this model. The tibial defect was likely due to damage of the medial meniscus, even though we could not identify a correlation between the severity of medial meniscal grade in our study to the gross score of the articular cartilage in this location, a finding corroborated by Smith, et al[249]. However, in a canine cadaver study, Tirgari, et al. noted that when the meniscus was torn, the cartilage underneath was deeply eroded[159]. In addition, in a concomitant study in our laboratory, we serially examined 3 dogs arthroscopically at 2, 4, 10, and 18 weeks after CrCL transection (Chapter 3). We noted that the cranial meniscotibial ligament of the medial meniscus stretched or ruptured in each of these dogs by 10 weeks, allowing

increased mobility of the cranial horn of the medial meniscus. Only one of these dogs had severe (grade 3) meniscal damage, highlighting the potential for the cranial horn of the medial meniscus to become more mobile and potentially causing damage to the articular cartilage underneath, without having significant pathology itself. It is also possible that the focal lesions of the femur could be due to this increased meniscal mobility combined with the hyperextension that is created by the cranial tibial thrust after CrCL transection. As previously, stated, however, this femoral lesion is most likely due to the abnormal movement of the patella in response to joint instability, causing it to impinge on the femur in that location[104,124]. Why these lesions have not been identified in more studies is not known, but could likely be due to the timing of lesion occurrence combined with the need to have adequate numbers of dogs to identify the lesions.

In general, the variability in lesions produced in our study were likely due to inherent differences of each individual animal in response to the surgically created instability. The most obvious component of this is the potential difference in pain threshold between each dog that would likely alter the degree of load bearing. Altered load bearing would no doubt affect the degree of damage sustained to the menisci, articular cartilage, and subchondral bone. As a component of this, based on the dog's own inherent activity level, the joint could be loaded differently. In other words, some dogs will jump around in their pens or runs, as well as during controlled exercise, while others will move around their pens/runs very little, and will only consistently move during controlled exercise. Still others will not bear weight on the CrCL deficient limb for a given time throughout the study. These simple differences in movement could have rather large implications in terms of the biomechanical and pathological response of the

joint to the instability. Another important component that is related to joint stability after CrCL transection is the effect of the periarticular musculature[139]. This musculature can help prevent much of the instability that is created after cruciate transection. We did not objectively examine this, but it appeared that dogs that ambulated quicker and better over time were those with relatively well built quadriceps and hamstring musculature. All of these are potential contributors to differences in load bearing between dogs and are almost impossible to control. However, it is the authors' opinion that some sort of controlled exercise program at least partially minimizes some of these inherent differences.

In summary, the results of our study demonstrate that the gross and histologic pathology changes present after CrCL transection in a large group of dogs was highly variable between dogs with respect to incidence, location, severity, and type of lesions present. This between-subject variation should be an important consideration when planning to use this model for future projects, or when drawing conclusions from studies that involve small group sizes.

6 SYNOVIAL FLUID LEVELS OF BONE-SPECIFIC ALKALINE PHOSPHATASE CORRELATE WITH OSTEOPHYTE FORMATION IN A CANINE CRANIAL CRUCIATE LIGAMENT TRANSECTION MODEL OF OSTEOARTHRITIS

Troy N. Trumble DVM, MS, R. Clark Billinghurst DVM, PhD, Richard D. Park DVM, PhD, C. Wayne McIlwraith BVSc, PhD

To be submitted to *Arthritis and Rheumatism* in spring 2003.

Presented in part at the 49th Annual Orthopaedic Research Society Meeting, New Orleans, LA, February 2-5, 2003.

6.1 Summary

Objective. To analyze biomarkers of bone formation in the serum and synovial fluid from a canine cranial cruciate ligament (CrCL) transection model of osteoarthritis (OA) to determine their temporal pattern and relationship to osteophyte production.

Methods. Nineteen mature male Walker Hounds had the right CrCL transected arthroscopically. Synovial fluid and serum samples were collected and radiographs were taken prior to surgery, and at various time points to 126 days post-transection. Immunoassays for bone alkaline phosphatase (BAP) and osteocalcin (OC) were used to detect osteoblastic activity in the serum. BAP levels were also evaluated in the synovial fluid. The ratio between the synovial fluid and serum concentrations of BAP was calculated (BAP SF:serum) to determine the relative source of BAP in the synovial fluid. Radiographs were scored for the presence and severity of osteophytes, and were compared to levels of the bone formation markers.

Results. Serum concentrations of BAP and OC decreased below baseline levels after CrCL transection, except for an early increase in OC levels at 7 days post-transection. BAP levels in the synovial fluid from the CrCL deficient stifle were increased significantly from baseline over time ($P<0.0001$), and had a significant positive correlation to the total osteophyte score ($r=0.6705$, $P<0.0001$). The BAP concentration in the synovial fluid from the contralateral joint was not significantly different from baseline, and the BAP SF:serum ratio was > 1 by days 70 and 126 post-CrCL transection.

Conclusion. The results of this study suggests that after CrCL transection in the dog, there is an increase in synovial fluid BAP levels that most likely originates directly from

osteophyte formation, indicating that synovial fluid BAP analysis may be a potential early biomarker of osteophyte development in the early stages of secondary OA.

6.2 Introduction

Osteoarthritis (OA) is a complex disease process that involves all components of the joint environment, including articular cartilage, synovium, and subchondral bone. When there is joint injury, such as rupture of the cranial cruciate ligament (CrCL – equivalent of human anterior cruciate ligament), there are abnormal biomechanical stresses placed on the entire joint. Invariably, this leads to loss of the articular cartilage accompanied by osteophyte formation along the margins of the bone surface in an attempt to stabilize the joint[1,100,119]. Even though a direct relationship between the severity of osteophyte formation and the degree of instability has not been established, radiographic evidence of osteophyte formation in typical locations within the canine stifle after CrCL rupture is one of the hallmarks used for the diagnosis of OA[100,119,171,182,186]. Classically, most biomarkers studied in osteoarthritis have examined turnover of collagen, proteoglycans, or other non-collagenous proteins. Few studies have used bone-specific biomolecular markers to examine bone turnover associated with osteoarthritis.

Alkaline phosphatases are a group of membrane-bound glycoproteins that can hydrolyze phosphate esters at an alkaline pH[271]. In humans, the tissue specific (liver, bone, and kidney) isoenzymes are coded by the same gene product, but differ from each other based on post-translational modifications[272]. With traditional analysis of total alkaline phosphatase activity, the liver- and bone-specific isoenzymes have been the most abundant forms identified in human serum[273]. The bone-specific alkaline phosphatase (BAP) has been localized to the vascular surface of the plasma membrane of

osteoblasts[274], and is released into the circulation after phospholipase cleavage from the membrane[275]. The exact role of BAP is not known, but it has been hypothesized that it may contribute to calcification of the matrix of bone[275-278]. Through the use of either precipitation by wheat germ lectin[279], or various immunoassays[280-282], BAP has been demonstrated to be a reliable serum marker of early osteoblastic activity of bone formation. BAP has been examined in the serum of human patients with metabolic bone disease, fractures, and cancer[279,280,282,283]. In human OA patients, the presence and location of total alkaline phosphatase and/or the bone-specific isoenzyme have been studied in bone[274,276,284], and the activity levels have been studied in serum[285-290], and synovial fluid (SF)[287]. The activity levels of BAP have also been evaluated in synovial fluid from horses with osteochondral fragmentation[291].

Osteocalcin (OC) is an abundant extracellular non-collagenous protein found in bone[292]. It has been called bone Gla-protein (BGP) due to vitamin K dependent carboxylation of its glutamic acid residues that allows it to have a selective affinity for calcium, and to bind to hydroxyapatite crystals[293-295]. OC is synthesized by osteoblasts, which can be markedly stimulated by vitamin D[296,297]. The exact role of OC in bone is not known. Most of the synthesized portion will bind to the mineral phase of bone formation while a small portion does not bind and is released into the circulation[298]. Its use as a specific marker of osteoblastic activity or bone formation has been demonstrated[299] but because it serves as a link between the organic and inorganic matrices of bone, it has been considered a marker of late osteoblastic activity, or bone turnover[300]. Using various immunoassays, the presence and levels of OC has been

examined in the serum and synovial fluid from human OA patients[301-304] and in naturally occurring canine OA[217].

Most of the studies utilizing BAP and OC as biomarkers of bone formation in OA have utilized serum and/or synovial fluid samples from patients at or close to end-stage disease. By this stage, bones making up the joint have already developed subchondral plate sclerosis and mature osteophytes, making it reasonable to assume that the relative levels of bone formation markers in the serum from the response of one joint would be relatively minimal. To the authors' knowledge, no studies have examined OC concentrations in the serum and BAP concentrations in the serum and synovial fluid from the early stages of an experimental animal model of OA. The canine CrCL transection model allows for analysis of the temporal pattern of bone formation, such as osteophytes, in the early stages of OA. Therefore, the purpose of this study was to examine the concentrations of BAP and OC in the serum and BAP in the synovial fluid from dogs that had unilateral CrCL transection and compare these concentrations to the radiographic findings. Our hypothesis was that the serum levels of BAP and OC would not differ from baseline after CrCL transection, and that the BAP levels in synovial fluid would increase and correlate with osteophytic progression.

6.3 Materials and methods

6.3.1 Experimental design. Nineteen purpose-bred adult male Walker Hounds with a mean ± SD weight of 22.42 ± 2.39 kg (range, 19-28.5 kg) were studied. These dogs were the placebo control group in a larger study of a novel therapeutic agent. Inclusion criteria required the dogs to be free of pre-existing orthopedic disease of the

stifles (equivalent to the human knee) based on routine physical, orthopedic, lameness, radiographic, and force plate examinations.

All dogs were anesthetized, and the right hind limb was prepared for aseptic surgery. A lateral parapatellar arthroscopic approach to the right stifle was used to examine the joint for the presence of any intra-articular pathology of the articular cartilage, cruciate ligaments and menisci. The CrCL was then transected arthroscopically using a meniscectomy blade (Chapter 2). Analgesia was administered via a 5 mg fentanyl patch (2.0 μg/kg/hr) that was applied the day before surgery and was maintained for 72 hours post-operatively. Morphine (1 mg/kg subcutaneously) was also administered post-operatively for pain, as needed. Cephalexin (Keflex) was administered intravenously during surgery and was continued orally (10 mg/kg) every 12 hours for 3 days to prevent infection. Throughout the study, all dogs were housed in individual runs. The animals were closely monitored during the first 48 hours post-operatively for any signs of pain, infection, anorexia, or intestinal complications. To encourage the development of OA, dogs were placed in an exercise protocol that required leash walking for 30 minutes every day for 5 days/week from the second day post-operatively until 126 days post-operatively.

All dogs were obtained through approved sources by the Colorado State University Laboratory Animal Resources, and the study was conducted under a protocol approved by the Colorado State University Animal Care and Use Committee.

6.3.2 Sample collection. Blood samples were collected in the morning, from the jugular vein prior to surgery (Day 0), one and two weeks post-operatively, followed by every 2 weeks thereafter until day 126. Samples were placed in serum separator tubes

and were allowed to clot at room temperature for approximately 30 minutes. The samples were then centrifuged for 10 minutes at 2,500 rpm. Synovial fluid samples were collected from both stifles using a lavage method where 5 ml of sterile saline was injected into the joint. The limb was then manipulated for 1-2 minutes to ensure adequate mixing of the saline and the synovial fluid prior to aspiration of as much synovial fluid as possible. Fluid was collected prior to surgery, and then again at 14, 70, and 126 days post-operatively in serum separator tubes. The samples were placed immediately on ice after collection and were centrifuged at 4 C for 10 minutes at 2,500 rpm. The serum and synovial fluid samples were then split into multiple aliquots with the interval between sample collection and freezing at -80 C being under 3 hours. All fluid samples were kept at -80 C until assayed. Most samples used for BAP analysis had 2 freeze/thaw cycles during sample analysis, with synovial fluid from the non-operated limb having as many as 4, due to less sample volume. A previously unthawed serum aliquot for each dog for each measurement period was used for osteocalcin analysis.

6.3.3 Radiographic analysis. Imaging procedures were performed with each dog sedated with a combination of acepromazine (0.05 mg/kg), butorphanol (0.2 mg/kg), and glycopyrolate (0.005 mg/kg) administered intramuscularly. Radiography was performed prior to synovial fluid aspiration to prevent artifacts due to arthrocentesis. Extended mediolateral and craniocaudal radiographs of both stifles were made prior to transection and then 14, 28, 70, and 126 days post-transection using computed radiography (CR). To quantify the radiographic osteophytic changes that occur after CrCL transection, the authors modified a previously reported numerical scoring system that assigned grades of 0, 1, 2, or 3 based on the presence and size of the osteophytes

present[171]. The following locations were examined for the presence of osteophytes or enthesophytes by a board-certified radiologist (RDP): proximal and distal patella, femoral trochlear ridges, medial and lateral tibial condyles, caudal proximal tibia, tibial intercondylar eminence, medial and lateral femoral condyles, and the insertion of the CrCL ligament (Figure 6.1). A total osteophyte score was then determined for each joint for each examination, by addition of the individual scores.

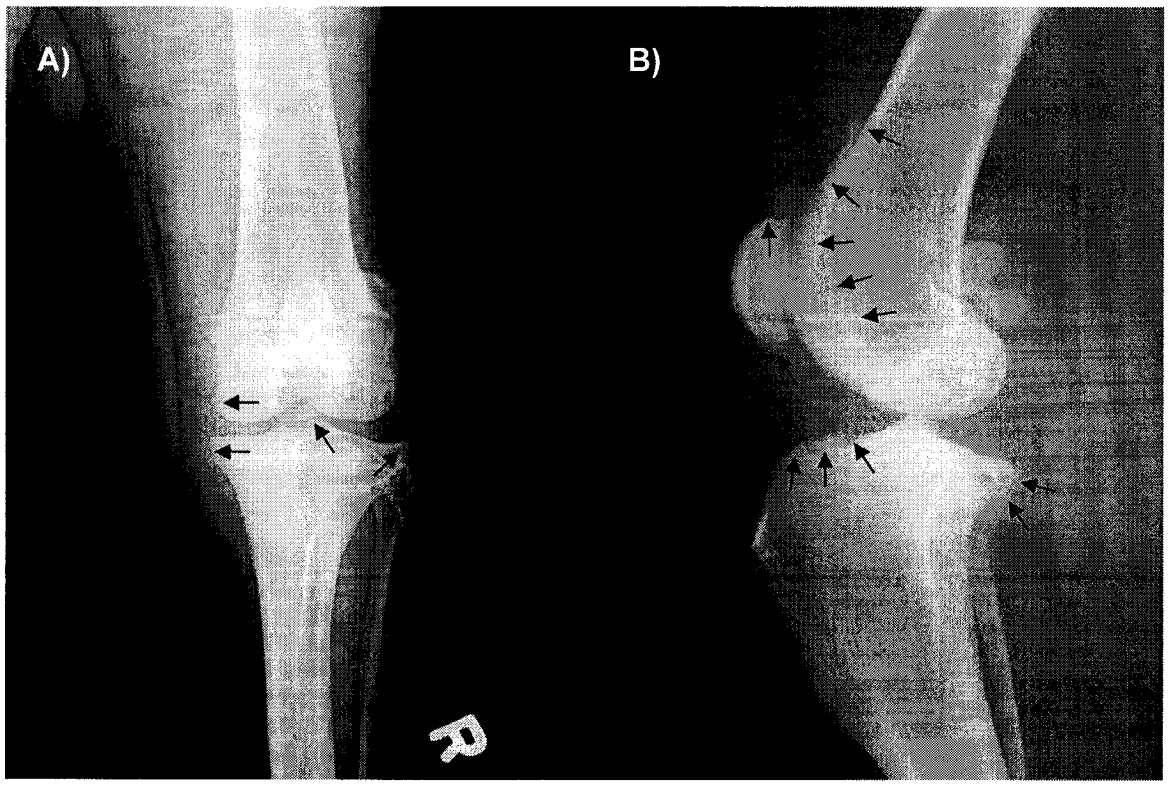

Figure 6.1. Craniocaudal (A) and mediolateral (B) radiographic views of one dog at day 126 post-CrCL transection using computed radiography. Arrows point out the presence of osteophytes that were graded as 1-3 based on size, and then summed to achieve the total osteophyte score for each joint of each dog for each examination. The total osteophyte score for this dog was 16. The lead marker (R) on the craniocaudal radiograph (A) indicates lateral. The locations of osteophyte production shown here include (counterclockwise from the medial femoral condyle in A): medial femoral condyle, medial tibial plateau, tibial intercondylar eminence, lateral tibial plateau, CrCL insertion, caudal proximal tibia, femoral trochlear ridges, proximal patella, and the distal patella.

6.3.4 Molecular biomarker for bone alkaline phosphatase analysis. Early osteoblastic activity was evaluated by measuring serum and synovial fluid levels of BAP using a commercially available ELISA (Metra™ BAP, Quidel Corporation, San Diego,

CA). This is an immunoassay based on a monoclonal antibody specific for human BAP. Cross-reactivity of the antibody to dog serum has been demonstrated by the manufacturer. Briefly, 125 µl of the assay buffer containing magnesium chloride, zinc sulfate, surfactant, and sodium azide was added to each coated well. This was followed by 20 µl of standards, high/low controls of BAP purified from human osteosarcoma SAOS-2 cells, or serum/synovial fluid samples added to the appropriate wells. All serum and synovial fluid samples were assayed at neet. The microtiter plate was incubated for 3 hours at room temperature. After washing, 150 µl of a p-Nitrophenyl Phosphate (pNPP) substrate solution was added to each well, and the plate was incubated for 30 minutes at room temperature. Then, 100µl of stop solution (1N NaOH) was added to each well. Within 15 minutes, the absorbance at 405 nm was measured in a microplate reader (Dynex Technologies GmbH, Denkendorf, GER), and the concentration of the unknown samples was determined by constructing a standard curve from absorbances of the standards with known concentrations of the BAP. Interassay coefficient of variation (CV) was < 9% for the serum and < 11% for the synovial fluid.

6.3.5 Molecular biomarker for osteocalcin analysis. Late osteoblastic activity was evaluated by measuring serum levels of intact osteocalcin only, using a commercially available ELISA (Biomedical Technologies, Inc., Stoughton, MA). This immunoassay is a sandwich ELISA based on monoclonal antibodies directed toward the amino- and carboxy- terminal regions of the intact 49 residue human protein. Cross-reactivity of the antibodies to dog serum has been demonstrated by the manufacturer. Briefly, 25 µl of diluent buffer (blank), standards, controls, and serum samples were added to the appropriate coated wells of the microtiter plate. Most serum samples were

analyzed at 1:3 dilution, with others being analyzed at 1:5, 1:2 or neet, as required. Then, 100 µl of the osteocalcin antiserum (biotinylated antibody to human osteocalcin) was added to each well. The microtiter plate was incubated for 2.5 hours at 37 C. After washing, 100 µl of Streptavidin-Horseradish Peroxidase reagent was added to all wells, and the plate was incubated for 30 minutes at room temperature. Then 100 µl of a TMB (3,3′,5,5′ Tetramethylbenzidine), hydrogen peroxide solution was added to all wells and incubated in the dark for 10 minutes at room temperature. Finally, 100 µl of stop solution (2M H_2SO_4) was added to each well. The absorbance at 450 nm was measured in a microplate reader (Dynex), and the concentration of the unknown samples were determined by subtracting the blank from all of the wells, and constructing a standard curve from absorbances of the standards with known concentrations. No interassay CV was performed due to financial considerations.

To determine the relative concentrations of BAP in the synovial fluid compared to the serum, a ratio of BAP synovial fluid values from the right CrCL transected limb was compared to the values in the serum (SF:serum) for each dog at each sampling point.

6.3.6 Statistical analysis. All data were expressed as the mean ± SD unless otherwise specified. The distribution of the data in the serum and synovial fluid BAP, serum OC, and total osteophyte score were assessed using the Kolmogorov-Smirnov test. Serum and synovial fluid from the right CrCL deficient stifle were normally distributed for BAP. Data for BAP values in the contralateral stifle, as well as the SF:serum ratio for BAP had to be transformed using the square root transformation to result in normalization of the data. The serum OC data had to be logarithmically transformed to

result in normalization of the data. Since the radiographic data was based on a subjective scoring system, it was non-parametric, and could not be normalized with transformations.

For each serum and/or synovial fluid data set, the overall effect of time was analyzed using a repeated measures ANOVA on the normalized data. Additional post-hoc Tukey's multiple comparisons tests were performed on each significant data set to determine significant differences between measurement periods. For the total osteophyte scores, Kruskal-Wallis analysis was performed using a Dunn's post-hoc test to determine significant differences between measurement periods. Correlations between and within the serum and synovial fluid markers of BAP and OC were assessed using Pearson correlation coefficient analysis on the normalized data. Correlations of the serum and synovial fluid values of BAP and OC to the total osteophyte score were performed using the Spearman Rank correlation analysis. Stepwise multiple regression was performed using BAP concentrations from the right CrCL deficient stifle as the dependent variable with each individual osteophyte location as the independent variables, knowingly violating the assumption of normality. A value of $P<0.05$ was considered significant for all analyses. All statistical analyses were performed using SAS software (SAS Institute, Cary, NC).

6.4 Results

6.4.1 Serum bone alkaline phosphatase and osteocalcin. The BAP concentrations in the serum were decreased significantly from baseline at 28 days ($P<0.05$), 42 days ($P<0.05$), 56 days ($P<0.001$), 70 days ($P<0.05$), and 84 days ($P<0.05$), and 126 days ($P<0.001$) post-CrCL transection (Figure 6.2). Serum OC significantly peaked at 1.1 fold higher than baseline at day 7 ($P<0.05$) and then was decreased

significantly below baseline at 84 days (P<0.01) and 112 days (P<0.05) post-CrCL transection (Figure 6.2).

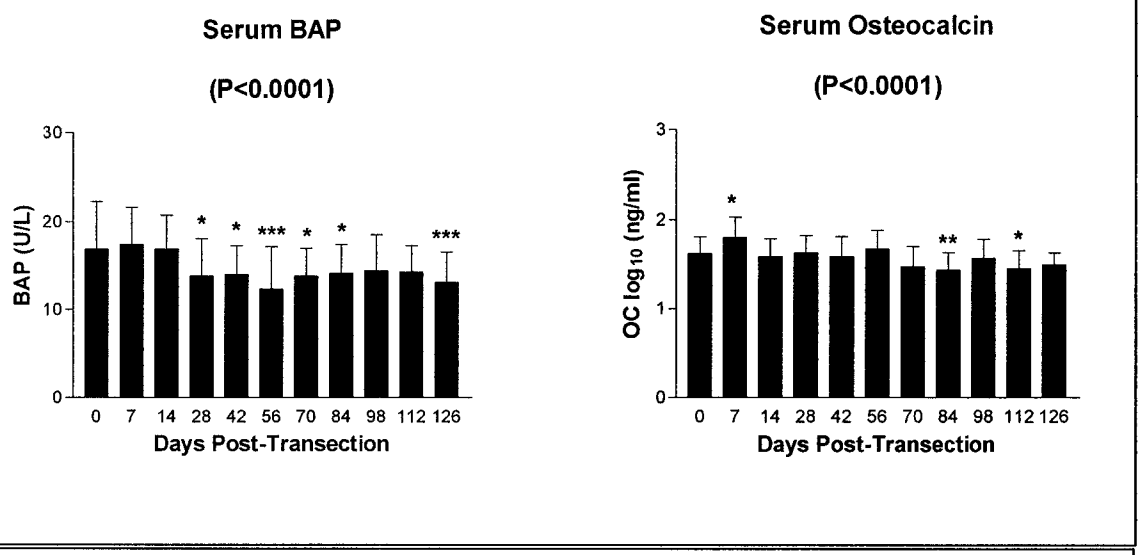

Figure 6.2. Mean (+ SD) serum values for BAP (A) and OC (B). The P value for overall effect of time is listed on each graph, and was determined by a repeated measures ANOVA, using Tukey's post-hoc test for comparison of values to baseline (Day 0). Significant differences from baseline are represented as * P<0.05, ** P<0.01, and *** P<0.001.

6.4.2 Synovial fluid bone alkaline phosphatase. The BAP concentration in the synovial fluid from the CrCL deficient stifle, increased significantly above baseline throughout the entire study, with concentrations 3.8 fold higher (P<0.01) at 14 days, 7.3 fold higher (P<0.001) at 70 and 126 days post-CrCL transection compared to baseline (Figure 6.3). The BAP concentration in the synovial fluid from the contralateral stifle did not reveal any significant differences from baseline concentrations (Figure 6.3).

The ratio of the BAP concentrations in the synovial fluid from the right CrCL deficient stifle to the serum (SF:serum), increased significantly above baseline throughout the entire study, with concentrations 3.4 fold higher (P<0.001) at 14 days, 8.3 fold higher (P<0.001) at 70 days, and 8.9 fold higher (P<0.001) at 126 days post-CrCL transection compared to baseline (Figure 6.3). The ratio was < 1 for all of the dogs prior

to (baseline) and 14 days after CrCL transection. Ratios were > 1 for 42% (8/19) of the dogs at 70 and 126 days post-CrCL transection, with a maximal ratio of 2.3 in one dog at 126 days (Figure 6.3).

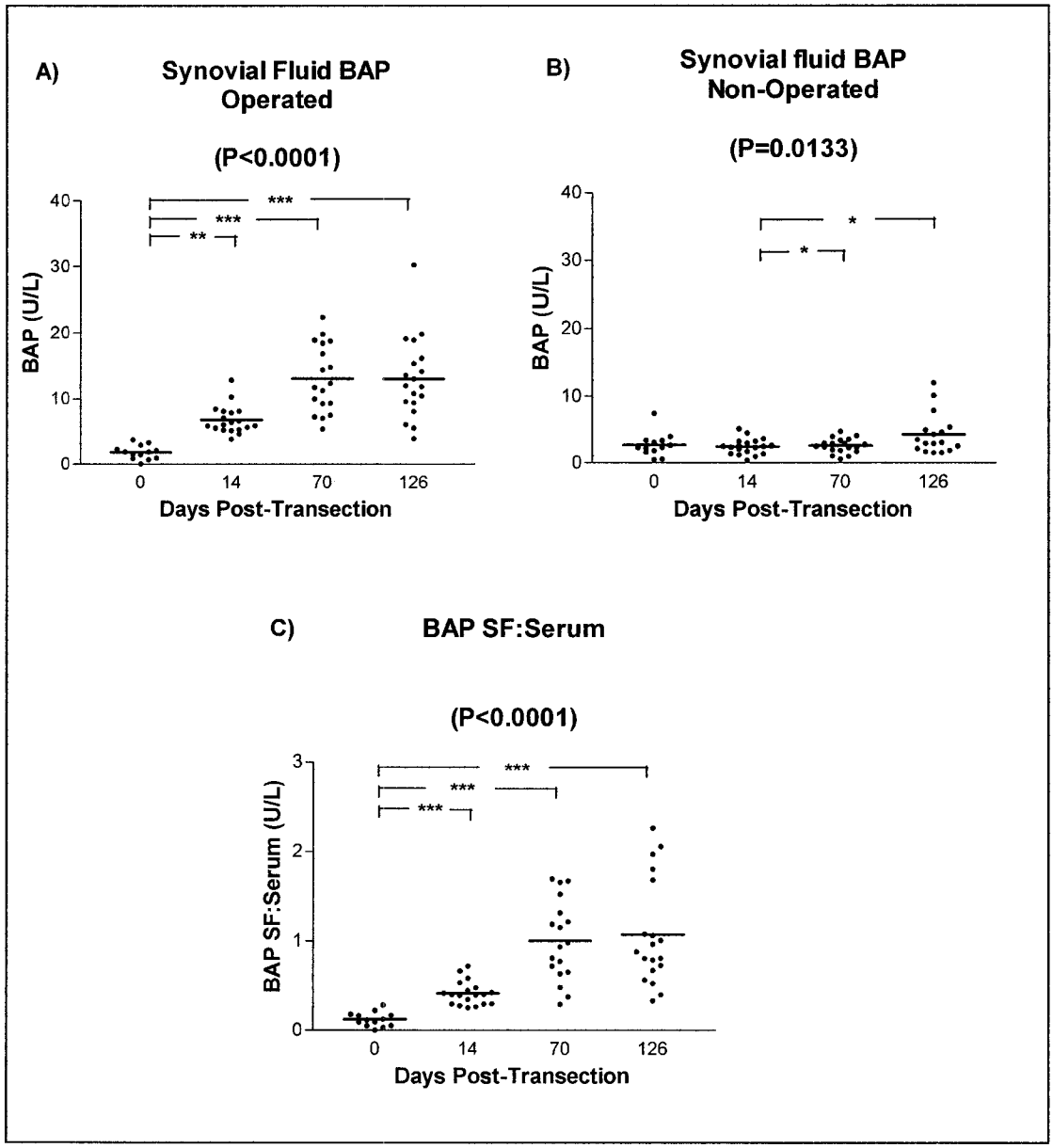

Figure 6.3. Individual BAP synovial values from the right CrCL transected stifle (A), the contralateral stifle (B), and the ratio between the BAP concentrations from the synovial fluid from the operated limb and serum (BAP SF:serum) (C). The transverse bar represents mean values. The P value for overall effect of time is listed on each graph, and was determined by a repeated measures ANOVA, using Tukey's post-hoc test for comparison of values to baseline (Day 0). Significant differences from baseline are represented as * P<0.05, ** P<0.01, *** P<0.0001, for (A) and (C), but in (B) there were no statistical differences from baseline, therefore comparisons are shown to day 14 to explain the overall significant effect.

6.4.3 Radiographic analysis. The total osteophyte score increased from baseline throughout the entire study, with a significant 15.3 fold elevation starting at 28 days (P<0.001), 35.8 fold increase at 70 days (P<0.001) and 67.7 fold increase at 126 days (P<0.001) post-CrCL transection when compared to baseline (Figure 6.4). Stepwise

Day	*Pat Distal*	*Pat Prox*	*Fem Tr*	*Tib L Plat*	*Tib M Plat*	*Tib Cd*	*Tib InCon*	*Fem L Con*	*Fem M Con*	*CrCL Insert*	*Total*
0	0.11 ± 0.46	0.05 ± 0.23	0	0	0	0	0	0.05 ± 0.23	0	0	0.21 ± 0.92
14	0.16 ± 0.50	0.11 ± 0.32	0.11 ± 0.32	0	0.05 ± 0.23	0	0	0.05 ± 0.23	0	0	0.47 ± 1.17
28	0.42 ± 0.61	0.16 ± 0.37	0.42 ± 0.51	0.05 ± 0.23	0.11 ± 0.32	0	0.05 ± 0.23	0.11 ± 0.32	0	0.05 ± 0.23	1.37 ± 1.61
70	1.11 ± 0.57	0.47 ± 0.70	1.21 ± 0.54	0.37 ± 0.50	0.37 ± 0.60	0.11 ± 0.32	1.42 ± 0.96	0.11 ± 0.32	0.05 ± 0.23	0.47 ± 0.61	5.68 ± 3.09
126	1.89 ± 0.66	1.05 ± 0.71	1.95 ± 0.71	0.95 ± 0.62	1.42 ± 0.77	0.74 ± 0.56	2.11 ± 0.99	0.68 ± 0.58	0.68 ± 0.75	0.89 ± 0.57	12.37 ± 3.52

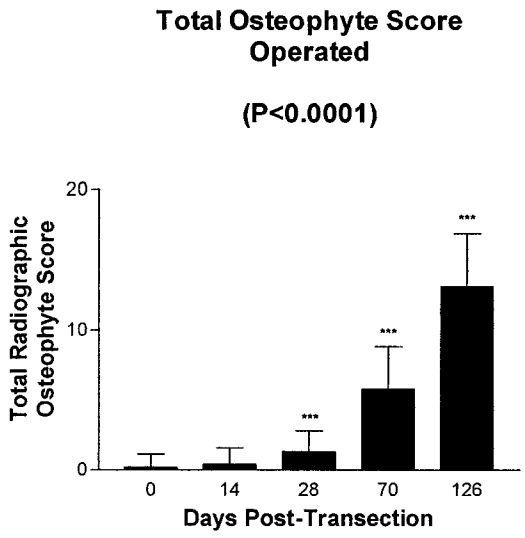

Figure 6.4. Table and graph of mean (± SD) osteophyte scores (0-3) for each location identified on radiographs for each examination period (Day 0, 14, 28, 70, and 126). The P value for overall effect of time is listed on the graph, and was determined by Kruskal-Wallis analysis, using Dunn's post-hoc test for comparison of values to baseline (Day 0). Significant differences from baseline are represented as *** P<0.001.
Pat = patella, Tib = tibia, Fem = femur, Prox = proximal, Tr = trochlear ridges, LPlat = lateral plateau, MPlat = medial plateau, Cd = caudal, InCon = intercondylar eminence, LCon = lateral condyle, MCon = medial condyle, and Insert = insertion.

multiple regression identified a significant relationship between the presence and severity of osteophytes along the femoral trochlear ridges, intercondylar eminence of the tibia,

and the caudal tibia and the concentration of BAP in the synovial fluid of the right CrCL deficient stifle ($r^2 = 0.5049$, $P<0.0001$).

6.4.4 Correlations. The BAP concentration in the synovial fluid from the CrCL deficient stifle positively correlated with the ratio of BAP SF:serum ($r=0.9226$, $P<0.0001$) (Table 6.1). The total osteophytic radiographic score positively correlated with the BAP concentration in the synovial fluid from the CrCL deficient stifle ($r=0.6705$, $P<0.0001$) as well as the ratio of BAP SF:serum ($r=0.6494$, $P<0.0001$) (Table 6.1). The concentration of BAP in the serum positively correlated with the concentration of OC in the serum ($r=0.3095$, $P<0.0001$) (Table 6.1).

	S-BAP	S-OC	SF-BAP	BAP SF:serum	Rad Score
S-BAP	1.000	**0.3095**	-0.0290	**-0.2385**	**-0.2417**
		(P<0.0001)		(P=0.0484)	(P=0.0183)
S-OC		1.000	-0.1819	-0.1764	-0.1965
SF-BAP			1.000	**0.9226**	**0.6705**
				(P<0.0001)	(P<0.0001)
BAP SF:serum				1.000	**0.6494**
					(P<0.0001)
Rad score					1.000

Table 6.1. Correlations between the serum (S) and synovial fluid (SF) concentrations from the right CrCL transected stifle of BAP, its SF:serum ratio, OC and the total osteophyte score (Rad score). Pearson correlation coefficients are reported for the S-BAP, S-OC, SF-BAP, and BAP SF:serum biomarkers, whereas Spearman rank correlation coefficients are reported for the total osteophyte score. Only significant P values ($P<0.05$) are listed in parentheses under its respective correlation coefficient that is highlighted in bold.

6.5 Discussion

In the mammalian body, bone goes through a finely regulated flux of formation and resorption to react and respond to the stresses placed on the skeleton from normal movement, as well as after injury. This osseous response can be monitored in various disease processes using biomolecular markers. Biomolecular markers of bone formation, such as BAP and OC have traditionally been measured in the serum of patients with fractures, cancer, or metabolic bone diseases[279,280,282,283]. These are all disease processes in which there should be a major response of the bone that can be easily detected by the serum. However, arthritic conditions usually have to involve more than one joint in order to result in detectable changes in the serum concentrations of biomarkers. This will generally occur in rheumatoid arthritis (RA), but rarely in OA secondary to trauma. Therefore, most of the studies examining the evaluation of BAP and OC levels in serum have involved humans with RA, and fewer have examined samples from OA patients[287,288,302,303]. The concentrations of OC in the serum from human OA patients have been reported to be below those in non-arthritic humans when there is no evidence of subchondral bone destruction[302], and similar to levels in normal humans when there is evidence of radiographic destruction[302,305]. In naturally occurring CrCL rupture in dogs, serum OC levels were significantly higher than controls[217]. This wide range of findings may reflect the subtle differences present between the stage of OA present in each group studied. In addition, lability and susceptibility of the OC molecule to fragmentation, as well as variability between assays in which fragments are examined can also lead to these conflicting results[306].

In our experimental OA model, we identified an early and significant elevation in serum OC concentrations 7 days after CrCL transection, followed by a return to normal, until it significantly decreased from baseline on days 84 and 112 post-CrCL transection. This increase was unexpected, since by one week after CrCL transection there was no evidence of any major changes to the bone such as osteophytes or subchondral changes that could be identified. The increase could be due to the acute difference in weight-bearing and use of the limb that occurs following CrCL transection[198], or associated with the exercise program that was started in these dogs 2 days post-operatively, both of which may have had an effect on the overall bone response in the rest of the body. The decrease in OC concentrations from baseline during the later stages of our study could be reflective of increased diffusion into the synovial fluid in response to osteophyte progression, increased fragmentation, with the intact molecule no longer being present, or increased clearance by the kidney.

The serum total alkaline phosphatase activity has been measured in human OA patients[285,287-289], as well as from dogs with naturally occurring CrCL rupture[217]. In these BAP the specific isoenzyme concentrations were being determined from wheat germ lectin precipitation, electrophoresis, or other immunoassay methods, resulting in potential cross-reactivity with the liver isoenzyme[288]. Serum total alkaline phosphatase activity has been reported to be normal in naturally occurring CrCL rupture in dogs[217], as have the specific BAP levels in human OA patients[289]. Similar to the OC studies, these studies examined alkaline phosphatase levels at the end-stage of the OA process as opposed to the acute phases reported in our study. We identified significant decreases from baseline in the serum levels of BAP, starting at day 28 and throughout most of the remainder of

the study and hypothesize that these decreases in serum BAP levels might be related to increased diffusion into the synovial fluid in response to an increase in osteophyte formation. Since synovial fluid is an ultrafiltrate of plasma, the potential exists that in order for osteophytes to form, diffusion of BAP from the blood must increase to adequately provide the necessary amounts of BAP.

To the authors' knowledge, this is the first study to examine BAP concentrations in the synovial fluid after cruciate ligament disruption in the dog. Total alkaline phosphatase levels in the synovial fluid have been reported from calcium pyrophosphate crystal deposition disease[307], and comparing human OA and RA patients[287]. In addition, increased levels of BAP have been reported in synovial fluid from joints with naturally occurring osteochondral fragmentation compared to the contralateral joints in horses[291]. Our study indicates that BAP levels in the synovial fluid significantly increased above baseline 2 weeks after CrCL transection and continued to rise throughout the remainder of the study whereas, the BAP concentration in the synovial fluid from the contralateral stifle did not differ from baseline throughout the study. SF:serum ratios were calculated in an attempt to distinguish whether the synovial fluid content was likely elevated due to local production or via diffusion from the plasma[287]. Prior to CrCL transection, when BAP levels were assumed to be normal in the serum and synovial fluid, serum levels were higher than the synovial fluid levels. This suggests that most of the BAP found in the synovial fluid in a normal joint, likely diffused from the blood into the joint. This trend continued two weeks after CrCL transection, but from day 70 post CrCL transection to the end of the study, the synovial fluid levels became higher than the serum in 42% of the dogs. This switch, combined with no changes from baseline in the synovial fluid

BAP concentrations from the contralateral stifle suggests that there was local production of BAP within the joint.

In previous reports that have utilized this model, the earliest osteophytic changes that have been identified either grossly or histologically, occurred by 2-4 weeks after injury[100,186,308], with the earliest radiographic evidence present between 4-5 weeks[100,308,309]. Sabistan, et al. demonstrated, via gross and magnetic resonance (MR) imaging, that osteophytes first appeared by 4 weeks after injury, then increased in size up to 32 weeks, after which the rate of progression decreased[186]. This would tend to indicate that the most likely active early source of bone formation markers after CrCL disruption would be osteophytes and rather than subchondral bone. Any major change to subchondral bone formation, as identified by biomarker analysis, at this stage of the disease process would be expected to be detected in the serum and not the synovial fluid, since subchondral bone is not exposed to the synovial fluid unless full thickness articular cartilage erosion is present.

In our study, computed radiography was used to demonstrate an increasing production of osteophytes that could be quantified, allowing documentation of the progression in size and location over time, as previously reported[171]. We found a significant positive correlation between our total osteophyte score and the BAP concentrations in the synovial fluid from the CrCL deficient stifle ($r=0.6705$). In addition, multiple regression was used to identify that 3 of the scores for osteophyte locations represented approximately 50% of the variation in the synovial fluid BAP levels. The potential exists for BAP concentrations in the synovial fluid to be used as an early biomarker of osteophyte formation with more sensitivity than radiographs.

However, we did not examine enough time points in the synovial fluid to be able to definitively make this conclusion.

The exact role and mechanism of BAP and OC in osteophyte formation is not completely understood. Our study, as well as others[1,100,119], have demonstrated that osteophytes have resulted from joint instability created by CrCL transection, but the direct relationship has been poorly understood. We theorize that the instability could be responsible for stimulating anabolic growth factors such as transforming growth factor-β (TGF-β), since its active form has been shown to be present in high levels with enhanced mechanical loading and excessive tissue damage[310,311]. In addition, injection of recombinant TGF-β into murine stifles has resulted in sustained over expression and origination of osteophyte formation from the periosteum in locations similar to those seen with OA[310-312]. Therefore, it is likely that instability causes increased TGF-β activity that is at least partially responsible for the stimulation of periosteum in generating chondrophytes that can undergo a process similar to endochondral ossification (Figure 6.5)[100,119]. During endochondral ossification, vascular infiltration has been shown to be linked to differentiation of chondrocytes[313,314], and is associated with[315] and maybe even precede osteophyte development[308]. In osteophytes, hypertrophic chondrocytes have been shown to express vascular endothelial cell growth factor (VEGF)[316] which helps regulate chondrocyte differentiation and triggers cartilage remodeling[317]. VEGF may, therefore, stimulate angiogenesis in response to TGF-β in osteophytes. This vascular invasion has been linked to apoptosis of differentiated chondrocytes by endothelial-derived nitric oxide (NO) around the blood vessels, resulting in recruitment of osteoblasts and the formation of mineralizing matrix vesicles (Figure 6.5)[316,318].

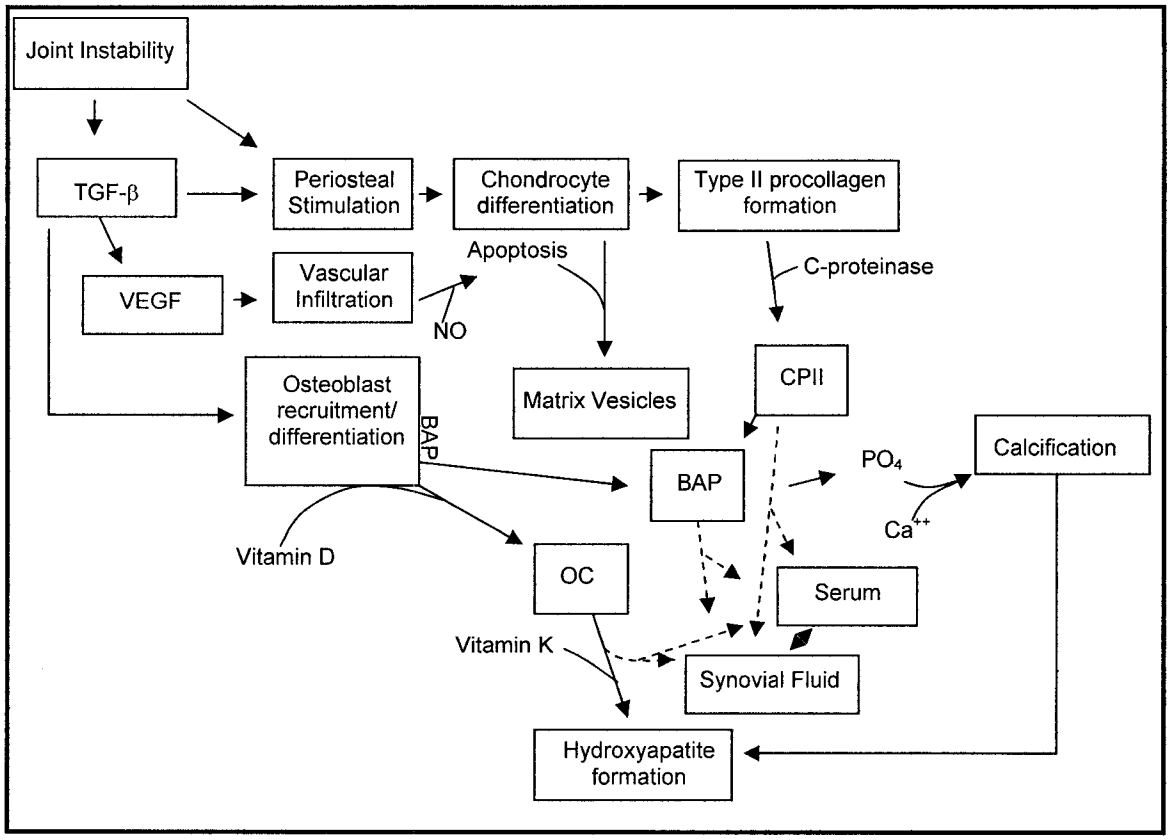

Figure 6.5. Schematic representation of potential pathways and involvement of BAP and OC in osteophyte formation. The dotted lines represent release of OC, BAP, and CPII into either the serum or synovial fluid. The matrix vesicle represents the general location around which the BAP, CPII, OC, PO_4 and Ca^{++} are located. TGF-β = Transforming growth factor-beta, VEGF = vascular endothelial growth factor, NO = nitric oxide, BAP = bone alkaline phosphatase, OC = osteocalcin, CPII = carboxy-propeptide of type II collagen, PO_4 = phosphate, Ca^{++} = calcium, C = carboxy

Bone alkaline phosphatase has been located on the vascular surface of the plasma membrane of osteoblasts[274], extending into the newly formed matrix vesicles[277], whereas osteocalcin is synthesized within the osteoblast by vitamin D stimulation[296,297]. Alkaline phosphatase concentrations have been shown to be elevated around matrix vesicles in the hypertrophic zone of endochondral ossification[277,319]. Most of the calcification in a growth plate occurs around these matrix vesicles due to the presence of focal concentrations of proteoglycans as well as the carboxy-propeptide of type II collagen (CPII)[278,320]. CPII is cleaved from the procollagen molecule of type II collagen shortly after synthesis, and accumulates next to the matrix vesicles, where alkaline phosphatase

is located, as well as focal accumulation of OC and calcium[278]. The CPII has been hypothesized to activate the BAP such that is mobilizes soluble inorganic phosphate which then reacts with calcium, resulting in mineral formation of hydroxyapatite[278]. This process is likely further enhanced by vitamin K activation of OC, giving it selective affinity for calcium, and allowing it to bind to hydroxyapatite[293-295]. Adding credence to this explanation, we compared the synovial fluid BAP levels in our study to the synovial fluid CPII levels in the same dogs (Chapter 7), and found a significant positive correlation ($r=0.5134$, $P<0.0001$). The exact mechanism for release of BAP, CPII and OC from osteoid is not completely understood, but it is reasonable to assume that since osteophytes have a large vascular supply, and are exposed to the synovial fluid, that all three molecules could be cleared into either fluid (Figure 6.5).

The bone markers evaluated in this study have been reported to vary in their levels in body fluids depending upon breed, age, sex, time of day, season, renal or hepatic function, and sample handling[321,322]. These potential sources of variability were minimized in our study, as our dogs were shown to have normal renal and hepatic function via hematologic exam, and all dogs were the same breed, age, and sex. In addition, all of the serum samples were collected at the same time of day and were processed quickly, with no excess in freeze/thaw cycles. The synovial fluid was collected by lavage technique to ensure enough synovial fluid for multiple biomarker analysis. The disadvantages of the lavage technique are that the volume of fluid within the joint is unknown, and it has the potential to affect the metabolism of the articular tissues. We feel that these concerns were minimized by the length of time between

collection periods and the fact that all of the joints were similarly treated for each dog at each time period.

In summary, we identified decreased levels of BAP and OC biomarkers from baseline in the serum, except for an early increase in OC levels at 7 days after CrCL transection in dogs. The BAP concentration in the synovial fluid of the CrCL deficient stifle increased over time, and positively correlated with the total osteophyte score. The increased ratio of BAP SF:serum by days 70 and 126 post-transection, combined with the lack of significant difference from baseline in the contralateral stifle, suggests that the BAP in the synovial fluid is being locally produced by newly forming osteophytes. These results suggest that the evaluation of BAP levels in the synovial fluid has the potential to be a sensitive indicator of osteophyte development in the early stages of secondary OA.

7 EVALUATION OF COLLAGEN SYNTHESIS (TYPE II) AND DEGRADATION (TYPE I AND II) BY COLLAGENASE CLEAVAGE AND PROTEOGLYCAN TURNOVER IN THE SYNOVIAL FLUID AND SERUM FROM A CANINE CRANIAL CRUCIATE TRANSECTION MODEL OF OSTEOARTHRITIS

Troy N. Trumble DVM, MS, R. Clark Billinghurst DVM, PhD, Megan S. Knowlton BS, C. Wayne McIlwraith BVSc, PhD

To be submitted to *Arthritis and Rheumatism* in spring 2003.

Presented in part at the 48th Annual Orthopaedic Research Society Meeting, Dallas, TX, February 10-13, 2002, and the 49th Annual Orthopaedic Research Society Meeting, New Orleans, LA, February 2-5, 2003.

7.1 Summary

Objective. To determine the temporal patterns and amount of type II collagen synthesis and degradation, as well as estimate type I collagen degradation and proteoglycan turnover by the use of biomarkers in a canine cranial cruciate ligament (CrCL) transection model of osteoarthritis.

Methods. Nineteen mature male Walker Hounds had the right CrCL transected arthroscopically. Synovial fluid and serum samples were collected prior to surgery, and then at various points post-transection. ELISAs were used to detect the carboxy-propeptide of type II collagen (CPII), type II collagen degradation (234CEQ), and type I and II collagen degradation (COL2-3/4C_{short}) products in the serum and synovial fluid, from which type I collagen degradation was calculated (COL2-3/4C_{short} - 234CEQ). The amount of proteoglycan turnover (sGAG) was also determined in the serum and synovial fluid. Cross-reactivity of the 234CEQ antibody with canine articular cartilage was analyzed.

Results. Serum concentrations of all biomarkers significantly decreased below baseline, except for the 234CEQ levels, which significantly increased by day 126 post-CrCL transection. The synovial fluid CPII, COL2-3/4C_{short} and type I collagen levels in the CrCL deficient stifle increased significantly above baseline by day 14 post-transection and then decreased over time. The synovial fluid 234CEQ levels increased over time, but were not statistically different from baseline, and sGAG levels increased above baseline, reaching a significant peak by day 126. Type II synthesis and degradation were both increased after CrCL transection, with synthesis predominating early and degradation predominating at the end of the study. Type I collagen degradation products were greater

than type II collagen degradation products in the synovial fluid, and predominated early whereas type II collagen degradation products predominated at the end of the study.

Conclusion. The ELISAs for CPII, 234CEQ, and COL2-3/4C_{short} can all be used to monitor the temporal pattern and levels of type II collagen synthesis and degradation, and combined type I and II collagen degradation, respectively, as well as to estimate type I collagen degradation from the synovial fluid and serum of dogs with CrCL transection.

7.2 Introduction

In the mammalian body, collagen is an abundant protein, compromising approximately 60% of the dry weight of articular cartilage with type II collagen accounting for 90% of the collagen content[16]. Type I collagen is also abundant in other articular tissues such as the menisci, ligaments, joint capsule, and subchondral bone. These collagens are responsible for providing strength and structure to these tissues. Proteoglycans function to arrest the flow of interstitial water when an external force is applied by forming large aggregates interspersed between the collagen fibrils. In a normal joint environment, homeostasis occurs between synthesis and degradation of type II collagen proteoglycan. However, when there are abnormal biomechanical stresses applied to the joint due to injury, such as rupture to the cranial cruciate ligament (CrCL – canine equivalent of the human anterior cruciate ligament), secondary osteoarthritis (OA) often develops[323]. The homeostatic balance changes, with catabolism of type II collagen and proteoglycan predominating. Biomolecular markers allow identification of the relative degree and temporal pattern of synthesis and degradation related to joint injury.

During fibril formation of type II collagen, the procollagen molecule is secreted from the chondrocytes into the extracellular matrix (ECM) with its helical carboxy- (C-)

and amino- (N-) propeptide extensions still attached. These propeptides are then cleaved and released from the tropocollagen molecule by specific C- and N- proteinases, allowing the tropocollagen molecule to get incorporated into collagen fibril formation (Figure 7.1) [324,325]. The type II collagen C-propeptide is equivalent to the calcium-binding protein chondrocalcin[326], and its content and release from the cartilage matrix has been directly correlated with type II collagen synthesis[222]. Through the use of radioimmunoassays (RIA)[327,328] and ELISA[329], the relative location and/or concentrations of the C-propeptide in cartilage[222,330], synovial fluid[222,329,331-334], and serum[222,328] of humans with OA and rheumatoid arthritis (RA) have been reported to represent disease-induced changes in type II collagen synthesis compared to controls.

Degradation of collagen and turnover of proteoglycan are presumed to be primarily initiated by pro-inflammatory cytokines that can cause up-regulation and activation of zinc dependent endopeptidases, called matrix metalloproteinases (MMPs). The collagenases (MMP -1, -8, and -13)[57-60] as well as the membrane bound MT1-MMP (MMP-14)[61] have been shown to cleave the fibrillar collagen triple helix at a specific site (Gly_{775}-Leu/Ile_{776}) approximately three fourths of the distance from the amino- terminal end of each α chain, resulting in the generation of a new three-quarter length fragment (TC^A) and one-quarter length fragment (TC^B)[57-59,61,62]. As a result of this cleavage, specific peptide sequences that were not accessible in the intact molecule (neoepitopes) on the new C-terminal end of the ¾ fragment now become exposed (Figure 7.1).

A polyclonal (COL2-3/4C_{short})[62] and a monoclonal (9A4)[335] antineoepitope antibody have been developed and shown to recognize the TC^A fragments of type I and II collagens in humans[62], and hamsters[335]. By lengthening the peptide sequence recognized

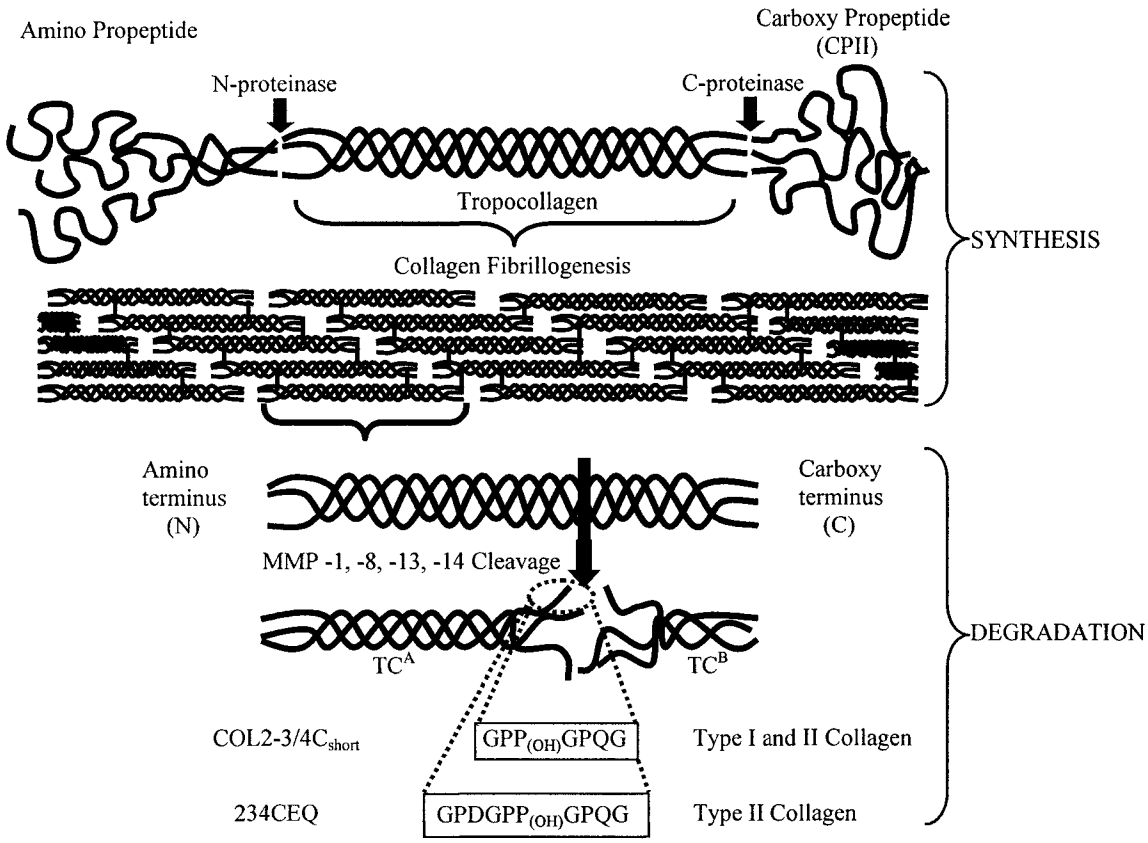

Figure 7.1. Schematic of collagen synthesis and degradation. The procollagen molecule of type II collagen is secreted extracellularly with amino- (N-) and carboxy- (C-) propeptides still attached. Each are cleaved off of the tropocollagen molecule by their respective proteinase prior to the tropocollagen incorporation into the collagen fibril. The carboxy-propeptide (CPII) is then released into cartilage, followed by the proximal body fluids, in which it can be identified and quantified using a polyclonal antibody to give an estimate of type II collagen synthesis. The collagenases (MMP -1, -8, and -13) as well as MMP-14 are capable of cleaving the collagen triple helix into a ¾ amino- fragment (TC^A) and a ¼ carboxy- fragment (TC^B). This cleavage exposes neoepitopes on the C- terminal end of the ¾ fragment that are not exposed in the uncleaved molecule. These fragments are released into the proximal body fluids and can be identified using the polyclonal antibodies COL2-3/4C_{short} and 234CEQ. The neoepitope recognized by COL2-3/4C_{short} represents both type I and II collagen cleavage, whereas the neoepitope recognized by 234CEQ represents only type II collagen cleavage. (Adapted from Manicourt, et al. 1999, and Billinghurst, et al. 1997, and 2001)

by the COL2-3/4C_{short} antibody in the N-terminal direction, a type II collagen specific antineoepitope antibody was developed for humans (COL2-3/4C_{long}) (Billinghurst, unpublished data). However, there was poor reactivity with this polyclonal antibody for cleaved equine type II collagen[223], and in our preliminary studies of canine type II

collagen degradation. Billinghurst, et al. developed an equine specific type II collagen antineoepitope antibody (234CEQ) that was based on a Glu-Asp substitution present in the peptide sequence of the immunogen to make it more equine specific, compared to the human sequence[223]. Since the peptide sequence for canine type II collagen is exactly the same in this region as that in the horse, we thought that cross-reactivity of the 234CEQ polyclonal antibody with canine type II collagen was likely[336,337]. Immunostaining has identified the relative location and/or concentrations of the COL2-3/4C_{short} and 234CEQ antineoepitope antibodies in articular cartilage[223,338-340], and in culture media[60,62,223,231,242], using an ELISA[341].

During the process of OA, the C-propeptide, collagen neoepitopes, as well as proteoglycan fragments are released from articular cartilage into the synovial fluid and eventually blood. Therefore, the aim of this study was to utilize the CPII, COL2-3/4C_{short}, and 234CEQ antibodies in ELISAs for quantitation of the C-propeptide, combined type I and II collagen and type II collagen specific collagenase cleavage fragments, respectively, in the synovial fluid and serum of cranial cruciate deficient dogs to be able to distinguish the relative amounts and temporal patterns of synthesis and degradation. The difference between the concentrations of COL2-3/4C_{short} and 234CEQ in both fluids was also used to estimate the relative amounts of types I collagen degradation during the acute stages of OA secondary to CrCL transection, and quantification of sulfated glycosaminoglycans (sGAG) was performed to estimate the proteoglycan turnover in both fluids. Our hypothesis was that both type II collagen synthesis and degradation would increase after CrCL transection, with synthesis diminishing and degradation predominating over time.

7.3 Materials and methods

7.3.1 Experimental design. Nineteen purpose-bred adult male Walker Hounds with a mean ± SD weight of 22.42 ± 2.39 kg (range, 19-28.5 kg) were used for this study. These dogs formed the placebo control group in a larger study evaluating a novel therapeutic agent for arthritis. Inclusion criteria required the dogs to be free of pre-existing orthopedic disease of the stifles (equivalent to the human knee) based on routine physical, orthopaedic, lameness, radiographic, and force plate examinations.

All dogs were anesthetized, and the right hind limb was prepared for aseptic surgery. A lateral parapatellar arthroscopic approach to the right stifle was used to examine the joint for the presence of any intra-articular pathology of the articular cartilage, cruciate ligaments and menisci. The CrCL was then transected arthroscopically using a meniscectomy blade (Chapter 2). Analgesia was administered via a 5 mg fentanyl patch (2.0 μg/kg/hr) that was applied the day before surgery and was maintained for 72 hours post-operatively. Morphine (1 mg/kg subcutaneously) was also administered post-operatively for pain, as needed. Cephalexin (Keflex) was administered intravenously during surgery and was continued orally (10 mg/kg) every 12 hours for 3 days to prevent infection. Throughout the study, all dogs were housed in individual runs. The animals were closely monitored during the first 48 hours post-operatively for any signs of pain, infection, anorexia, or intestinal complications. To encourage the development of OA, dogs were placed in an exercise protocol that required leash walking for 30 minutes every day for 5 days/week from the second day post-operatively until 126 days post-operatively.

All dogs were obtained through approved sources by the Colorado State University Laboratory Animal Resources, and the study was conducted under a protocol approved by the Colorado State University Animal Care and Use Committee.

7.3.2 Sample collection. Blood samples were collected in the morning from the jugular vein prior to surgery (Day 0), one and two weeks post-operatively, followed by every 2 weeks thereafter until day 126. Samples were placed in serum separator tubes and were allowed to clot at room temperature for approximately 30 minutes. The samples were then centrifuged for 10 minutes at 2,500 rpm. Synovial fluid samples were collected from both stifles using a lavage method where 5 ml of saline was injected into the joint. The limb was then manipulated for 1-2 minutes to ensure adequate mixing of the saline and the synovial fluid prior to aspiration of as much synovial fluid as possible. Fluid was collected prior to surgery, and then again at 14, 70, and 126 days post-operatively in serum separator tubes. The samples were placed immediately on ice after collection and were centrifuged at 4 C for 10 minutes at 2,500 rpm. The serum and synovial fluid samples were then split into multiple aliquots with the interval between sample collection and freezing at -80 C being under 3 hours. All samples were kept at -80 C until assayed. Most samples had 2 freeze/thaw cycles during sample analysis, with synovial fluid from the non-operated limb having as many as 4, due to less sample volume.

7.3.3 Molecular biomarker of type II collagen synthesis. Synthesis of type II collagen was evaluated by measuring serum and synovial fluid levels of CPII using a commercially available ELISA (IBEX Technologies, Montreal, CAN). This assay is a two-step competitive immunoassay based on a rabbit polyclonal antibody specific for

CPII (R160). Cross-reactivity of the antibody with the canine propeptide has been demonstrated by the manufacturer.

Briefly, 96-well microtiter plates were coated overnight at 4 C with 100 µl/well of CPII coating antigen stock diluted in a Tris based coating buffer. After washing, plates were stored at 4 C for no more than one week. In a separate polypropylene mixing plate, 50 µl of bovine CPII standards, serum or synovial fluid samples were added along with 50 µl of R160 anti-CPII antibody diluted in a protein-based buffer containing BSA and goat normal serum to all wells. Serum and synovial fluid samples were assayed at neet or a 1:2 dilution with a protein-based buffer containing BSA. The polypropylene plate was incubated on a high-speed shaker for 30 minutes at room temperature, followed by transfer of 80 µl of the antibody-standard/sample mix from each well of the polypropylene plate to the ELISA plate using a multi-channel pipette. The ELISA plate was then incubated on a high-speed shaker for 2 hours at room temperature. After washing, 100 µl of goat anti-rabbit Horse Radish Peroxidase (HRP) conjugate diluted in 6% BSA buffer was added to each well and incubated on a high-speed shaker for 30 minutes at room temperature. After washing, 100 µl of TMB (3,3′,5,5′ Tetramethylbenzidine) and hydrogen peroxide in an HRP substrate buffer was added to each well. After 30 minutes of incubation on a high-speed shaker at room temperature, 100 µl of stopping solution (2 M H_2SO_4) was added to each well. The absorbance at 450 nm was measured in a microplate reader (Dynex Technologies GmbH. Denkendorf, GER), and the concentration of the unknown samples were determined by constructing a standard curve from absorbances of the standards with known concentrations of bovine CPII. Interassay coefficient of variation (CV) was < 9% for the serum and synovial fluid.

7.3.4 Molecular biomarker of type I and II collagen degradation. Type I and II collagen degradation from collagenase-mediated cleavage was assessed by measuring neoepitope levels in the serum and synovial fluid with the COL2-3/4C$_{short}$ polyclonal antibody using an inhibition ELISA[341]. Serum samples were assayed at neet and synovial fluid samples were assayed at neet or 1:2 dilution. The interassay CV for the serum was < 14% and for the synovial fluid it was < 21%.

7.3.5 Molecular biomarker of type II collagen degradation. Type II specific collagen degradation from collagenase-mediated cleavage was assessed by measuring neoepitope levels in the serum and synovial fluid with the 234CEQ polyclonal antibody using a slightly modified inhibition ELISA from that used for the COL2-3/4C$_{short}$[223,341]. The primary 234CEQ antibody dilution was modified to 1:16,000. Serum and synovial fluid samples were assayed at neet. The interassay CV for the serum was < 12%, and for the synovial fluid it was < 20%.

7.3.6 Immunoblotting for 234CEQ specificity. Equine and canine type II collagen w ere c ollected from m acroscopically normal-appearing articular c artilage a nd isolated by pepsin digestion and differential salt precipitation[342]. Solutions of each were prepared by dissolving the lyophilized collagen in 0.5 *M* acetic acid and diluting to a final concentration of 1.5 mg/ml of digestion buffer that consisted of 50 m*M* Tris, 10 m*M* $CaCl_2$, 600 m*M* NaCl, and 0.01% Brij 35 (Sigma Chemical Co., St. Louis, MO), at pH 7.6. Recombinant human pro MMP-13 (Calbiochem-Novabiochem Corp., La Jolla, CA) was activated by incubation with 2 m*M* (final concentration) aminophenyl mercuric acetate (Sigma) in the same digestion buffer for 2 hours at 37 C. The activated MMP-13 was added to the collagen solutions at a final molar ratio of 1:60 (MMP-13:collagen).

Samples were incubated for 8 hours at 30 C, and the collagenase was inactivated with 166 m*M* EDTA (Sigma). To study the time-dependent collagenase cleavage of native type II collagen, aliquots were removed at 0, 1, 4 and 8 hours of incubation and the MMP-13 in each aliquot was inactivated with EDTA.

The MMP-13 cleaved fragments of the purified collagens were separated, using sodium dodecyl sulfate-polyacrylamide gel electrophoresis (Bio-Rad Laboratories, Hercules, CA) as previously described[343]. The 10% 1-mm thick mini-Protean gels were stained with Coomassie Blue R-250 (Bio-Rad). Electrophoretic transfer to nitrocellulose membranes (Bio-Rad) and immunodetection of the TC^A collagen fragments were performed as previously described[254], with the following exceptions: the BSA-blocked membranes were incubated for 1 hour with the 234CEQ antibody at 1:1,000 dilution in PBS-3% BSA-Tween, and after three 10-minute washes in PBS-1% BSA-Tween, alkaline phosphatase-conjugated goat anti-rabbit IgG $F(ab')_2$ fragment diluted 1:20,000 with PBS-3% BSA-Tween was added for 1 hour at 30 C.

7.3.7 Estimation of type I collagen degradation. Since the COL2-3/4C_{short} antineoepitope antibody recognizes both type I and type II collagen cleavage, whereas the 234CEQ antibody recognizes only type II collagen cleavage, the amount of type I collagen cleavage can be estimated. This was performed by subtracting the serum and synovial fluid 234CEQ values for each given dog and measurement period from the matching values obtained from the COL2-3/4C_{short} immunoassay. Negative values were assumed to be zero.

7.3.8 Determination of proteoglycan turnover. The serum and synovial fluid were assayed for the sulfated glycosaminoglycans (sGAG) content using a modification

of the colorimetric 1,9-dimethylmethylene blue dye-binding assay[224]. All serum and synovial fluid samples were digested with papain (Sigma), and then 10 µl of the sample or standard (chondroitin sulfate C; Sigma) were added to 190 µl of the dye reagent in the microtiter plate wells. The absorbance was read at 530 nm within 10 minutes. All serum samples were diluted 1:2, whereas the synovial fluid dilution was started at 1:10 and subsequently decreased, as required, to 1:5, 1:2, or neet. The interassay CV for the serum was < 23%, and for the synovial fluid it was < 28%.

7.3.9 Statistical analysis. All data were expressed as the mean ± SD unless otherwise specified. The distribution of the serum and synovial fluid CPII, COL2-3/4C_{short}, 234CEQ, type I collagen, and sGAG data were assessed using the Kolmogorov-Smirnov test. Serum and synovial fluid CPII levels were normally distributed. The serum and synovial fluid sGAG levels, as well as the serum 234CEQ, and the synovial fluid 234CEQ and COL2-3/4C_{short} from the right CrCL deficient stifle had to be transformed using the square root transformation to result in normalization of the data. However, due to the inordinate amount of zero values for the synovial fluid from the contralateral stifle for the 234CEQ and COL2-3/4C_{short} as well as the serum and synovial fluid values from both stifles for type I collagen, and the serum COL2-3/4C_{short}, no transformation could normalize the data. Square root transformation improved the distribution on this data, but did not normalize them. Separate non-parametric analyses were performed on this data and showed no overall difference from parametric analysis using square root transformation. Therefore, for ease of graphical comparison this data was presented with square root transformation and normality was assumed.

For each serum and synovial fluid data set, the overall effect of time was analyzed using a repeated measures ANOVA. Additional post-hoc Tukey's multiple comparisons tests were performed on each significant data set to determine significant differences from baseline (Day 0). Significant differences between other time points were ignored. Correlations between and within all of the serum and synovial fluid markers were assessed using Pearson correlation coefficient analysis using transformed data. A value of $P<0.05$ was considered significant for all analyses. All statistical analyses were performed using SAS software (SAS Institute, Cary, NC).

7.4 Results

7.4.1 Characterization of 234CEQ antibody as an antineoepitope antibody for collagenase-generated fragments of canine type II collagen. Immunoblotting of the aliquots removed during the 8 hour digestion of purified equine and canine type II collagens by the collagenase MMP-13, demonstrated recognition by the 234CEQ antibody of increasing concentrations of ¾-length fragments (Figure 7.2). The antibody recognized the monomeric ¾-length α chain fragments (αTC^{A}) of the cleaved equine and canine type II collagen, with equal intensity of staining.

7.4.2 Type II collagen synthesis, type I and II collagen cleavage by collagenases, and proteoglycan turnover in serum. The CPII concentrations (type II collagen synthesis) in the serum decreased significantly from baseline at 28 days ($P<0.001$), 42 days ($P<0.001$), 56 days ($P<0.001$), 70 days ($P<0.001$), and 112 days ($P<0.01$) post-CrCL transection (Figure 7.3). Conversely, the 234CEQ neoepitope levels (type II collagen degradation) in the serum remained elevated above baseline at all time

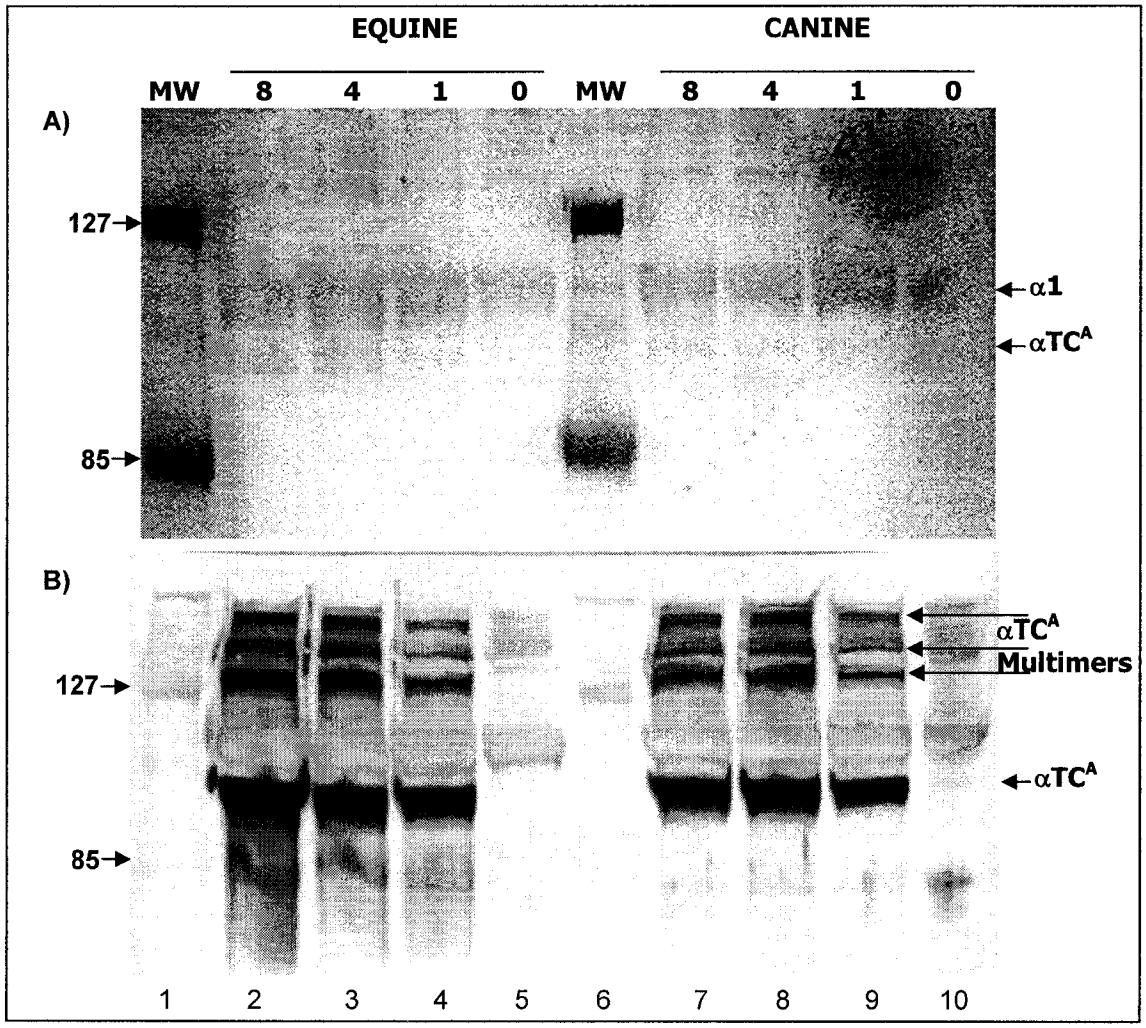

Figure 7.2. Immunoblot analysis of the time course of triple helical equine and canine type II collagen by recombinant human MMP-13 (rHuMMP-13). Type II collagen was collected from macroscopically normal appearing equine and canine articular cartilage, and was digested in solution over 8 hours with aminophenyl mercuric acetate-activated rHuMMP-13 at a final molar ratio of 1:60 (enzyme:collagen). Aliquots were removed at 0, 1, 4, and 8 hours, and the MMP-13 was inactivated with 166 m*M* EDTA. Each sample was separated under reducing conditions by sodium dodecyl sulfate (SDS)-polyacrylamide gel electrophoresis (PAGE; 10%) and either stained with Coomassie Blue (A) or eletrophoretically transferred to nitrocellulose and incubated with a 1:1,000 dilution of the 234CEQ $F(ab')_2$ preparation (B). The molecular weight (MW) standards and digestion times are indicated above the corresponding sample lanes for equine (lanes 1-5) and canine (lanes 6-10) type II collagens. The right margin indicates the positions of uncleaved α1(II) and the single αTC^A form of the ¾ length fragments produced by MMP-13 cleavage, as well as the ¾ fragment multimers (B). The left margin indicates the molecular weights of the standards in lanes 1 and 6.

points except for 28 days post-CrCL transection, peaking at 1.8 times higher than baseline at 126 days ($P<0.05$) post-CrCL transection (Figure 7.3).

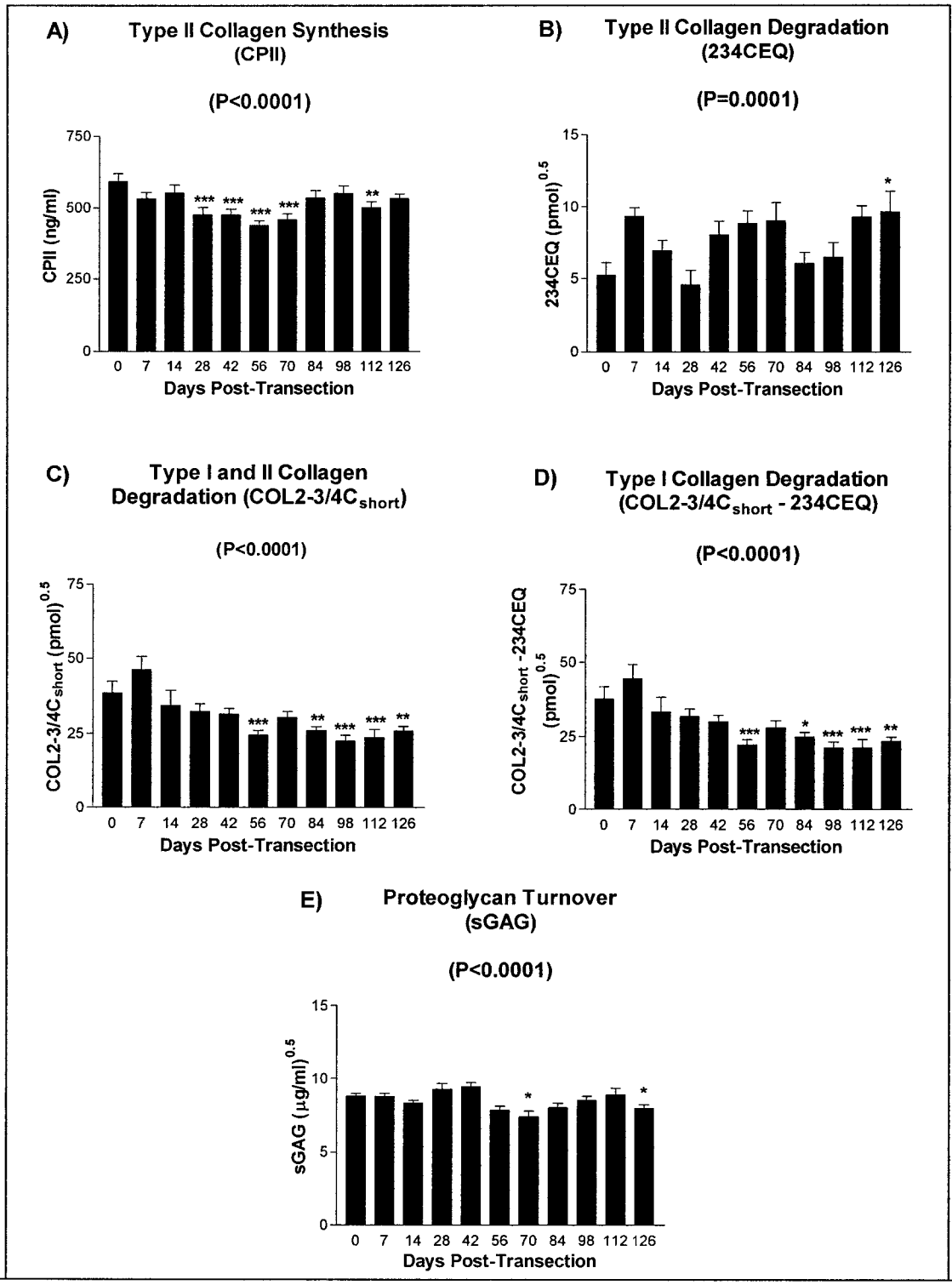

Figure 7.3. Mean (+ SEM) serum values for type II collagen synthesis (A) as represented by the carboxy-propeptide (CPII), and degradation (B and C) represented by collagenase cleavage of type II collagen (234CEQ) and combined type I and II collagen (COL2-3/4C_{short}). Type I collagen degradation (D) was calculated by subtracting the 234CEQ concentration from the COL2-3/4C_{short} concentration. Proteoglycan turnover (sulfated glycosaminoglycans, or sGAG) was also measured (E). The P value for overall effect of time is listed on each graph, as determined by repeated measures ANOVA, with Tukey's post-hoc test to compare values to baseline (Day 0). Significant differences from baseline are represented as *P<0.05, **P<0.01, and ***P<0.001.

The COL2-3/4C_{short} neoepitope levels (type I and II collagen degradation) in the serum peaked at 7 days post-CrCL transection and then decreased significantly from baseline at 56 days ($P<0.001$), 84 days ($P<0.01$), 98 days ($P<0.001$), 112 days ($P<0.001$), and 126 days ($P<0.01$) post-CrCL transection (Figure 7.3).

The estimation of type I collagen degradation (COL2-3/4C_{short} - 234CEQ levels) in the serum was similar to COL2-3/4C_{short} with a peak at 7 days post-CrCL transection followed by significant decrease from baseline at 56 days ($P<0.001$), 84 days ($P<0.05$), 98 days ($P<0.001$), 112 days ($P<0.001$), and 126 days ($P<0.01$) post-CrCL transection (Figure 7.3).

The amount of sGAG (proteoglycan turnover) in the serum, also decreased significantly from baseline at 70 days ($P<0.05$) and 126 days ($P<0.05$) post-CrCL transection (Figure 7.3).

7.4.3 Type II collagen synthesis, type I and II collagen cleavage by collagenases, and proteoglycan turnover in synovial fluid. The CPII concentrations (type II collagen synthesis) in the synovial fluid from the right CrCL deficient stifle, increased significantly above baseline throughout the entire study, with concentrations 2.3 fold higher ($P<0.001$) at 14 days, 1.9 fold higher ($P<0.001$) at 70 days, and 1.8 fold higher ($P<0.001$) at 126 days post-CrCL transection compared to baseline (Figure 7.4). Moreover, the 234CEQ neoepitope (type II collagen degradation) levels in the synovial fluid from the right CrCL deficient stifle, increased from baseline throughout the study, but was not significant (Figure 7.4).

The COL2-3/4C_{short} neoepitope (type I and II collagen degradation) levels in the synovial fluid from the right CrCL deficient stifle, increased significantly above baseline

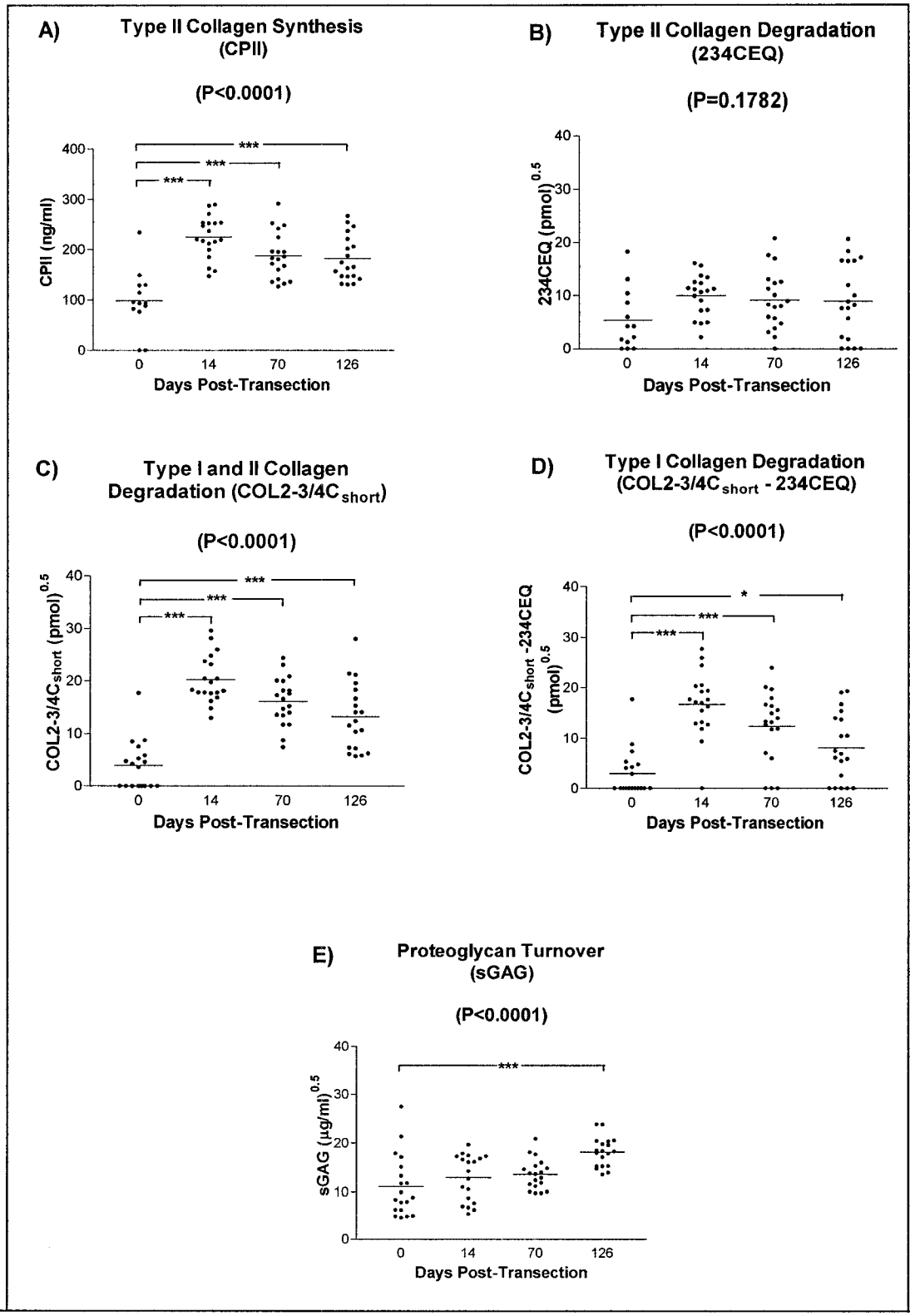

Figure 7.4. Individual synovial fluid values from the right CrCL transected stifle for the synthesis and degradation/turnover markers described in Figure 3. The transverse bar represents mean values. The P value for overall effect of time is listed on each graph, and was determined by a repeated measures ANOVA, with Tukey's post-hoc test for comparison of values to baseline (Day 0). Significant differences from baseline are represented as *P<0.05, **P<0.01, and ***P<0.001.

throughout the entire study, with concentrations 5.1 fold higher ($P<0.001$) at 14 days, 4.1 fold higher ($P<0.001$) at 70 days, and 3.3 fold higher ($P<0.001$) at 126 days post-CrCL transection when compared to baseline (Figure 7.4).

The estimation of type I collagen degradation (COL2-3/4C_{short} - 234CEQ levels) in the synovial fluid from the right CrCL deficient stifle increased significantly above baseline throughout the entire study, with concentrations 5.8 fold higher ($P<0.001$) at 14 days, 4.3 fold higher ($P<0.001$) at 70 days, and 2.8 fold higher ($P<0.05$) at 126 days post-CrCL transection compared to baseline (Figure 7.4).

The amount of sGAG (proteoglycan turnover) in the synovial fluid from the right CrCL deficient stifle, increased significantly above baseline, with concentrations being 1.6 fold higher ($P<0.001$) than baseline at 126 days post CrCL transection. (Figure 7.4).

The estimations of combined type I and II (COL2-3/4C_{short} neoepitope), type II specific (234CEQ neoepitope), and type I collagen degradation, as well as proteoglycan turnover (sGAG) in the synovial fluid from the left non-operated stifle did not reveal any significant differences from baseline concentrations (Figure 7.5).

7.4.4 Correlations. The relative predominance of type I collagen degradation compared to type II collagen degradation, as calculated by subtracting the 234CEQ concentration from the COL2-3/4C_{short} concentration, leads to an expected strong positive correlation between the calculated type I collagen and the COL2-3/4C_{short} levels in the serum ($r=0.9924$, $P<0.0001$), and synovial fluid from the right CrCL deficient stifle ($r=0.8713$, $P<0.0001$) (Table 7.1). There were no other statistically significant correlations of note between any of the biomarkers in the serum or between those in the serum compared to synovial fluid from the CrCL deficient stifle. The CPII

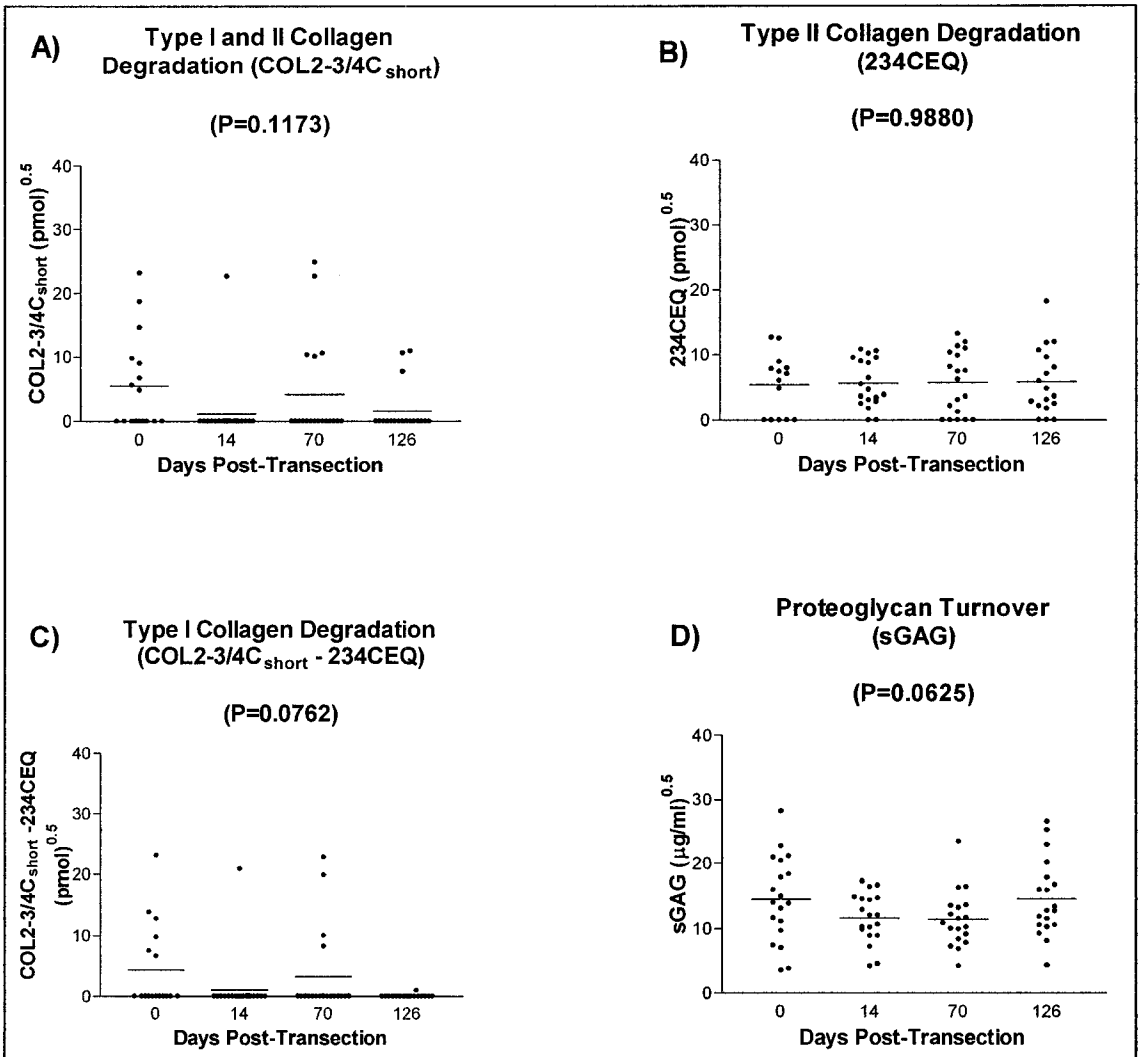

Figure 7.5. Individual synovial fluid values from the left non-operated stifle for the degradation/turnover markers described in Figure 3. The transverse bar represents mean values. The P value for overall effect of time is listed on each graph, and was determined by a repeated measures ANOVA, with Tukey's post-hoc test for comparison of values to baseline (Day 0). Note that CPII analysis was not performed on the left stifle.

concentrations in the synovial fluid from the CrCL deficient stifle positively correlated with synovial fluid concentrations from the same joint for COL2-3/4C$_{short}$ (r=0.7410, P<0.0001), type I collagen (r=0.5604, P<0.0001), 234CEQ (r=0.3106, P=0.0094), and sGAG (r=0.3030, P=0.0108) (Table 7.1). In addition, the 234 CEQ and COL2-3/4C$_{short}$ concentrations from the synovial fluid from the CrCL deficient stifle was also positively correlated (r=0.3594, P=0.0022) (Table 7.1).

Table 7.1. Pearson correlation coefficients between the serum (S) and synovial fluid (SF) from the right CrCL transected stifle of the collagen synthesis and degradation / proteoglycan turnover biomarkers identified in Figure 3. Only significant P values (P<0.05) are listed in parenthesis under its respective correlation coefficient that are highlighted in bold.

	S-CPII	S-234CEQ	S-COL2-3/4C$_{short}$	S-Type I	S-sGAG	SF-CPII	SF-234CEQ	SF-COL2-3/4C$_{short}$	SF-Type I	SF-sGAG
S-CPII	1.000	-0.0201	**0.1862** (P=0.0070)	**0.1930** (P=0.0051)	0.0997	-0.1364	-0.2202	-0.1069	0.0387	**-0.2577** (P=0.0246)
S-234CEQ		1.000	0.0539	-0.0456	0.0324	**0.2444** (P=0.0415)	0.1175	**0.2301** (P=0.0471)	**0.2286** (P=0.0470)	0.400
S-COL2-3/4C$_{short}$			1.000	**0.9924** (P<0.0001)	0.0956	0.0171	-0.0628	0.1084	0.1480	-0.1027
S-Type I				1.000	0.0927	0.0069	-0.0675	0.0953	0.1340	-0.0985
S-sGAG					1.000	-0.0509	0.0100	-0.0520	-0.0980	0.0520
SF-CPII						1.000	**0.3106** (P=0.0094)	**0.7410** (P<0.0001)	**0.5604** (P<0.0001)	**0.3030** (P=0.0108)
SF-234CEQ							1.000	**0.3594** (P=0.0022)	-0.0654	0.1181
SF-COL2-3/4C$_{short}$								1.000	**0.8713** (P<0.0001)	0.1782
SF-Type I									1.000	0.0792
SF-sGAG										1.000

7.5 Discussion

In articular cartilage, the C-propeptide has been shown to have a dual role. It helps to deliver the tropocollagen molecule outside of the cell so that fibril formation can occur, and then remains bound to the highly charged chondroitin sulfate chains of proteoglycans in the ECM and participates in calcification of the articular cartilage near the tidemark[278,326,344,345]. Nelson, et al. demonstrated that its half-life in cartilage is short and that the levels of CPII found in articular cartilage positively correlated with the amount of type II collagen synthesis that occurred[222]. In addition, they found that there was a positive correlation between the cartilage content of CPII and what was released into the culture media[222]. Likewise, the COL2-3/4C_{short}[60,62,231,242] as well as the 234CEQ[223] antineoepitope antibodies have also been shown to reflect the amount of collagenase-cleaved collagen released from the articular cartilage into culture media. These results all suggest that the levels of CPII, COL2-3/4C_{short} and 234CEQ neoepitopes identified in the synovial fluid and serum of our study by ELISA techniques should represent type II collagen synthesis, as well as type I and II collagen degradation derived from collagenase cleavage.

During normal joint homeostasis, there is a balance between synthesis and degradation of type II collagen within articular cartilage. However, after joint injury, such as cranial cruciate ligament transection/rupture, it is presumed the synthesis of type II collagen by chondrocytes is limited. In previous reports of human patients with primary or secondary OA, the synovial fluid CPII concentration increased over normal levels as the severity worsened, until end-stage OA was reached[329,331-334]. Lohmander, et al. also demonstrated that the CPII levels can increase as early as 1-2 days after injury

and can reach maximum levels before any radiographic changes of OA are present[329,332]. In our study, we also identified significantly increased CPII levels in the synovial fluid at all time points after CrCL transection, with a peak at 14 days post-transection. This indicated a significant, early response of the articular cartilage to synthesize type II collagen in the face of instability created by CrCL transection. This response decreased over time, but always remained significantly elevated compared to baseline. Serum levels of CPII in our study, however, decreased to below baseline, similar to what has been described in human OA patients compared to controls[222]. Dilution of the propeptides, slower release from articular cartilage, as well as further proteolytic processing of the propeptide in the serum may prevent detection of the elevations in CPII levels by the immunoassay[346].

The amino acid sequence of the C-termini created after collagenase cleavage of canine type II collagen, contains a Glu-Asp substitution from the human sequence that is recognized by the COL2-3/4C_{long} antineoepitope antibody. This substitution and amino acid sequence is exactly the same as the peptide sequence in the horse used for production of the 234CEQ antineoepitope antibody.[336,337] It was, therefore, likely that the 234CEQ antineoepitope antibody would also recognize canine type II collagen fragments derived from collagenase cleavage. As expected, immunoblot analysis demonstrated that the 234CEQ antineoepitope antibody recognizes the ¾ fragments (TC^A) of cleaved type II collagen from canine articular cartilage similar to collagenase cleaved equine type II collagen (Figure 7.2)[223]. Therefore, the 234CEQ polyclonal antibody could be used with canine samples to identify degradation specific to collagenase cleavage of the triple helix of type II collagen.

Synovial fluid type II collagen degradation increased above baseline at all time points in our study, but these increases were not significantly different from baseline. In the serum, however, the amount of type II degradation increased over time, peaking and becoming significantly higher than baseline at 126 days post-CrCL transection. This difference between the sensitivity of identification of the 234CEQ antineoepitope in the two fluids was interesting because usually one would expect the assay to detect greater differences in the synovial fluid compared to the serum due to its relative proximity to the articular cartilage. This difference could indicate that for consistent detection of the neoepitope, further denaturation of the collagenase-cleaved triple helix may be required. In addition, it could be due to potential variability in the use of the assay with synovial fluid, since the synovial fluid interassay SV (20%) was much greater than that for the serum (12%).

The combination of our results of type II synthesis and degradation indicate that both are locally stimulated after joint injury. Synthesis appears to occur more acutely, peaking at day 14 post-CrCL transection in the synovial fluid, whereas degradation peaks in the serum at day 126 post-CrCL transection. At day 126, we also demonstrated that the proteoglycan turnover in the synovial fluid significantly increased from baseline, showing that proteoglycan turnover also increases, along with, or because of collagen degradation. It is important to note that throughout the length of our study, type II collagen synthesis remains significantly elevated from baseline values, which agrees with the human OA studies[329,331-334]. This demonstrates that type II collagen synthesis responds quickly, in an attempt to maintain a relative homeostatic environment, but diminishes over time, while type II collagen degradation increases over time. It would be

likely that if we followed these dogs out for a longer time frame, the CPII content in the synovial fluid would return to baseline levels or lower, and the 234CEQ levels would continue to increase in both the synovial fluid and serum.

Garnero, et al. suggested that an uncoupling between synthesis and degradation occurs in human OA, where the rate of each becomes independent of the other[347]. However, in our study, the CPII levels were positively correlated with all of the other synovial fluid biomarkers that represented degradation (COL2-3/4C_{short}, 234CEQ, type I collagen, and sGAG). This would suggest that the synthetic response of type II collagen in the dog is likely to be greater when there is simultaneous degradation of type I and II collagen as well as proteoglycans. Similarly, in human patients with secondary OA from cruciate ligament or meniscal injury, it was demonstrated that the synovial fluid levels of CPII significantly correlated with cartilage damage scores, suggesting that it may actually reflect the overall extent of damage to the articular cartilage[334]. Therefore, even though synthesis and degradation may uncouple over time, in the early stages of secondary OA after CrCL transection in the dog, synthesis appeared to increase as degradation increased.

The COL2-3/4C_{short} antineoepitope antibody has been shown to recognize the peptide sequence for both human type I and type II collagen cleavage, due to the relative homology between the two[62]. Since there is relatively little species differences between these sequences, it was likely that this antibody would also recognize both type I and II collagen cleavage in canine tissues. In previous studies examining the use of the COL2-3/4C_{short} antibody in articular tissues, only articular cartilage has been examined, through immunostaining[338-340] or cartilage explant studies[60,62,231,242]. Since type II collagen

represents 90% of the collagen in articular cartilage[16], it could be assumed that cleavage identified in those cartilage studies was mostly representative of type II collagen degradation, and not type I collagen. However, when examining the articular environment via the synovial fluid and serum, as in our CrCL transection model, the amount of type II collagen compared to type I collagen becomes much smaller. In the serum, the most likely sources of type I collagen are the skin and bone, whereas in the synovial fluid, type I collagen fragments could be derived from the menisci, ligaments, joint capsule, and subchondral bone. This would indicate that both type I and type II collagen cleavage would be identified in the serum and synovial fluid of our study with no distinction between the two. Through the use of both the COL2-3/4C_{short} and 234CEQ antineoepitope antibodies, we were able to estimate the amount of type I collagen cleavage after CrCL transection.

Subtraction of the 234CEQ concentrations from the COL2-3/4C_{short} levels demonstrated that the COL2-3/4C_{short} antibody predominantly identifies type I collagen cleavage in the serum and synovial fluid of this study compared to type II collagen. Because of this, the estimated type I collagen degradation was similar to the COL2-3/4C_{short} findings described above. This study demonstrated that type I (predominantly) and type II collagen degradation are key features of our model of OA in the dog. This can be monitored by measurement of biomarker levels in serum and synovial fluid. Type I collagen degradation tended to predominant early in the disease process (day 14), whereas type II collagen degradation tended to predominate later (day 126).

To further evaluate the predominance of type I collagen degradation in the early stages after CrCL transection, we arthroscopically examined the stifles of 3 dogs in a

companion study at 14, 70 and 126 days post-CrCL transection (Chapter 3). The peak of cleaved collagen at day 14 post-transection (supporting peak collagenase levels) appeared to be associated with the acute inflammatory process that was evident arthroscopically. The source of type I cleavage products likely varied depending on the stage of the disease process. In the initial stages of injury (day 14), there was a generalized fibrous response within the joint. Fibrin covered the transected ends of the CrCL, and there was fraying of the menisci. By day 70 and 126, there were adhesions to the CrCL, as well as thickening of the joint capsule, synovial membrane, and fat pad. There was increasing damage to the meniscus at this stage, and this may have been the primary source of type I collagen degradation products measured at this stage of experimental OA.

Our study did have some limitations. The variability of cartilaginous as well as medial meniscal injury that occurred after CrCL transection is likely reflected in the variability of the biomarker data. In addition, the COL2-3/4C_{short} and 234CEQ ELISAs were in-house assays that inherently had interassay CVs that were >10% for the serum and synovial fluid, which will increase the variability of the results. The synovial fluid was collected by lavage technique because of the difficulty in aspirating enough synovial fluid to be able to analyze multiple biomarkers. The disadvantages of the lavage technique are that the volume of fluid within the joint is unknown, and it has the potential to affect the metabolism of the articular tissues. We feel that these concerns were minimized by the length of time between collection periods and the fact that all of the joints were similarly treated for each dog at each time period.

In summary, we identified that the 234CEQ antineoepitope antibody recognizes the ¾ fragment created by collagenase cleavage of canine type II collagen. The CPII,

COL2-3/4C_{short}, and 234CEQ assays were able to detect the C-propeptide, and respective type I and II collagen neoepitopes created after collagenase cleavage of the collagen triple helix in the synovial fluid and serum from dogs with a transected CrCL, allowing determination of the temporal pattern and relative amounts of type II synthesis, type I and II collagen degradation and specific type II collagen degradation, respectively. Synovial fluid was the superior fluid for analysis of these biomarkers compared to serum. Type II synthesis (CPII) and degradation (234CEQ) were both increased after CrCL transection in the dog, with synthesis predominating early and degradation predominating at the end of the study. In addition, the relative contribution of type I collagen degradation was determined (COL2-3/4C_{short} – 234CEQ), with type I collagen degradation predominating early and type II collagen degradation predominating at the end of the study.

8 CORRELATION OF SYNOVIAL FLUID PROSTAGLANDIN (PGE_2) CONCENTRATIONS TO GROUND REACTION FORCES AND CLINICAL PARAMETERS OF PAIN AND INFLAMMATION IN A CANINE CRANIAL CRUCIATE TRANSECTION MODEL OF OSTEOARTHRITIS

Troy N. Trumble DVM, MS, R. Clark Billinghurst DVM, PhD, C. Wayne McIlwraith BVSc, PhD

To be submitted to *American Journal of Veterinary Research* in spring 2003.

8.1 Summary

Objective. Evaluate the temporal pattern of prostaglandin (PGE_2) concentrations in the synovial fluid after transection of the cranial cruciate ligament (CrCL) in the dog, in an attempt to correlate it to ground reaction forces and subjective clinical parameters of lameness and/or pain.

Methods. Nineteen purpose-bred adult male Walker Hounds had the right CrCL transected arthroscopically. Force plate measurements, subjective clinical analysis of pain or lameness and synovial fluid were collected prior to surgery (baseline), and then at various time points post-transection. PGE_2 analysis was performed on the synovial fluid samples, and the PGE_2 concentrations were correlated to the ground reaction forces and clinical parameters.

Results. The PGE_2 concentration significantly increased above baseline throughout the entire study ($P<0.0001$), peaking 14 days after transection. The peak vertical force and impulse significantly decreased ($P<0.0001$) by day 14 post-transection, followed by an increase over time without returning to baseline levels. All of the clinical parameters (lameness, degree of weight bearing, joint extension, overall pain score, effusion score, and synovial fluid total protein content) except for synovial fluid WBC count significantly increased above baseline ($P<0.0001$). Significant negative correlations ($P<0.0001$) were present between the PGE_2 concentration and the peak vertical force ($r = -0.5720$) and impulse ($r = -0.4573$), and significant positive correlations ($P<0.0001$) were present between the PGE_2 concentration and the subjective lameness score ($r = 0.5016$) and the effusion score ($r = 0.6817$).

Conclusion. The correlations between PGE_2 concentrations in synovial fluid and the parameters used to measure pain and lameness suggests significant involvement of PGE_2 in the acute inflammatory process occurring within the joint in this model.

8.2 Introduction

Cranial cruciate ligament (CrCL) transection in dogs has been an accepted experimental model of osteoarthritis (OA) that results in changes typical of the early stages of OA in both humans and dogs[1]. Transection of the CrCL in the dog ultimately results in damage to all of the intra-articular structures, including the synovium, menisci, articular cartilage, and subchondral bone[1,101,249]. This injury has been presumed to be due to the combination of many events that are primarily related to joint instability and inflammation[101]. Traditionally, it has been thought that the instability leads to increased inflammation, however, with surgical transection of the CrCL, inflammation is usually present at the same time as the creation of the instability, and the combination will cause the dog to be lame[97].

With the onset of inflammation, cytokines such as interleukin-1 (IL-1) and tumor necrosis factor alpha (TNFα) are upregulated, and they in turn activate the cyclo-oxygenase (COX) pathway. The induction of the COX-2 pathway, in particular, stimulates the synovium to produce a variety of inflammatory mediators such as prostaglandins, thromboxanes, leukotrienes, and kinins[348-350]. Prostaglandin E_2 (PGE_2) has been shown to be the most important inflammatory mediator in experimentally induced inflammatory exudates[351]. It is an eicosanoid that is capable of mediating a number of features characteristic of inflammation including vasodilation and increased permeability of small blood vessels, leading to erythema[352]. In addition, it sensitizes

peripheral nocioceptors[353,354], stimulates the formation of new blood vessels[355], and alters expression of matrix metalloproteinases (MMPs) via promotion of plasminogen activators[356]. The diversity of these reactions are due to the existence of multiple receptor subtypes and isoforms that are responsible for the regulation of the prostaglandin cycle[357]. PGE_2 has both anabolic and catabolic effects via its regulation of chondrocyte proliferation and the synthesis of extracellular matrix components[358-360]. It has been shown to be present in greater amounts from synovial fluid of horses with varying degrees of OA compared to that from normal joints[351,361], and due to its high levels in the synovial fluid early in the disease process, it has been suggested to be a useful indicator of the existing inflammatory status[361].

Force plate analysis has been used as a research tool in dogs to objectively measure normal and abnormal forces[192,196-202,263-265]. It allows for description of the peak forces and impulses (total force applied over time) applied in vertical, craniocaudal (braking and propulsion), and mediolateral directions. Many canine orthopedic studies have included analysis of these ground reaction forces to objectively determine the normal forces applied for different gait cycles at varying velocities[192,196,197,263-265]. In addition, force plate analysis has been used to measure the abnormal forces that result from insult to the appendicular skeleton, as well as the response of the limb to various surgical techniques or medical therapies used to treat joint impairment[198-202]. Force plate analysis has been used to document changes in the ground reaction forces that occur as a result of CrCL rupture/transection compared to preoperative values[198-202]. Certain surgical techniques have been shown to improve this kinetic data in the early period, suggesting that the force plate is a sensitive tool for identification of subtle differences

that can occur over time[199]. To the authors' knowledge, PGE_2 concentrations in the synovial fluid of dogs have not been correlated to the ground reaction forces produced after cruciate ligament injury.

The purpose of this study was to evaluate the temporal pattern of PGE_2 concentrations in the synovial fluid after experimental transection of the CrCL in the dog, in an attempt to correlate these levels with subjective and objective analysis of pain and/or lameness. Our hypothesis was that PGE_2 concentrations in the synovial fluid would peak early and would correlate to objective analysis of lameness via force plate analysis.

8.3 Materials and methods

8.3.1 Experimental design. Nineteen purpose-bred adult male Walker Hounds with a mean ± SD weight of 22.42 ± 2.39 kg (range, 19-28.5 kg) were studied. These dogs were the placebo control group in a larger study of a novel therapeutic agent. Inclusion criteria required the dogs to be free of pre-existing orthopaedic disease of the stifles based on routine physical, orthopaedic, lameness, radiographic, and force plate examinations. Orthopaedic examination included a separate lameness and physical examination of both hind limbs as well as radiographs of both stifles. In anticipation of gait analyses, each dog was acclimated for several weeks to the force platform analysis laboratory and was led by a leash at a trot across the force plate prior to inclusion into the study. Selection and subsequent inclusion required the dogs to be free of pre-existing orthopaedic disease of the stifles based on orthopedic examination and radiography. In addition, the dogs had to be able to adequately trot across the force plate with minimal effort or coaxing from the handler.

All dogs were anesthetized, and the right hind limb was prepared for aseptic surgery. A lateral parapatellar arthroscopic approach to the right stifle was used to examine the joint for the presence of any intra-articular pathology of the articular cartilage, cruciate ligaments and menisci. The CrCL was then transected arthroscopically using a meniscectomy blade (Chapter 2). Analgesia was administered via a 5 mg fentanyl patch (2.0 μg/kg/hr) that was applied the day before surgery and was maintained for 72 hours post-operatively. Morphine (1 mg/kg subcutaneously) was also administered post-operatively for pain, as needed. Cephalexin (Keflex) was administered intravenously during surgery and was continued orally (10 mg/kg) every 12 hours for 3 days to prevent infection. Throughout the study, all dogs were housed in individual runs. The animals were closely monitored during the first 48 hours post-operatively for any signs of pain, infection, anorexia, or intestinal complications. To encourage the development of OA, dogs were placed in an exercise protocol that required leash walking for 30 minutes every day for 5 days/week from the second day post-operatively until 126 days post-operatively.

All dogs were obtained through approved sources by the Colorado State University Laboratory Animal Resources, and the study was conducted under a protocol approved by the Colorado State University Animal Care and Use Committee.

8.3.2 Synovial fluid collection. Synovial fluid samples were collected from the right CrCL transected stifle using a lavage method where 5 ml of sterile saline was injected into the joint. The limb was then manipulated for 1-2 minutes to ensure adequate mixing of the saline and the synovial fluid prior to aspiration of as much synovial fluid as possible. Fluid was collected prior to surgery, and then again at 14, 70, and 126 days

post-operatively. Of the total volume collected, 0.5-1.0 ml was added to a tube containing EDTA and the remainder was placed in serum separator tubes. The EDTA tubes were analyzed for total protein content and white blood cell count. The samples from the serum separator tubes were placed immediately on ice after collection and were centrifuged at 4 C for 10 minutes at 2,500 rpm. The samples were then split into multiple aliquots with the interval between sample collection and freezing at -80 C being under 3 hours. All samples were kept at -80 C until assayed. Most samples used for PGE_2 analysis had 2-4 freeze/thaw cycles during sample analysis, due to the volume of synovial fluid required for analysis.

8.3.3 Prostaglandin E_2 (PGE_2) Analysis.

Extraction – Synovial fluid samples were subjected to solid phase extraction procedures. Synovial fluid (500 µl) was mixed with 500 µl of 80% ethanol and 10 µl of glacial acetic acid, and then incubated at room temperature for 5 minutes prior to centrifugation (5500 rpm) for 8 minutes. The supernatant was applied to 1-ml, C2 minicolumns (Amprep Minicolumns, Amersham Pharmacia Biotech Limited, UK) that had been washed twice with 1 ml of 10% ethanol, under vacuum. The columns were then washed with 1 ml of deionized water and 1 ml of hexane, and the PGE_2 was eluted, under vacuum, with 1.5 ml of ethyl acetate. The eluted sample was evaporated to dryness under a continuous nitrogen flow, using a multi-port gas evaporation system (Savant Speed Vac Plus, Thermo Savant, Holbrook, NY), and then stored at -20 C.

Assay – The PGE_2 concentration was estimated using a commercially available enzyme immunoassay kit (Correlate-EIA, Assay Designs, Inc., Ann Arbor, MI). This immunoassay uses a monoclonal antibody that competitively binds to PGE_2 or an alkaline

phosphatase molecule bound with PGE_2. Prior to analysis, each extracted sample was resuspended in 400 µl of the supplied assay buffer. Then 100 µl of assay buffer, PGE_2 standards or synovial fluid samples (neet) were applied to the appropriate wells that were coated with a goat antibody specific to mouse IgG. This was followed by addition of 50 µl of assay buffer, alkaline phosphatase conjugated with PGE_2 and/or the monoclonal antibody to PGE_2 to the appropriate wells, and the plate was sealed and incubated overnight (18-24 hours) at 4 C. After washing, 5 µl of alkaline phosphatase conjugated with PGE_2 was added to each well indicating total activity, followed by 200 µl of p-nitrophenyl phosphate (p-Npp) substrate solution. After incubation for 1 hour at 37 C, 50 µl of stop solution (trisodium phosphate) was added to each well. The absorbance at 405 nm was measured immediately in a microplate reader (Dynex MRX plate reader, Dynex Technologies GmbH, Denkendorf, GER). The binding percentage for each standard and sample was calculated, and the concentration of PGE_2 in the samples was determined from a standard curve created using a log-logit transformation. Due to limited sample volume, no interassay coefficient of variation (CV) was performed.

8.3.4 Force plate evaluation. The force plate (Model ORS6-5, Advanced Mechanical Technologies, Inc., Newton, MA) was mounted in the center of, and level with, the surface of a 15-m runway. The signal from the force plate was processed and stored by use of computer software programs (IBM 486Dx, IBM Co., Boca-Raton, FL, and Acquire, Version 6.3W, Sharon Software Inc., Dewitt, MI). As each dog was trotted over the force plate, velocity was recorded by use of 2 photoelectric cells, placed 2 m apart, and a start-interrupt timer system. Care was taken to ensure that the dog triggered the photoelectric cells and that a constant speed was maintained across the force plate

during each trial. Dogs were trotted across the force plate by one handler prior to having the CrCL transected (baseline), and then again at 14, 28, 70 and 126 days post-transection. An evaluation was considered valid if the dog struck the plate with its right forelimb followed by its right hind limb at a velocity between 1.45 and 2.05 m/s with less than 10% acceleration/deceleration. If a dog was distracted during an evaluation, or any other paw or combination of limbs struck the force plate, then the data was considered invalid. Due to the severity of lameness present in some dogs, each dog was trotted across the force plate a maximum of 75 times per trial session, with a maximum of five acceptable trials collected per dog, per session. If the dog was completely non-weight bearing on the right hind limb, then the value entered for each trial was zero. All trials were recorded and archived on digital video. Peak vertical force and impulse were recorded for each limb at 1-millisecond intervals for 650 milliseconds after foot strike. All forces were normalized to the dog's body weight recorded at each measurement period.

8.3.5 Subjective clinical pain scoring. Subjective assessment of lameness and pain was performed just before each force plate evaluation, prior to CrCL transection (baseline), and then again at 14, 28, 70, and 126 days post-transection. All subjective scores were performed by the same evaluator (TNT). Lameness was graded on a scale from 1-4, with 1 = no lameness, 2 = mild lameness at a walk or trot, 3 = moderate lameness at a walk or trot, or 4 = severe lameness at a walk or trot. The degree of weight bearing when the limb was at rest was assessed on a scale from 1-3, 1 = normal weight bearing at rest, 2 = partial weight bearing at rest, or 3 = non-weight bearing at rest. For subjective assessment of pain, the limb was lifted off the ground and maximally

extended. The response to this limb extension was assessed on a scale from 1-4, with 1 = no response, 2 = mild response (turn head toward affected limb), 3 = moderate response (withdraws affected limb), or 4 = severe response (vocalizes or becomes aggressive). A cumulative overall pain score was calculated by summing the scores for lameness, weight bearing and joint extension. In addition, the degree of joint effusion was subjectively assessed at the time of arthrocentesis on days 0, 14, 70 and 126. The scale for the effusion score ranged from 0-3, with 0 = no effusion, 1 = mild effusion, 2 = moderate effusion, or 3 = severe effusion.

8.3.6 Statistical analysis. All data were expressed as the mean ± SD unless otherwise specified. The distribution of the data for the synovial fluid PGE_2, total protein and white blood cell count, peak vertical force and impulse, as well as subjective scores for lameness, degree of weight bearing, joint extension, overall pain score, and effusion score were assessed for normality using the Kolmogorov-Smirnov test. The peak vertical force was normally distributed. Data for the PGE_2 concentrations had to be transformed using logarithms to result in normalization of the data. All of the other data sets (synovial fluid total protein and white blood cell count, vertical impulse, subjective scores for lameness, degree of weight bearing, joint extension, overall pain scoring, and effusion score) could not be normalized with transformations and were analyzed non-parametrically.

For the peak vertical force and the PGE_2 data, the overall effect of time was analyzed using a repeated measures ANOVA on the normalized data. Additional post-hoc Tukey's multiple comparisons tests were performed on each significant data set to determine significant differences from baseline. For the non-parametric data (vertical

impulse, synovial fluid total protein and white blood cell count, lameness, degree of weight bearing, joint extension, overall pain score, and effusion score), Kruskal-Wallis analyses were performed using a Dunn's post-hoc test to determine significant differences from baseline. Correlations between the peak vertical force and PGE_2 concentrations were assessed using Pearson's correlation coefficient on the normalized data. Correlations made to the non parametric data, including the vertical impulse and the clinical parameters (synovial fluid total protein and white blood cell count, lameness, degree of weight bearing, joint extension, overall pain score and effusion score) were performed using the Spearman Rank correlation. A value of $P<0.05$ was considered significant for all analyses. All statistical analyses were performed using SAS software (SAS Institute, Cary, NC).

8.4 Results

8.4.1 PGE_2 analysis. PGE_2 concentrations in the synovial fluid significantly increased above baseline throughout the entire study, with concentrations 1.5 fold higher ($P<0.001$) at 14 days, 1.4 fold higher as 70 days ($P<0.001$), and 1.3 fold higher ($P<0.001$) at 126 days post-CrCL transection compared to baseline (Figure 8.1).

8.4.2 Force plate analysis. The peak vertical force from the CrCL deficient limb significantly decreased below baseline throughout the entire study, with the mean force being 62% lower on day 14 ($P<0.001$), 49% lower on day 28 ($P<0.001$), 42% lower

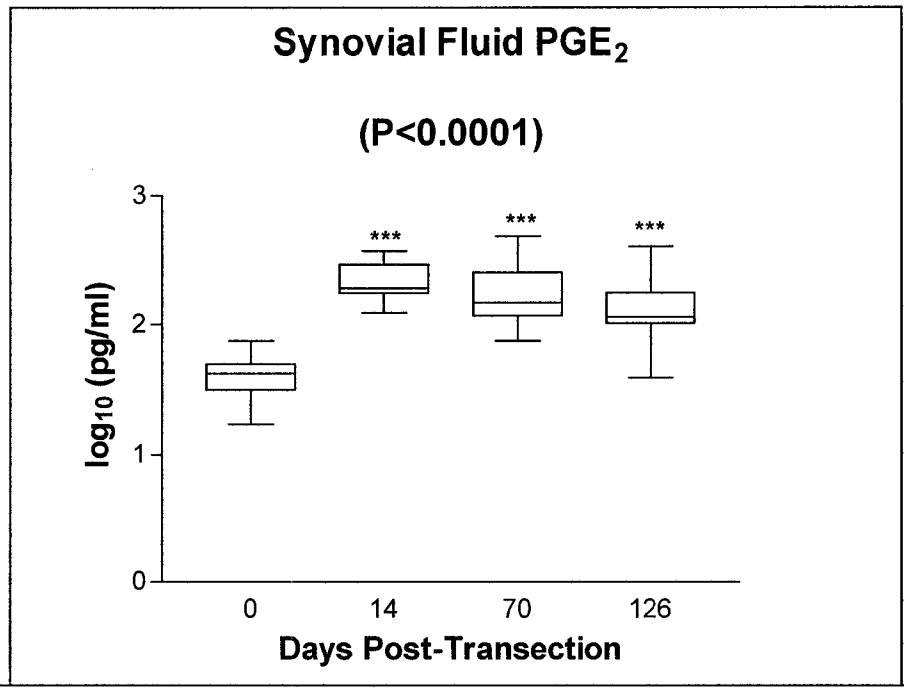

Figure 8.1. Concentrations of PGE_2 in the synovial fluid (expressed as logarithmic transformation of pg/ml) from the CrCL transected stifle for each measurement period (Day 0, 14, 70, and 126). The box represents the 25^{th}-75^{th} percentiles, the line represents the median and the whiskers represent the 10^{th} and 90^{th} percentiles. The P value for overall effect of time was P<0.0001, as determined by a repeated measures ANOVA, with Tukey's post-hoc test for comparison of values to baseline (Day 0). Significant differences from baseline are represented as *** P<0.001.

on day 70 (P<0.001), and 27% lower on day 126 (P<0.001) post-CrCL transection than the mean force measured at baseline (Figure 8.2). The corresponding peak vertical

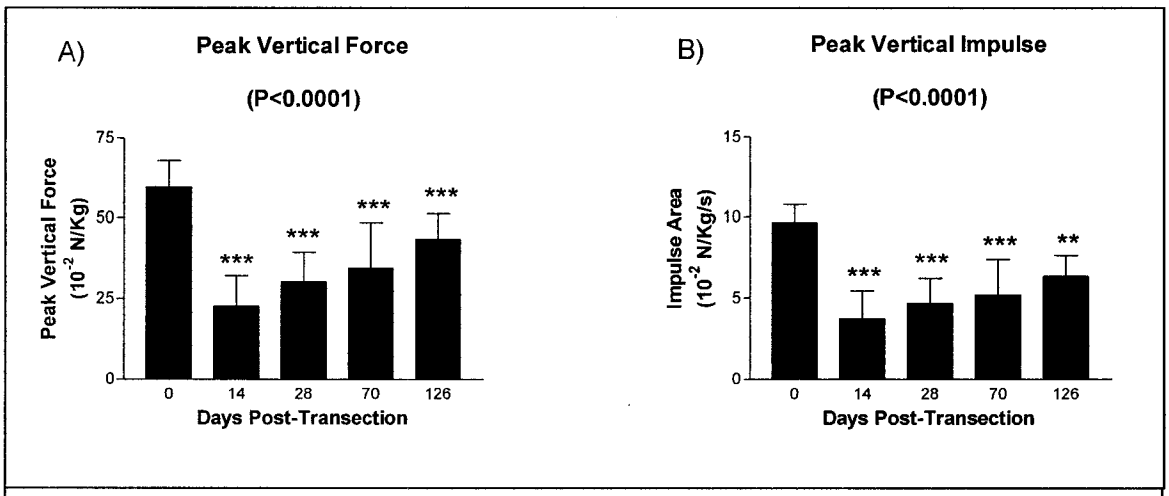

Figure 8.2. Mean + SD for the peak vertical force (A) and peak vertical impulse (B) for each measurement period (Day 0, 14, 28, 70, and 126). The P value for overall effect of time is listed above each graph, and was determined by a repeated measures ANOVA, with Tukey's post-hoc test for the peak vertical force, and Kruskal-Wallis analysis with a Dunn's post-hoc test for the peak vertical impulse. Significant differences from baseline are represented as ** P<0.01, and *** P<0.001.

impulse for the CrCL deficient limb was also significantly lower than baseline throughout the entire study, with the mean impulse being 61% lower on day 14 ($P<0.001$), 52% lower on day 28 ($P<0.001$), 46% lower on day 70 ($P<0.001$), and 34% lower on day 126 ($P<0.01$) post-CrCL transection than the mean impulse measured at baseline (Figure 8.2).

8.4.3 Clinical parameters. The total protein content in the synovial fluid was significantly higher ($P<0.0001$) than baseline throughout the entire study, peaking at day 14 post-CrCL transection (Table 8.1). The white blood cell count in the synovial fluid was significantly higher than baseline on day 14 ($P<0.05$) and day 126 ($P<0.001$) post-CrCL transection (Table 8.1). The effusion score was significantly higher ($P<0.0001$) than baseline throughout the entire study (Table 8.1). The lameness grade was

Table 8.1. Mean ± SD for the total protein content, white blood cell count, and effusion score for fluid of CrCL transected joints during each measurement period (Day 0, 14, 70, and 126). The P value for overall effect of time for each parameter was $P<0.0001$, and was determined by Kruskal-Wallis analysis with a Dunn's post-hoc test to determine significant differences from baseline. Significant differences from baseline are represented as * $P<0.05$, and *** $P<0.001$.

Day	*Total Protein*	*White Blood Cell Count*	*Effusion score*
0	0.38 ± 0.21	192.86 ± 126.88	0 ± 0
14	2.16 ± 0.61 ***	536.84 ± 586.15 *	2.26 ± 0.45 ***
70	1.63 ± 0.60 ***	321.05 ± 201.60	2.11 ± 0.32 ***
126	1.49 ± 0.73 ***	915.79 ± 1498.99 ***	2.80 ± 0.41 ***

significantly higher than baseline throughout the entire study, peaking at day 14 ($P<0.001$) post-CrCL transection, and decreasing thereafter (Table 8.2). The degree of weight bearing on the CrCL transected limb was significantly worse than baseline on days 14, 28, and 70 ($P<0.001$) post-CrCL transection, before returning to baseline levels 126 days post-transection (Table 8.2). The response to joint extension was significantly greater than baseline throughout the entire study peaking at day 70 ($P<0.001$) post-CrCL

transection before decreasing 126 days post-transection (Table 8.2). The overall pain score was significantly higher than baseline values throughout the entire study, peaking at day 14 ($P<0.001$), and decreased thereafter (Table 8.2).

Table 8.2. Mean ± SD for the subjective clinical parameters including lameness, degree of weight bearing, joint extension, and the cumulative total of all three as the overall pain score for the operated limb during each measurement period (Day 0, 14, 28, 70, and 126). A score of 1.00 at day 0 was indicative of no lameness, normal weight bearing and no response to joint extension. The P value for overall effect of time for each parameter was $P<0.0001$, and was determined by Kruskal-Wallis analysis with a Dunn's post-hoc test to determine significant differences from baseline. Significant differences from baseline are represented as * $P<0.05$, ** $P<0.01$, and *** $P<0.001$.

Day	*Lameness*	*Weight bearing*	*Joint extension*	*Overall pain score*
0	1.00 ± 0	1.00 ± 0	1.00 ± 0	3.00 ± 0
14	3.50 ± 0.51 ***	2.00 ± 0 ***	2.32 ± 0.67 ***	7.89 ± 0.81 ***
28	3.37 ± 0.60 ***	2.00 ± 0 ***	2.42 ± 0.51 ***	7.79 ± 0.63 ***
70	3.16 ± 0.60 ***	2.05 ± 0.23 ***	2.47 ± 0.51 ***	7.68 ± 0.89 ***
126	2.84 ± 0.76 ***	1.53 ± 0.51	1.89 ± 0.57 **	6.26 ± 1.33 *

8.4.4 Correlations. Significant negative correlations were present between the synovial fluid PGE_2 concentrations and the peak vertical force ($r = -0.5720$, $P<0.0001$), and peak vertical impulse ($r = -0.4573$, $P=0.0001$) (Table 8.3). Significant positive correlations were present between the PGE_2 concentration and all of the clinical parameters except WBC count, including the subjective lameness score ($r = 0.5016$, $P<0.0001$) and the effusion score ($r = 0.6817$, $P<0.0001$) (Table 8.3). In addition, the peak vertical force and impulse both were significantly and negatively correlated with all of the clinical parameters except WBC count.

Table 8.3. Table of correlation coefficients between the synovial fluid PGE_2 concentrations, ground reaction forces (peak vertical force and vertical impulse), and clinical parameters (lameness, degree of weight bearing, joint extension, overall pain score, and synovial fluid effusion score, total protein content and white blood cell count (WBC)). The correlation between PGE_2 concentration and peak vertical force was determined using the Pearsons correlation coefficients. All other correlations were determined using a Spearman rank correlation. P values ($P<0.05$) are listed in parentheses underneath their respective correlation coefficient (r value) highlighted in bold.

	PGE_2	*Vertical Force*	*Vertical Impulse*	*Lameness*	*Weight Bearing*	*Joint extension*	*Overall Pain Score*	*Effusion Score*	*Total Protein*	*WBC*
PGE_2	1.000	**-0.5720**	**-0.4573**	**0.5016**	**0.5785**	**0.2955**	**0.4673**	**0.6817**	**0.4771**	0.1336
		(P<0.0001)	(P=0.0001)	(P<0.0001)	(P<0.0001)	(P=0.0169)	(P<0.0001)	(P<0.0001)	(P<0.0001)	
Peak Vertical Force		1.000	**0.9434**	**-0.7846**	**-0.7325**	**-0.5203**	**-0.7580**	**-0.4775**	**-0.5643**	-0.2185
			(P<0.0001)	(P<0.0001)	(P<0.0001)	(P<0.0001)	(P<0.0001)	(P<0.0001)	(P<0.0001)	
Vertical Impulse			1.000	**-0.8123**	**-0.7309**	**-0.5002**	**-0.7689**	**-0.5400**	**-0.5478**	-0.1935
				(P<0.0001)	(P<0.0001)	(P<0.0001)	(P<0.0001)	(P<0.0001)	(P<0.0001)	
Lameness				1.000	**0.7258**	**0.5355**	**0.8822**	**0.6009**	**0.6232**	**0.3115**
					(P<0.0001)	(P<0.0001)	(P<0.0001)	(P<0.0001)	(P<0.0001)	(P=0.0082)
Weight Bearing					1.000	**0.6546**	**0.8028**	**0.5430**	**0.6205**	**0.3805**
						(P<0.0001)	(P<0.0001)	(P<0.0001)	(P<0.0001)	(P=0.0011)
Joint Extension						1.000	**0.8151**	**0.5101**	**0.4411**	0.1060
							(P<0.0001)	(P<0.0001)	(P=0.0001)	
Overall Pain Score							1.000	**0.5476**	**0.5702**	0.1780
								(P<0.0001)	(P<0.0001)	
Effusion Score								1.000	**0.7705**	**0.4928**
									(P<0.0001)	(P=0.0002)
Total Protein									1.000	**0.3504**
										(P=0.0027)
WBC										1.000

8.5 Discussion

Production of PGE_2 has been shown to be stimulated through an upregulation of COX-2, via the pro-inflammatory cytokines, IL-1 and TNFα[349,350,362], or IL-18[363]. This inflammatory process stimulates primary afferent neurons within the joint to release neuropeptides, such as substance P, that further drives the inflammatory process by causing the release of IL-1 and TNFα[364], as well as initiating and enhancing PGE_2 production[365,366]. A positive correlation between substance P and PGE_2 has been identified in the synovial fluid from OA joints of horses[361]. Kirker-Head, et al. suggested that because of the early peak of both substance P and PGE_2 in the early phase of OA, that the synovial fluid content of PGE_2 likely plays a predominant role in the acute-phase of the inflammatory process[361]. The results of our study support this statement since the PGE_2 concentrations in the synovial fluid from the CrCL transected dogs were significantly elevated from baseline, peaking at 14 days post-transection.

In further support of our current finding, a separate study from our laboratory examined 3 dogs that underwent serial arthroscopic examinations 14, 28, 70, and 126 days after CrCL transection (Chapter 3). Results of that study indicated that the degree of synovitis reached a peak by 28 days after transection, and then diminished over time, but never completely abated. Since we did not collect synovial fluid for PGE_2 analysis 28 days after transection, we cannot say whether the PGE_2 concentration would have actually peaked then as opposed to the currently observed 14 days post-transection. However, both studies indicate that there is an early inflammatory peak in PGE_2 levels that most likely occurs in the synovial fluid within the first month after CrCL transection.

The lameness that occurs following CrCL transection is likely the result of a multifactorial process in which both instability and inflammation contribute to the process. It has been demonstrated that in the presence of joint inflammation, afferent nerve fibers of the joint exhibit increased sensitivity with activation of nociceptors and neuropeptides, such as substance P[353,354,366]. When combined with the joint instability, this results in increased neural activity of the receptors, or hyperalgesia, which is presumably perceived as pain, especially during movement and joint loading[353]. However, pain can also be present when the joint is at rest[353], which may be partially due to increased intra-articular volume and the enhanced sensitivity of the joint afferents due to increased pressure[367]. Our results demonstrated that PGE_2 levels in the synovial fluid are strongly associated with clinical assessments of pain in that there were significant correlations with PGE_2 concentrations to peak vertical force ($r = -0.5720$) and impulse ($r = -0.4573$), subjective lameness assessment ($r = 0.5016$), the degree of weight bearing when the limb was at rest ($r = 0.5785$), in addition to the joint effusion score ($r = 0.6817$).

Our force plate results are similar to previous reports of naturally-occurring or experimentally-induced CrCL rupture[198-202]. There was an acute decrease in the peak vertical force and impulse by 2 weeks, followed by an increase in the amount of weight bearing over time, without returning to pre-CrCL transection values. This improvement has been stated to be due to the inherent increase in stability of the joint over time because of the increasing fibrous response of the joint capsule[198,202]. This fibrous response likely contributes some to this stability, but often, even though the dog has improved clinically, cranial drawer instability is still present[198]. Our results suggest that the decrease in the inflammatory process over time, after CrCL transection/rupture, might

actually contribute to some of this improvement in weight bearing, presumably due to less pain associated with joint loading. Following this line of thinking, any further pathologic change within the joint, such as meniscal tearing, may also result in increased lameness due to exacerbation of the inflammatory process as the menisci are themselves capable of spontaneous production of PGE_2[362]. Our results also support previous findings of a significant negative correlation between the subjective lameness score and both the peak vertical force ($r = -0.7846$) and impulse ($r = -0.8123$) identified via force plate analysis[199].

Synovial fluid PGE_2 has been thought to originate from the articular tissues, and not from the blood since no relationship was established with the total leukocyte count in the blood[368]. Even though we did not examine the total leukocyte count in the blood, our results indicated that no correlation exists between the synovial fluid white blood cell count and the PGE_2 concentration. It has also been stated that PGE_2 depresses proteoglycan synthesis by chondrocytes, accelerating the loss of glycosaminoglycans (GAG) from articular cartilage[358,359]. However, when we attempted to correlate the synovial fluid PGE_2 concentration to the synovial fluid and serum sulfated GAG (sGAG) content from these same dogs (Chapter 7), no correlation could be identified. PGE_2 stimulates the synthesis of degradative enzymes, such as MMPs, by chondrocytes via the promotion of plasminogen activators[356]. One of the primary groups of MMPs responsible for cleavage of the type II collagen are the collagenases (MMP-1, -8, and -13). When we compared the PGE_2 concentrations in this study to our results from synovial fluid analysis measuring levels of collagenase-cleaved fragments of type I and II collagen in the same dogs (COL 2-3/4C_{short}) (Chapter 7), there was a significant positive correlation

($r = 0.6808$, $P < 0.0001$). In addition, type II collagen synthesis, as represented by the carboxy-propeptide of type II collagen (CPII) levels in the synovial fluid of these dogs (Chapter 7), also was significantly correlated to PGE_2 concentrations in this study ($r = 0.5164$, $P < 0.0001$). These correlations suggested that collagenase levels are upregulated, along with, and perhaps due to PGE_2, resulting in increased type II collagen cleavage. As a result of this cleavage, type II collagen synthesis likely increases to try to maintain a homeostatic balance within the extracellular matrix. The relative lack of correlation between PGE_2 levels and sGAG content in our study compared to the other *in vitro* studies is likely because our samples were obtained *in vivo*, and were probably not exposed to the same levels of cytokines as those *in vitro* studies.

The actual content of PGE_2 in the synovial fluid may have been higher than what we measured since the synovial fluid was collected by lavage technique because of the difficulty in aspirating enough synovial fluid to be able to evaluate multiple biomarkers. The disadvantages of the lavage technique are that it dilutes the synovial fluid, making the actual volume of fluid within the joint unknown, and it has the potential to affect the metabolism of the articular tissues. We feel that these concerns were minimized by the length of time between collection periods and the fact that all of the joints were similarly treated for each dog at each time period. The collection of the force plate data in this study was performed so that the previously identified sources of variability would be minimized[196,197,264,265]. However, individual variation among and within each dog with regards to its response to CrCL transection was difficult if not impossible to control, and could have affected some of the results.

In summary, PGE_2 concentrations in the synovial fluid from the joints dogs that had CrCL transection were significantly elevated from baseline for 4 months after surgery, peaking acutely at 14 days post-transection. Correlation analyses revealed a significant negative correlation between the synovial fluid levels of PGE_2 and both the peak vertical force and impulse derived from force plate analysis. In addition, there were significant positive correlations of the PGE_2 concentrations with all of the clinical parameters examined (lameness, degree of weight bearing, joint extension, overall pain score, effusion score, and synovial fluid total protein content) except for synovial fluid white blood cell count. These results suggest that PGE_2 in the synovial fluid likely is involved in the acute inflammation and associated lameness and pain during the early stage after CrCL transection in the dog.

9 THE INEFFECTIVENESS OF A SYNTHETIC MATRIX METALLOPROTEINASE INHIBITOR DETERMINED IN A CANINE CRANIAL CRUCIATE LIGAMENT TRANSECTION MODEL OF OSTEOARTHRITIS USING PATHOLOGY, CLINICAL PARAMETERS, AND BIOMARKERS ANALYSES

Troy N. Trumble DVM, MS, R. Clark Billinghurst DVM, PhD, Alison M. Bendele DVM, PhD, Richard D. Park DVM, PhD, C. Wayne McIlwraith BVSc, PhD

To be submitted to *Arthritis and Rheumatism* in spring 2003.

9.1 Summary

Objective. To test the efficacy of a synthetic matrix metalloproteinase (MMP) inhibitor (BAY 12-9566) in a canine cranial cruciate ligament (CrCL) transection model of osteoarthritis (OA).

Methods. Thirty-nine dogs had the right CrCL successfully transected arthroscopically. Twenty and 19 dogs were orally administered BAY 12-9566 or a placebo, respectively, starting at 2 weeks post-transection and continued daily throughout week 18. Serum and synovial fluid collection, subjective pain scores (lameness, degree of weight bearing, response to joint extension, overall pain score, and effusion score), radiographs, and force plate analyses were all performed prior to CrCL transection, and then at various time points throughout the study until sacrifice at 18 weeks post-transection. Immunoassays were performed using the serum and/or synovial fluid to determine the relative amounts of inflammation (prostaglandin-E_2), proteoglycan turnover (sulfated glycosaminoglycans-sGAG), bone formation (bone alkaline phosphatase-BAP, and osteocalcin-OC), collagen synthesis (carboxy-propeptide of type II collagen-CPII), type II collagen degradation (234CEQ neoepitope), type I and II collagen degradation (COL2-3/4C_{short} neoepitope), and type I collagen degradation (calculated as COL2-3/4C_{short} – 234CEQ). Gross and histologic gradings were performed for the articular cartilage, synovium, menisci, and osteophyte formation.

Results. Pathology, clinical effects, and biomarker analyses did not reveal any significant differences between dogs treated with BAY 12-9566 and those given a placebo with the exception of more severe histological lesions of the medial tibia for dogs treated with BAY 12-9566 compared to placebo treated controls.

Conclusion. BAY 12-9566 was ineffective in inhibiting the pathological, clinical, and biomarker responses that occur in response to CrCL transection in the dog.

9.2 Introduction

The extracellular matrix of articular cartilage is composed primarily of large proteoglycans (aggrecan) interspersed between a fibrillar network of type II collagen. The combination of these two molecules allows the articular cartilage to resist compressive and tensile forces placed upon a normal joint. However, when joint injury occurs, such as with rupture of the cranial cruciate ligament (CrCL – equivalent to human anterior cruciate ligament) abnormal forces and inflammation can cause a cascade of events that leads to articular cartilage degradation, the hallmark of osteoarthritis (OA)[1].

The exact pathogenesis of OA is not completely understood, but it is thought that cytokines, such as interleukin-1 (IL-1) and tumor necrosis factor alpha (TNF α) stimulate chondrocytes and other cellular sources to produce degradative enzymes, called matrix metalloproteinases (MMPs). MMPs are a family of zinc-containing, calcium-dependent proteinases that are synthesized in a latent form[52]. MMPs are believed to become activated *in situ* by other proteinases removing the propeptide that is attached to the active site, allowing the zinc atom in the active site to hydrolyze susceptible protein substrates[54]. They are classified based upon the substrates they digest[369]. The MMPs of importance in OA include the collagenases -1, -2, and -3 (MMP -1, -8, and -13), stromelysins -1 and -2 (MMP-3 and -10), gelatinases A and B (MMP -2 and -9) and membrane-type metalloproteinase 1 (MMP -14)[56].

Under normal conditions within the joint, MMPs play an important role in the normal turnover of aggrecan and type II collagen. However, during pathological

conditions such as in OA, MMPs can be over-produced causing abnormally high turnover of articular cartilage[370]. MMPs are carefully controlled by endogenous inhibitors, such as the general inhibitor α2-macroglobulin, or a family of specific tissue inhibitors of metalloproteinases (TIMPs)[52]. TIMPs are capable of preventing the activation of proenzymes as well as blocking the action of activated MMPs by forming irreversible, noncovalent 1:1 complexes, preventing the MMP from reacting with its substrate[69,70]. However, it has been demonstrated that there are increased levels of MMPs present without corresponding increases in TIMP levels in articular cartilage and synovial fluid from human OA. This suggests that much of the pathology observed in OA may be due to local imbalances between activated MMPs and TIMPs[371-374]. Therefore, a potential therapeutic approach in controlling OA would be to inhibit MMPs with synthetically designed inhibitors.

Many synthetic inhibitors of MMPs have been developed to counteract the action of MMPs in cancer and OA[226]. Many of the first synthetic inhibitors were designed to mimic the peptide sequences of the MMP substrates. However, these first-generation inhibitors had low oral bioavailability and were replaced by second-generation inhibitors that were based on the 3-dimensional structure of the active sites of specific MMPs as identified by X-ray crystallography[227]. Tanomastat (BAY 12-9566) is a non-peptidic biphenyl second-generation MMP inhibitor with a zinc-binding carboxyl group[237]. Although it is a broad-spectrum inhibitor, it selectively targets MMP -3, -2, -9, and -14, compared to the collagenases (MMP -1, -8, and -13) (Figure 9.1). It has been shown to inhibit metastasis and angiogenesis in cancer patients[238] and halt or slow the progression of OA[239,240]. In IL-1 stimulated cartilage explant studies, BAY 12-9566 significantly

reduced the amount of proteoglycan release and collagen degradation in a dose-dependent manner[223,242]. Histologic evidence of decreased cartilage lesions after administration of oral BAY 12-9566 has been demonstrated in a rat adjuvant arthritis model[243], as well as in canine and guinea pig meniscectomy models of OA, where cartilage loss was reduced by 50-60% compared to controls in the canine model[241]. These reports suggest that BAY 12-9566 has the potential to be a useful anti-arthritic agent.

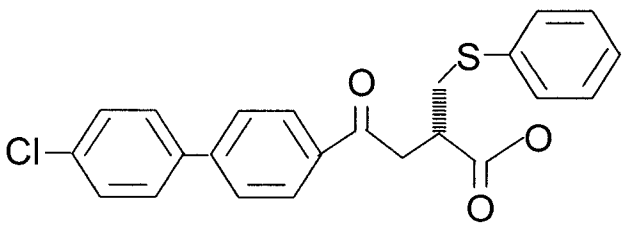

BAY 12-9566

IC_{50}	nM
MMP -2	11
MMP -3	134
MMP -9	301
MMP -14	414
MMP -8	2200
MMP -1	>5000
MMP -13	66000

Figure 9.1. Chemical structure for 4-[4-4-(chlorophenyl)phenyl]-4-oxo-2S-phenylthiomethyl) butanoic acid, a non-peptidic biphenyl second generation MMP inhibitor with a zinc-binding carboxyl group that is commonly known as Tanomastat or BAY 12-9566. The nanomolar constants for 50% inhibition of specific MMPs by BAY 12-9566 is listed in the table to the right of the structure.

The purpose of this study was to evaluate the efficacy of orally administered BAY 12-9566 in slowing the progression of degradative changes in the stifle joint that occur secondary to CrCL transection in the dog. Efficacy of BAY 12-9566 was based on differences detected in the degree of pathology (gross and histologic), clinical parameters of pain and inflammation (lameness, degree of weight bearing, response to joint extension, and overall pain score), radiographs, force plate analysis, as well as biomarker analyses of inflammation (prostaglandin $-E_2$), proteoglycan turnover (sulfated glycosaminoglycans – sGAG)[224], bone formation markers (bone alkaline phosphatase –

BAP, and osteocalcin – OC) type II collagen synthesis (carboxy-propeptide of type II collagen – CPII)[222], and type I and/or II collagen degradation by collagenase cleavage (COL2-3/4C_{short} and 234CEQ neoepitopes)[62,223], in dogs treated with BAY 12-9566 compared to controls. Our hypothesis was that treatment with BAY 12-9566 would result in significantly less pathologic changes, collagen degradation and proteoglycan turnover in stifle joints after CrCL transection compared to placebo-treated dogs.

9.3 Materials and methods

The study was conducted under a protocol approved by the Colorado State University Animal Care and Use Committee. Dogs were obtained through approved sources by the Colorado State University Laboratory Animal Resources. The study was designed as a randomized, double-blinded, placebo controlled study to confirm the dose of BAY 12-9566.

9.3.1 Animals and Experimental Protocol. Forty purpose-bred adult male Walker Hounds with a mean ± SD weight of 22.36 ± 2.71 kg (range, 16.8 – 29.5 kg) were studied. Upon arrival, dogs were given routine physical and hematologic examinations. Orthopedic examination included a separate lameness and physical examination of both hind limbs as well as radiographs of both stifles. In anticipation of gait analyses, each dog was acclimated for several weeks to the force platform analysis laboratory and was led across the force plate by leash, at a trot prior to the start of the study. Selection and subsequent inclusion required the dogs to be free of pre-existing orthopedic disease of the stifles based on orthopedic examination and radiographs. In addition, the dogs had to be able to adequately trot across the force plate with minimal effort or coaxing from the handler.

All dogs were anesthetized, and the right hind limb was prepared for aseptic surgery. A lateral parapatellar arthroscopic approach to the right stifle was used to examine the joint for the presence of any intra-articular pathology. The CrCL was then transected arthroscopically using a meniscectomy blade (Chapter 2). Analgesia was administered via a 5 mg fentanyl patch (2.0 μg/kg/hr) that was applied the day before surgery and was maintained for 72 hours post-operatively. Morphine (1 mg/kg subcutaneously) was also administered post-operatively for pain, as needed. Cephalexin (Keflex) was administered intravenously during surgery and was continued orally (10 mg/kg) every 12 hours for 3 days to prevent infection. Throughout the study, all dogs were housed in individual runs. The animals were closely monitored during the first 48 hours post-operatively for any signs of pain, infection, anorexia, or intestinal complications. To encourage the development of OA, dogs were exercised by leash walking for 30 minutes every day for 5 days/week, from the second day post-operatively until 18 weeks.

At 2 weeks post-CrCL transection, dogs were randomized into one of two treatment groups. Group 1 consisted of 20 dogs that received BAY 12-9566 (5 mg/kg orally, once a day) (BAYER Corp., West Haven, CT) and group 2 consisted of 20 dogs that received placebo tablets (5 mg/kg orally, once a day) (BAYER Corp.) Each dog started receiving their respective treatment on day 14 post-CrCL transection, continuing daily for 16 weeks. All dogs were euthanized with sodium pentobarbital euthanasia solution (88 mg/kg) via intravenous injection at 18 weeks post-operatively and both stifles were disarticulated and examined grossly.

9.3.2 Sample collection for biomarker analyses. Blood samples were collected in the morning from the jugular vein prior to surgery (baseline), 1 and 2 weeks post-operatively, and every 2 weeks thereafter until week 18. Samples were placed in serum separator tubes and were allowed to clot at room temperature for approximately 30 minutes. The samples were then centrifuged for 10 minutes at 2,500 rpm. Synovial fluid samples were collected from both stifles using a lavage method where 5 ml of sterile saline was injected into the joint. The limb was then manipulated for 1-2 minutes to ensure adequate mixing of the saline and the synovial fluid prior to aspiration of as much synovial fluid as possible. Fluid was collected prior to surgery, and then again at 2, 10, and 18 weeks post-operatively. Of the total volume collected, 0.5-1.0 ml was added to a tube containing EDTA and the remainder was placed in serum separator tubes. The EDTA tubes were analyzed for total protein (TP) content and white blood cell (WBC) count. The samples were placed immediately on ice after collection and were centrifuged at 4 C for 10 minutes at 2,500 rpm. The serum and synovial fluid samples were then split into multiple aliquots with the interval between sample collection and freezing at -80 C being under 3 hours. All samples were kept at -80 C until assayed.

9.3.3 Analysis of pathology.

9.3.3.1 Macroscopic grading of lesions. Immediately after sacrifice, the right and left stifles of all dogs were opened and the lesions were described, measured, and photographed by a board-certified pathologist (AMB). Gross pathology was subjectively graded (0-3) for synovial thickening, the degree of medial and lateral meniscal damage, osteophyte formation, and articular cartilage degeneration, as previously described (Chapter 5). The evaluations of articular cartilage degeneration and

osteophyte formation were divided into two basic compartments: the tibial plateaus and the femoral condyles. Lesion locations for the tibial plateaus were identified as cranial, middle, the area not protected by the meniscus, and caudal. Lesion locations for the femoral condyles were proximal, central weight bearing, and central non-weight bearing. Actual measurements of articular cartilage lesions were made using a micrometer to derive a calculated set of data points based on length X width X depth score. The depth of articular cartilage damage was graded on a scale from 0-4, as previously described (Chapter 5).

9.3.3.2 Microscopic grading of lesions. After gross examination, the proximal end of the tibia and distal end of the femur were removed using a band saw to preserve the articular surfaces and placed in 10% neutral buffered formalin for 5 days. The sections of femurs and tibias from both stifles were then decalcified in formic acid and prepared for histopathologic evaluation. The surface area of the articular cartilage of the tibia and femur were each divided into 2 compartments (medial and lateral). Each compartment was further subdivided into 3 basic regions (cranial, weight bearing, and caudal). For each region, 1-2 slabs of bone/cartilage, approximately 2-3 mm thick, were processed, embedded in paraffin, and sectioned for each dog. Histologic sections were stained with toluidine blue. Synovial membrane was removed from the cranial portion of the joint, placed in formalin, sectioned (5μm), and stained with hematoxylin and eosin. Synovial pathology was scored on a scale from 0-3 as previously described (Chapter 5). Osteophytes were scored on a scale from 0-3 based on presence and size as previously described (Chapter 5).

Compartmentalized articular cartilage lesions of the medial tibia, medial femur, lateral tibia and lateral femur were scored. For cartilage degeneration, lesions were graded according to the depth/severity (0-5) and area involved (fraction of the total surface), as previously described (Chapter 5). The area involved was multiplied by the depth/severity score to arrive at a value for a single section, and values for each of the 3 regions (cranial, weight bearing, and caudal) were summed to give a total for each compartment. Total values for cartilage degeneration parameters were separately determined for tibia and femur, and were summed to derive a total joint score. Measurements of the total lesion width for chondrocyte death, cloning, fibrillation, or proteoglycan loss were taken across the tibial and femoral surfaces.

9.3.4 Clinical parameters.

9.3.4.1 Subjective pain scoring. Subjective assessments of lameness and pain were performed before each radiograph and force plate evaluation, prior to CrCL transection (baseline), and then again at 2, 4, 10, and 18 weeks post-transection. All subjective scores were performed by the same author (TNT), as previously described (Chapter 8). Lameness was graded on a scale from 1-4, with 1 representing no lameness and 4 being severely lame at a walk or trot. The degree of weight bearing when the limb was at rest was assessed on a scale from 1-3, with 1 representing normal weight bearing at rest and 3 being non-weight bearing at rest. For subjective assessment of pain, the limb was lifted off the ground and maximally extended. The response to this limb extension was assessed on a scale from 1-4, with 1 representing no response and 4 representing a severe response (vocalizes or becomes aggressive). A cumulative overall pain score was calculated by summing the scores for lameness, weight bearing and joint

extension. In addition, the degree of joint effusion was subjectively assessed during arthrocentesis at baseline, 2, 10 and 18 weeks post-surgery. The scale for the effusion score ranged from 0-3, with 0 representing no effusion and 3 representing severe effusion.

9.3.4.2 Radiographic analysis. Imaging procedures were performed with each dog sedated with a combination of acepromazine (0.05 mg/kg), butorphanol (0.2 mg/kg), and glycopyrolate (0.005 mg/kg) administered intramuscularly. Radiographs were performed prior to synovial fluid aspiration to prevent artifacts due to arthrocentesis. Extended mediolateral and craniocaudal radiographs of both stifles were made prior to transection and then 2, 4, 10, and 18 weeks post-transection using computed radiography (CR). To quantify the radiographic osteophytic changes that occurred after CrCL transection, a board-certified radiologist (RDP) assigned grades of 0-3 based on the presence and size of the osteophytes present in the following locations: proximal and distal patella, femoral trochlear ridges, medial and lateral tibial condyles, caudal proximal tibia, tibial intercondylar eminence, medial and lateral femoral condyles, and the insertion of the CrCL ligament. A total osteophyte score was then determined by addition of the individual scores for each joint for each examination.

9.3.4.3 Force plate evaluation. The force plate (Model OR6-5, Advanced Mechanical Technologies Inc., Newton, MA) was mounted in the center of, and level with, the surface of a 15-m runway. The signal from the force plate was processed and stored by use of computer software programs (Acquire, Version 6.3W, Sharon Software Inc., Dewitt, MI). Dogs were trotted across the force plate by one

handler prior to having the CrCL transected (baseline), and then again at 2, 4, 10, and 18 weeks post transection, as previously described (Chapter 4).

9.3.5 Biomarker analyses.

9.3.5.1 Prostaglandin-E_2 (PGE_2) analysis. Synovial fluid samples were subjected to solid phase extraction procedures, as previously described (Chapter 8). Analysis of the PGE_2 concentration from the extracted samples was estimated at neet, using a commercially available ELISA kit (Correlate-EIA, Assay Designs, Inc., Ann Arbor, MI), as previously described (Chapter 8). Due to limited sample volume, no interassay coefficient of variation (CV) was performed.

9.3.5.2 Biomarker of type II collagen synthesis. The serum and synovial fluid levels of CPII were measured using a commercially available two-step competitive ELISA (IBEX Technologies, Montreal, CAN) based on a rabbit polyclonal antibody specific for CPII (R160). Cross-reactivity with dog serum has been demonstrated by the manufacturer. Serum and synovial fluid samples were analyzed at neet or 1:2 dilution as previously described (Chapter 7). Interassay coefficient of variation (CV) was < 9% for the serum and synovial fluid.

9.3.5.3 Biomarker of collagenase-induced type I and II collagen degradation. Collagenase-mediated cleavage of type I and II collagen was assessed by measuring the neoepitope in the serum and synovial fluid recognized by the COL2-3/4C_{short} polyclonal antibody using an inhibition ELISA.[341] Cross-reactivity with the dog has been demonstrated (Chapter 7).[62] Serum samples were assayed at neet and synovial fluid samples were assayed at neet or 1:2 dilution. The interassay CV for the serum was < 14% and for the synovial fluid it was < 21%.

9.3.5.4 Biomarker of collagenase-induced type II collagen degradation. Collagenase-mediated cleavage of type II collagen was assessed by measuring the neoepitope in the serum and synovial fluid recognized by the 234CEQ polyclonal antibody using a slightly modified inhibition ELISA from that used for the COL2-3/4C_{short}.[223,341] Cross-reactivity with the dog has been previously demonstrated (Chapter 7). The primary 234CEQ antibody dilution was modified to 1:16,000. Serum and synovial fluid samples were assayed at neet. The interassay CV for the serum was < 12%, and for the synovial fluid it was < 20%.

9.3.5.5 Estimation of collagenase-induced type I collagen degradation. Since the COL2-3/4C_{short} antineoepitope antibody recognizes both type I and type II collagen cleavage, and the 234CEQ antibody recognizes only type II collagen cleavage, then the amount of type I collagen cleavage can be estimated. This was performed by subtracting the serum and synovial fluid values for each given dog and measurement period obtained with the 234CEQ immunoassay from the matching values obtained with the COL2-3/4C_{short} immunoassay. Negative values were assumed to be zero.

9.3.5.6 Determination of proteoglycan turnover. The serum and synovial fluid were assayed for the sulfated glycosaminoglycan (sGAG) content using a modification of the colorimetric 1,9-dimethylmethylene blue dye-binding assay.[224] Serum samples were diluted 1:2, whereas the synovial fluid dilutions started at 1:10 and subsequently decreased, as required, to 1:5, 1:2, or neet, as previously described (Chapter 7). The interassay CV for the serum was < 23%, and for the synovial fluid it was < 28%.

9.3.5.7 Biomarker for early osteoblastic activity. The serum and synovial fluid levels of BAP were measured using a commercially available ELISA

(Metra™ BAP, Quidel Corporation, San Diego, CA) that is based on a monoclonal antibody specific for human BAP. Cross-reactivity of the antibody to dog serum has been demonstrated by the manufacturer. Serum and synovial fluid samples were assayed at neet, as previously described (Chapter 6). Interassay coefficient of variation (CV) was < 9% for the serum and < 11% for the synovial fluid.

9.3.5.8 Biomarker for late osteoblastic activity. The serum levels of intact osteocalcin were measured using a commercially available sandwich ELISA (Biomedical Technologies, Inc., Stoughton, MA) that is based on monoclonal antibodies directed toward the amino- and carboxy- terminal regions of the intact human 49 residue protein. Cross-reactivity of the antibodies to dog serum has been demonstrated by the manufacturer. Most serum samples were analyzed at 1:3 dilution, as previously described (Chapter 6), with others being analyzed at 1:5, 1:2 or neet, as required. No interassay CV was performed due to financial restrictions.

9.3.6 Statistical analysis. All data were expressed as the mean ± SD unless otherwise specified. The distribution of the pathology, clinical, and biomarker data were assessed using the Kolmogorov-Smirnov test. The peak vertical force, and the serum CPII and synovial fluid CPII data from the right CrCL deficient stifle were normally distributed. Data for the 234CEQ, COL2-3/4C_{short}, calculated type I collagen degradation, sGAG, and BAP for the serum and synovial fluid had to be transformed using the square root, and the serum OC and synovial fluid PGE_2 data had to be logarithmically transformed to result in normalization of the data. Data for the subjective scoring (gross and histologic pathology, lameness, degree of weight bearing, response to joint extension, overall pain score, effusion score, and radiographic data), as well as the

peak vertical impulse, and the synovial fluid TP and WBC count were not normally distributed.

For each of the gross and histologic pathology scores, differences between means of the treated group and control group were compared using a two-tailed student's t test. For all of the biomarker data sets (234CEQ, COL2-3/4C_{short}, type I degradation, sGAG, BAP, CPII, OC, and PGE_2) as well as the peak vertical force, the normalized data was analyzed using a two-way ANOVA with time as the repeated measure and treatment as a fixed effect. The remainder of the non-parametric data was analyzed using a Wilcoxon rank sum, to distinguish significant differences between treatment groups as well as due to time post-transection. A value of $P<0.05$ was considered significant for all analyses. All statistical analyses were performed using SAS software (SAS Institute, Cary, NC).

9.4 Results

All dogs had complete transection of the right CrCL except for one dog in the control group. Data from this dog was excluded from the remainder of the analyses, leaving the control group with 19 dogs. No adverse effects due to treatment were noted in any of the dogs.

9.4.1 Pathology.

9.4.1.1 Macroscopic pathology findings. Comparison of mean subjective gross scores for the treatment groups demonstrated highly comparable synovial fibrosis and thickening, and medial and lateral meniscal damage (Figure 9.2A). Formation of patellar groove osteophytes were more abundant than those on the femur and tibia (Figure 9.2B). Medial tibial and lateral tibial osteophyte scores were similar with no significant differences between treatment groups, while lateral femoral

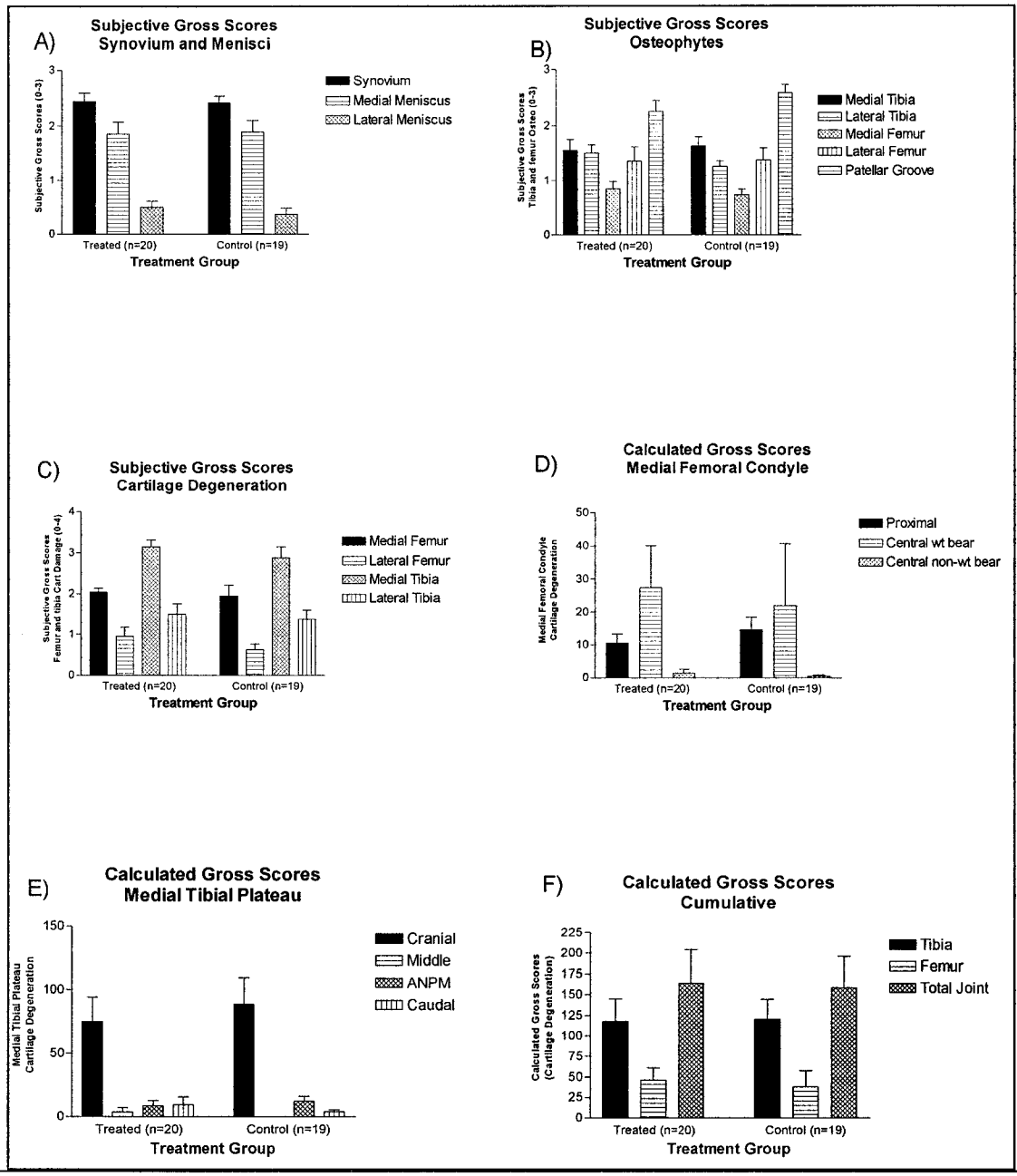

Figure 9.2. Mean ± SEM for the subjective gross pathology scores for the synovium and menisci (A), osteophytes (B), and cartilage degeneration (C), and the calculated gross pathology scores for the medial femoral condyle (D), medial tibial plateau (E), and cumulative tibia, femur and total joint score (F) for each treatment group (treated and control). The legend next to each graph identifies each bar. A two-tailed student's t-test was performed to identify no significant differences between treatment groups. wt=weight, bear=bearing, ANPM=area not protected by the meniscus.

osteophyte scores were greater than medial femoral osteophytes with no significant difference between the treatment groups (Figure 9.2B). However, in general, the treated group had a greater amount of fibrous tissue surrounding the joint capsule. Medial

femoral and tibial subjective gross scores for cartilage degeneration were greater than the lateral femoral and tibial scores, but no significant differences were noted between treatment groups (Figure 9.2C).

Evaluation of the data for cartilage degeneration as the calculated gross scores for the various regions at risk for damage (quantitation of length X width X depth score) revealed that medial femoral cartilage degeneration was similar between the treatment groups for proximal, central weight bearing and central non weight bearing areas (Figure 9.2D). Lateral femoral condylar degenerative changes were highly variable with no significant differences between the treatment groups. The cranial medial tibial plateau which was the area with the overall highest calculated values for cartilage damage was similar between the treatment groups as were the various other medial tibial regions (Figure 9.2E). Lateral tibial degenerative changes were highly variable with no significant differences between the treatment groups. Expressing the data as the sum of calculated gross scores for tibia or femur indicated that the greatest cartilage damage was on the tibia where values were slightly greater than double the values calculated for femur, with no significant differences between the treatment groups for either (Figure 9.2F). Finally, adding the values for tibia and femur to arrive at a total joint score, yielded similar values between the treatment groups (Figure 9.2F).

9.4.1.2 Microscopic pathology findings. Synovial membrane pathology was not significantly different between the treatment groups. Evaluation of cartilage degeneration using calculated scores did not reveal significant treatment differences for the various medial and lateral compartments (Figure 9.3A). Combining medial and lateral compartments and expressing the data as a comparison of tibia vs. femur also revealed no

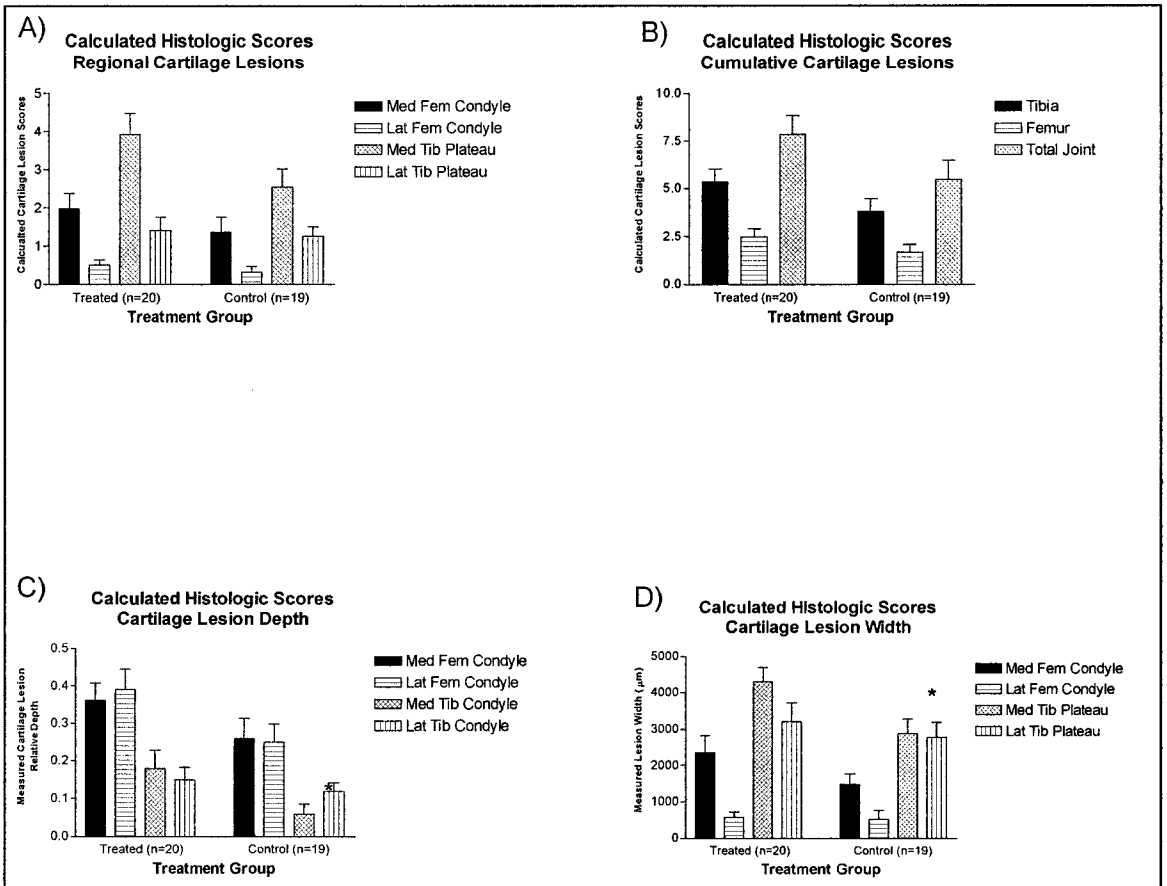

Figure 9.3. Mean ± SEM for the calculated histologic pathology scores for medial and lateral femoral and tibial cartilage degeneration scores (A), cumulative tibia, femur and total joint score (B), medial and lateral femoral and tibial lesion depth scores (C), and medial and lateral femoral and tibial lesion width scores (D) for each treatment group (treated and control). The legend next to each graph identifies each bar. A two-tailed student's t-test was performed to identify any significant differences between treatment groups. Significant differences between treatment groups on the graphs are shown as *P<0.05. Med=medial, Lat=lateral, Fem=femur, Tib=tibia.

differences between treatment groups, as well as when the scores for tibia and femur were combined to achieve a total joint score (Figure 9.3B). The depth of cartilage degeneration was similar for the medial and lateral femoral condyles in both treatment groups with depths of femoral degeneration being greater than depths of tibial degeneration. Significant differences for medial tibial depths of degeneration were seen between the groups with the control group having significantly less than the treated group ($P<0.05$) (Figure 9.3C). Measurement of the widths of the medial and lateral femoral lesions did not reveal significant differences between the treatment groups (Figure 9.3D).

The widths of medial tibial lesions were significantly greater in treated dogs compared to controls ($P<0.05$), while the width of lateral tibial lesions did not show significant differences between the treatment groups (Figure 9.3D).

9.4.2 Clinical parameters.

9.4.2.1 Subjective scoring. Both the degree of lameness and weight bearing on the CrCL deficient limb became significantly worse compared to baseline over time ($P<0.0001$) with no treatment effect ($P=0.2463$ and $P=0.9480$, respectively) (Figure 9.4A and 9.4B). The response to extension of the CrCL deficient stifle became

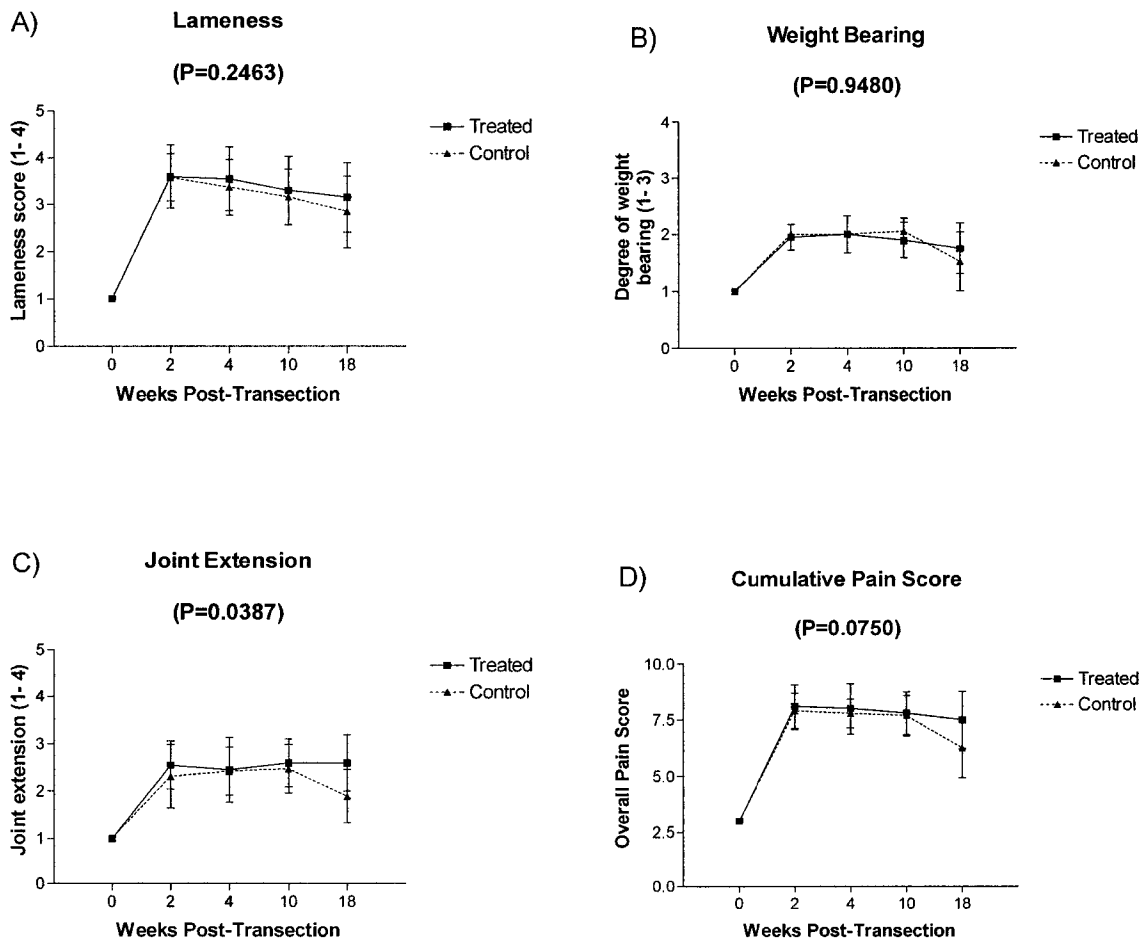

Figure 9.4. Mean ± SD for the subjective scoring of the clinical parameters of pain and inflammation, including lameness (A), degree of weight bearing (B), response to joint extension (C), and overall pain score (D) for each treatment group (treated ■ and control ▲) over each evaluation period (0, 2, 4, 10, and 18 weeks). A two-way ANOVA was performed, with time as the repeated measure and treatment as a fixed effect. The P value for the effect of treatment is listed on each graph.

significantly greater over time compared to baseline (P<0.0001), and the treated dogs had a significantly greater response to joint extension than control dogs (P=0.0387), that was evident at 18 weeks post-CrCL transection (Figure 9.4C). The overall pain score for the CrCL deficient limb was significantly greater than baseline throughout the study (P<0.0001) with no treatment effect (P=0.0750) (Figure 9.4D). The effusion score increased significantly from baseline throughout the study (P<0.0001) with no treatment effect (P=0.3016) (Figure 9.5A). The total protein content and the WBC count in the synovial fluid from the CrCL deficient stifle both increased significantly from baseline over time (P<0.0001) with no treatment effect (P=0.7998 and P=0.7017, respectively) (Figure 9.5B and 9.5C).

9.4.2.2 Radiographic analysis. The total radiographic osteophyte scores increased significantly from baseline throughout the study (P<0.0001) with no treatment effect (P=0.4255) (Figure 9.5D).

9.4.2.3 Force plate analysis. The peak vertical force and its respective impulse decreased significantly from baseline throughout the entire study (P<0.0001), with no treatment effect (P=0.3906 and P=0.8321, respectively) (Figures 9.5E and 9.5F).

9.4.3 Biomarker analyses.

9.4.3.1 Articular cartilage markers in the serum. The serum CPII concentrations (type II collagen synthesis) decreased significantly from baseline over time (P<0.0001) with no treatment effect (P=0.4037) (Figure 9.6A). The serum 234CEQ concentrations (type II collagen degradation) increased significantly from baseline over time (P=0.0002) with no treatment effect (P=0.2924) (Figure 9.6B). The serum COL2-3/4C_{short} concentrations (type I and II collagen degradation) as well as the estimation of

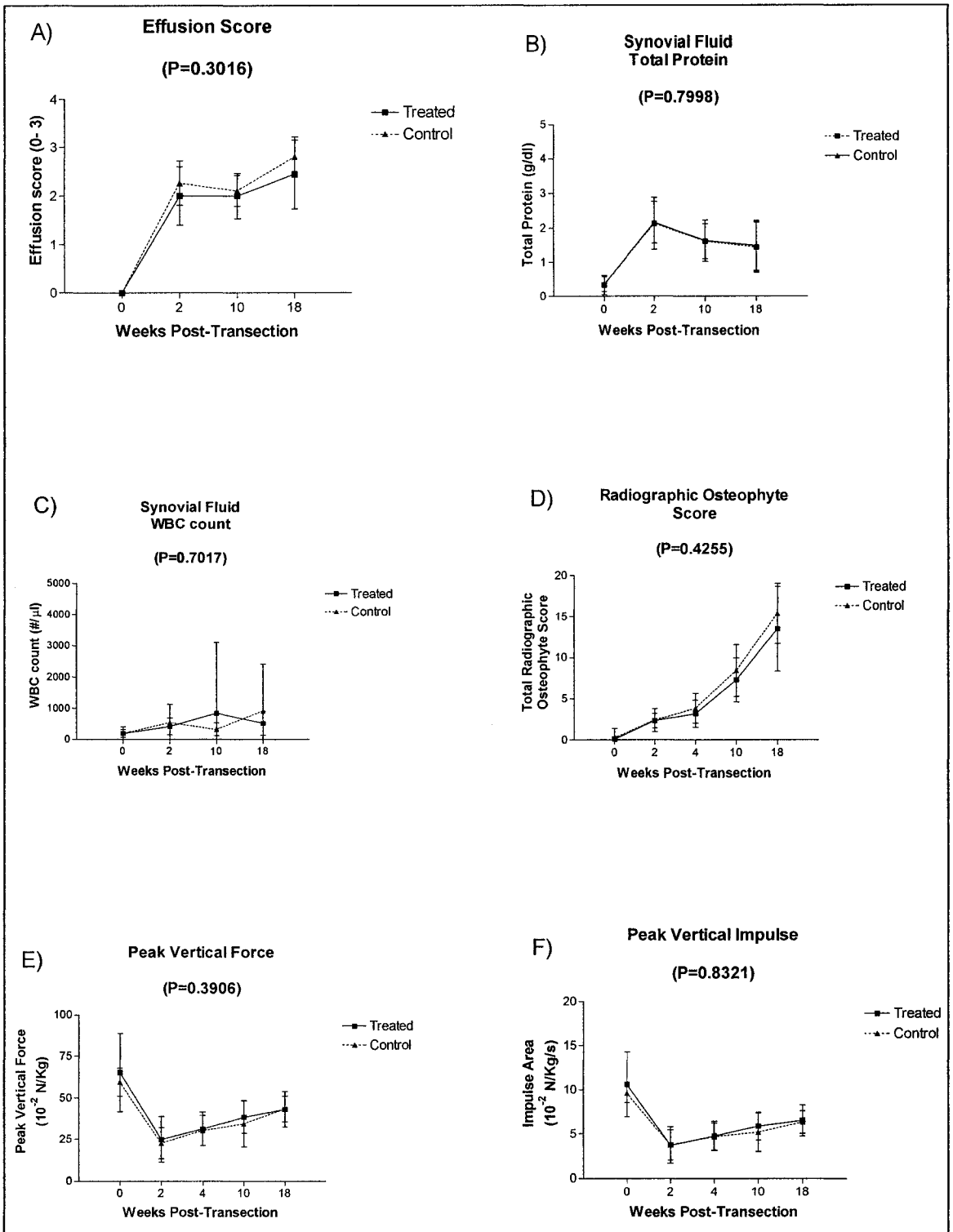

Figure 9.5. Mean ± SD for the treated (■) and control (▲) dogs over each evaluation period (0, 2, 10, and 18 weeks for A-C and 0, 2, 4, 10, and 18 weeks for D-F) for the following clinical parameters: effusion score (A), synovial fluid TP content (B), synovial fluid WBC count (C), total radiographic osteophyte score (D) and the peak vertical force and impulse (E and F). A two-way ANOVA was performed, with time as the repeated measure and treatment as a fixed effect. The P value for the effect of treatment is listed on each graph.

type I collagen degradation (COL2-3/4C_{short} – 234CEQ) decreased significantly from baseline over time (P<0.0001) with no treatment effect (P=0.4567 and P=0.3755, respectively) (Figure 9.6C and 9.6D). The serum sGAG concentrations (proteoglycan turnover) decreased significantly from baseline over time (P<0.0001) with no treatment effect (P=0.2588) (Figure 9.6E).

9.4.3.2 Inflammatory and articular cartilage markers in synovial fluid. The synovial fluid CPII concentrations (type II collagen synthesis) in the CrCL deficient stifle increased significantly from baseline throughout the study (P<0.0001) with no treatment effect (P=0.5320) (Figure 9.7A). No analyses for CPII were performed on the synovial fluid from the contralateral joint. The synovial fluid 234CEQ concentration (type II collagen degradation) from the CrCL deficient stifle increased significantly from baseline throughout the study (P<0.0001) with no treatment effect (P=0.9618), and the concentrations in the contralateral stifle did not differ from baseline over time (P=0.5721) and had no treatment effect (P= 0.7710) (Figure 9.7B). The synovial fluid COL2-3/4C_{short} concentration (type I and II collagen degradation) and the estimated synovial fluid type I collagen degradation (COL2-3/4C_{short} – 234CEQ) from the CrCL deficient stifle increased significantly from baseline throughout the study (P<0.0001) with no treatment effect (P=0.0572 and P=0.0554, respectively) (Figure 9.7C and 9.7D). The synovial fluid COL2-3/4C_{short} concentrations and the estimated type I collagen degradation in the contralateral stifle did not differ from baseline over time (P=0.0958 and P=0.2301, respectively) and had no treatment effect (P= 0.2279 and P=0.3902, respectively) (Figure 9.7C and 9.7D). The synovial fluid sGAG concentration (proteoglycan turnover) from the CrCL deficient stifle increased significantly from

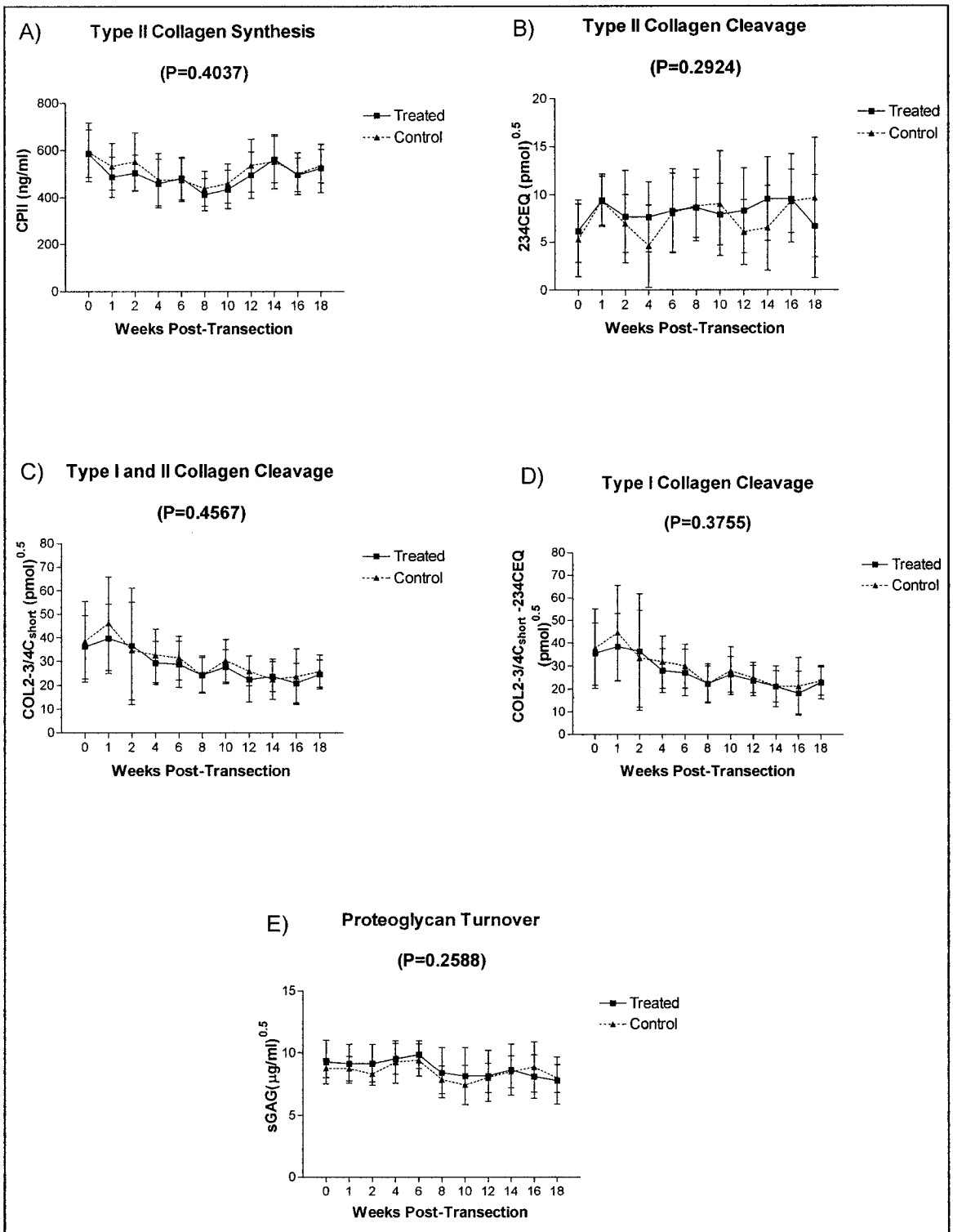

Figure 9.6. Mean ± SD for the articular cartilage biomarkers in the serum, including CPII (A), 234CEQ (B), COL2-3/4C_{short} (C), calculated type I collagen (D) and sGAG (E) for each treatment group (treated ■ and control ▲) over each evaluation period (0, 1, 2, 4, 6, 8, 10, 12, 14, 16 and 18 weeks). A two-way ANOVA was performed, with time as the repeated measure and treatment as a fixed effect. The P value for the effect of treatment is listed on each graph.

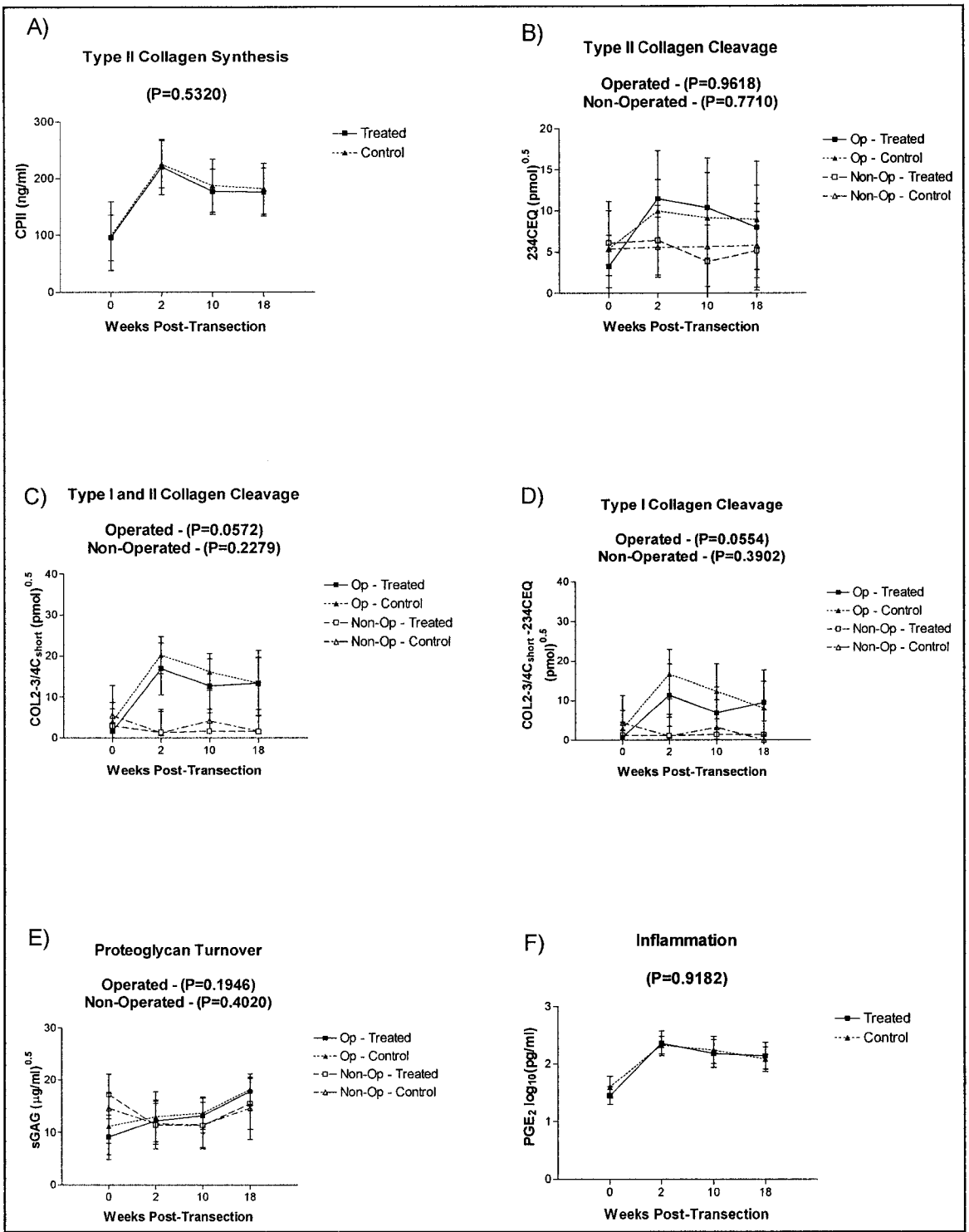

Figure 9.7. Mean ± SD for the articular cartilage biomarkers (A-E) listed in Figure 6, and Prostaglandin-E2 (PGE_2) (F) from the synovial fluid of the treated (■) and control (▲) dogs of the CrCL deficient stifles in A and F. Graphs B-E shows the synovial fluid values in the CrCL deficient stifles (Op – Operated) for the treated (■) and control (▲) dogs, as well as the levels from the contralateral joint (Non-Op – Non-operated) for the treated (□) and control (Δ) dogs for each evaluation period (0, 2, 10, and 18 weeks). A two-way ANOVA was performed, with time as the repeated measure and treatment as a fixed effect. The P value for the effect of treatment is listed on each graph.

baseline over time (P<0.0001) with no treatment effect (P=0.1946), and the concentrations in the contralateral stifle decreased significantly from baseline over time (P<0.0001), with no treatment effect (P=0.4020) (Figure 9.7E). The synovial fluid concentrations of PGE_2 (synovial inflammation) in the CrCL deficient stifle increased significantly from baseline throughout the study (P<0.0001) with no treatment effect (P=0.9182) (Figure 9.7F).

9.4.3.3 Bone formation markers. The serum BAP and OC concentrations decreased significantly from baseline over time (P<0.0001) with no treatment effect (P=0.7890 and P=0.1419, respectively) (Figure 9.8A and 9.8B). The

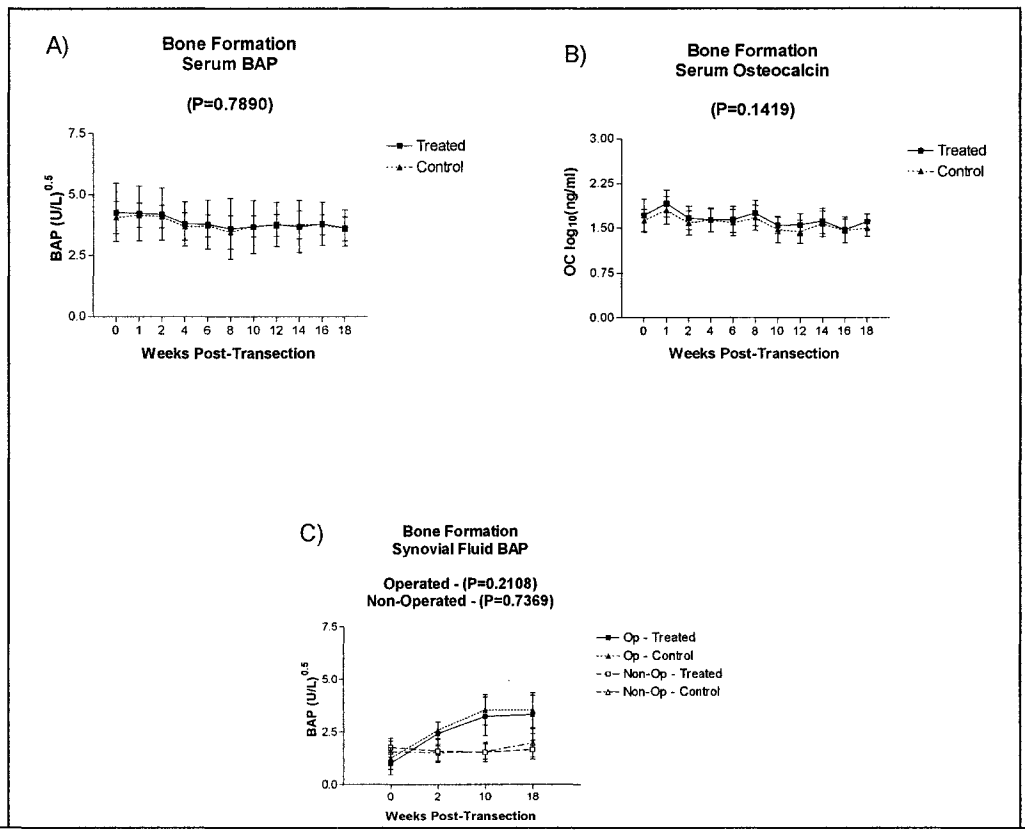

Figure 9.8. Mean ± SD for the bone formation markers BAP (A) and OC (B) in the serum, and BAP in the synovial fluid (C). Serum samples are shown for the treated (■) and control (▲) dogs for each evaluation period (0, 1, 2, 4, 6, 8, 10, 12, 14, 16, and 18 weeks). Synovial fluid BAP values are shown in the in the CrCL deficient stifles (Op – Operated) for the treated (■) and control (▲) dogs, as well as the levels from the contralateral joint (Non-Op – Non-operated) for the treated (□) and control (Δ) dogs for each evaluation period (0, 2, 10, and 18 weeks). A two-way ANOVA was performed, with time as the repeated measure and treatment as a fixed effect. The P value for the effect of treatment is listed on each graph.

synovial fluid BAP concentration from the CrCL deficient stifle increased significantly from baseline throughout the study ($P<0.0001$) with no treatment effect ($P=0.2108$), and the concentrations in the contralateral stifle did not differ from baseline over time ($P=0.2790$), with no treatment effect ($P=0.7369$) (Figure 9.8C).

9.5 Discussion

MMPs are potent degradative enzymes that have to be carefully controlled to minimize their effect upon extracellular matrix turnover. Endogenous control by α2-macroglobulin and TIMPs, have limited potential to inhibit increased MMP activity during OA[374]. This may be partially due to their size, limiting access to the extracellular matrix[375]. Many synthetic MMP inhibitors have been designed[226], but only a few have been shown to have adequate bioavailability, successful delivery to the intra-articular environment with effective tissue concentrations and minimal side effects[52]. One of these synthetic inhibitors is BAY 12-9566. It is a second-generation inhibitor designed primarily to inhibit MMP-3. It has been shown to have good oral bioavailability at multiple doses, with good penetration into the synovial fluid and articular cartilage even though it is highly protein bound (99.9%)[239-241], with minimal side effects, showing only mild to moderate thrombocytopenia and elevated liver enzymes in human cancer patients[376-378]. *In vitro*, IL-1 stimulated cartilage explant studies have demonstrated dose dependent inhibition of proteoglycan release and type II collagen degradation[223,242], and early studies in animal models of OA demonstrated reduced histopathologic cartilage loss[241,243].

These preliminary studies of BAY 12-9566 demonstrated that it has the potential to decrease cartilage degeneration and be a novel therapeutic for delaying the progression

of OA. In our study, the macroscopic and histologic lesions induced by CrCL transection were highly variable between dogs with respect to incidence, location, severity and type, as previously described (Chapter 5), with the variability between the treatment groups being similar. Comparisons of gross pathology data demonstrated no significant differences between the BAY 12-9566 and placebo treated dogs for the various joint compartments whether the data was evaluated as an overall subjective score or a calculated value that was based on actual measurement of lesions. Moreover, the histologically-determined depth and width of the medial tibial plateau lesions were significantly worse when the dogs were treated with BAY 12-9566, than the control dogs. Therefore, results of this study did not demonstrate a significant difference between BAY 12-9566 and placebo treated dogs in terms of overall cartilage degeneration, synovial pathology or osteophyte formation after CrCL transection. This apparent lack of protection of articular cartilage and failure to improve limb function in the BAY 12-9566 treated dogs in our study was supported by the biomarker analyses and clinical parameters of pain and inflammation.

The results of our study are similar to clinical trials of OA and rheumatoid arthritis (RA), in which no therapeutic benefits of MMP inhibitors could be established[227,230]. Potential reasons for the lack of efficacy of MMP inhibitors could be due to the fact that the role of each MMP in physiological and pathological processes of OA are not completely understood[369]. BAY 12-9566 is similar to most MMP inhibitors in that it is broad-spectrum, but focuses on a particular group of MMPs, such as the stromelysins. However, there is debate as to which particular MMP would be most beneficial to focus on to obtain maximal efficacy against OA[227]. MMP-3 was targeted in

the development of BAY 12-9566 because MMP-3 can degrade aggrecan, link protein, gelatins, type IV collagen, collagen cross-links, and other non-collagenous proteins[65,67], while also having the ability to activate procollagenases[64,66]. Therefore, inhibition of MMP-3 has the potential to directly inhibit aggrecan degradation as well as indirectly inhibit collagenase-induced cleavage of type II collagen. However, the levels of BAY 12-9566 administered in our model of OA did not prevent cartilage damage when compared to the placebo-treated controls.

There are many potential reasons why BAY 12-9566 did not result in significantly less articular cartilage degradation than the controls in our study. First of all, it has been suggested that in order for MMP inhibitors to have the most dramatic effect in preventing irreversible joint destruction, they must be given early in the disease process[379]. In our study, we did not start administering BAY 12-9566 until 2 weeks post-CrCL transection. The timing was based on the assumption that treatment of OA is generally initiated well after the original insult. The potential exists for a prophylactic effect if we began administration prior to CrCL transection or just after transection. However, the OA changes in our canine CrCL transection model are representative of the early stages of the disease process in which a therapeutic effect should be seen when compared to humans where the natural disease process is generally further advanced. Secondly, it should be noted that MMPs are not the only enzymes capable of causing breakdown of articular cartilage. Other proteinases such as serine and cysteine proteinases or aggrecanase[380] could still contribute to cartilage degradation even if the MMPs were inhibited. In addition, since multiple MMPs have overlapping specificity, it is also possible that MMP inhibition of one MMP at the protein level can be overcome by upregulation of MMP

production at the genetic level, or that another MMP could intervene and degrade articular cartilage in place of the inhibited one[381].

Most of the scores for the clinical parameters as well as the concentrations of the synovial fluid biomarkers in our study increased significantly between baseline examinations and when BAY 12-9566 administration was started at 2 weeks post-CrCL transection. This response was due to the instability and inflammation created by the model, which has been described elsewhere (Chapters 4-8). This suggests that the efficacy of BAY 12-9566 may have been improved if anti-inflammatories, such as non-steroidal anti-inflammatory drugs (NSAIDs), were administered either immediately after transection, as occurs in many clinical situations, and/or concurrently with BAY 12-9566. The combination of NSAIDs and BAY 12-9566 have been shown to be well tolerated in humans[382] and would have the potential to maximize the inhibitory activity against MMPs. NSAIDs block prostaglandin production through inhibition of the cyclo-oxygenase (COX) pathway, which in turn will decrease the inflammatory process, likely decreasing the levels of IL-1 and TNF α. Therefore, when combined with BAY 12-9566, NSAIDs have the potential to decrease gene expression of the MMPs by regulating IL-1 and TNF α mediation of MMP synthesis[56] while BAY 12-9566 would inhibit MMP activity at the protein level by preventing activation and/or inhibiting previously activated MMPs[56].

In general, when studying MMP inhibitors such as BAY 12-9566, animal models of OA have been advantageous over clinical trials in humans. Therapy can be started early in the disease process, allowing for the maximal potential efficacy of the drug, as well as being able to directly examine the resulting pathological changes. It has been

stated that additional ways of examining OA progression need to be established that would allow for identification of cartilage preservation, especially in short term studies of human OA[240]. Our study attempted to address this issue by using multiple biomarkers of collagen synthesis and degradation and proteoglycan turnover, as well as indirect markers of joint damage, such as PGE_2, the bone formation markers, and effusion scores. In addition, we combined subjective analysis of symptoms of abnormal joint function (lameness scores, degree of weight bearing, etc.) with objective analysis of lameness (force plate) and physical measures of cartilage damage (radiographs) to determine the efficacy of BAY 12-9566 in our model. To the authors' knowledge, this is the first time data for the synthetic, degradative, symptomatic, and physical changes have been assimilated in examining the efficacy of a MMP inhibitor in an animal model of OA. The combination of these analyses proved to be sensitive indicators of changes occurring in this model of OA, while at the same time identifying that BAY 12-9566 does not significantly alter the progression of the disease process.

It is also important to mention that BAY 12-9566 is only one of many MMP inhibitors that have been designed[226]. Many of these inhibitors are structurally and functionally different with potentially radically different inhibitory patterns. Therefore, the lack of success of BAY 12-9566 in this model of OA cannot necessarily be considered to be representative of the efficacy of other MMP inhibitors in this or any other model of OA. Moreover, given the severity and variability of this model, it is still possible that BAY 12-9566 could prove beneficial with models involving milder OA changes and/or combined with other agents, such as NSAIDs. The results of this study do suggest that other pathways of articular cartilage degradation, such as the

inflammatory cascade, or other proteinases (aggrecanase), may need to be inhibited as well, in order to preserve articular cartilage. All phase III clinical trials for the use of BAY 12-9566 in human patients with OA and cancer have been halted by an independent Data Safety Monitoring Board. This was done because of safety concerns identified in a phase III clinical study of small cell lung cancer in which there was a significant increase in both disease progression and mortality in those individuals receiving BAY 12-9566 compared to those receiving the placebo[383]. Therefore, the combination of this human health concern, combined with the lack of articular cartilage preservation demonstrated in our study, suggests that BAY 12-9566 will not be used as a sole therapeutic for the treatment of OA in humans or animals.

In summary, the administration of BAY 12-9566 did not significantly affect the development of OA secondary to CrCL transection in the dog, as determined by examination of the pathological changes (gross and histology), clinical effects (subjective pain and effusion scores, radiographs, and force plate), and biomarker analyses (inflammation, collagen synthesis, collagen degradation, proteoglycan turnover, and bone formation).

10 SUMMARY

The main objectives of this study were described in chapter 1. This chapter will be divided by each objective and will briefly summarize and discuss the relevant findings related to each objective.

10.1 Objective 1: to develop and describe an arthroscopic approach to transect the cranial cruciate ligament (CrCL) in dogs for the creation of an experimental model of OA.

Arthroscopy of the canine stifle requires patience and practice with little margin for error. Even though there are other studies that report the use of arthroscopy for CrCL transection (Chapter 1 and 2), a complete description of the technique was lacking. Therefore we described our arthroscopic technique for CrCL transection using a meniscectomy blade. It produced a model of OA with little post-operative morbidity and iatrogenic damage to the other intra-synovial structures (Chapter 2). This was accomplished by placing the limb in maximal flexion while establishing and maintaining adequate distention throughout the procedure so that a sharp meniscectomy blade could be easily inserted through a medial approach. Two passes of the meniscectomy blade in a medial to lateral direction were generally required (57% of the dogs) to completely transect the CrCL. This transection could be performed with minimal resection of the fat pad (13% of the dogs). However, when visualization of the ligament became difficult due to the fat pad, hemorrhage, or periarticular fluid, visual

confirmation of transection was difficult. This resulted in partial transection of the CrCL in one of the original dogs utilized in this study (Chapter 2). Once the surgeon has experience with the arthroscopic procedure for CrCL transection described in this report, it is a very reliable and reproducible technique for the induction of OA in the dog allowing evaluation of novel anti-arthritic agents for both animals and humans.

10.2 Objective 2: to determine, using clinical, macroscopic, microscopic, and biomolecular analyses, the efficacy of a disease modifying drug that inhibits the action of some of the major degradative enzymes responsible for catabolic changes in a joint after CrCL transection.

Tanomastat, BAY 12-9566, is a broad-spectrum synthetic inhibitor of matrix metalloproteinases (MMPs). Since MMPs are potent degradative enzymes that have been shown to degrade the extracellular matrix of articular cartilage, then inhibition by BAY 12-9566 should protect against articular cartilage degradation during OA (Chapter 1 and 9). The efficacy of BAY 12-9566 in our study was evaluated by examination of the pathological changes (gross and histology), clinical effects (subjective pain and effusion scores, radiographs, and force plate), and biomarker analyses (inflammation, collagen synthesis, collagen degradation, proteoglycan turnover, and bone formation) secondary to CrCL transection in the dog. All of these analyses did not demonstrate any cartilage preservation of the joints of dogs that received BAY 12-9566 (20 dogs) compared to those receiving a placebo (19 dogs) (Chapter 9). To the authors' knowledge, this was the first time that the efficacy of an MMP inhibitor designed for OA has been examined using all of the analyses described. However, additional analyses of MMP activity or MMP mRNA expression would have also been beneficial to determine whether inhibition

of MMPs was indeed accomplished at the dosage administered in this study. Activity assays were not performed due to a lack of cross-reactivity of commercially available kits to the dog, and mRNA expression was to be determined using real-time polymerase chain reaction, (RT-PCR) but our source for the sequences of canine MMPs did not materialize. Reasons for the failure of BAY 12-9566 to protect articular cartilage may be related to the variability of the model (Chapter 5), the timing of initial administration (day 14 post-CrCL transection), and the potential that other pathways need to be inhibited in addition to MMPs. This includes the need for anti-inflammatory agents, as well as inhibitors of other proteinases, such as aggrecanase (Chapter 9).

10.3 Objective 3: to characterize the temporal pattern of clinical, macroscopic and biomolecular changes that occur in a joint after CrCL transection using non-invasive methods including: arthroscopy, force plate and radiographic analyses, as well as biomarker analyses of inflammation, collagen synthesis and degradation, proteoglycan turnover, and bone formation.

Arthroscopy was performed serially after CrCL transection (day 14, 28, 70, and 126) in three additional dogs to allow temporal identification of the damage sustained to the synovium, articular cartilage, menisci, and meniscotibial ligament after CrCL transection (Chapter 3). Articular cartilage and medial meniscal damage started as early as 2 weeks after CrCL transection, and generally progressed from there. Stretching or rupture of the cranial meniscotibial ligament of the medial meniscus was identified to a variable degree in all three dogs for the first time, and the clinical importance of this injury still needs to be defined. The degree of synovitis peaked at one month after CrCL transection and then decreased over time but never completely subsided (Chapter 3).

Overall, this study demonstrated that clinically relevant osteoarthritic changes start to occur as early as 2 weeks after CrCL transection and will likely progress when the joint is not stabilized.

Due to the fact that meniscal damage was identified in the early period after CrCL transection, and is presumed to cause the dog to become acutely lame (Chapter 1 and 4), force plate examination was used to try to determine whether meniscal damage could be identified objectively. Out of the 39 dogs with complete CrCL transection in our study, 12 (31%) had a $\geq$ 10% decrease in the peak vertical force identified in successive force plate measurements made at some point between 2 and 18 weeks after CrCL transection. This was theorized to represent recent medial meniscal injury. The mean ± SD meniscal grade for these 12 dogs was 2.58 ± 0.67 (out of a maximum of 3) which was significantly higher (P=0.0035) than for the remaining 27 dogs (1.56 ± 0.89) that represented the "typical" changes in peak vertical force identified in previous reports following CrCL rupture/transection (Chapter 4). The results of this study provide a potential non-invasive way to objectively delineate the temporal pattern of meniscal injury after CrCL rupture/transection.

Radiographic evidence of osteophytes is one of the hallmarks of diagnosis of OA, however, its relationship to biomarker levels of bone formation identified by bone alkaline phosphatase (BAP) or osteocalcin (OC) has not been previously reported. In addition, the identification of BAP and OC in the serum and/or synovial fluid has rarely been examined in osteoarthritis models (Chapter 6). Using the 19 placebo dogs, we identified decreased levels of BAP and OC biomarkers from baseline in the serum, except for an early increase in OC levels at 7 days after CrCL transection in dogs. This peak at

day 7 may be explained by an early response of the entire skeleton to a regimented exercise protocol started at day 2. OC was not examined in the synovial fluid in deference to examination of other biomarkers in the synovial fluid. The BAP concentration in the synovial fluid of the CrCL deficient stifle increased over time, and positively correlated with the total osteophyte score (r=0.6705, P=0.0001). The ratio of BAP in the synovial fluid compared to the serum increased by days 70 and 126 post-transection. When combined with a lack of significant difference from baseline in the contralateral stifle, these results suggest that the BAP in the synovial fluid was being locally produced by newly forming osteophytes (Chapter 6). Therefore, the evaluation of BAP levels in the synovial fluid has the potential to be a more sensitive indicator of osteophyte development in the early stages of secondary OA than radiographs.

In order to understand the relative contribution of synthesis and degradation to this model of OA, we used biomarker analyses of the carboxy-propeptide of type II collagen (CPII) as a representative of type II collagen synthesis, and the COL2-3/4C_{short} and 234CEQ anti-neoepitope antibodies for identification of type I and II collagen degradation and type II collagen degradation, respectively, in the serum and synovial fluid (Chapter 7). This was the first report to identify that the 234CEQ antineoepitope antibody recognizes the ¾ fragment created by collagenase cleavage of canine type II collagen, as well as demonstrating that the CPII, COL2-3/4C_{short}, and 234CEQ assays were able to be detected in the synovial fluid and serum from dogs with a transected CrCL (Chapter 7). Using the placebo dogs, synovial fluid was the superior fluid for analysis of these biomarkers compared to serum. Type II synthesis (CPII) and degradation (234CEQ) were both increased after CrCL transection in the dog, with

synthesis predominating early and degradation predominating at the end of the study, when proteoglycan turnover was also shown to significantly increase. In addition, the relative contribution of type I collagen degradation was determined by subtracting the values of 234CEQ from COL2-3/4C_{short}, and showed that type I collagen degradation predominated early and type II collagen degradation predominated at the end of the study. The source of type I collagen likely varies based upon the stage of the disease process, ranging from the early fibrinous response to the late damage sustained by the meniscus (Chapter 7).

Inflammation is considered to be one of the main causes for the initiation and continuation of the OA process after the stifle is made unstable from CrCL transection (Chapter 1 and 8). Therefore, we examined the levels of prostaglandin E_2 (PGE_2) in the synovial fluid after CrCL transection, and compared its values to the clinical parameters related to pain and inflammation, as well as force plate analysis (Chapter 8). Using the 19 placebo dogs, PGE_2 concentrations in the synovial fluid from the joints of dogs that had CrCL transection were significantly elevated from baseline throughout the study, peaking at 14 days post-transection. Correlation analyses revealed a significant negative correlation between the synovial fluid levels of PGE_2 and both the peak vertical force and impulse derived from force plate analysis. In addition, there were significant positive correlations of the PGE_2 concentrations with all of the clinical parameters examined (lameness, degree of weight bearing, joint extension, overall pain score, effusion score, and synovial fluid total protein content) except for synovial fluid white blood cell count (Chapter 8). These results suggest that PGE_2 in the synovial fluid likely is involved in

the acute inflammation and associated lameness and pain during the early stage after CrCL transection in the dog.

Through the use of the above listed biomarkers, valuable information was gained regarding the identification and use of these markers in body fluids. However, when examining which fluid provided the most information with regards to the changes identified after CrCL transection in the dog, synovial fluid was superior to serum. This is most likely due to its proximity to the articular surface combined with the fact that further proteolytic cleavage of the matrix fragments occurs in the serum potentially making them unidentifiable by the antibodies used for their detection (Chapter 1). An attempt was made to identify biomarkers that would represent changes related to inflammation, as well as synthesis and degradation of type II collagen synthesis, and bone turnover. The use of these markers in this model of OA was among the first described in body fluids, especially when related to other clinical parameters. However, to complete the picture, it would have been good to include a marker of aggrecan synthesis, such as CS846 to complement the proteoglycan turnover, and a bone degradation marker such as the carboxy-telopeptide of type I collagen (CTx) to complement the bone formation markers. However, we did attempt to identify pyridinoline cross-links in the serum (Serum Pyd) of 7 dogs, but found no differences over time. The bone formation markers, BAP and OC in the serum had similar findings, indicating that both did not have to be performed (Chapter 6). Based on the levels of BAP identified in the synovial fluid, it would be the logical marker to use in future studies.

10.4 Objective 4: to analyze the macroscopic variability of this osteoarthritis model.

When examining all of the analyses used in this study, we noticed that there was considerable variation in the pathology present between dogs. This has rarely been mentioned in previous reports, using this model, in which ≤ 4 dogs were generally used per group (Chapter 1 and 5). The coefficient of variation (CV) for the macroscopic and microscopic changes identified in our study were 21-436% and 27-424%, respectively, with the CV being much greater the more specific the analysis. Based on these findings, 12 dogs would be required to obtain 80% power (Chapter 5). The results of our study demonstrate that the gross and histologic pathology changes present after CrCL transection in a large group of dogs was highly variable between dogs with respect to incidence, location, severity, and type of lesions present. This between-subject variation should be an important consideration when planning to use this model for future projects, or when drawing conclusions from studies that involve small group sizes. This variability makes it difficult to determine whether treatment effects are not being elucidated because of the variability or because the inhibitor does not protect articular cartilage. However, when the variability was examined between the two treatment groups, it was very similar between the groups, making it more likely that the MMP inhibitor was not effective. However, further studies in a model with less variability in pathology, such as a meniscectomy model, may be prudent before determining that BAY 12-9566 has no chondroprotective effect.

In summary, we designed and created a model of osteoarthritis in the dog by arthroscopically transecting the CrCL. We managed to help distinguish some of the

temporal patterns of clinical and biochemical changes that occur after CrCL transection that may be valuable in predicting or identifying various aspects of early OA. Moreover, we determined the lack of efficacy of the MMP inhibitor, BAY 12-9566, in this experimental model of OA.

BIBLIOGRAPHY

1. Brandt KD, Myers SL, Burr D, et al: Osteoarthritic changes in canine articular cartilage, subchondral bone, and synovium fifty-four months after transection of the anterior cruciate ligament. Arthritis Rheum 34:1560-1570., 1991

2. Johnson JA, Austin, C., Breur, G. J.: Incidence of canine appendicular musculoskeletal disorders in 16 veterinary teaching hospitals from 1980 through 1989. Vet Comp Orthop Traumatol 7:56-69, 1994

3. Robins G: The canine stifle joint, in Whittick W (ed): Canine Orthopedics (ed second edition). Philadelphia, Lea and Febiger, 1990, pp 693-760

4. Arnoczky S, Wilson, J.: The connective tissues, in Whittick W (ed): Canine Orthopedics (ed second edition). Philadelphia, Lea and Febiger, 1990, pp 21-41

5. Mow VC, Ateshian GA, Spilker RL: Biomechanics of diarthrodial joints: a review of twenty years of progress. J Biomech Eng 115:460-467., 1993

6. Arnoczky SP, Marshall JL: The cruciate ligaments of the canine stifle: an anatomical and functional analysis. Am J Vet Res 38:1807-1814., 1977

7. Johnson JM, Johnson AL: Cranial cruciate ligament rupture. Pathogenesis, diagnosis, and postoperative rehabilitation. Vet Clin North Am Small Anim Pract 23:717-733., 1993

8. Arnoczky SP, Marshall, J.L.: Pathomechanics of cruciate and meniscal injuries, in Bojrab MJ (ed): Pathophysiology in Small Animal Surgery. Philadelphia, Lea & Febiger, 1981, pp 590-603

9. Harari J: Caudal cruciate ligament injury. Vet Clin North Am Small Anim Pract 23:821-829., 1993

10. Hulse D, Shires, PK.: The meniscus: Anatomy, function, and treatment. Compend Cont Educ 5:765-774, 1983

11. Krause WR, Pope MH, Johnson RJ, et al: Mechanical changes in the knee after meniscectomy. J Bone Joint Surg Am 58:599-604., 1976

12. Fithian DC, Kelly MA, Mow VC: Material properties and structure-function relationships in the menisci. Clin Orthop:19-31., 1990

13. Leach D, Jacobs, K.: Normal arthrology, in Whittick W (ed): Canine Orthopedics (ed second edition). Philadelphia, Lea and Febiger, 1990, pp 42-58

14. Bennett D, May, C.: Meniscal damage associated with cruciate disease in the dog. J Small Anim Pract 32:111-117, 1991

15. Eikenberry EF, Bruckner, P.: Supramolecular structure of cartilage matrix, in Seibel MJ, Robins, S. P., Bilezikian, J. P. (ed): Dynamics of bone and cartilage metabolism. San Diego, Academic Press, 1999, pp 289-300

16. von der Mark K: Structure, biosynthesis, and gene regulation of collagens in cartilage and bone, in Seibel MJ, Robins SP, Bilezikian JP (eds): Dynamics of Bone and Cartilage Metabolism. San Diego, Academic Press, 1999, pp 3-29

17. Hardingham T: Proteoglycans and glycosaminoglycans, in Seibel MJ, Robins, S. P., Bilezikian, J. P. (ed): Dynamics of bone and cartilage metabolism. San Diego, Academic Press, 1999, pp 71-81

18. Hardingham T: Proteoglycans: their structure, interactions and molecular organization in cartilage. Biochem Soc Trans 9:489-497., 1981

19. Comper WD, Williams RP, Zamparo O: Water transport in extracellular matrices. Connect Tissue Res 25:89-102, 1990

20. Maroudas A: Proteoglycan osmotic-pressure and the collagen tension in normal, osteoarthritic human cartilage. Seminars in Arthritis and Rheumatism 11:36-39, 1981

21. Lai WM, Hou JS, Mow VC: A triphasic theory for the swelling and deformation behaviors of articular cartilage. J Biomech Eng 113:245-258, 1991

22. Muir H: Proteoglycans as organizers of the intercellular matrix. Biochem Soc Trans 11:613-622, 1983

23. Todhunter RJ: Anatomy and physiology of synovial joints, in McIlwraith CW, Trotter, G. W. (ed): Joint Disease in the Horse. Philadelphia, WB Saunders, 1996, pp 1-28

24. Palmer JL, Bertone AL: Joint structure, biochemistry and biochemical disequilibrium in synovitis and equine joint disease. Equine Vet J 26:263-277., 1994

25. Edwards JC: The nature and origins of synovium: experimental approaches to the study of synoviocyte differentiation. J Anat 184:493-501., 1994

26. Levick JR, Knight AD: Osmotic flows across the blood-joint barrier. Ann Rheum Dis 46:534-539., 1987

27. Kerr HR, Warburton B: Surface rheological properties of hyaluronic acid solutions. Biorheology 22:133-144, 1985

28. Walker ER, Boyd RD, Wu DD, et al: Morphologic and morphometric changes in synovial membrane associated with mechanically induced osteoarthrosis. Arthritis Rheum 34:515-524, 1991

29. Barlow Y, Willoughby J: Pathophysiology of soft tissue repair. Br Med Bull 48:698-711, 1992

30. Bennett D: Joints and Joint Diseases, in Whittick W (ed): Canine Orthopedics (ed second edition). Philadelphia, Lea and Febiger, 1990, pp 776-778

31. Palmer JL, Bertone, A. L.: Joint biomechanics in the pathogenesis of traumatic arthritis, in McIlwraith CW, Trotter, G. W. (ed): Joint Disease in the Horse. Philadelphia, WB Saunders, 1996, pp 104-119

32. Nade S, Newbold PJ: Factors determining the level and changes in intra-articular pressure in the knee joint of the dog. J Physiol 338:21-36, 1983

33. Levick JR: The influence of hydrostatic pressure on trans-synovial fluid movement and on capsular expansion in the rabbit knee. J Physiol 289:69-82, 1979

34. McDonald JN, Levick JR: Hyaluronan reduces fluid escape rate from rabbit knee joints disparately from its effect on fluidity. Exp Physiol 79:103-106, 1994

35. Baumgarten M, Bloebaum RD, Ross SD, et al: Normal human synovial fluid: osmolality and exercise-induced changes. J Bone Joint Surg Am 67:1336-1339., 1985

36. Myers SL, Brandt KD, Eilam O: Even low-grade synovitis significantly accelerates the clearance of protein from the canine knee. Implications for measurement of synovial fluid "markers" of osteoarthritis. Arthritis Rheum 38:1085-1091., 1995

37. Amiel D, Abel MF, Kleiner JB, et al: Synovial fluid nutrient delivery in the diathrial joint: an analysis of rabbit knee ligaments. J Orthop Res 4:90-95, 1986

38. Simkin PA: Friction and lubrication in synovial joints. J Rheumatol 27:567-568., 2000

39. Dahlin LB, Hanff G, Myrhage R: Healing of ligaments in synovial fluid. An experimental study in rabbits. Scand J Plast Reconstr Surg Hand Surg 25:97-102, 1991

40. Redler I, Mow VC, Zimny ML, et al: The ultrastructure and biomechanical significance of the tidemark of articular cartilage. Clin Orthop:357-362, 1975

41. Boskey AL: Mineralization, structure, and function of bone, in Seibel MJ, Robins, S. P., Bilezikian, J. P. (ed): Dynamics of bone and cartilage metabolism. San Diego, Academic Press, 1999, pp 153-164

42. Boskey AL: Current concepts of the physiology and biochemistry of calcification. Clin Orthop:225-257, 1981

43. Kawcak CE, McIlwraith CW, Norrdin RW, et al: The role of subchondral bone in joint disease: a review. Equine Vet J 33:120-126., 2001

44. Dingle JT, Page Thomas DP, Hazleman B: The role of cytokines in arthritic diseases: in vitro and in vivo measurements of cartilage degradation. Int J Tissue React 9:349-354, 1987

45. Kimura JH, Hardingham TE, Hascall VC: Assembly of newly synthesized proteoglycan and link protein into aggregates in cultures of chondrosarcoma chondrocytes. J Biol Chem 255:7134-7143, 1980

46. Ratcliffe A, Hughes C, Fryer PR, et al: Immunochemical studies on the synthesis and secretion of link protein and aggregating proteoglycan by chondrocytes. Coll Relat Res 7:409-421, 1987

47. Bayliss MT, Roughley PJ: The properties of proteoglycan prepared from human articular cartilage by using associative caesium chloride gradients of high and low starting densities. Biochem J 232:111-117, 1985

48. Martel-Pelletier J, Alaaeddine N, Pelletier JP: Cytokines and their role in the pathophysiology of osteoarthritis. Front Biosci 4:D694-703., 1999

49. Xie D, Hui F, Homandberg GA: Fibronectin fragments alter matrix protein synthesis in cartilage tissue cultured in vitro. Arch Biochem Biophys 307:110-118, 1993

50. Sah RL, Kim YJ, Doong JY, et al: Biosynthetic response of cartilage explants to dynamic compression. J Orthop Res 7:619-636, 1989

51. Hall AC, Urban JP, Gehl KA: The effects of hydrostatic pressure on matrix synthesis in articular cartilage. J Orthop Res 9:1-10., 1991

52. Elliott S, Cawston T: The clinical potential of matrix metalloproteinase inhibitors in the rheumatic disorders. Drugs Aging 18:87-99, 2001

53. Cawston TE: Proteinases and inhibitors. Br Med Bull 51:385-401., 1995

54. Kleiner DE, Jr., Stetler-Stevenson WG: Structural biochemistry and activation of matrix metalloproteases. Curr Opin Cell Biol 5:891-897, 1993

55. Wernicke D, Seyfert C, Hinzmann B, et al: Cloning of collagenase 3 from the synovial membrane and its expression in rheumatoid arthritis and osteoarthritis. J Rheumatol 23:590-595., 1996

56. Cawston TE: Metalloproteinase inhibitors and the prevention of connective tissue breakdown. Pharmacol Ther 70:163-182, 1996

57. Miller EJ, Harris ED, Jr., Chung E, et al: Cleavage of Type II and III collagens with mammalian collagenase: site of cleavage and primary structure at the NH2-terminal portion of the smaller fragment released from both collagens. Biochemistry 15:787-792, 1976

58. Hasty KA, Pourmotabbed TF, Goldberg GI, et al: Human neutrophil collagenase. A distinct gene product with homology to other matrix metalloproteinases. J Biol Chem 265:11421-11424, 1990

59. Mitchell PG, Magna HA, Reeves LM, et al: Cloning, expression, and type II collagenolytic activity of matrix metalloproteinase-13 from human osteoarthritic cartilage. J Clin Invest 97:761-768., 1996

60. Billinghurst RC, Wu W, Ionescu M, et al: Comparison of the degradation of type II collagen and proteoglycan in nasal and articular cartilages induced by interleukin-1 and the selective inhibition of type II collagen cleavage by collagenase. Arthritis Rheum 43:664-672., 2000

61. Ohuchi E, Imai K, Fujii Y, et al: Membrane type 1 matrix metalloproteinase digests interstitial collagens and other extracellular matrix macromolecules. J Biol Chem 272:2446-2451, 1997

62. Billinghurst RC, Dahlberg L, Ionescu M, et al: Enhanced cleavage of type II collagen by collagenases in osteoarthritic articular cartilage. J Clin Invest 99:1534-1545., 1997

63. Hardingham TE, Fosang AJ: The structure of aggrecan and its turnover in cartilage. J Rheumatol Suppl 43:86-90., 1995

64. Brinckerhoff CE, Auble DT: Regulation of collagenase gene expression in synovial fibroblasts. Ann N Y Acad Sci 580:355-374, 1990

65. Matrisian LM: The matrix-degrading metalloproteinases. Bioessays 14:455-463, 1992

66. Murphy G, Cockett MI, Stephens PE, et al: Stromelysin is an activator of procollagenase. A study with natural and recombinant enzymes. Biochem J 248:265-268., 1987

67. Murphy G, Cockett MI, Ward RV, et al: Matrix metalloproteinase degradation of elastin, type IV collagen and proteoglycan. A quantitative comparison of the activities of 95 kDa and 72 kDa gelatinases, stromelysins-1 and -2 and punctuated metalloproteinase (PUMP). Biochem J 277 (Pt 1):277-279, 1991

68. Clegg PD, Carter SD: Matrix metalloproteinase-2 and -9 are activated in joint diseases. Equine Vet J 31:324-330., 1999

69. Henriet P, Blavier L, Declerck YA: Tissue inhibitors of metalloproteinases (TIMP) in invasion and proliferation. Apmis 107:111-119, 1999

70. Denhardt DT, Feng B, Edwards DR, et al: Tissue inhibitor of metalloproteinases (TIMP, aka EPA): structure, control of expression and biological functions. Pharmacol Ther 59:329-341, 1993

71. Sandy JD, Neame PJ, Boynton RE, et al: Catabolism of aggrecan in cartilage explants. Identification of a major cleavage site within the interglobular domain. J Biol Chem 266:8683-8685., 1991

72. Lohmander LS, Lark MW, Dahlberg L, et al: Cartilage matrix metabolism in osteoarthritis: markers in synovial fluid, serum, and urine. Clin Biochem 25:167-174., 1992

73. Lotz M, Blanco FJ, von Kempis J, et al: Cytokine regulation of chondrocyte functions. J Rheumatol Suppl 43:104-108., 1995

74. Pelletier JP, DiBattista JA, Roughley P, et al: Cytokines and inflammation in cartilage degradation. Rheum Dis Clin North Am 19:545-568., 1993

75. Towle CA, Trice ME, Ollivierre F, et al: Regulation of cartilage remodeling by IL-1: evidence for autocrine synthesis of IL-1 by chondrocytes. J Rheumatol 14 Spec No:11-13, 1987

76. Chizzonite R, Truitt T, Kilian PL, et al: Two high-affinity interleukin 1 receptors represent separate gene products. Proc Natl Acad Sci U S A 86:8029-8033, 1989

77. Pelletier JP, Faure MP, DiBattista JA, et al: Coordinate synthesis of stromelysin, interleukin-1, and oncogene proteins in experimental osteoarthritis. An immunohistochemical study. Am J Pathol 142:95-105., 1993

78. Seckinger P, Lowenthal JW, Williamson K, et al: A urine inhibitor of interleukin 1 activity that blocks ligand binding. J Immunol 139:1546-1549, 1987

79. Hughes CE, Caterson B, Fosang AJ, et al: Monoclonal antibodies that specifically recognize neoepitope sequences generated by 'aggrecanase' and matrix metalloproteinase cleavage of aggrecan: application to catabolism in situ and in vitro. Biochem J 305:799-804., 1995

80. Tyler JA: Chondrocyte-mediated depletion of articular cartilage proteoglycans in vitro. Biochem J 225:493-507, 1985

81. Tyler JA, Benton HP: Synthesis of type II collagen is decreased in cartilage cultured with interleukin 1 while the rate of intracellular degradation remains unchanged. Coll Relat Res 8:393-405, 1988

82. Smith RA, Baglioni C: Multimeric structure of the tumor necrosis factor receptor of HeLa cells. J Biol Chem 264:14646-14652, 1989

83. Kohno T, Brewer MT, Baker SL, et al: A second tumor necrosis factor receptor gene product can shed a naturally occurring tumor necrosis factor inhibitor. Proc Natl Acad Sci U S A 87:8331-8335, 1990

84. Fernandes JC, Martel-Pelletier J, Pelletier JP: The role of cytokines in osteoarthritis pathophysiology. Biorheology 39:237-246, 2002

85. Guerne PA, Carson DA, Lotz M: IL-6 production by human articular chondrocytes. Modulation of its synthesis by cytokines, growth factors, and hormones in vitro. J Immunol 144:499-505, 1990

86. Nietfeld JJ, Wilbrink B, Helle M, et al: Interleukin-1-induced interleukin-6 is required for the inhibition of proteoglycan synthesis by interleukin-1 in human articular cartilage. Arthritis Rheum 33:1695-1701, 1990

87. Lotz M, Guerne PA: Interleukin-6 induces the synthesis of tissue inhibitor of metalloproteinases-1/erythroid potentiating activity (TIMP-1/EPA). J Biol Chem 266:2017-2020, 1991

88. Shingu M, Nagai Y, Isayama T, et al: The effects of cytokines on metalloproteinase inhibitors (TIMP) and collagenase production by human chondrocytes and TIMP

production by synovial cells and endothelial cells. Clin Exp Immunol 94:145-149., 1993

89. Malemud CJ: The role of growth factors in cartilage metabolism. Rheum Dis Clin North Am 19:569-580., 1993

90. Tesch GH, Handley CJ, Cornell HJ, et al: Effects of free and bound insulin-like growth factors on proteoglycan metabolism in articular cartilage explants. J Orthop Res 10:14-22, 1992

91. Rayan V, Hardingham T: The recovery of articular cartilage in explant culture from interleukin-1 alpha: effects on proteoglycan synthesis and degradation. Matrix Biol 14:263-271, 1994

92. Trippel SB: Growth factor actions on articular cartilage. J Rheumatol Suppl 43:129-132., 1995

93. Tardif G, Pelletier JP, Dupuis M, et al: Collagenase 3 production by human osteoarthritic chondrocytes in response to growth factors and cytokines is a function of the physiologic state of the cells. Arthritis Rheum 42:1147-1158., 1999

94. Huh YH, Kim SH, Kim SJ, et al: Differentiation status-dependent regulation of cyclooxygenase-2 expression and prostaglandin E2 production by epidermal growth factor via mitogen-activated protein kinase in articular chondrocytes. J Biol Chem, 2002

95. Adams ME, Billingham ME: Animal models of degenerative joint disease. Curr Top Pathol 71:265-297, 1982

96. Palmoski MJ, Brandt KD: Immobilization of the knee prevents osteoarthritis after anterior cruciate ligament transection. Arthritis Rheum 25:1201-1208., 1982

97. Myers SL, Brandt KD, O'Connor BL, et al: Synovitis and osteoarthritic changes in canine articular cartilage after anterior cruciate ligament transection. Effect of surgical hemostasis. Arthritis Rheum 33:1406-1415., 1990

98. Brandt KD, Braunstein EM, Visco DM, et al: Anterior (cranial) cruciate ligament transection in the dog: a bona fide model of osteoarthritis, not merely of cartilage injury and repair. J Rheumatol 18:436-446., 1991

99. Dedrick DK, Goldstein SA, Brandt KD, et al: A longitudinal study of subchondral plate and trabecular bone in cruciate-deficient dogs with osteoarthritis followed up for 54 months. Arthritis Rheum 36:1460-1467., 1993

100. Marshall JL: Periarticular osteophytes. Initiation and formation in the knee of the dog. Clin Orthop 62:37-47., 1969

101. Pond MJ, Nuki G: Experimentally-induced osteoarthritis in the dog. Ann Rheum Dis 32:387-388., 1973

102. McDevitt C, Gilbertson E, Muir H: An experimental model of osteoarthritis; early morphological and biochemical changes. J Bone Joint Surg Br 59:24-35., 1977

103. Sandy JD, Adams ME, Billingham ME, et al: In vivo and in vitro stimulation of chondrocyte biosynthetic activity in early experimental osteoarthritis. Arthritis Rheum 27:388-397., 1984

104. Visco DM, Hill MA, Widmer WR, et al: Experimental osteoarthritis in dogs: a comparison of the Pond-Nuki and medial arthrotomy methods. Osteoarthritis Cartilage 4:9-22., 1996

105. Altman RD, Tenenbaum J, Latta L, et al: Biomechanical and biochemical properties of dog cartilage in experimentally induced osteoarthritis. Ann Rheum Dis 43:83-90., 1984

106. Stockwell RA, Billingham ME, Muir H: Ultrastructural changes in articular cartilage after experimental section of the anterior cruciate ligament of the dog knee. J Anat 136:425-439., 1983

107. McDevitt CA, Muir H: Biochemical changes in the cartilage of the knee in experimental and natural osteoarthritis in the dog. J Bone Joint Surg Br 58:94-101., 1976

108. Pelletier JP, Martel-Pelletier J, Altman RD, et al: Collagenolytic activity and collagen matrix breakdown of the articular cartilage in the Pond-Nuki dog model of osteoarthritis. Arthritis Rheum 26:866-874., 1983

109. Fernandes JC, Martel-Pelletier J, Jovanovic D, et al: The effects of tenidap on canine experimental osteoarthritis: II. Study of the expression of collagenase-1 and interleukin 1beta by in situ hybridization. J Rheumatol 25:951-958., 1998

110. Pelletier JP, Lajeunesse D, Jovanovic DV, et al: Carprofen simultaneously reduces progression of morphological changes in cartilage and subchondral bone in experimental dog osteoarthritis. J Rheumatol 27:2893-2902., 2000

111. Fernandes JC, Martel-Pelletier J, Otterness IG, et al: Effects of tenidap on canine experimental osteoarthritis. I. Morphologic and metalloprotease analysis. Arthritis Rheum 38:1290-1303., 1995

112. Fernandes JC, Caron JP, Martel-Pelletier J, et al: Effects of tenidap on the progression of osteoarthritic lesions in a canine experimental model. Suppression of metalloprotease and interleukin-1 activity. Arthritis Rheum 40:284-294., 1997

113. Pelletier JP, Jovanovic D, Fernandes JC, et al: Reduced progression of experimental osteoarthritis in vivo by selective inhibition of inducible nitric oxide synthase. Arthritis Rheum 41:1275-1286., 1998

114. Jovanovic D, Caron JP, Martel-Pelletier J, et al: The therapeutic effects of tenidap in canine experimental osteoarthritis: relationship with biochemical markers. J Rheumatol 24:916-925., 1997

115. Howell DS, Pita JC, Muller FJ, et al: Treatment of osteoarthritis with tiaprofenic acid: biochemical and histological protection against cartilage breakdown in the Pond-Nuki canine model. J Rheumatol Suppl 27:138-142., 1991

116. Carney SL: Effect of diacetyl rhein on the development of experimental osteoarthritis. A biochemical investigation. Osteoarthritis Cartilage 4:251-261., 1996

117. Eyre DR, McDevitt CA, Billingham ME, et al: Biosynthesis of collagen and other matrix proteins by articular cartilage in experimental osteoarthrosis. Biochem J 188:823-837., 1980

118. Johnson RG, Poole AR: The early response of articular cartilage to ACL transection in a canine model. Exp Pathol 38:37-52, 1990

119. Marshall JL, Olsson SE: Instability of the knee. A long-term experimental study in dogs. J Bone Joint Surg Am 53:1561-1570., 1971

120. Vignon E, Hartmann JD, Vignon G, et al: Cartilage destruction in experimentally induced osteoarthritis. J Rheumatol 11:202-207., 1984

121. Vignon E, Arlot M, Hartmann D, et al: Hypertrophic repair of articular cartilage in experimental osteoarthrosis. Ann Rheum Dis 42:82-88., 1983

122. Pidd JG, Gardner DL, Adams ME: Ultrastructural changes in the femoral condylar cartilage of mature American foxhounds following transection of the anterior cruciate ligament. J Rheumatol 15:663-669., 1988

123. Myers SL, Brandt KD, Burr DB, et al: Effects of a bisphosphonate on bone histomorphometry and dynamics in the canine cruciate deficiency model of osteoarthritis. J Rheumatol 26:2645-2653., 1999

124. Smith GN, Jr., Myers SL, Brandt KD, et al: Diacerhein treatment reduces the severity of osteoarthritis in the canine cruciate-deficiency model of osteoarthritis. Arthritis Rheum 42:545-554., 1999

125. Slowman-Kovacs SD, Albrecht ME, Brandt KD: Effects of salicylate on chondrocytes from osteoarthritic and contralateral knees of dogs with unilateral anterior cruciate ligament transection. Arthritis Rheum 32:486-490., 1989

126. Fife RS: Alterations in a cartilage matrix glycoprotein in canine osteoarthritis. Arthritis Rheum 29:1493-1500., 1986

127. Fife RS, Palmoski MJ, Brandt KD: Metabolism of a cartilage matrix glycoprotein in normal and osteoarthritic canine articular cartilage. Arthritis Rheum 29:1256-1262., 1986

128. Adams ME: Cartilage hypertrophy following canine anterior cruciate ligament transection differs among different areas of the joint. J Rheumatol 16:818-824., 1989

129. Marshall KW, Chan AD: Bilateral canine model of osteoarthritis. J Rheumatol 23:344-350., 1996

130. Marshall KW, Chan AD: Arthroscopic anterior cruciate ligament transection induces canine osteoarthritis. J Rheumatol 23:338-343., 1996

131. Fernandes JC, Jovanovic D, Dehnade F, et al: [Resection of the anterior cruciate ligament of the knee using arthroscopy induces arthrosis in dogs. Validity of the Pond-Nuki model]. Ann Chir 52:768-775, 1998

132. Guilak F, Ratcliffe A, Lane N, et al: Mechanical and biochemical changes in the superficial zone of articular cartilage in canine experimental osteoarthritis. J Orthop Res 12:474-484., 1994

133. Adams M, Pelletier, JP: Canine anterior cruciate transection model of osteoarthritis. CRC Handbook of animal models for the rheumatic diseases:57-81, 1988

134. Paatsama S, Sittnikow K: Early changes in the knee joint due to instability induced by cutting of the anterior cruciate ligament. An experimental study in young dogs. Acta Radiol Suppl 319:169-173, 1972

135. Adams ME GM, Ho A: Cartilage proteoglycan changes in experimental canine osteoarthritis. J Rheumatol suppl 14:107-109, 1987

136. Adams ME, Brandt KD: Hypertrophic repair of canine articular cartilage in osteoarthritis after anterior cruciate ligament transection. J Rheumatol 18:428-435., 1991

137. Brandt KD: Pain, synovitis, and articular cartilage changes in osteoarthritis. Semin Arthritis Rheum 18:77-80., 1989

138. Braunstein EM, Brandt KD, Albrecht M: MRI demonstration of hypertrophic articular cartilage repair in osteoarthritis. Skeletal Radiol 19:335-339, 1990

139. Brandt KD: Animal models of osteoarthritis. Biorheology 39:221-235, 2002

140. Johnson RG: Transection of the canine anterior cruciate ligament: a concise review of experience with this model of degenerative joint disease. Exp Pathol 30:209-213, 1986

141. Caron JP, Fernandes JC, Martel-Pelletier J, et al: Chondroprotective effect of intraarticular injections of interleukin-1 receptor antagonist in experimental osteoarthritis. Suppression of collagenase-1 expression. Arthritis Rheum 39:1535-1544., 1996

142. Slocum B, Devine T: Cranial tibial thrust: a primary force in the canine stifle. J Am Vet Med Assoc 183:456-459, 1983

143. Flo GL: Meniscal injuries. Vet Clin North Am Small Anim Pract 23:831-843, 1993

144. Williams J, Tomlinson, J., Constantinescu, G.M.: Diagnosing and treating meniscal injuries in the dog. Veterinary Medicine 89:42-47, 1994

145. Flo GL: Classification of meniscal lesions in 26 consecutive canine meniscectomies. J Am Anim Hosp Assoc 19:335-340, 1983

146. Innes JF, Barr AR: Clinical natural history of the postsurgical cruciate deficient canine stifle joint: year 1. J Small Anim Pract 39:325-332., 1998

147. Hulse D, Shires, PK.: Observation of posteromedial compartment of the stifle joint. J Am Anim Hosp Assoc 17:575-578, 1981

148. Elkins AD, Pechman, R., Kearney, M. T., Herron, M.: A retrospective study evaluating the degree of degenerative joint diseases in the stifle joint of dogs following surgical repair of anterior cruciate ligament rupture. J Am Anim Hosp Assoc 27:533-540, 1991

149. Flo G, DeYoung, D., Tvedten, H., Johnson, L.: Classification of meniscal injuries in the canine stifle based upon gross pathological appearance. J Am Anim Hosp Assoc 19:325-334, 1983

150. Flo GL: Modification of the lateral retinacular imbrication technique for stabilizing cruciate ligament injuries. J Am Anim Hosp Assoc 11:570-575, 1975

151. Flo GL, DeYoung, D.: Meniscal injuries and medial meniscectomy in the canine stifle. J Am Anim Hosp Assoc 14:683-689, 1978

152. Gambardella PC, Wallace, L. J., Cassidy, F.: Lateral suture technique for management of anterior cruciate ligament rupture in dogs: A retrospective study. J Am Anim Hosp Assoc 17:33-38, 1981

153. Metelman L, Schwarz, P., Salman, M., Alvis, M.: An evaluation of three different cranial cruciate ligament surgical stabilisation procedures as they relate to post-operative meniscal injuries. Vet Comp Orthop Traumatol 8:118-123, 1995

154. Moore KW, Read RA: Cranial cruciate ligament rupture in the dog--a retrospective study comparing surgical techniques. Aust Vet J 72:281-285., 1995

155. Vasseur PB, Berry, C. R.: Progression of stifle osteoarthritis following reconstruction of the cranial cruciate ligament in 21 dogs. J Am Anim Hosp Assoc 28:129-136, 1992

156. Anderson DR, Woo SL, Kwan MK, et al: Viscoelastic shear properties of the equine medial meniscus. J Orthop Res 9:550-558., 1991

157. Siemering GH, Eilert, R. E.: Arthroscopic study of cranial cruciate ligament and medial meniscal lesions in the dog. Vet Surg 15:265-269, 1986

158. Dieppe P: Osteoarthritis: clinical and research perspective. Br J Rheumatol 30:1-4., 1991

159. Tirgari M, Vaughan LC: Arthritis of the canine stifle joint. Vet Rec 96:394-399., 1975

160. Henrotin Y, Deby-Dupont G, Deby C, et al: Active oxygen species, articular inflammation and cartilage damage. Exs 62:308-322, 1992

161. Sandy JD, Sriratana A, Brown HL, et al: Evidence for polymorphonuclear-leucocyte-derived proteinases in arthritic cartilage. Biochem J 193:193-202, 1981

162. Wolfe GC, MacNaul KL, Buechel FF, et al: Differential in vivo expression of collagenase messenger RNA in synovium and cartilage. Quantitative comparison

with stromelysin messenger RNA levels in human rheumatoid arthritis and osteoarthritis patients and in two animal models of acute inflammatory arthritis. Arthritis Rheum 36:1540-1547., 1993

163. Lark MW, MacNaul KA, Donatelli S, et al: Induction of increased levels of proteoglycan fragments in synovial fluid (SF) and increased levels of stromelysin in cartilage, synovium and SF by intraarticular injection of canine monocyte conditioned medium into dogs. J Rheumatol 21:1716-1724., 1994

164. Lohmander LS, Roos H, Dahlberg L, et al: Temporal patterns of stromelysin-1, tissue inhibitor, and proteoglycan fragments in human knee joint fluid after injury to the cruciate ligament or meniscus. J Orthop Res 12:21-28., 1994

165. Tyler JA: Insulin-like growth factor 1 can decrease degradation and promote synthesis of proteoglycan in cartilage exposed to cytokines. Biochem J 260:543-548, 1989

166. Matyas JR, Adams ME, Huang D, et al: Discoordinate gene expression of aggrecan and type II collagen in experimental osteoarthritis. Arthritis Rheum 38:420-425., 1995

167. Mankin HJ, Lippiello L: Biochemical and metabolic abnormalities in articular cartilage from osteo-arthritic human hips. J Bone Joint Surg Am 52:424-434., 1970

168. Mankin HJ, Dorfman H, Lippiello L, et al: Biochemical and metabolic abnormalities in articular cartilage from osteo-arthritic human hips. II. Correlation of morphology with biochemical and metabolic data. J Bone Joint Surg Am 53:523-537., 1971

169. van den Berg WB: Growth factors in experimental osteoarthritis: transforming growth factor beta pathogenic? J Rheumatol Suppl 43:143-145., 1995

170. Middleton J, Arnott N, Walsh S, et al: Osteoblasts and osteoclasts in adult human osteophyte tissue express the mRNAs for insulin-like growth factors I and II and the type 1 IGF receptor. Bone 16:287-293, 1995

171. Widmer WR, Buckwalter, K. A., Braunstein, E. M., Hill, M. A., O' Connor, B. L., Visco D. M.: Radiographic and magnetic resonance imaging of the stifle joint in

experimental osteoarthritis of dogs. Veterinary Radiology and Ultrasound 35:371-383, 1994

172. Radin EL, Rose RM: Role of subchondral bone in the initiation and progression of cartilage damage. Clin Orthop:34-40., 1986

173. Roush JK: Hind limb lameness in the mature dog. Vet Clin North Am Small Anim Pract 31:125-141, vi., 2001

174. Lewis DD, Goring, RL., Parker, RB., Curasi, PA.: A comparison of diagnostic methods used in the evaluationof early degenerative joint disease in the dog. J Am Anim Hosp Assoc 23:305-315, 1987

175. van Gestel MA: Diagnostic accuracy of stifle arthroscopy in the dog. J Am Anim Hosp Assoc 21:757-763, 1985

176. Miller C, Presnell, K. R.: Examination of the canine stifle: Arthroscopy versus arthrotomy. J Am Anim Hosp Assoc 21:623-629, 1985

177. Kivumbi CW, Bennett D: Arthroscopy of the canine stifle joint. Vet Rec 109:241-249., 1981

178. Siemering GH: Arthroscopy of dogs. J Am Vet Med Assoc 172:575-577., 1978

179. Person MW: A procedure for arthroscopic examination of the canine stifle joint. J Am Anim Hosp Assoc 21:179-186, 1985

180. van Gestel MA: Arthroscopy of the canine stifle. Vet Q 7:237-239., 1985

181. Pond MJ, Campbell JR: The canine stifle joint. I. Rupture of the anterior cruciate ligament. An assessment of conservative and surgical treatment. J Small Anim Pract 13:1-10., 1972

182. Heffron LE, Campbell JR: Osteophyte formation in the canine stifle joint following treatment for rupture of the cranial cruciate ligament. J Small Anim Pract 20:603-611., 1979

183. Brandt KD, Fife RS, Braunstein EM, et al: Radiographic grading of the severity of knee osteoarthritis: relation of the Kellgren and Lawrence grade to a grade based on joint space narrowing, and correlation with arthroscopic evidence of articular cartilage degeneration. Arthritis Rheum 34:1381-1386., 1991

184. Spindler KP, Schils JP, Bergfeld JA, et al: Prospective study of osseous, articular, and meniscal lesions in recent anterior cruciate ligament tears by magnetic resonance imaging and arthroscopy. Am J Sports Med 21:551-557., 1993

185. Mink JH, Deutsch AL: Magnetic resonance imaging of the knee. Clin Orthop:29-47, 1989

186. Sabiston CP, Adams ME, Li DK: Magnetic resonance imaging of osteoarthritis: correlation with gross pathology using an experimental model. J Orthop Res 5:164-172, 1987

187. Brandt KD, Schauwecker DS, Dansereau S, et al: Bone scintigraphy in the canine cruciate deficiency model of osteoarthritis. Comparison of the unstable and contralateral knee. J Rheumatol 24:140-145., 1997

188. Boyd SK, Matyas JR, Wohl GR, et al: Early regional adaptation of periarticular bone mineral density after anterior cruciate ligament injury. J Appl Physiol 89:2359-2364., 2000

189. Boyd SK, Muller R, Matyas JR, et al: Early morphometric and anisotropic change in periarticular cancellous bone in a model of experimental knee osteoarthritis quantified using microcomputed tomography. Clin Biomech (Bristol, Avon) 15:624-631., 2000

190. Anderson MA MF: Force plate analysis: A noninvasive tool for gait evaluation. Compendium for Continuing Education 16:857-867, 1994

191. DeCamp CE: Kinetic and kinematic gait analysis and the assessment of lameness in the dog. Vet Clin North Am Small Anim Pract 27:825-840., 1997

192. Budsberg SC, Verstraete MC, Soutas-Little RW: Force plate analysis of the walking gait in healthy dogs. Am J Vet Res 48:915-918., 1987

193. Rumph PF, Lander JE, Kincaid SA, et al: Ground reaction force profiles from force platform gait analyses of clinically normal mesomorphic dogs at the trot. Am J Vet Res 55:756-761., 1994

194. McLaughlin RM, Jr., Roush JK: Effects of subject stance time and velocity on ground reaction forces in clinically normal greyhounds at the trot. Am J Vet Res 55:1666-1671., 1994

195. McLaughlin R, Jr., Roush JK: Effects of increasing velocity on braking and propulsion times during force plate gait analysis in greyhounds. Am J Vet Res 56:159-161., 1995

196. Riggs CM, DeCamp CE, Soutas-Little RW, et al: Effects of subject velocity on force plate-measured ground reaction forces in healthy greyhounds at the trot. Am J Vet Res 54:1523-1526., 1993

197. Jevens DJ, Hauptman JG, DeCamp CE, et al: Contributions to variance in force-plate analysis of gait in dogs. Am J Vet Res 54:612-615., 1993

198. Budsberg SC, Verstraete MC, Soutas-Little RW, et al: Force plate analyses before and after stabilization of canine stifles for cruciate injury. Am J Vet Res 49:1522-1524., 1988

199. Jevens DJ, DeCamp CE, Hauptman J, et al: Use of force-plate analysis of gait to compare two surgical techniques for treatment of cranial cruciate ligament rupture in dogs. Am J Vet Res 57:389-393., 1996

200. O'Connor BL, Visco DM, Heck DA, et al: Gait alterations in dogs after transection of the anterior cruciate ligament. Arthritis Rheum 32:1142-1147., 1989

201. Rumph PF, Kincaid SA, Visco DM, et al: Redistribution of vertical ground reaction force in dogs with experimentally induced chronic hindlimb lameness. Vet Surg 24:384-389., 1995

202. Budsberg SC: Long-term temporal evaluation of ground reaction forces during development of experimentally induced osteoarthritis in dogs. Am J Vet Res 62:1207-1211., 2001

203. Lohmander LS, Felson DT: Defining the role of molecular markers to monitor disease, intervention, and cartilage breakdown in osteoarthritis. J Rheumatol 24:782-785., 1997

204. Lohmander LS: Articular cartilage and osteoarthrosis. The role of molecular markers to monitor breakdown, repair and disease. J Anat 184:477-492., 1994

205. Simkin PA: Synovial perfusion and synovial fluid solutes. Ann Rheum Dis 54:424-428., 1995

206. Kraus VB, Huebner JL, Fink C, et al: Urea as a passive transport marker for arthritis biomarker studies. Arthritis Rheum 46:420-427., 2002

207. Manicourt DH, Lenz ME, Thonar EJ: Levels of serum keratan sulfate rise rapidly and remain elevated following anterior cruciate ligament transection in the dog. J Rheumatol 18:1872-1876., 1991

208. Ratcliffe A, Beauvais PJ, Saed-Nejad F, et al: Synovial fluid analyses detect and differentiate proteoglycan metabolism in canine experimental models of osteoarthritis and disuse atrophy. Agents Actions Suppl 39:63-67, 1993

209. Ratcliffe A, Billingham ME, Saed-Nejad F, et al: Increased release of matrix components from articular cartilage in experimental canine osteoarthritis. J Orthop Res 10:350-358., 1992

210. Brandt KD, Thonar EJ: Lack of association between serum keratan sulfate concentrations and cartilage changes of osteoarthritis after transection of the anterior cruciate ligament in the dog. Arthritis Rheum 32:647-651., 1989

211. Carney SL, Billingham ME, Caterson B, et al: Changes in proteoglycan turnover in experimental canine osteoarthritic cartilage. Matrix 12:137-147., 1992

212. Innes JF, Sharif M, Barr AR: Relations between biochemical markers of osteoarthritis and other disease parameters in a population of dogs with naturally acquired osteoarthritis of the genual joint. Am J Vet Res 59:1530-1536., 1998

213. Innes JF, Sharif M, Barr AR: Changes in concentrations of biochemical markers of osteoarthritis following surgical repair of ruptured cranial cruciate ligaments in dogs. Am J Vet Res 60:1164-1168., 1999

214. Johnson KA, Hart RC, Chu Q, et al: Concentrations of chondroitin sulfate epitopes 3B3 and 7D4 in synovial fluid after intra-articular and extracapsular reconstruction of the cranial cruciate ligament in dogs. Am J Vet Res 62:581-587., 2001

215. Johnson KA, Hay CW, Chu Q, et al: Cartilage-derived biomarkers of osteoarthritis in synovial fluid of dogs with naturally acquired rupture of the cranial cruciate ligament. Am J Vet Res 63:775-781., 2002

216. Johnson KA, Hulse DA, Hart RC, et al: Effects of an orally administered mixture of chondroitin sulfate, glucosamine hydrochloride and manganese ascorbate on synovial fluid chondroitin sulfate 3B3 and 7D4 epitope in a canine cruciate ligament transection model of osteoarthritis. Osteoarthritis Cartilage 9:14-21., 2001

217. Arican M, Carter SD, Bennett D: Osteocalcin in canine joint diseases. Br Vet J 152:411-423., 1996

218. Arican M, Carter SD, Bennett D, et al: Measurement of glycosaminoglycans and keratan sulphate in canine arthropathies. Res Vet Sci 56:290-297., 1994

219. Chu Q, Lopez M, Hayashi K, et al: Elevation of a collagenase generated type II collagen neoepitope and proteoglycan epitopes in synovial fluid following induction of joint instability in the dog. Osteoarthritis Cartilage 10:662-669, 2002

220. Manicourt DH, Cornu O, Lenz ME, et al: Rapid and sustained rise in the serum level of hyaluronan after anterior cruciate ligament transection in the dog knee joint. J Rheumatol 22:262-269., 1995

221. Arican M, Carter SD, May C, et al: Hyaluronan in canine arthropathies. J Comp Pathol 111:185-195., 1994

222. Nelson F, Dahlberg L, Laverty S, et al: Evidence for altered synthesis of type II collagen in patients with osteoarthritis. J Clin Invest 102:2115-2125., 1998

223. Billinghurst RC, Buxton EM, Edwards MG, et al: Use of an antineoepitope antibody for identification of type-II collagen degradation in equine articular cartilage. Am J Vet Res 62:1031-1039., 2001

224. Farndale RW, Buttle DJ, Barrett AJ: Improved quantitation and discrimination of sulphated glycosaminoglycans by use of dimethylmethylene blue. Biochim Biophys Acta 883:173-177., 1986

225. Vincenti MP, White LA, Schroen DJ, et al: Regulating expression of the gene for matrix metalloproteinase-1 (collagenase): mechanisms that control enzyme activity, transcription, and mRNA stability. Crit Rev Eukaryot Gene Expr 6:391-411, 1996

226. Skiles JW, Gonnella NC, Jeng AY: The design, structure, and therapeutic application of matrix metalloproteinase inhibitors. Curr Med Chem 8:425-474., 2001

227. Brown PD: Ongoing trials with matrix metalloproteinase inhibitors. Expert Opin Investig Drugs 9:2167-2177., 2000

228. Shapiro SD: Mighty mice: transgenic technology "knocks out" questions of matrix metalloproteinase function. Matrix Biol 15:527-533, 1997

229. Vincenti MP, Clark IM, Brinckerhoff CE: Using inhibitors of metalloproteinases to treat arthritis. Easier said than done? Arthritis Rheum 37:1115-1126., 1994

230. Greenwald RA: Thirty-six years in the clinic without an MMP inhibitor. What hath collagenase wrought? Ann N Y Acad Sci 878:413-419, 1999

231. Dahlberg L, Billinghurst RC, Manner P, et al: Selective enhancement of collagenase-mediated cleavage of resident type II collagen in cultured osteoarthritic cartilage and arrest with a synthetic inhibitor that spares collagenase 1 (matrix metalloproteinase 1). Arthritis Rheum 43:673-682., 2000

232. Spirito S, Doughty J, O'Byrne E, et al: Metalloprotease inhibitors halt collagen breakdown in IL-1 induced bovine nasal cartilage cultures. Inflamm Res 44 Suppl 2:S131-132., 1995

233. Bottomley KM, Borkakoti N, Bradshaw D, et al: Inhibition of bovine nasal cartilage degradation by selective matrix metalloproteinase inhibitors. Biochem J 323:483-488., 1997

234. Bonassar LJ, Sandy JD, Lark MW, et al: Inhibition of cartilage degradation and changes in physical properties induced by IL-1beta and retinoic acid using matrix metalloproteinase inhibitors. Arch Biochem Biophys 344:404-412, 1997

235. Ellis AJ, Curry VA, Powell EK, et al: The prevention of collagen breakdown in bovine nasal cartilage by TIMP, TIMP-2 and a low molecular weight synthetic inhibitor. Biochem Biophys Res Commun 201:94-101, 1994

236. Kozaci LD, Buttle DJ, Hollander AP: Degradation of type II collagen, but not proteoglycan, correlates with matrix metalloproteinase activity in cartilage explant cultures. Arthritis Rheum 40:164-174, 1997

237. Levy DE, Ezrin, A.M.: Matrix metalloproteinas inhibiting drugs. Emerg Drugs 2:205-230, 1997

238. Gatto C, Rieppi M, Borsotti P, et al: BAY 12-9566, a novel inhibitor of matrix metalloproteinases with antiangiogenic activity. Clin Cancer Res 5:3603-3607., 1999

239. Leff R, Elias, I., Ionescu, M., Reiner, A., Poole, A.: Molecular changes in human osteoarthritic cartilage after 3 weeks of oral administration of BAY 12-9566, a novel matrix metalloproteinase inhibitor. Arthritis and Rheumatism 42:S404, 1999

240. Leff RL: Clinical trials of a stromelysin inhibitor. Osteoarthritis, matrix metalloproteinase inhibition, cartilage loss, surrogate markers, and clinical implications. Ann N Y Acad Sci 878:201-207., 1999

241. Chau T, Jolly, G., Plym, M-J., McHugh, M., Bortolon, E., Wakefield, J., Gianpaolo-Ostravage, C., Maniglia, C.: Inhibition of articular cartilage degradation in dog and guinea pig models of osteoarthritis by the stromelysin inhibitor, BAY 12-9566. Arthritis and Rheumatism 41:S300, 1998

242. Billinghurst RC, O'Brien K, Poole AR, et al: Inhibition of articular cartilage degradation in culture by a novel nonpeptidic matrix metalloproteinase inhibitor. Ann N Y Acad Sci 878:594-597., 1999

243. Hamada T, Arima N, Shindo M, et al: Suppression of adjuvant arthritis of rats by a novel matrix metalloproteinase-inhibitor. Br J Pharmacol 131:1513-1520., 2000

244. Ratcliffe A, Rosenwasser MP, Mahmud F, et al: The in vivo effects of naproxen on canine experimental osteoarthritic articular cartilage: composition, metalloproteinase activities and metabolism. Agents Actions Suppl 39:207-211, 1993

245. Jarvinen M, Jozsa L, Johnson RJ, et al: Effect of anterior cruciate ligament reconstruction with patellar tendon or prosthetic ligament on the morphology of the other ligaments of the knee joint. An experimental study in dogs. Clin Orthop:176-182., 1995

246. Damyanovich AZ, Staples JR, Marshall KW: 1H NMR investigation of changes in the metabolic profile of synovial fluid in bilateral canine osteoarthritis with unilateral joint denervation. Osteoarthritis Cartilage 7:165-172., 1999

247. Damyanovich AZ, Staples JR, Chan AD, et al: Comparative study of normal and osteoarthritic canine synovial fluid using 500 MHz 1H magnetic resonance spectroscopy. J Orthop Res 17:223-231., 1999

248. Marshall KW, Manolopoulos V, Mancer K, et al: Amelioration of disease severity by intraarticular hylan therapy in bilateral canine osteoarthritis. J Orthop Res 18:416-425., 2000

249. Smith GN, Mickler EA, Albrecht ME, et al: Severity of medial meniscus damage in the canine knee after anterior cruciate ligament transection. Osteoarthritis Cartilage 10:321-326., 2002

250. Dupuis J, Harari, J.: Cruciate ligament and meniscal injuries in dogs. Compend Cont Educ 15:215-233, 1993

251. Vasseur PB: Clinical results following nonoperative management for rupture of the cranial cruciate ligaments in dogs. Vet Surg 13:243-246, 1984

252. Chauvet AE, Johnson AL, Pijanowski GJ, et al: Evaluation of fibular head transposition, lateral fabellar suture, and conservative treatment of cranial cruciate ligament rupture in large dogs: a retrospective study. J Am Anim Hosp Assoc 32:247-255., 1996

253. Shires PK, Hulse, D. A., Liu, W.: The under-and-over fascial replacement technique for anterior cruciate ligament rupture in dogs: A retrospective study. J Am Anim Hosp Assoc 20:69-77, 1984

254. Dodge GR, Poole AR: Immunohistochemical detection and immunochemical analysis of type II collagen degradation in human normal, rheumatoid, and osteoarthritic articular cartilages and in explants of bovine articular cartilage cultured with interleukin 1. J Clin Invest 83:647-661., 1989

255. Orford CR, Gardner DL, O'Connor P: Ultrastructural changes in dog femoral condylar cartilage following anterior cruciate ligament section. J Anat 137 (Pt 4):653-663, 1983

256. Korvick DL: Joint motion studies of the normal and cranial cruciate ligament deficient stifle in large breed dogs, in. Urbana, University of Illinois, 1991

257. Kurosawa H, Fukubayashi T, Nakajima H: Load-bearing mode of the knee joint: physical behavior of the knee joint with or without menisci. Clin Orthop:283-290, 1980

258. Fukubayashi T, Kurosawa H: The contact area and pressure distribution pattern of the knee. A study of normal and osteoarthrotic knee joints. Acta Orthop Scand 51:871-879, 1980

259. Berlet GC, Fowler PJ: The anterior horn of the medical meniscus. An anatomic study of its insertion. Am J Sports Med 26:540-543., 1998

260. Nelson EW, LaPrade RF: The anterior intermeniscal ligament of the knee. An anatomic study. Am J Sports Med 28:74-76., 2000

261. Evans CH, Mears DC, Cosgrove JL: Release of neutral proteinases from mononuclear phagocytes and synovial cells in response to cartilaginous wear particles in vitro. Biochim Biophys Acta 677:287-294, 1981

262. Budsberg SC, Jevens DJ, Brown J, et al: Evaluation of limb symmetry indices, using ground reaction forces in healthy dogs. Am J Vet Res 54:1569-1574., 1993

263. Budsberg SC, Verstraete MC, Brown J, et al: Vertical loading rates in clinically normal dogs at a trot. Am J Vet Res 56:1275-1280., 1995

264. Rumph PF, Steiss JE, West MS: Interday variation in vertical ground reaction force in clinically normal Greyhounds at the trot. Am J Vet Res 60:679-683., 1999

265. Rumph PF, Steiss JE, Montgomery RD: Effects of selection and habituation on vertical ground reaction force in greyhounds. Am J Vet Res 58:1206-1208., 1997

266. Renberg WC, Johnston SA, Ye K, et al: Comparison of stance time and velocity as control variables in force plate analysis of dogs. Am J Vet Res 60:814-819., 1999

267. Rumph PF, Kincaid SA, Baird DK, et al: Vertical ground reaction force distribution during experimentally induced acute synovitis in dogs. Am J Vet Res 54:365-369., 1993

268. Shoemaker SC, Markolf KL: The role of the meniscus in the anterior-posterior stability of the loaded anterior cruciate-deficient knee. Effects of partial versus total excision. J Bone Joint Surg Am 68:71-79., 1986

269. Allen CR, Wong EK, Livesay GA, et al: Importance of the medial meniscus in the anterior cruciate ligament- deficient knee. J Orthop Res 18:109-115., 2000

270. Pelletier JP, Martel-Pelletier J: Protective effects of corticosteroids on cartilage lesions and osteophyte formation in the Pond-Nuki dog model of osteoarthritis. Arthritis Rheum 32:181-193., 1989

271. Moss DW: Perspectives in alkaline phosphatase research. Clin Chem 38:2486-2492, 1992

272. Weiss MJ, Henthorn PS, Lafferty MA, et al: Isolation and characterization of a cDNA encoding a human liver/bone/kidney-type alkaline phosphatase. Proc Natl Acad Sci U S A 83:7182-7186, 1986

273. Moss DW: Diagnostic aspects of alkaline phosphatase and its isoenzymes. Clin Biochem 20:225-230, 1987

274. Hoshi K, Ejiri S, Ozawa H: Localizational alterations of calcium, phosphorus, and calcification- related organics such as proteoglycans and alkaline phosphatase during bone calcification. J Bone Miner Res 16:289-298., 2001

275. Howard AD, Berger J, Gerber L, et al: Characterization of the phosphatidylinositol-glycan membrane anchor of human placental alkaline phosphatase. Proc Natl Acad Sci U S A 84:6055-6059, 1987

276. Mansell JP, Bailey AJ: Abnormal cancellous bone collagen metabolism in osteoarthritis. J Clin Invest 101:1596-1603., 1998

277. de Bernard B, Bianco P, Bonucci E, et al: Biochemical and immunohistochemical evidence that in cartilage an alkaline phosphatase is a Ca2+-binding glycoprotein. J Cell Biol 103:1615-1623, 1986

278. Poole AR, Matsui Y, Hinek A, et al: Cartilage macromolecules and the calcification of cartilage matrix. Anat Rec 224:167-179., 1989

279. Leung KS, Fung KP, Sher AH, et al: Plasma bone-specific alkaline phosphatase as an indicator of osteoblastic activity. J Bone Joint Surg Br 75:288-292., 1993

280. Garnero P, Delmas PD: Assessment of the serum levels of bone alkaline phosphatase with a new immunoradiometric assay in patients with metabolic bone disease. J Clin Endocrinol Metab 77:1046-1053., 1993

281. Woitge HW, Scheidt-Nave C, Kissling C, et al: Seasonal variation of biochemical indexes of bone turnover: results of a population-based study. J Clin Endocrinol Metab 83:68-75., 1998

282. Kyd PA, Vooght KD, Kerkhoff F, et al: Clinical usefulness of bone alkaline phosphatase in osteoporosis. Ann Clin Biochem 35:717-725., 1998

283. Stepan J, Pacovsky V, Horn V, et al: Relationship of the activity of the bone isoenzyme of serum alkaline phosphatase to urinary hydroxyproline excretion in metabolic and neoplastic bone diseases. Eur J Clin Invest 8:373-377, 1978

284. Lereim P, Linde A, Goldie JF: The presence of alkaline phosphatase in the subchondral bone of the medial tibial condyle in the normal state and in osteoarthritis and rheumatoid arthritis. Arch Orthop Unfallchir 83:181-185., 1975

285. Stepan J, Susta A: The clinical significance of serum alkaline phosphatase isoenzymes in locomotor diseases. Z Rheumatol 34:261-269, 1975

286. Hazell K, Ortiz S: The blood alkaline phosphatase level as an aid to diagnosis, treatment and prognosis. Gerontol Clin 8:111-117, 1966

287. Cimmino MA, Dato G, Cutolo M: Synovial fluid alkaline phosphatase. Arthritis Rheum 30:235-237., 1987

288. Cimmino MA, Buffrini L, Barisone G, et al: Alkaline phosphatase activity in the serum of patients with rheumatoid arthritis. Z Rheumatol 49:143-146., 1990

289. Siede WH, Seiffert UB, Merle S, et al: Alkaline phosphatase isoenzymes in rheumatic diseases. Clin Biochem 22:121-124., 1989

290. Arican M, Carter SD, Bennett D, et al: Increased metabolism of collagen VI in canine osteoarthritis. J Comp Pathol 114:249-256., 1996

291. Fuller CJ, Barr AR, Sharif M, et al: Cross-sectional comparison of synovial fluid biochemical markers in equine osteoarthritis and the correlation of these markers with articular cartilage damage. Osteoarthritis Cartilage 9:49-55., 2001

292. Price PA, Poser JW, Raman N: Primary structure of the gamma-carboxyglutamic acid-containing protein from bovine bone. Proc Natl Acad Sci U S A 73:3374-3375, 1976

293. Hauschka PV, Reid ML: Vitamin D dependence of a calcium-binding protein containing gamma-carboxyglutamic acid in chicken bone. J Biol Chem 253:9063-9068, 1978

294. Poser JW, Price PA: A method for decarboxylation of gamma-carboxyglutamic acid in proteins. Properties of the decarboxylated gamma-carboxyglutamic acid protein from calf bone. J Biol Chem 254:431-436, 1979

295. Hauschka PV, Carr SA: Calcium-dependent alpha-helical structure in osteocalcin. Biochemistry 21:2538-2547, 1982

296. Beresford JN, Gallagher JA, Poser JW, et al: Production of osteocalcin by human bone cells in vitro. Effects of 1,25(OH)2D3, 24,25(OH)2D3, parathyroid hormone, and glucocorticoids. Metab Bone Dis Relat Res 5:229-234, 1984

297. Camarda AJ, Butler WT, Finkelman RD, et al: Immunocytochemical localization of gamma-carboxyglutamic acid-containing proteins (osteocalcin) in rat bone and dentin. Calcif Tissue Int 40:349-355, 1987

298. Price PA, Williamson MK, Lothringer JW: Origin of the vitamin K-dependent bone protein found in plasma and its clearance by kidney and bone. J Biol Chem 256:12760-12766, 1981

299. Delmas PD, Malaval L, Arlot ME, et al: Serum bone Gla-protein compared to bone histomorphometry in endocrine diseases. Bone 6:339-341, 1985

300. Azria M: The value of biomarkers in detecting alterations in bone metabolism. Calcif Tissue Int 45:7-11, 1989

301. Fairney A, Patel KV, Hollings NP, et al: Abnormal osteocalcin binding in rheumatoid arthritis. Ann Rheum Dis 49:229-230., 1990

302. Campion GV, Delmas PD, Dieppe PA: Serum and synovial fluid osteocalcin (bone gla protein) levels in joint disease. Br J Rheumatol 28:393-398., 1989

303. Mattei JP, Ferrera V, Boutsen Y, et al: Serum and synovial fluid osteocalcin in rheumatic diseases. Int J Clin Pharmacol Res 12:103-107, 1992

304. Salisbury C, Sharif M: Relations between synovial fluid and serum concentrations of osteocalcin and other markers of joint tissue turnover in the knee joint compared with peripheral blood. Ann Rheum Dis 56:558-561., 1997

305. Wollheim FA: Predictors of joint damage in rheumatoid arthritis. Apmis 104:81-93., 1996

306. Heuck C, Wolthers OD: A placebo-controlled study of three osteocalcin assays for assessment of prednisolone-induced suppression of bone turnover. J Endocrinol 159:127-131., 1998

307. McCarty DJ, Solomon SD, Warnock ML, et al: Inorganic pyrophosphate concentrations in the synovial fluid of arthritic patients. J Lab Clin Med 78:216-229, 1971

308. Gilbertson EM: Development of periarticular osteophytes in experimentally induced osteoarthritis in the dog. A study using microradiographic, microangiographic, and fluorescent bone-labelling techniques. Ann Rheum Dis 34:12-25., 1975

309. Heffron LE, Campbell JR: Morphology, histology and functional anatomy of the canine cranial cruciate ligament. Vet Rec 102:280-283., 1978

310. van Beuningen HM, van der Kraan PM, Arntz OJ, et al: Transforming growth factor-beta 1 stimulates articular chondrocyte proteoglycan synthesis and induces osteophyte formation in the murine knee joint. Lab Invest 71:279-290., 1994

311. van Beuningen HM, Glansbeek HL, van der Kraan PM, et al: Differential effects of local application of BMP-2 or TGF-beta 1 on both articular cartilage composition and osteophyte formation. Osteoarthritis Cartilage 6:306-317, 1998

312. van Beuningen HM, Glansbeek HL, van der Kraan PM, et al: Osteoarthritis-like changes in the murine knee joint resulting from intra-articular transforming growth factor-beta injections. Osteoarthritis Cartilage 8:25-33, 2000

313. Roach HI: New aspects of endochondral ossification in the chick: chondrocyte apoptosis, bone formation by former chondrocytes, and acid phosphatase activity in the endochondral bone matrix. J Bone Miner Res 12:795-805, 1997

314. Hatori M, Klatte KJ, Teixeira CC, et al: End labeling studies of fragmented DNA in the avian growth plate: evidence of apoptosis in terminally differentiated chondrocytes. J Bone Miner Res 10:1960-1968, 1995

315. Moskowitz RW, Goldberg VM: Studies of osteophyte pathogenesis in experimentally induced osteoarthritis. J Rheumatol 14:311-320., 1987

316. Hashimoto S, Creighton-Achermann L, Takahashi K, et al: Development and regulation of osteophyte formation during experimental osteoarthritis. Osteoarthritis Cartilage 10:180-187., 2002

317. Gerber HP, Vu TH, Ryan AM, et al: VEGF couples hypertrophic cartilage remodeling, ossification and angiogenesis during endochondral bone formation. Nat Med 5:623-628, 1999

318. Hashimoto S, Takahashi K, Amiel D, et al: Chondrocyte apoptosis and nitric oxide production during experimentally induced osteoarthritis. Arthritis Rheum 41:1266-1274, 1998

319. Vaananen HK: Immunohistochemical localization of alkaline phosphatase in the chicken epiphyseal growth cartilage. Histochemistry 65:143-148, 1980

320. Poole AR, Pidoux I, Reiner A, et al: Association of an extracellular protein (chondrocalcin) with the calcification of cartilage in endochondral bone formation. J Cell Biol 98:54-65., 1984

321. Seibel MJ: Molecular markers of bone turnover: biochemical, technical and analytical aspects. Osteoporos Int 11:S18-29., 2000

322. Lepage OM, Hartmann DJ, Eicher R, et al: Biochemical markers of bone metabolism in draught and warmblood horses. Vet J 156:169-175., 1998

323. Brandt KD: Transection of the anterior cruciate ligament in the dog: a model of osteoarthritis. Semin Arthritis Rheum 21:22-32., 1991

324. Uitto J, Allan RE, Polak KL: Conversion of type II procollagen to collagen. Extracellular removal of the amino-terminal and carboxy-terminal extensions without a preferential sequence. Eur J Biochem 99:97-103, 1979

325. Peltonen L, Halila R, Ryhanen L: Enzymes converting procollagens to collagens. J Cell Biochem 28:15-21, 1985

326. Van der Rest M, Rosenberg LC, Olsen BR, et al: Chondrocalcin is identical with the C-propeptide of type II procollagen. Biochem J 237:923-925., 1986

327. Hinek A, Reiner A, Poole AR: The calcification of cartilage matrix in chondrocyte culture: studies of the C-propeptide of type II collagen (chondrocalcin). J Cell Biol 104:1435-1441., 1987

328. Mansson B, Carey D, Alini M, et al: Cartilage and bone metabolism in rheumatoid arthritis. Differences between rapid and slow progression of disease identified by serum markers of cartilage metabolism. J Clin Invest 95:1071-1077., 1995

329. Shinmei M, Ito K, Matsuyama S, et al: Joint fluid carboxy-terminal type II procollagen peptide as a marker of cartilage collagen biosynthesis. Osteoarthritis Cartilage 1:121-128., 1993

330. Lee ER, Matsui Y, Poole AR: Immunochemical and immunocytochemical studies of the C-propeptide of type II procollagen in chondrocytes of the growth plate. J Histochem Cytochem 38:659-673., 1990

331. Shinmei M, Kobayashi T, Yoshihara Y, et al: Significance of the levels of carboxy terminal type II procollagen peptide, chondroitin sulfate isomers, tissue inhibitor of metalloproteinases, and metalloproteinases in osteoarthritis joint fluid. J Rheumatol Suppl 43:78-81., 1995

332. Lohmander LS, Yoshihara Y, Roos H, et al: Procollagen II C-propeptide in joint fluid: changes in concentration with age, time after knee injury, and osteoarthritis. J Rheumatol 23:1765-1769., 1996

333. Kobayashi T, Yoshihara Y, Samura A, et al: Synovial fluid concentrations of the C-propeptide of type II collagen correlate with body mass index in primary knee osteoarthritis. Ann Rheum Dis 56:500-503., 1997

334. Kobayashi T, Yoshihara Y, Samura A, et al: Chondrocalcin as a marker of articular cartilage degeneration in anterior cruciate ligament-deficient knees. Orthopedics 21:773-776., 1998

335. Otterness IG, Downs JT, Lane C, et al: Detection of collagenase-induced damage of collagen by 9A4, a monoclonal C-terminal neoepitope antibody. Matrix Biol 18:331-341., 1999

336. Du F, Acland GM, Ray J: Differential splicing of type II procollagen mRNA in canine retina. Anim Biotechnol 9:15-20, 1998

337. Richardson DW, Dodge GR: Cloning of equine type II procollagen and the modulation of its expression in cultured equine articular chondrocytes. Matrix Biol 16:59-64, 1997

338. Stoop R, van der Kraan PM, Buma P, et al: Denaturation of type II collagen in articular cartilage in experimental murine arthritis. Evidence for collagen degradation in both reversible and irreversible cartilage damage. J Pathol 188:329-337., 1999

339. Stoop R, Buma P, van der Kraan PM, et al: Differences in type II collagen degradation between peripheral and central cartilage of rat stifle joints after cranial cruciate ligament transection. Arthritis Rheum 43:2121-2131., 2000

340. Price JS, Chambers MG, Poole AR, et al: Comparison of collagenase-cleaved articular cartilage collagen in mice in the naturally occurring STR/ort model of osteoarthritis and in collagen-induced arthritis. Osteoarthritis Cartilage 10:172-179., 2002

341. Billinghurst RC, Ionescu M, Poole AR: Immunoassay for collagenase-mediated cleavage of types I and II collagens. Methods Mol Biol 151:457-472, 2001

342. Kielty CM, Hopkinson, I., Grant, M.E.: The collagen family, in Royce PM, Steinmann, B. (ed): Connective tissue and its heritable disorders. New York, Wiley-Liss, Inc., 1992, pp 103-147

343. Laemmli UK: Cleavage of structural proteins during the assembly of the head of the bacteriophage T4. Nature (Lond) 227:680-685, 1970

344. Poole AR, Rosenberg LC: Chondrocalcin and the calcification of cartilage. A review. Clin Orthop:114-118., 1986

345. Niyibizi C, Wu JJ, Eyre DR: The carboxypropeptide trimer of type II collagen is a prominent component of immature cartilages and intervertebral-disc tissue. Biochim Biophys Acta 916:493-499., 1987

346. Poole AR: Can serum biomarker assays measure the progression of cartilage degeneration in osteoarthritis? Arthritis Rheum 46:2549-2552, 2002

347. Garnero P, Ayral X, Rousseau JC, et al: Uncoupling of type II collagen synthesis and degradation predicts progression of joint damage in patients with knee osteoarthritis. Arthritis Rheum 46:2613-2624, 2002

348. Henderson B, Higgs GA: Synthesis of arachidonate oxidation products by synovial joint tissues during the development of chronic erosive arthritis. Arthritis Rheum 30:1149-1156, 1987

349. Newton R, Kuitert LM, Bergmann M, et al: Evidence for involvement of NF-kappaB in the transcriptional control of COX-2 gene expression by IL-1beta. Biochem Biophys Res Commun 237:28-32, 1997

350. Yamamoto K, Arakawa T, Ueda N, et al: Transcriptional roles of nuclear factor kappa B and nuclear factor-interleukin-6 in the tumor necrosis factor alpha-

dependent induction of cyclooxygenase-2 in MC3T3-E1 cells. J Biol Chem 270:31315-31320, 1995

351. Gibson KT, Hodge H, Whittem T: Inflammatory mediators in equine synovial fluid. Aust Vet J 73:148-151, 1996

352. Crofford LJ: COX-2 in synovial tissues. Osteoarthritis Cartilage 7:406-408, 1999

353. Schaible HG, Grubb BD: Afferent and spinal mechanisms of joint pain. Pain 55:5-54, 1993

354. Schaible HG, Schmidt RF: Excitation and sensitization of fine articular afferents from cat's knee joint by prostaglandin E2. J Physiol 403:91-104, 1988

355. Ben-Av P, Crofford LJ, Wilder RL, et al: Induction of vascular endothelial growth factor expression in synovial fibroblasts by prostaglandin E and interleukin-1: a potential mechanism for inflammatory angiogenesis. FEBS Lett 372:83-87, 1995

356. Vignon E, Mathieu P, Louisot P, et al: Phospholipase A2 activity in human osteoarthritic cartilage. J Rheumatol Suppl 18:35-38, 1989

357. Negishi M, Sugimoto Y, Ichikawa A: Prostanoid receptors and their biological actions. Prog Lipid Res 32:417-434, 1993

358. Malemud CJ, Sokoloff L: The effect of prostaglandins of cultured lapine articular chondrocytes. Prostaglandins 13:845-860, 1977

359. Fulkerson JP, Ladenbauer-Bellis IM, Chrisman OD: In vitro hexosamine depletion of intact articular cartilage by E-prostaglandins: prevention by chloroquine. Arthritis Rheum 22:1117-1121, 1979

360. Blanco Garcia FJ: Catabolic events in osteoarthritic cartilage. Osteoarthritis Cartilage 7:308-309, 1999

361. Kirker-Head CA, Chandna VK, Agarwal RK, et al: Concentrations of substance P and prostaglandin E2 in synovial fluid of normal and abnormal joints of horses. Am J Vet Res 61:714-718, 2000

362. LeGrand A, Fermor B, Fink C, et al: Interleukin-1, tumor necrosis factor alpha, and interleukin-17 synergistically up-regulate nitric oxide and prostaglandin E2 production in explants of human osteoarthritic knee menisci. Arthritis Rheum 44:2078-2083., 2001

363. Futani H, Okayama A, Matsui K, et al: Relation between interleukin-18 and PGE2 in synovial fluid of osteoarthritis: a potential therapeutic target of cartilage degradation. J Immunother 25 Suppl 1:S61-64, 2002

364. Fortier LA, Nixon AJ: Distributional changes in substance P nociceptive fiber patterns in naturally osteoarthritic articulations. J Rheumatol 24:524-530, 1997

365. Lotz M, Carson DA, Vaughan JH: Substance P activation of rheumatoid synoviocytes: neural pathway in pathogenesis of arthritis. Science 235:893-895, 1987

366. Marshall KW, Chiu B, Inman RD: Substance P and arthritis: analysis of plasma and synovial fluid levels. Arthritis Rheum 33:87-90., 1990

367. Jayson MI, St Dixon AJ: Intra-articular pressure in rheumatoid arthritis of the knee. I. Pressure changes during passive joint distension. Ann Rheum Dis 29:261-265, 1970

368. Sturge RA, Yates DB, Gordon D, et al: Prostaglandin production in arthritis. Ann Rheum Dis 37:315-320, 1978

369. Cawston T: Matrix metalloproteinases and TIMPs: properties and implications for the rheumatic diseases. Mol Med Today 4:130-137., 1998

370. Birkedal-Hansen H, Moore WG, Bodden MK, et al: Matrix metalloproteinases: a review. Crit Rev Oral Biol Med 4:197-250, 1993

371. Dean DD, Azzo W, Martel-Pelletier J, et al: Levels of metalloproteases and tissue inhibitor of metalloproteases in human osteoarthritic cartilage. J Rheumatol 14 Spec No:43-44., 1987

372. Dean DD, Martel-Pelletier J, Pelletier JP, et al: Evidence for metalloproteinase and metalloproteinase inhibitor imbalance in human osteoarthritic cartilage. J Clin Invest 84:678-685., 1989

373. Lohmander LS, Hoerrner LA, Dahlberg L, et al: Stromelysin, tissue inhibitor of metalloproteinases and proteoglycan fragments in human knee joint fluid after injury. J Rheumatol 20:1362-1368., 1993

374. Martel-Pelletier J, McCollum R, Fujimoto N, et al: Excess of metalloproteases over tissue inhibitor of metalloprotease may contribute to cartilage degradation in osteoarthritis and rheumatoid arthritis. Lab Invest 70:807-815, 1994

375. Nagase H, Itoh Y, Binner S: Interaction of alpha 2-macroglobulin with matrix metalloproteinases and its use for identification of their active forms. Ann N Y Acad Sci 732:294-302, 1994

376. Hirte H, Goel, R., Bennet, K., Elias, I., Shah, A., Seymour, L.: Phase I study of the matrix metalloproteinase inhibitor (MMPI) BAY 12-9566 in patients with advanced cancer. Annals of Oncology Suppl 2:75, 1998

377. Goel R, Hirte, H., Shah, A., Major, P., Waterfield, B., Holohan, S.: Phase I study of the metalloproteinase inhibitor Bayer 12-9566, in American Society of Clinical Oncologists, p 217a

378. Rowinsky E, Hammond, L., Aylesworth, C., Humphrey, R., Siu, L., Smith, L.: Prolonged administration of BAY 12-9566, an oral non-peptidic biphenyl matrix: a phase I and pharmacologic study. Annals of Oncology 9:76a, 1998

379. Mengshol JA, Mix KS, Brinckerhoff CE: Matrix metalloproteinases as therapeutic targets in arthritic diseases: bull's-eye or missing the mark? Arthritis Rheum 46:13-20., 2002

380. Cawston T, Carrere S, Catterall J, et al: Matrix metalloproteinases and TIMPs: properties and implications for the treatment of chronic obstructive pulmonary disease. Novartis Found Symp 234:205-218, 2001

381. Erlichman C, Adjei AA, Alberts SR, et al: Phase I study of the matrix metalloproteinase inhibitor, BAY 12-9566. Ann Oncol 12:389-395., 2001

382. Shah A, Woodruff M, Agarwal V, et al: Pharmacokinetics, safety, and tolerability of BAY 12-9566 and nonsteroidal anti-inflammatory agents (naproxen, ibuprofen) during coadministration in patients with osteoarthritis. J Clin Pharmacol 41:330-339., 2001

383. Hughes S: Bayer drug casts shadow over MMP inhibitor in cancer. Scrip Daily News Alert:40301, 1999